SUBSTITUTION AND REDOX CHEMISTRY OF RUTHENIUM COMPLEXES

by

Paul Stuart Moritz, B. Sc. (Hons)

*

A Thesis submitted for the Degree of Doctor of Philosophy.

The Department of Physical and Inorganic Chemistry,
The University of Adelaide.

JUNE 1987
Awarded 1/12/87

STATEMENT.

This Thesis contains no material which has been accepted for the award of any other Degree or Diploma in any University and, to the best of my knowledge and belief, contains no material previously published or written by another person, except where due reference is made in the text. I give consent that, if this Thesis is accepted for the award of the Degree of Doctor of Philosophy, it may be made available for photocopying and, if applicable, loan.

Paul Stuart Moritz.

SUMMARY

The coordination chemistry of ruthenium is dominated by the oxidation states, +2 and +3. Within these oxidation states, the ammine complexes form a large and well-characterized group. This thesis reports on the chemistry of the hitherto neglected triammine complexes, with particular reference to their redox chemistry, and the possible formation of Ru(IV) triammine complexes with terminal oxo ligands. The chemistry of the +4 oxidation state is further explored through the formation of stable chelate complexes.

The salt, $[Ru(NH_3)_3(OH_2)_3](CF_3SO_3)_3$, was prepared by hydrolysis of $Ru(NH_3)_3Cl_3$ in triflic acid solution. Its spectra, electrochemistry and substitution reactions are similar to those of the well-known hexa-, penta-, and tetraammine complexes. At freshly polished platinum and glassy carbon electrodes, a quasi reversible redox wave was detected, corresponding to a proton-coupled reduction involving the Ru^{3+}/Ru^{2+} couple. At anodically-activated glassy carbon electrodes, an additional, irreversible CV wave was detected,which was attributed to the $RuO^{2+}/RuOH_2^{3+}$ couple.

The uv/vis spectrum of the Ru(III) complex was also pH-dependent, and the pK_a values associated with two proton disssociation steps were measured. Solvolysis of the aqua ligands by organic solvents was studied electrochemically and spectroscopically. Coordination of methanol is favoured by the +3 oxidation state, and acetonitrile can coordinate to either the +3 or +2 oxidation state, with the reaction occurring more rapdily on the +2 state. Dimethylsulphoxide can coordinate to either oxidation state, through a S-bound, π-bonding interaction. Acetone appears to coordinate through the carbonyl oxygen atom to the +3 state, and to the +2 state through an η^2 π-interaction involving both atoms of the carbonyl group.

Substitution reactions were carried out with a variety of ligands to give three types of complexes:

(1) substituted triammineaquaruthenium(III) complexes, where the ligands are uni- or dinegative bidentate ligands, such as diketonates and dicarboxylic acids.

(2) substituted triammineruthenium(II) complexes with mono- and bidentate π-acceptor ligands such as pyridines and nitriles.

(3) triammineruthenium(II) complexes with tripodal, tridentate ligands containing three pyridine molecules bound to a central heteroatom.

The spectra and electrochemistry of these complexes showed features similar to those of the analogous Ru(III) and Ru(II) tetra- and pentaammine complexes. In all three cases, the complexes exhibited reversible or quasi reversible electron transfers attributable to the Ru^{3+}/Ru^{2+} couple. In the cases where an aqua ligand was present, pH-dependent electron transfers were evident. At anodically-activated glassy carbon electrodes, irreversible waves attributable to the $RuOH_2^{3+}/RuO^{2+}$ oxidation were also observed. In the case of the complex, $[Ru(NH_3)_3(C_2O_4)(OH_2)]^+$, this latter redox couple was also quasi-reversible at a highly polished glassy carbon electrode.

The chemistry of the triammine series was further extended by the isolation and characterization of a triammine nitrosyl complex, and the reaction of this complex to give dinitrogen complexes.

Complexes with dinegative, tridentate ligands based on aromatic hydrazones, were formed by the reaction of $RuCl_3.3H_20$ with two equivalents of the appropriate protonated ligand in the presence of base. Depending on the ligand used, either a Ru(III) or Ru(IV) complex was obtained. The spectra, magnetochemistry, and electrochemistry of these complexes were studied. The oxidation state of the complex, and the $E_{1/2}$ potential of the Ru^{4+}/Ru^{3+} couple were shown to be dependent on the electronic properties of the ligand. In some cases, two reversible electron transfer reactions could be detected in DMSO, corresponding to the Ru^{4+}/Ru^{3+} and Ru^{3+}/Ru^{2+} couples.

ACKNOWLEDGEMENTS.

I acknowledge and thank my Supervisor, Dr. Alex Diamantis. Without his encouragement, guidance and friendship this work would not have come to fruition.

I would also like to thank Dr. B. J. Steel, who was always willing to discuss electrochemical aspects of my work, and Dr. J. H. Coates, who acted as my Supervisor during Dr. Diamantis's absence on study leave. Dr. F. R. Keene of James Cook University kindly supplied ligands and preprints of his publications, and Dr. G. A. Heath, formerly of Edinburgh University, provided a copy of some recent, unpublished, results.

Thanks are also due to Dr. E. R. T. Tiekink, who determined the crystal structures, Mr. T. Blumenthal and Mr. M. Liddell, who recorded the mass spectra and Ms. Andrea Hounslow who recorded the NMR spectra. Mr. Michael Hounslow provided invaluable advice on the finer points of Macintosh word processing.

Dr. Md. Abdus Salam, Tom Horr, Robert Jones (who proof read this Thesis) and Mary Manikas patiently humoured me while we shared the laboratory. They, and the rest of my friends and fellow students, gave much me much support and many hours of fruitful conversation.

I also thank the Technical, Laboratory and Secretarial staff of the Department of Physical and Inorganic Chemistry.

The financial assistance of a Commonwealth Postgraduate Research Award and a short term University of Adelaide Scholarship is acknowledged.

ABBREVIATIONS

acac	penta-2,4-dione
ampy	2(aminomethyl)pyridine
BH	benzoylhydrazine
bzac	1-phenylbuta-1,3-dione
dbm	1,3-diphenylpropa-1,3-dione
DMSO	dimethylsulphoxide
dpm	2,2,6,6-tetramethylhepta-3,5-dione
EtOH	ethanol
hap	2-hydroxyacetophenone
hna	2-hydroxyanaphthaldehyde
HTFMS	trifluoromethanesulphonic acid
MeCN	acetonitrile(cyanomethane)
MEK	butanone
MeOH	methanol
$MeSO_3$	methanesulphonate anion
$MeSO_3H$	methanesulphonic acid
OAP	2-aminophenol
oxine	8-hydroxyquinoline
phen	1,10-phenanthroline
PPh_3	triphenylphosphine
py	pyridine
py_3COH	tris(pyridyl)methanol
py_3CH	tris(pyridyl)methane
py_3N	tris(pyridyl)amine
RuA_n	$Ru(NH_3)_n$
sal	salicylaldehyde
SalH	salicyloylhydrazinze
terpy	2,2',2"-terpyridine
TFMS	trifluoromethanesulphonate anion

The abbreviations for the dinegative tridentate ligands are derived from the trivial names of the ketone-type and amine-type portions which make up the Schiff's base ligand.
For example, bzacBH = benzoylacetonebenzoylhydrazone. (Systematic name = N'-(1-methyl-3-oxo-3-phenylpropylidene)benzohydrazide.

ABBREVIATIONS (cont.)

ELECTROCHEMISTRY.

CV	cyclic voltammetry
DPV	differential pulse voltammetry
$E_{1/2}$	half-wave potential
E_p	peak potential (subscript c refers to cathodic peaks, subscript a refers to anodic peaks
GCE	glassy carbon electrode
LSV	linear sweep voltammetry
OSWV	Osteryoung square wave voltammetry
SCE	saturated calomel electrode
SCP	sampled current polarography

SPECTRA

A	absorbance
B.M.	Bohr magneton
FAB	fast atom bombardment
ir	infrared
sh	shoulder
uv/vis	ultra violet/ visible
(υ)	stretching mode
(δ)	bending mode
λ	wavelength
υ	frequency

"It is better to ask some of the questions than to know all the answers."

(James Thurber, "Fables of Our Time and Illustrated Poems.")

TABLE 0F CONTENTS.

CHAPTER 6. EXPERIMENTAL.

Chapter 1.

INTRODUCTION.

1.1. Aims of the Project.

Ruthenium is capable of forming compounds in at least 9 different oxidation states from 0 to +8, but the most prevalent states are +2, +3 and +4. [1] However, there is a large difference in the number of compounds formed in each of these oxidation states. In a recent comprehensive work on the chemistry of ruthenium [2], the chapters dealing with the oxidation state +2, +3 and +4 were respectively 549, 180 and 62 pages long. While the discussion of the chemistry of Ru(II) also dealt with a large number of organometallic compounds, where the concept of oxidation state is more formal than in compounds with more electronegative donor atoms, there is still obviously a much larger number of compounds of Ru(II) known than there is of Ru(III), and in turn more of Ru(III) than of Ru(IV).

Additionally, the chemistry of Ru(IV) is dominated by multinuclear species. There are relatively few mononuclear coordination complexes known in this oxidation state, [2a] whereas the mononuclear complexes of Ru(II) and Ru(III) are, by far, the most prevalent.

In recent times there has been a growing interest in the area of higher oxidation state complexes of ruthenium, and many of the new complexes which have been synthesized are in the +4 oxidation state. Meyer's group has demonstrated the existence of a relatively stable series of oxoruthenium(IV) complexes containing diimine ligands [3-7], and also, in one case, ammine ligands. [8] Poon's group has been able to obtain oxoruthenium complexes containing macrocyclic tertiary amine ligands,[9-13] and Chakravorty's group has demonstrated the existence of a range of Ru(IV) complexes containing N-donor ligands. [14-18] Finally, several groups have studied the existence of Ru(IV) diketonate complexes. [19-23]

The aim of this project was to study the formation of simple coordination compounds containing the oxoruthenium(IV), $Ru{=}O^{2+}$, group. The hitherto little-known triammine series of complexes was chosen as the group which offered the best scope to vary the coordination environment by substitution at two coordination sites while maintaining the presence of an oxo ligand. It was proposed to form the oxoruthenium group by proton-coupled oxidation of a $RuOH_2^{3+}$ group. A previous study has shown that it is possible to generate $[Ru(NH_3)_5(O)]^{2+}$ by electrochemical oxidation of $[Ru(NH_3)_5(OH_2)]^{3+}$ at an anodically activated glassy carbon voltammetric electrode. [8]

It was also intended to use the aqua ligand in the substituted triammineaqua ruthenium(II) complexes as a site for reaction with dinitrogen gas, and so form a series of substituted triammine dinitrogen complexes. It was hoped that any increased electron density on Ru(II) which might be induced by the substituting ligand would enhance the binding of the dinitrogen ligand to the metal centre.

As an adjunct to this work, studies were also made of complex formation with a series of dinegative, tridentate ligands based on aroyl hydrazones. These ligands have been shown to stabilize vanadium(IV) in the absence of the vanadyl(V=O) group. [24, 25]

1.2. Factors Affecting the Stability of Ruthenium Oxidation States.

The relative stability of a complex in either of two oxidation states can be judged from the reduction potential for the electron transfer between the two states. For the reaction:

$$Ox + e^- \rightleftharpoons Red \quad \textbf{(1.1)}$$

with a reduction potential, E, the free energy change upon electron transfer will be given by the equation:

$$\Delta G = -nFE \quad \textbf{(1.2)}$$

If a series of 6 coordinate complexes is studied, in which only one ligand is varied, (e.g. $[Ru(NH_3)_5L]$) then the entropy contributions to the free energy change associated with electron transfer will be much the same for each complex in the series. The variation in E as the ligand is changed may then be related to the contribution of the d electrons to the overall free energy change which would be expected to be associated with the enthalpy term. Similarly, in the same series of complexes, the variations in the equilibrium constant, K, for the attachment of the ligand would be expected to reflect the effect of the ligand in altering the electronic energy of the complex.

The ruthenium oxidation states, +2, +3, and +4 are d^6, d^5 and d^4 systems respectively. The complexes in the +2 and +3 states are most often low-spin mononuclear species while those of the +4 state are sometimes low-spin mononuclear complexes, but more often diamagnetic,multinuclear species. [2a, 2b, 2c]

The d_π electrons of Ru(II) participate in π-backbonding to a greater extent than those in d^6 complexes in higher oxidation states such as Co(III) and Rh(III). [26] Because of this, the Ru(II) complexes tend to contain ligands capable of strong π-acceptance. This is the case with ligands such as dinitrogen, carbon monoxide, organonitriles and pyridine ligands.

Clearly, when the π-accepting ability of the ligand is quite good, it might be expected that the Ru(II) complex will be better stabilized to oxidation. If the reduction in the ir stretching frequency of a ligand X-Y, (υ)XY, is taken as a measure of the ligand's ability to act as a π-acceptor, then some correlation might be expected between the reduction potential and the reduction in (υ)X-Y. This is exactly what is observed in the limited series shown in Table 1.1. It can be seen that the higher potential required to oxidize the terminal dinitrogen complex [27] ,compared with those of the two organonitrile complexes [26], is consistent with the much greater reduction in (υ)X-Y for the dinitrogen ligand than for the nitriles. [28, 29] As there is also some σ-donor ability in the nitrile ligands, the above comparison is made on the assumption that the π-accepting ability of the nitriles is the major contribution to the Ru(II)-NCR bond.

A similar trend can be seen in the formation constant data displayed in Table 1.2. It can be seen that when the ligand is a good π-acceptor, such as N_2, the formation constant for the Ru(II) complex is very much larger than that for the Ru(III) complex with the same ligand. At the same time, the formation constant for Ru(III) complexes with poor π-acceptor ligands, such as Cl^-, are very much larger than those for the Ru(II) complexes with the same ligands. [30]

As illustrated by the prevalence of Ru(II) nitrile pyridine and polypyridine complexes, Ru(II) is not stabilized solely by π-acceptor ligands, but also by ligands which have some σ-donor ability. Also, besides those ligands which are both π-acceptors and σ-donors, there are also compounds of moderate stability which have purely σ-donor ligands. These compounds include those with ammine ligands, e.g. $[Ru(NH_3)_6]^{2+}$ and $[Ru(NH_3)_5(OH_2)]^{2+}$ [26], but such complexes do not favour further substitution by π-donors. Hence, within the ammine series, there are no known examples of complexes with π-donors such as diketonates or carboxylates. Similarly, there are no examples in which the Ru(II) ion is complexed entirely by carboxylate ligands, and the only fully characterized example of a tris diketonate complex of Ru(II) involves trifluoropentanedionate as the ligand, which has some π-acceptor ability due to the electron withdrawing effects of the fluorine atoms. [31] There are Ru(II) complexes containing ligands such as diketonates and carboxylates where the co-ligands are good π-acceptors such as phosphines and carbon monoxide. [2e, 2f]

To conclude, the +2 oxidation state of ruthenium is stable with both σ-donor and π-acceptor ligands, and in some cases one ligand provides a suitable combination of both properties. π-donors will only coordinate to Ru(II) when π-acceptors are present.

The +3 oxidation state is also capable of existing with ligands which are both π-acceptors and σ-donors, such as nitriles and pyridyls. Within the pentaammine and tetraammine series, the nitrile and pyridine ligands form complexes which are quite stable and the Ru(III)/Ru(II) electrochemical

L	$(\upsilon)L^a$	$(\upsilon)Ru(NH_3)_5L^a$	$\delta\upsilon^a$	E(V vs SCE)
MeCN[b]	2254	2239	15	+0.19
PhCN[b]	2232	2194	27	+0.23
N_2*	2331[c]	2118[d]	213	+0.81[e]

Table 1.1. Comparison of changes in ir absorptions with oxidation potential in $Ru(NH_3)_5L^{2+}$ complexes. * Raman spectrum. (a) cm^{-1} (b) Reference 26 (c) Reference 28 (d) Reference 29 (e)Reference 27

Ligand	$[Ru(NH_3)_5(OH_2)]^{2+}$	$[Ru(NH_3)_5(OH_2)]^{3+}$	Ratio
N_2	3.3×10^4	4.0×10^{-13}	8×10^{16}
Pyridine	2.4×10^7	6.0×10^3	4×10^3
Imidazole	2.8×10^6	1.9×10^6	1.5
Cl^-	0.41.	1×10^2	4×10^{-1}
HO^-	6.0×10^2	6.0×10^{11}	1×10^{-9}

Table 1.2. Equilibrium constants for the replacement of water by various ligands. (Reference 30)

couples are reversible. However, in the case of Ru(III) complexes, the major contribution to metal-ligand bond formation comes from the ability of the ligand to form a σ-bond. This is illustrated by the case of the nitrile ligands where the frequency of the ir absorption due to (υ)CN increases on complex formation as a result of the loss of delocalization of electron density from the nitrogen lone pair into the C-N antibonding orbitals, without concomitant back donation from the metal centre. [26]

The importance of σ-donation from the ligand to the Ru(III) centre is further exemplified by the existence of a large number of ammine carboxylates and diketonates, as well as the tris carboxylate and diketonate complexes. [2d, 19, 21-23]

The coordination chemistry of Ru(IV) is dominated by bridged, multinuclear complexes. [2a] The bridging ligands are quite often very strong π-donors such as oxo and nitride ions. Also there are a number of complexes containing phosphinimate, $R_3P{=}N^-$, ligands.[32] In the aqueous chemistry of Ru(IV), also, there are many examples of bridged multinuclear complexes. These are mostly the aqua halo complexes, and may consist of up to four ruthenium ions, often with these ions existing in several different oxidation states within the complex.

The existence of the large number of bridged complexes of Ru(IV) is a direct consequence of the ability of some ligands to stabilize this oxidation state. The very strong π-donors, such as O^{2-} and N^{3-} are also ligands which tend to act as very good bridging groups. [33] The existence of the stable hexachlororuthenium(IV) ion provides good evidence that the Cl^- ligand is also a sufficiently strong π–donor to stabilize the Ru(IV) centre. [34]

Recent electrochemical studies on the tris diketonate Ru(III) complexes have also indicated that these ligands are capable of stabilizing the +4 oxidation state. [20-23] With these ligands, and perhaps other strong π-donors, it may be possible to isolate other stable mononuclear Ru(IV) complexes in the ammineruthenium series.

1.3. Oxoruthenium(IV) Complexes With N-Donor Ligands.

There are three classes of N-donor ligands under consideration. The polypyridyl groups employed by Meyer's group, the macrocylic tertiary amines used by Poon's group and the arylazopyridine ligands used by Chakravorty.

1.3.1. Polypyridyl Ligands. Interest in this class of compounds stems from the ability of $[Ru(trpy)(bpy)OH_2]^{2+}$ and similar complexes to act as catalytic oxygen atom transfer agents. [3] In aqueous solution $[Ru(trpy)(bpy)OH_2]^{2+}$ is capable of undergoing two one electron oxidations with coupled proton transfer.

$$[Ru(trpy)(bpy)(O)]^{2+} + e^- + H^+ \rightleftharpoons [Ru(trpy)(bpy)OH]^{2+} \quad (1.3)$$

$$[Ru(trpy)(bpy)OH]^{2+} + e^- + H^+ \rightleftharpoons [Ru(trpy)(bpy)OH_2]^{2+} \quad (1.4)$$

The $E_{1/2}$ values are +0.61 V vs SCE* and +0.48 V vs SCE ,respectively, at pH 7. In the presence of organic molecules such as ethanol, propan-2-ol or ethanal, the organic molecule reduces the Ru(IV) oxo complex to the Ru(II) aqua complex, and the organic molecule is oxidized. For propan-2-ol, the overall reaction is:

$$[Ru(trpy)(bpy)(O)]^{2+} + CH_3CH(OH)CH_3 \rightleftharpoons [Ru(trpy)(bpy)OH_2]^{2+} + CH_3C(O)CH_3 \quad (1.5)$$

Under conditions of electrolytic oxidation of the Ru(II) complex, the whole cycle could be made catalytic and, over 100 redox cycles, 10-20% of the alcohol was oxidized. [3] The electrochemistry of $[Ru(trpy)(bpy)OH_2]^{2+}$ was investigated over a wide range of pH values, and the pH dependence of the $E_{1/2}$ values was consistent with the pK_a values measured by pH titration of the Ru(II) and Ru(III) complexes. [4]

The electrochemistry of the $[Ru(bpy)_2(py)O]^{2+}/[Ru(bpy)_2(py)OH_2]^{2+}$ system was consistent with the existence of two reversible electron transfer steps, which were pH dependent. At pH 7, the $E_{1/2}$ value for the Ru(IV)/Ru(III) couple was +0.53 V, and for the Ru(III)/Ru(II) couple, +0.42 V. $[Ru(bpy)_2(py)O]^{2+}$ was isolated as its perchlorate salt, and the presence of the oxoruthenium group, $Ru{=}O^{2+}$, was confirmed by isotopic labelling with O^{18}. In the ir spectrum, $(\upsilon)Ru{=}O^{16}$ was observed at 792 cm^{-1} and $(\upsilon)Ru{=}O^{18}$ at 752 cm^{-1}. [5]

The complex *cis* $[Ru(bpy)_2(OH_2)_2]^{2+}$ was shown to be capable of four one electron/one proton oxidations to give a dioxoruthenium (VI) complex according to reactions 1.6 to 1.9. [6]

$$cis\,[Ru(bpy)_2(O)_2]^{2+} + e^- + H^+ \rightleftharpoons cis\,[Ru(bpy)_2(OH)(O)]^{2+} \quad (1.6)$$

$$cis\,[Ru(bpy)_2(OH)(O)]^{2+} + e^- + H^+ \rightleftharpoons cis\,[Ru(bpy)_2(OH_2)(O)]^{2+} \quad (1.7)$$

$$cis\,[Ru(bpy)_2(OH_2)(O)]^{2+} + e^- + H^+ \rightleftharpoons cis\,[Ru(bpy)_2(OH_2)(OH)]^{2+} \quad (1.8)$$

$$cis\,[Ru(bpy)_2(OH_2)(OH)]^{2+} + e^- + H^+ \rightleftharpoons cis\,[Ru(bpy)_2(OH_2)_2]^{2+} \quad (1.9)$$

The $E_{1/2}$ values for these reactions were reported as +1.07, +0.94, +0.76 and +0.53 V respectively, at pH 4.

---

*Henceforth, all E values will be quoted vs the SCE unless otherwise stated.

Oxidation of *cis* $[Ru(bpy)_2(OH_2)_2]^{2+}$ with 3 equivalents of Ce^{4+} ion resulted in the Ru(V) complex *cis* $[Ru(bpy)_2(OH)(O)]^{2+}$, the perchlorate salt of which had an ir absorption at 857 cm^{-1} which was assigned to the (υ)RuO vibration. The perchlorate salt of *cis* $[Ru(bpy)_2(O)_2]^{2+}$, obtained by the reaction of excess Ce^{4+} ion with *cis* $[Ru(bpy)_2(OH_2)_2]^{2+}$, showed two bands attributable to (υ)RuO in the ir spectrum, at 860 cm^{-1} and 835 cm^{-1}.

A phosphineoxoruthenium(IV) complex has also been isolated. [7] By oxidation of *cis* $[Ru(bpy)_2(OH_2)PEt_3]^{2+}$ with Ce^{4+}, it was possible to obtain *cis* $[Ru(bpy)_2(O)PEt_3]^{2+}$. This compound also had a well behaved electrochemistry and, at pH 7, it was possible to observe the redox couples 1.10 and 1.11 with $E_{1/2}$ values of +0.72 V and +0.46 V respectively.

$$[Ru(bpy)_2(O)PEt_3]^{2+} + e^- + H^+ \rightleftharpoons [Ru(bpy)_2(OH)PEt_3]^{2+} \quad \textbf{(1.10)}$$

$$[Ru(bpy)_2(OH)PEt_3]^{2+} + e^- + H^+ \rightleftharpoons [Ru(bpy)_2(OH_2)PEt_3]^{2+} \quad \textbf{(1.11)}$$

The presence of the oxo group was confirmed by the presence of an ir absorption at 790 cm^{-1}. The Ru(IV) complex was also shown to be capable of oxidizing a variety of organic and inorganic substrates. [7]

1.3.2. Macrocyclic Tertiary Amine Ligands. In 1984, Poon and co-workers reported that reaction of *trans* $[Ru(tmc)Cl_2]Cl$ (tmc = 1,4,8,11-tetramethyl-1,4,8,11-tetraazacyclotetradecane) with 30% hydrogen peroxide gave a complex which they formulated as *trans* $[Ru(tmc)(H_2O)(O)]^{2+}$. [9] As its perchlorate salt, this compound had an intense ir absorption at 855 cm^{-1}. However, this product was later positively identified as the Ru(VI) complex *trans* $[Ru(tmc)(O)_2]^{2+}$. [10] The cyclic voltammogram of this complex showed one two electron and two one electron waves, which were assigned to the electron transfer couples shown as 1.12 to 1.14:

$$trans\,[Ru(tmc)(O)_2]^{2+} + 2e^- + 2H^+ \rightleftharpoons trans\,[Ru(tmc)(H_2O)(O)]^{2+} \quad \textbf{(1.12)}$$

$$trans\,[Ru(tmc)(H_2O)(O)]^{2+} + e^- + 2H^+ \rightleftharpoons trans\,[Ru(tmc)(H_2O)_2]^{3+} \quad \textbf{(1.13)}$$

$$trans\,[Ru(tmc)(H_2O)_2]^{3+} + e^- \rightleftharpoons trans\,[Ru(tmc)(H_2O)_2]^{2+} \quad \textbf{(1.14)}$$

The $E_{1/2}$ values were +0.66 V, +0.36 V and +0.15 V, respectively, in 0.1 mol dm^{-3} $HClO_4$.

The dioxoruthenium complex was shown to be capable of reacting with PPh_3 in acetonitrile to give *trans* $[Ru(tmc)(MeCN)(O)]^{2+}$. [11] The crystal structure of the PF_6^- salt revealed a Ru=O bond distance of 1.765(5) Å. The (υ)RuO absorption in the ir spectrum could not be positively identified because of absorptions due to the tmc ligand in the region 700-820 cm^{-1}. The other product of

the reaction was $O=PPh_3$, indicating that the reduction of the Ru(VI) complex was accompanied by an oxo atom transfer to the phosphine. There was also a report of the complex *trans* $[Ru(tmc)(Cl)(O)]^+$, with a Ru=O bond length of 1.765(7) Å, and having a quasi-reversible one electron reduction couple in acetonitrile at +1.1 V vs cp_2Fe^+/cp_2Fe. [12] This complex was capable of acting as an electrocatalytic agent for the oxidation of benzyl alcohol.

In later work, the same workers were able to show that the Ru=O distance in the *trans* dioxoruthenium(VI) complexes was insensitive to the ring size of the macrocycle. [13]

1.3.3. Arylazopyridine Ligands. The existence of well-defined proton-coupled electron transfer reactions involving $Ru\text{-}OH_2^{2+}$ and $Ru{=}O^{2+}$ compounds has also been demonstrated for complexes containing arylazopyridine ligands. For $[Ru(pap)_2(py)OH_2]^{2+}$ (pap = phenylazopyridine), the two electron redox couple 1.15 has been observed.[14]

$$[Ru(pap)_2(py)(O)]^{2+} + 2e^- + 2H^+ \rightleftharpoons [Ru(pap)_2(py)OH_2]^{2+} \quad \textbf{(1.15)}$$

$E_{1/2}$ for the couple is +1.20 V in the pH range 1-4. The Ru(IV) complex was shown to be capable of oxidizing H_2O to O_2.

Later, it was demonstrated that the hydroxoaqua and dihydroxo complexes, such as $[Ru(pap)_2(OH_2)(OH)]^{2+}$and $[Ru(pap)_2(OH)_2]^+$ are capable of one electron oxidation to the corresponding Ru(IV) complex. [15] e.g. $E_{1/2}$ for couple 1.16 is +1.89 V, and for couple 1.17 is +1.53 V

$$[Ru^{IV}(pap)_2(OH_2)(OH)]^{3+} + e^- \rightleftharpoons [Ru^{III}(pap)_2(OH_2)(OH)]^{2+} \quad \textbf{(1.16)}$$

$$[Ru^{IV}(pap)_2(OH)_2]^{2+} + e^- \rightleftharpoons [Ru^{III}(pap)_2(OH)_2]^{+} \quad \textbf{(1.17)}$$

It is apparent from these data that the hydroxo ligand is not as good at stabilizing the Ru(IV) oxidation state as the oxo ligand.

1.4. Ruthenium(IV) Complexes With Bidentate Ligands

1.4.1. Arylazopyridine Ligands. The diaqua complexes, $[Ru(pap)_2(OH_2)_2]^{2+}$, react with bidentate ligands such as acac-, bpy, en and triazene-1-oxides to give complexes of the type, $[Ru(pap)_2(LL)]^{n+}$ in solution. [16] In the case of the complex, $[Ru(tap)_2(acac)]^+$ (tap = tolylazopyridine), the Ru(II)/Ru(III) oxidation occurs at +1.34 V and the Ru(III)/Ru(IV) oxidation wave was observed at about +2 V in the CV. However, it was not possible to isolate the oxidized species.

1.4.2. RuN_3O_3 Complexes. A series of complexes, $[RuL_3]$, ($L = [X\text{-}C_6H_4\text{-}N\text{-}N{=}N(O)R]^-$) has been synthesized. [17] In acetonitrile, these complexes displayed a quasi-reversible wave in the region –0.060 V to –1.20 V, assigned to the Ru(III)/Ru(II) couple, and a reversible wave in the region +0.20 V to + 0.70 V, assigned to the Ru(IV)/Ru(III) couple.

Electrolysis of several of the complexes was reported, and the uv/vis spectra of the oxidized species were determined and compared with those of the Ru(III) complexes. None of the Ru(IV) complexes were isolated. On electrolytic reduction of the complexes in acetonitrile, the reduced species were observed to decompose. For both the Ru(IV)/Ru(III) and Ru(III)/Ru(II) couples there was a good correlation between the $E_{1/2}$ values and the Hammett constant for the sustituent X.

When two of the triazene-1-oxide ligands in the above complexes were replaced by a bipyridine ligand, to give $[Ru(bpy)_2L]^+$, the Ru(III)/Ru(II) couple was shifted to a potential in the range +0.16 V to +0.44 V. [18] A further oxidation wave in the CV was observed in the region +1.40 V to +1.70V, but there was some uncertainty about whether this oxidation was metal or ligand-based.

1.4.3. $Ru(diket)_3$ Complexes. The one electron oxidation of Ru(III) diketonate complexes in non-aqueous solutions has been the subject of much study. [19-23] Fackler and co-worker investigated the redox chemistry of the $M(acac)_3$ complexes for a number of metals. [20] In the case of the ruthenium complex, it was found that there was a reversible oxidation in the CV at +1.05 V vs the Ag/AgCl electrode in a number of organic solvents. Although the oxidized species showed no tendency to undergo further reaction on the voltammetric time scale, it proved to be unstable over the longer time period required for electrosynthesis. In N, N'-dimethylformamide, the oxidation process was irreversible, and there was no evidence of the return cathodic wave after oxidation.

In two studies on the electrochemistry of the Ru(III) complexes with the ligands $[R\text{-}C(O)\text{-}C(R')\text{-}C(O)\text{-}R"]^-$, the substituents R and R" were varied with R' =H [21] and the substituent R' was varied with $R = R" = CH_3$. [22] For R' = H, the $E_{1/2}$ values for oxidation and for reduction were plotted against the sum of the Hammett constants of the substituents. The $E_{1/2}$ values for reduction lie along a straight line, while the $E_{1/2}$ values for oxidation appear to lie along two horizontal lines. In the second case, it was found that the oxidation and reduction potentials could be expressed as a function of the sum of the Hammett constants if the *para*- position value was used for R', and the *meta*- position values were used for R and R".

A later study was concerned with the redox chemistry of a greater number of tris diketonate complexes than the previous work. [23] It was found that both the reduction potential and oxidation potential of the Ru(III) complexes varied linearly with the Taft parameters, and with almost identical

slopes. The reduction potentials were in the range –0.67 V to +0.27 V and the oxidation potentials were in the range +1.09 V to +1.88 V vs Ag/AgCl.

The uv/vis spectra of $Ru(diket)_3$ complexes were recorded in dichloromethane, and the OTTLE technique was used to study the spectra of the Ru(II) and Ru(IV) complexes. [23] It was found that all spectra contained intra- ligand absorptions in addition to absorptions assigned to charge transfer transitions. When the Ru(III) complexes were subjected to reductive electrolysis, the intensity of the intra-ligand bands increased markedly, sometimes with a shift in the absorption maximum, and one of the LMCT bands disappeared while that at lower energy increased in intensity, possibly due to MLCT. Under conditions of oxidative electrolysis, the intensity of the intraligand bands did not increase by a great amount, but the absorption maximum shifted to a longer wavelength as an intense absorption was induced at wavelengths shorter than 250 nm (the absorption cutoff for the solvent). One charge transfer band disappeared and the low intensity band at lower energy was shifted to a longer wavelength, with a higher absorbance. For example, in the case of $Ru(acac)_3$, the Ru(III) complex had absorptions at 275 nm (A = 0.49 in the spectroelectrochemical cell), 347 nm (A = 0.21) and 504 nm (A = 0.03). After reduction, there were bands at 275 nm (A = 0.92), 347 nm (a shoulder with A = 0.012) and 504 nm (A = 0.38). After oxidation, there were bands at 284 nm (A = 0.43), 347 nm (A = 0.05) and 700 nm (A = 0.13). [23]

1.5. Ruthenium(IV) Complexes With Chloro Ligands.

1.5.1. Macrocyclic Tertiary Amine Ligand Complexes. By electrochemical oxidation of the complexes, *trans* $[Ru(tmc)_2X_2]^+$ (X = Cl, Br, or NCO), Poon and co-workers were able to form the Ru(IV) complexes, *trans* $[Ru(tmc)X_2]^{2+}$. [35] In acetonitrile, *trans* $[Ru(tmc)Cl_2]^+$ had a cyclic voltammogram which consisted of two quasi-reversible waves at –0.56 V and +1.21 V vs the cp_2Fe^+/cp_2Fe couple. (i.e. –0.25 V and +1.54 V vs SCE. [36]) These waves were assigned to the Ru(III)/Ru(II) and Ru(IV)/Ru(III) couples respectively. It was possible to follow the electrochemical formation of *trans* $[Ru(tmc)Cl_2]^{2+}$ by spectroscopic means, but the controlled-potential oxidation at +1.30 V showed that the oxidative current did not decay to a background level, but remained at a constant value as oxidation proceeded. It was proposed that some of the electrochemically generated Ru(IV) complex reacted with a non-electroactive species to regenerate the starting material.

The large difference in the oxidation potentials of *trans* $[Ru(tmc)_2Cl_2]^+$ and *trans* $[Ru(tmc)(H_2O)_2]^{3+}$ (as shown in Table 1.3) is a good illustration of the ability of strong π-donor ligands to stabilize Ru(IV). Cl^- is a weaker π-donor ligand than O^{2-}, and it can be seen that it lacks sufficient π-donating power to be able to stabilize the +4 oxidation state as well as O^{2-}. The

decrease in the oxidation potential of a ruthenium complex by replacing Cl^- ligands with O^{2-}, or its precursor, H_2O, is also observed when the potential of the *cis* $[Ru(bpy)_2Cl_2]^{2+/+}$ couple (+1.97 V) is compared with that of the *cis* $[Ru(bpy)_2(OH_2)(O)]^{2+}$/ *cis* $[Ru(bpy)_2(OH_2)(OH)]^{2+}$ couple (+0.76 V at pH 4). [6] Certainly, part of the large difference in the oxidation potentials in these cases is because the O^{2-} ligand is a better π-donor than its precursors H_2O and OH^-, but there still remains a large degree of stabilization by the O^{2-} ligand over the Cl^- ligand which probably reflects the effects of a dinegative ion versus a uninegative ion.

Couple	$E_{1/2}$(V vs SCE)	Reference
cis $[Ru(bpy)_2(OH_2)(O)]^{2+}$/ *cis* $[Ru(bpy)_2(OH_2)(OH)]^{2+}$	+0.76 (pH4)	6
cis $[Ru(bpy)_2Cl_2]^{2+}$/ *cis* $[Ru(bpy)_2Cl_2]^{+}$	+1.97	"
trans $[Ru(tmc)(H_2O)_2(O)]^{2+}$/ *trans* $[Ru(tmc)(H_2O)_2]^{3+}$	+0.36	10
trans $[Ru(tmc)_2Cl_2]^{2+}$/ *trans* $[Ru(tmc)_2Cl_2]^{+}$	+1.54	35

Table 1.3. Oxidation potentials of dichloro- and diaquaruthenium(III) complexes.

1.5.2. Triazene-1-oxide Complexes.. When the $[RuL_3]$ complexes (L = $[X\text{-}C_6H_4\text{-}N\text{-}N{=}N(O)R]^-$) were treated with a hydrohalic acid, it was possible to obtain a stable, crystalline complex of the form, $[RuL_2X_2]$. [37] These complexes exhibited two single electron reductions in the CV, presumably to $[RuL_2X_2]^-$ and $[RuL_2X_2]^{2-}$. The first reduction wave was reversible, and found in the region +0.1 V to +0.2 V. The second reduction was irreversible, with the cathodic peak potential in the region –1.20 V to –1.55 V. The crystal structure of the Ru(IV) complex with X =Cl and L = $CH_3\text{-}C_6H_4\text{-}N\text{-}N{=}N(O)C_2H_5$ was determined and showed a slightly distorted octahedral coordination sphere, with the chloro ligands *trans* to each other.

1.6. Ru(IV)edta complexes.

The chemistry of the Ru(III) and Ru(II) complexes with edta has been the subject of study over the last decade, [38-40] but it is only recently that the chemistry of Ru(IV)edta complexes has been investigated. It has been shown that in aqueous solution, $[Ru^{III}(edta\text{-}H)(H_2O)]$ will react with molecular oxygen or hydrogen peroxide to give either a μ-peroxo or μ-hydroperoxo Ru(IV) complex. [41] In water/dioxane mixtures, it was found that $[Ru^{III}(edta\text{-}H)(H_2O)]$ acted as a catalyst for the

oxidation of PPh_3 by oxygen. [42] It was proposed that the oxidation reaction proceeded through the intermediates $[Ru^{IV}(edta)(PPh_3)]_2O_2$ and $[Ru^{V}{=}O(edta)(PPh_3)]$.

1.7. Tridentate Dinegative Ligands.

The demonstrated ability of the oxo ligand to stabilize the Ru(IV) ion, parallels the importance of the oxo ligand in stabilizing the vanadium (IV) oxidation state. The vanadyl, $V{=}O^{2+}$, group is almost ubiquitous in the chemistry of vanadium(IV). However, some recent studies have demonstrated that other π-donor ligands are capable of stabilizing this oxidation state.

In 1975, Diamantis and co-workers reported the synthesis of a non-vanadyl V(IV) complex containing a tridentate dinegative ligand. [24] The ligand, penta-2,4-dionebenzoylhydrazonate, was formed in situ in the reaction between $V(O)(acac)_2$ and benzoylhydrazine. Later work by the same group showed that it was possible to synthesize a large number of analogous complexes using a variety of diketones and aroylhydrazones to pre-form the ligand prior to reacting it with a vanadium compound. [25]

In the light of this information it is reasonable to expect that the ligands which have proved to be sufficiently strong π-donors to stabilize V(IV) may also stabilize Ru(IV). For this reason, attempts were made to synthesize ruthenium(IV) complexes with these ligands.

1.8. Electrochemical Techniques and Materials

1.8.1. Fundamentals. Voltammetry is concerned with the current-potential relationship in an electrochemical cell and, in particular, with the current-time response at a solid electrode at a controlled potential. If the potential is held, or stepped, to a potential at which charge transfer occurs between the oxidized and reduced forms of a redox couple, a faradaic current will flow. Reversible charge transfer reactions are those for which the rate of charge transfer is fast compared with the time scale of the experiment. When the rate of electron transfer is slow compared with the time scale of the experiment, the charge transfer is deemed irreversible.

In the course of this work three techniques have been used mainly: Cyclic Voltammetry (CV), Differential Pulse Voltammetry (DPV) and Osteryoung Square Wave Voltammetry (OSWV). As the theoretical basis of each of these techniques is described at great length in the literature [43-46] the discussion which follows will be confined to the application of these techniques to the study of transition metal complexes. The potential waveforms and corresponding current responses for these techniques are shown in Fig. 1.1.

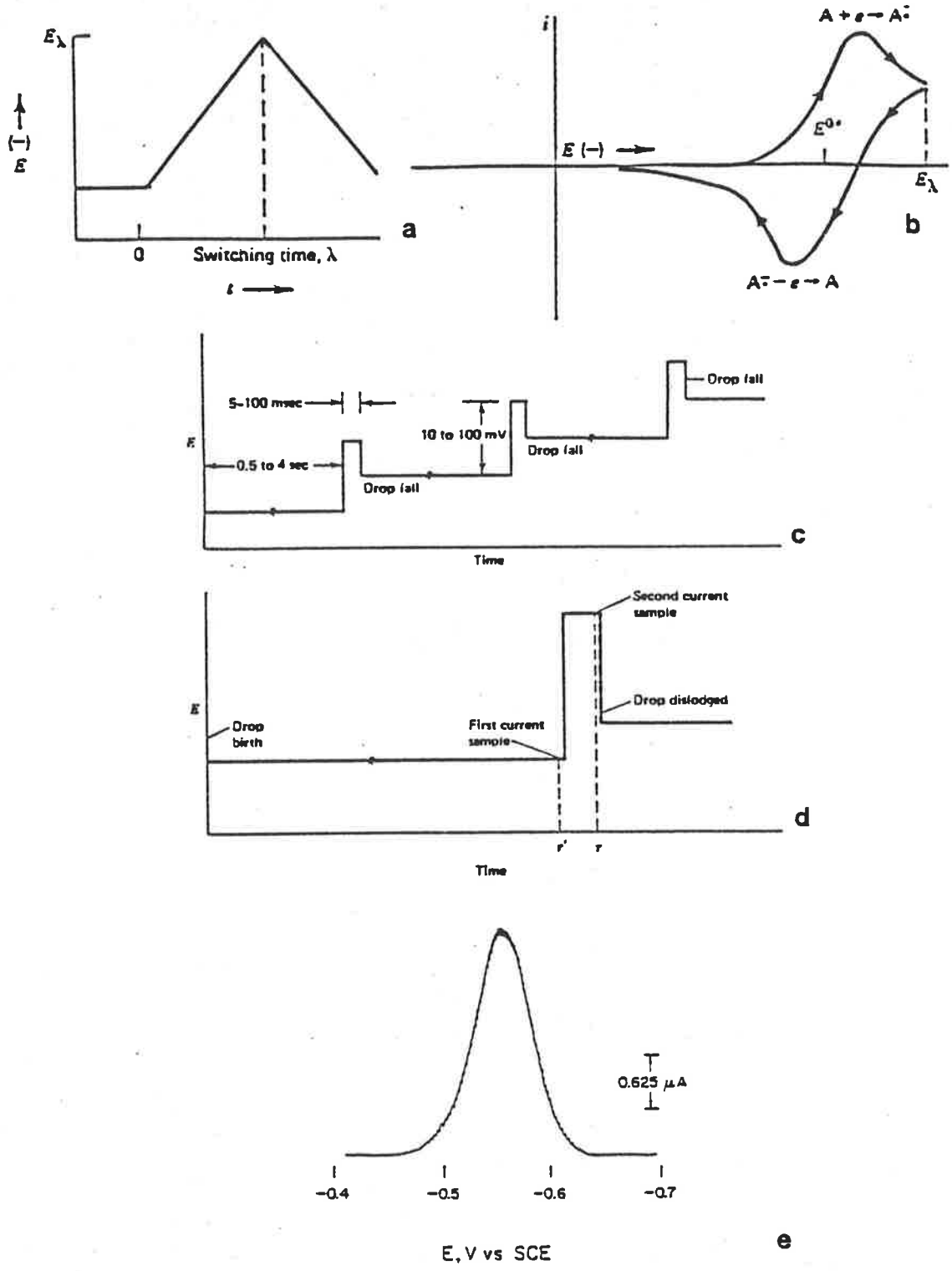

Fig. 1.1. Potential waveforms and current responses. (a) Cyclic potential sweep. (b) Typical cyclic voltammogram. (c) Potential programme for several pulse cycles in a DPV experiment. (d) Events for a single pulse cycle in a DPV experiment. (e) Typical differential pulse voltammogram.

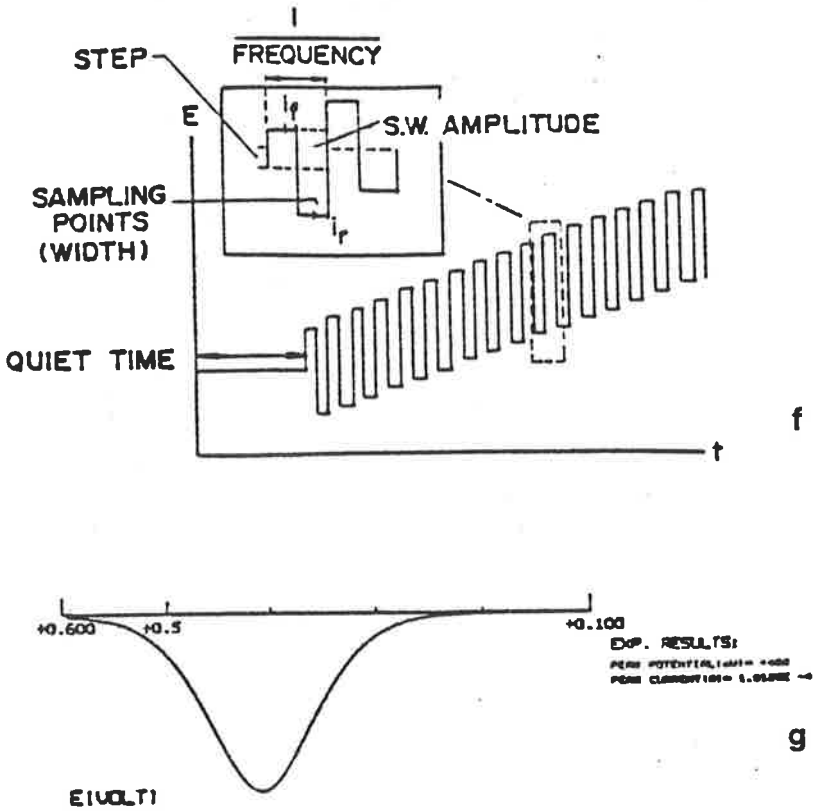

Fig. 1.1.(cont.) (f) Potential programme for Osteryoung square wave voltammetry.
(g) Typical Osteryoung square wave voltammogram.

For CV, the characteristic features of the voltammogram are the peak potentials on the cathodic and anodic scans (E_{pc} and E_{pa} respectively), the peak separation ($\Delta E_p = E_{pc} - E_{pa}$), and the $E_{1/2}$ potential ($E_{1/2} = E_{pc} + \Delta E_p/2$). At the $E_{1/2}$ potential, the concentration of the oxidized species and the reduced species at the electrode surface are equal, as given by the Nernst equation, 1.18:

For a redox reaction: $Ox + ne^- \rightleftharpoons Red$

$$E = E^o - RT/nF \ln [Red]/[Ox] \qquad (E_{1/2} \approx E^o) \qquad \textbf{(1.18)}$$

In both DPV and OSWV, the main features are the peak potential, E_p and the current at the peak potential, Δi_p. In the case of DPV, $E_p = E_{1/2} + \Delta E/2$, where ΔE is the amplitude of the potential pulse. For OSWV, the peak potential equals $E_{1/2}$. In all three modes, the current at the peak potential is proportional to the bulk concentration of the substrate.

Reversible charge transfer reactions are characterized by CV peak separations of approximately 60/n mV (where n is the number of electrons involved in the charge transfer). If ΔE_p is greater than this value, the electrochemical process is said to be quasi-reversible. For irreversible charge transfers, there is no reverse peak on reversing the potential scan and the peak potential shifts to more negative values for reductive reactions and to more positive values for oxidative reactions. In the cases of DPV and OSWV, as the reversibility of the electron transfer decreases, the peak becomes broader and, for OSWV, the peak potential is shifted at higher scan rates, as in the CV experiment.

CV experiments are best performed at scan rates greater than 20 mV sec^{-1} to avoid complications arising from diffusion effects which affect the resolution of E_p. In DPV experiments, E_p is not constant at high scan rates because the technique is, essentially, a differentiation of the CV wave and experiments must be performed at scan rates less than 20 mV sec^{-1}. Thus, electron transfer reactions which are irreversible on the CV time scale may be reversible or quasi-reversible on the DPV time scale. The advantage of OSWV and DPV is that both techniques differentiate between the charging (background) currents associated with the the CV process and the Faradaic current. The peaked current response in these two techniques is especially useful because it allows electron transfer reactions to be studied when the solubility of the substrate limits its concentration in solution, and when the electron transfer occurs at potentials close to the decomposition limits of the solvent.

1.8.2. The Effect of the Electrode Surface. The electron transfer reaction is a heterogeneous reaction, and so the rate of the reaction is dependent on the characteristics of the electrode/substrate interface. Consequently, the rate of electron transfer is highly dependent on

the state of the electrode surface. Generally, to obtain reproducible results, it is necessary for the solid electrode surface to be highly polished. In the case of glassy carbon electrodes, other pre-treatment procedures have been used in order to enhance the electron transfer, such as coating the electrode with a film which reversibly binds the substrate. [47]

Another such pre-treatment has been the application of high anodic potentials to the working electrode. This procedure has been found to increase the anodic current for oxidative electron transfers, and to improve the reversibility of the response. Anodic activation has also facilitated the observation of reactions not normally observed on platinum or untreated glassy carbon electrodes. [48-50]

Meyer's group has studied the surface of anodically activated glassy carbon using X-ray photoelectron spectroscopy. [49] Their studies revealed that the activated electrodes had a much higher surface oxygen content than the unactivated electrodes. Most of the oxygen seemed to be present in either phenol/alcohol or quinone/carbonyl groups. Confirmation of this assignment comes from another study in which glassy carbon electrodes modified by the adsorption of quinone/hydroquinone groups on the electrode surface, improved the reversibility of the oxidation of ascorbic acid. [51]

Other workers have established that similar surface groups are to be found on electrodes that have been polished to a high degree with alumina having a particle size of 0.05 μm. [52] These authors reported that the electrode was reproducibly activated towards the oxidation of a variety of substrates, and that the electrode had surface groups similar to those on the anodically activated electrodes. It was noted that the small residual amounts of alumina on the surface were unlikely to be the cause of the activation, as had been observed previously. [53]

There has been much discussion concerning the mechanism by which the anodic activation procedure enhances the electron transfer at the electrode. Engstrom [48] has proposed that the activation must involve either the oxidation of the surface to produce functionalities capable of catalysing the electrochemical reaction or the oxidative removal of impurities from the surface. It has been proposed that the activation process occur either directly by electrochemical oxidation of the electrode surface or indirectly by oxygen produced during anodization. It has also been argued that the increased oxygen content at the surface of the electrode acted by altering surface charge density or by the creation of catalytically active sites. [52]

In studying the electrochemical oxidation of $[Ru(NH_3)_5OH_2]^{3+}$ and $[Ru(bpy)_2(OH_2)]^{3+}$, Meyer has argued that the surface groups formed by the anodization procedure would be capable of mediating the coupled proton transfer. [49] It was argued that the presence of these surface

groups increases the rate of electron transfer by maintaining an equilibrium concentration of protons at the electrode surface. The existence of a strong deuterium isotope effect in the oxidation of *cis* $[Ru(bpy)_2(OH_2)]^{3+}$ by hydrogen peroxide is evidence that proton transfer is the rate limiting step in the oxidation reaction. [54]

1.8.3. Chemical Reaction After Electron Transfer. In discussing reversible CV experiments, it is assumed that the product of the charge transfer reaction will be long-lived. However, if the product of electron transfer undergoes some chemical reaction, viz:

$$\begin{aligned} Ox + ne^- &\rightleftharpoons Red \\ Red &\rightleftharpoons Z \end{aligned} \qquad \textbf{(1.19)}$$

there may be none of the species, Red, in the vicinity of the electrode when, after the scan direction has been reversed, the potential of the cell passes through the value at which electron transfer occurs. Thus, even though the electron transfer may satisfy the criteria of electrochemical reversibility, the reverse electrochemical process will not be observed. The CV will resemble that for an irreversible charge transfer. This situation is referred to as the "EC" (Electrochemical followed by Chemical reaction) mechanism of electron transfer. [44b] Fig 1.2. shows the shape of an EC CV wave.

If the product of the chemical reaction of Red is also capable of undergoing electron transfer reactions, the peak potential associated with electron transfer to or from Z may be detected if it falls within the potential limits of the CV experiment. This situation is referred to as the "ECE" (Electrochemical followed by Chemical followed by Electrochemical reaction)mechanism. [44b] Fig. 1.2 shows the shape of an ECE CV wave.

EC and ECE mechanisms are also discernible in the DPV and OSWV modes, usually giving rise to peak potentials and current maxima which are scan rate and direction dependent. If the rate of the reaction of Red is comparable to the voltammetric time scale, the relative heights of the various peaks in the voltammogram will be scan rate-dependent. There is an extensive treatment of the manner in which kinetic data may be obtained from CV experiments involving EC and ECE mechanisms in Chapter 11 of reference 44.

1.8.4. Proton-Coupled Electron Transfer. For a redox reaction in which electron transfer is accompanied by proton transfer, e.g.

$$Ox + ne^- + mH^+ \rightleftharpoons Red \qquad \textbf{(1.20)}$$

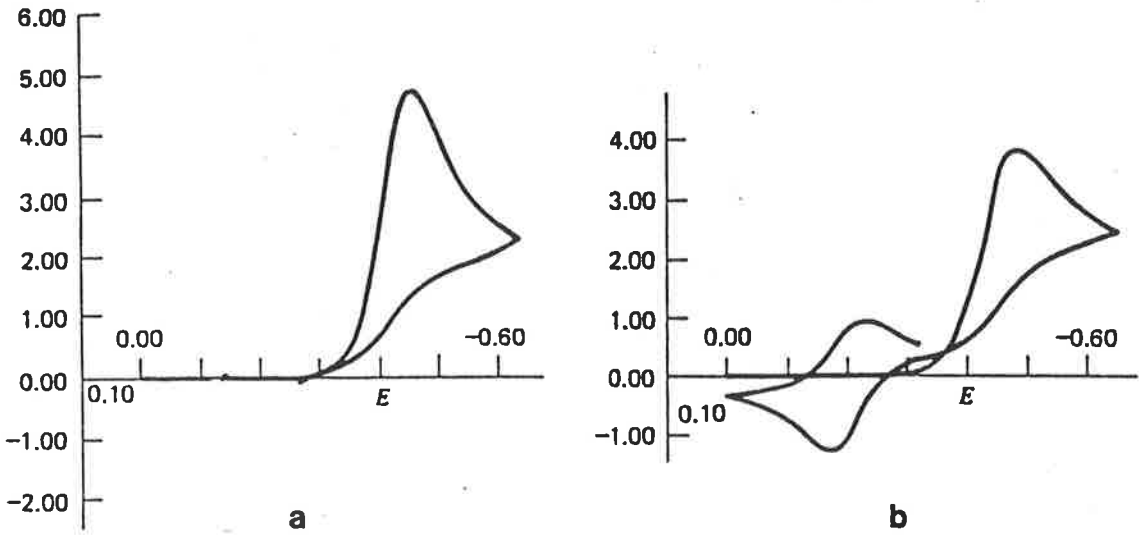

Fig. 1.2. (a) Shape of a cyclic voltammogram for an EC mechanism. (b) Shape of a cyclic voltammogram for an ECE mechanism.

rearrangement of the Nernst equation gives the relationship,

$$E = E_{1/2} - m/n \times .059\ pH. \qquad \textbf{(1.21)}$$

where E is in volts.

For a one electron reduction, the value of the constant will be 59 mV for m = 1, 118 mV for m = 2 and so on. If $E_{1/2}$ for a reaction is determined over a range of pH values, and $E_{1/2}$ plotted as a function of pH, it is possible to determine the ratio of protons to electrons in the electron transfer reaction from the slope of the graph. (Such a graph of $E_{1/2}$ vs pH is called a Pourbaix Diagram. [55]) By electrolysing a solution of the electroactive species at a large surface area electrode, it is possible to determine the charge transferred for a given amount of the substrate and so determine the number of electrons and protons involved in the charge transfer reaction.

REFERENCES

(1) "Handbook of Chemistry and Physics", 63rd Edition, CRC Press, Boca Raton, USA, 1982, p B35.

(2) E. A. Seddon, K. R. Seddon, "The Chemistry of Ruthenium", Elsevier, Amsterdam, 1984. (a) p 91. (b) p.155. (c) p 341. (d) p242. (e) p 559. (f) p 563

(3) B. A. Moyer, M. S. Thompson, T. J. Meyer, *J. Amer. Chem. Soc.*, **102**, 2310(1980)

(4) K. J. Takeuchi, M. S. Thompson, D. W. Pipes, T. J. Meyer, *Inorg. Chem.*, **23**, 1845(1984)

(5) B. A. Moyer, T. J. Meyer, *Inorg. Chem.*, **20**, 436(1981)

(6) K. J. Takeuchi, G. J. Samuels, S. W. Gersten, J. A. Gilbert, T. J. Meyer, *Inorg. Chem.*, **22**, 1407(1983)

(7) M. E. Marmion, K. J. Takeuchi, *J. Amer. Chem. Soc.*, **108**, 510(1986)

(8) A. A. Diamantis, W. R. Murphy, T. J. Meyer, *Inorg. Chem.*, **23**, 3230(1984)

(9) C. M. Che, T. W. Tang, C-K. Poon, *J. Chem. Soc., Chem. Comm.*,641(**1984**)

(10) C. M. Che, K-Y. Wong, C-K. Poon, *Inorg. Chem.*, **24**, 1797(1985)

(11) C. M. Che, K-Y. Wong, T. C. W.Mak, *J. Chem. Soc., Chem. Comm.*,546(**1985**)

(12) C. M. Che, K-Y. Wong, T. C. W.Mak, *J. Chem. Soc., Chem. Comm.*,988(**1985**)

(13) C. M. Che, K-Y. Wong, T. C. W.Mak, *J. Chem. Soc., Chem. Comm.*,986(**1985**)

(14) S. Goswami, A. R. Chakravarty, A. Chakravorty, *J. Chem. Soc., Chem. Comm.*,1288(**1982**)

(15) S. Goswami, A. R. Chakravarty, A. Chakravorty, *Inorg. Chem.*, **22**, 602(1983)

(16) S. Goswami, R. Mukherjee, A. Chakravorty, *Inorg. Chem.*, **22**, 2825(1983)

(17) R. Mukherjee, A. Chakravorty, *J. Chem. Soc., Dalton Trans.*, 955(**1983**)

(18) R. Mukherjee, A. Chakravorty, *J. Chem. Soc., Dalton Trans.*, 2197(**1983**)

(19) G. S. Patterson, R. H. Holm, *Inorg. Chem.*, **11**, 2285(1972)

(20) J. H. Tocher, J. P. Fackler, *Inorg. Chim. Acta,* **102**, 211(1985)

(21) Y. Takeuchi, A. Endo, K. Shimizu, G. P. Sato, *J. Electroanal. Chem.*, **185**, 185(1985)

(22) A. Endo, K. Shimizu, G. P. Sato, *Chem. Lett.*, 581(**1985**)

(23) G. A. Heath, K. R. Seddon, J. B. A. F. Smeulders, Unpublished results.

(24) A. A. Diamantis, M. R. Snow, J. A. Vanzo, *J. Chem. Soc., Chem. Comm.*,264(**1976**)

(25) Md. A. Salam, Ph. D. Thesis, The University of Adelaide, 1986.

(26) P. C. Ford, *Coord. Chem. Rev.*, **5**, 75(1970)

(27) C. M. Elson, J. Gulens, I. J. Itzkovitch, J. A. Page, *J. Chem. Soc., D.*, 875(**1970**)

(28) F. A. Cotton, G. Wilkinson, "Advanced Inorganic Chemistry", 3rd Edition, J. Wiley & Son, NewYork, 1972, p 710

(29) J. Chatt, G. J. Leigh, N. Thankarajan, *J. Chem. Soc.*, A., 3169(**1971**)

(30) H. Taube, *Coord. Chem. Rev.*, **26**, 75(1978)

(31) J. G. Gordon, M. J. O'Connor, R. H. Holm, *Inorg. Chim. Acta,* **5**, 381(1971)

(32) D. Pawson, W. P. Griffith, *J. Chem. Soc., Dalton Trans.*, 417(**1975**), and references therein.

(33) B. L. Haymore, *Coord. Chem. Rev.*, **31**, 123(1980)

(34) J. L. Howe, *J. Amer. Chem. Soc.*, **49**, 2381(1927)

(35) C. M. Che, K-Y. Wong, C-K. Poon, *Inorg. Chem.*, **25**, 1809(1986)

(36) G. J. Janz, R. P. T. Tompkins (Eds.), "Nonaqueous Electrolytes Handbook",Vol. 2, Academic Press, New York, 1973, p 472

(37) S. Battacharya, A. Chakravorty, F. A. Cotton, R. Mukherjee, W. Schwotzer, *Inorg. Chem.*, **23**, 1709(1984)

(38) T. Matsubara, C. Creutz, *Inorg. Chem.*, **18**, 1956(1979)

(39) A. A. Diamantis, J. V. Dubrawski, *Inorg. Chem.*, **20**, 1142(1981)

(40) A. A. Diamantis, J. V. Dubrawski, *Inorg. Chem.*, **22**, 1934(1983)

(41) M. M. Taqui-Khan, A. Hussain, G. Ramanchandraiah, M. A. Moiz, *Inorg. Chem.*, **25**, 3023(1986)

(42) M. M. Taqui-Khan, M. R. H. Siddiqui, A. Hussain, M. A. Moiz, *Inorg. Chem.*, **25**, 2765(1986)

(43) A. Weissberger, B. W. Rossiter (Eds.), "Techniques of Chemistry", Vol I, Part II, J. Wiley & Sons, Toronto, 1971.

(44) A. J. Bard, L. R. Faulkner, "Electrochemical Methods", J. Wiley & Sons, Toronto, 1980. (a) p 190. (b) p 430-480

(45) J. G. Osteryoung, R. A. Osteryoung, *Anal. Chem.*, **57**, 101A(1985)

(46) R. S. Nicholson, *Anal. Chem.*, **37**, 1351(1965)

(47) K. D. Snell, A. G. Keenan, *Chem. Soc. Rev.*, **8**, 259(1979)

(48) R. C. Engstrom, Anal. Chem., 54, 2310(1982)

(49) G. E. Cabaniss, A. A. Diamantis, W. R. Murphy, L. W. Linton, T. J. Meyer, *J. Amer. Chem. Soc.*, **107**, 1845(1985)

(50) J. C. Hoogvliet, C. M. B. van den Beld, C. J. van der Poel, W. P. van Bennekom, *J. Electroanal. Chem.*, **201**, 11(1986)

(51) H. Gomathi, G. P. Rao, *J. Electroanl. Chem.*, 190, 85(1985)

(52) G. N. Kamau, W. S. Willis, J. F. Rusling, *Anal. Chem.*, 57, 545(1985)

(53) J. Zak, T. Kuwana, *J. Amer. Chem. Soc.*, 104, 5514(1982)

(54) S. W. Gersten, J. A. Gilbert, T. J. Meyer, *J. Amer. Chem. Soc.*, 104, 6872(1982)

(55) B. Douglas, D. H. McDaniel, J. J. Alexander, "Concepts and Models of Inorganic Chemistry.", J. Wiley & Sons, New York, (1983), p495.

Chapter 2.

AMMINEAQUA RUTHENIUM COMPLEXES.

2.1. Introduction.

The pentaammine and tetraammine complexes of ruthenium have been the subjects of considerable interest since the pioneering work of Gleu, and the ammineaqua complexes are important intermediates in the synthesis of further substituted species. [1] Hydrolysis of $[Ru(NH_3)_5Cl]^{2+}$ salts yields pentaammineaquaruthenium(III), $[Ru(NH_3)_5OH_2]^{3+}$, according to reaction 2.1:

$$[Ru(NH_3)_5Cl]^{2+} + H_2O \xrightarrow{k_1} [Ru(NH_3)_5OH_2]^{3+} + Cl^- \qquad (2.1)$$

For acid hydrolysis, the rate constant, $k_1 = 3.1 \times 10^{-6}$ sec^{-1} at 35°C, and the base hydrolysis is about 10^6 times faster.[2] Base hydrolysis is the conventional method of synthesis of $[Ru(NH_3)_5OH_2]^{3+}$ salts via the hydroxo complex, $[Ru(NH_3)_5OH]^{2+}$. The same result may also be achieved using reductive catalysis, which utilizes the enhanced lability of Ru(II) complexes towards hydrolysis, according to reaction scheme 2.2:

$$[Ru(NH_3)_5Cl]^{2+} + H_2O + \text{reductant} \longrightarrow [Ru(NH_3)_5Cl]^{+}$$
$$[Ru(NH_3)_5Cl]^{+} + H_2O \rightleftharpoons [Ru(NH_3)_5OH_2]^{2+} + Cl^- \qquad (2.2)$$

k_1 for the hydrolysis step has been found to be of the order of 10^1 sec^{-1}. [3] In a solvent from which oxygen has not been excluded, the Ru(II) complexes are rapidly oxidized to the Ru(III) ion. $E_{1/2}$ for this reduction of the chloro complex is –0.24V vs SCE in acidic medium. [4]

The tetraamminediaquaruthenium complexes are less well known than the pentaammineaqua, but the *cis* and *trans* isomers of the Ru(II) and Ru(III) ions may be formed by the catalytic reduction process described above. $E_{1/2}$ = -0.14V for the couple, *cis* $[Ru(NH_3)_4(OH_2)]^{3+/2+}$. [5] This same complex may be synthesized from $[Ru(NH_3)_4C_2O_4]^{+}$ by hydrolysis in concentrated HTFMS. [6]

Reactions of the above complexes which have been studied include substitution by halide and carboxylate ions [7, 8], organonitriles [9] and pyridines [10, 11], and electron transfer reactions. [12] $[Ru(NH_3)_5OH_2]^{2+}$ was the first species from which a dinitrogen complex was synthesized by the direct reaction with nitrogen gas. [13] A dinitrogen complex was also obtained when $[Ru(NH_3)_4(OH_2)_2]^{2+}$ was reacted with nitrogen. [14]

Despite the abundance of pentaammine and tetraammine ruthenium complexes, very few triammine ruthenium complexes have been identified. $Ru(NH_3)_3Cl_3$ was synthesized by Gleu [1c] and, more recently, Bottomley was able to synthesize this complex from $[(NH_3)_5RuCl_3Ru(NH_3)_5]Cl_2$. [15] The triammine trichloride is insoluble in all common solvents, a fact which is attributed to the existence of hydrogen-bonded chains of octahedra of $Ru(NH_3)_3Cl_3$ in the solid.[15b] $Ru(NH_3)_3Cl_3$ is the logical starting point for the synthesis of triammine complexes and it is almost certain that its insolubility is the reason that so few triammine complexes are known.

2.2. Isolation of Triamminetriaquaruthenium(III)

Pentaammine solvento complexes of ruthenium [16] and cobalt [17] have been prepared by the acid hydrolysis of the appropriate chloro complex in concentrated, anhydrous triflic acid. The use of anhydrous conditions, and the distillation of HCl gas from the reaction mixture resulted in pentaamminetriflato complexes as the original products. However, in the presence Ag^+ ion, in concentrated aqueous solutions of triflic acid, $Ru(NH_3)_3Cl_3$ was readily hydrolysed to the title complex under conditions of mild heating.(Temperature between 45°C and 70°C). The preparative reaction is:

$$Ru(NH_3)_3Cl_3 + 3H_2O + 3Ag^+ \longrightarrow [Ru(NH_3)_3(OH_2)_3]^{3+} + 3AgCl \qquad (2.3)$$

The complex was isolated as its triflate salt after filtering off the solid silver chloride, concentrating the filtrate and then cooling it overnight. More than 98% of the theoretical amount of silver chloride can be separated, indicating that conversion of starting material to product is virtually complete. The overall yield of the product is 90%. Similar results were obtained when *p*-toluenesulphonic acid was used, but the overall yield was lower, due to contamination of the solid with precipitated acid.

That the reaction product was a triammine complex was confirmed by the formation of $Ru(NH_3)_3Cl_3$ on heating it in concentrated hydrochloric acid, and identified by its ir spectrum. If other non-coordinating organic acids, such as trifluoroacetic or methanesulphonic, were used in the hydrolysis reaction, no precipitate was obtained after concentrating the filtered reaction mixture. Treatment of the concentrated filtrate with concentrated hydrochloric acid did not result in the precipitation of $Ru(NH_3)_3Cl_3$. In these cases it would seem that the ammine ligands were also replaced, probably due to protonation by the acid.

2.3. Acid-Base Properties.

The pK_a of coordinated water is generally lower than that of the free molecule because of changes in its bonding. For the complex, $[Ru(NH_3)_5OH_2]^{3+}$, the pK_a value for the acid-base

equilibrium shown as reaction 2.4 has been found to be 3.9. [18]

$$[Ru(NH_3)_5OH_2]^{3+} \overset{Ka}{\rightleftharpoons} [Ru(NH_3)_5OH]^{2+} + H^+ \quad \textbf{(2.4)}$$

Having several potential acidic protons, $[Ru(NH_3)_3(OH_2)_3]^{3+}$ would be expected to be involved in more than one acid dissociation reaction. By potentiometric titration with 0.1 mol dm^{-3} sodium hydroxide solution, the pK_a values for the dissociation reactions 2.5 and 2.6 were measured.

$$[Ru(NH_3)_3(OH_2)_3]^{3+} \overset{Ka_1}{\rightleftharpoons} [Ru(NH_3)_3(OH_2)_2(OH)]^{2+} + H^+ \ (pK_{a_1} = 3.77\pm.04) \quad \textbf{(2.5)}$$

$$[Ru(NH_3)_3(OH_2)_2(OH)]^{2+} \overset{Ka_2}{\rightleftharpoons} [Ru(NH_3)_3(OH_2)(OH)_2]^{+} + H^+ (pK_{a_2} = 6.93\pm.04) \quad \textbf{(2.6)}$$

The pH of the solution rose to about 12.5 after the second inflection in the pH vs titre curve, precluding estimation of the third proton-dissociation reaction which, consequently, must be very high.

Because the properties of tetraamminediaquaruthenium(III) were also of interest, the acid-base properties of that complex were studied. By pH titration, two acid dissociations were detected, corresponding to reactions 2.7 and 2.8.

$$[Ru(NH_3)_4(OH_2)_2]^{3+} \overset{Ka_1}{\rightleftharpoons} [Ru(NH_3)_4(OH_2)(OH)]^{2+} + H^+ \ (pK_{a_1} = 3.96\pm.04) \quad \textbf{(2.7)}$$

$$[Ru(NH_3)_4(OH_2)(OH)]^{2+} \overset{Ka_2}{\rightleftharpoons} [Ru(NH_3)_4(OH)_2]^{+} + H^+ \ (pK_{a_2} = 7.09\pm.04) \quad \textbf{(2.8)}$$

These data are displayed in Table 2.1, where they are compared with the pK_a values previously determined for similar complexes. The main determinant of the pK_a is the oxidation state of the ruthenium ion. The first pK_a for the Ru(III) species is in the range 3.7 to 4.0, and those of the Ru(II) complexes are greater than 10. It should be noted that the pK_a also depends on the ionic strength of the solution in which the measurement is made. [19a]. For the pH titrations, the complexes were dissolved in 0.1 mol dm^{-3} sodium perchlorate solution in order to allow comparison between the pK_a values determined by titration and those determined in the course of the electrochemical experiments.

Compound	$\lambda_{max}(\varepsilon)^a$	pK_a	Reference
Ru(III) complexes.			
$[Ru(NH_3)_3(OH_2)_3]^{3+}$	251(1150) 340(114)	3.77	This work
$[Ru(NH_3)_3(OH_2)_2(OH)]^{2+}$	296(1600)	6.93	"
$[Ru(NH_3)_4(OH_2)_2]^{3+}$	254(1200) 337(107)	3.96	"
$[Ru(NH_3)_4(OH_2)(OH)]^{2+}$	296(2650)	7.09	"
$[Ru(NH_3)_5(OH_2)]^{3+}$	268(734)	3.9	18
$[Ru(NH_3)_5(OH)]^{2+}$	295(2100)		"
$[Ru(OH_2)_6]^{3+}$	225(2480)		21
Ru(II) complexes.			
$[Ru(NH_3)_3(OH_2)_3]^{2+}$	260sh (350) 445(60)		This work
$[Ru(NH_3)_4(OH_2)_2]^{2+}$	261(530) 435(54)		4
$[Ru(NH_3)_5(OH_2)]^{2+}$	268(640) 390sh(54)	13.1(μ = 1) 12.3(μ = 0.1)	4, 19a 19b

Table 2.1. Spectral and pK_a data for ammineaqua ruthenium complexes. (a) λ in nm, ε in M^{-1} cm^{-1}

2.4. Electronic Spectra.

The uv/vis spectrum of $[Ru(NH_3)_3(OH_2)_3]^{3+}$ was determined in aqueous solutions, and also in methanol. In aqueous solutions (Fig. 2.1) the spectrum was dependent on pH, as would be expected given the acid-base properties described above. In 0.1 mol dm^{-3} perchloric acid, an absorption maximum was observed at 251nm (ε =1150 M^{-1} cm^{-1}), and there was a shoulder to this peak at 340nm (ε = 114 M^{-1} cm^{-1}). At pH 5, the absorption maximum occurred at 296nm(ε = 1600 M^{-1} cm^{-1}). Above pH 7, the spectrum was initially almost identical with that at pH 5 (λ_{max} = 296nm, ε = 1760), but over a period of time, two additional absorptions were observed. The first was apparent as a shoulder at about 360nm, and reached its maximum intensity during the first 1.5 hours. The second peak, at 420nm, became more intense over a longer time scale (8 hours or more). It is apparent that the spectrum of $[Ru(NH_3)_3(OH_2)(OH)_2]^{+}$ is almost identical with that of $[Ru(NH_3)_3(OH_2)_2(OH)]^{2+}$. However, over time, reactions occur in solution, possibly leading to the formation of oxo-bridged multinuclear complexes as occurs with other ammineruthenium complexes in basic conditions. [20]

The spectrum of $[Ru(NH_3)_4(OH_2)_2]^{3+}$ was also determined. (Fig. 2.2) In 0.1 mol dm^{-3} perchloric acid there was an absorption maximum at 254nm (ε = 1200 M^{-1} cm^{-1}), and a shoulder to this peak at 337nm (ε = 107 M^{-1} cm^{-1}). At pH 5, the absorption maximum occured at 296nm (ε = 2650 M^{-1} cm^{-1}).

The salt, $[Ru(NH_3)_3(OH_2)_3](TFMS)_3$, is soluble in many organic solvents, including alcohols. In methanol, the spectrum of $[Ru(NH_3)_3(OH_2)_3]^{3+}$ was time-dependent, as shown in Fig. 2.3. About 5 minutes after dissolution, in addition to the peak at 250 nm, there was a small peak at about 305nm, which formed without an apparent isosbestic point. Over a 3 hour period, these peaks were replaced by another at 420nm, with a single isosbestic point at 300 nm. The peak at 420 nm eventually attained an intensity corresponding to ε = 2010. This result is indicative of the rapid formation of a comlex containing one or two methanol ligands, followed by the slow substiution of a further ligand. The final product is apparently $[Ru(NH_3)_3(MeOH_2)_3]^{3+}$, because there are no peaks in the region 250 to 260 nm, where ammine aqua complexes are expected to have absorptions.This result was significant in that it implied that ligand substitution reactions on alcoholic solutions of $[Ru(NH_3)_3(OH_2)_3]^{3+}$ would be feasible.

The highest energy peak in each spectrum described above was assigned to a LMCT transition by comparison with the spectrum of $[Ru(OH_2)_6]^{3+}$, where the band at 225 nm has been so assigned. [21] This assignment is supported by the observation that when one of the aqua ligands is deprotonated, the band is shifted to lower energy. The OH^{-} ligand is a better electron donor than H_2O, so the energy of a charge transfer from an hydroxo ligand will be of lower energy

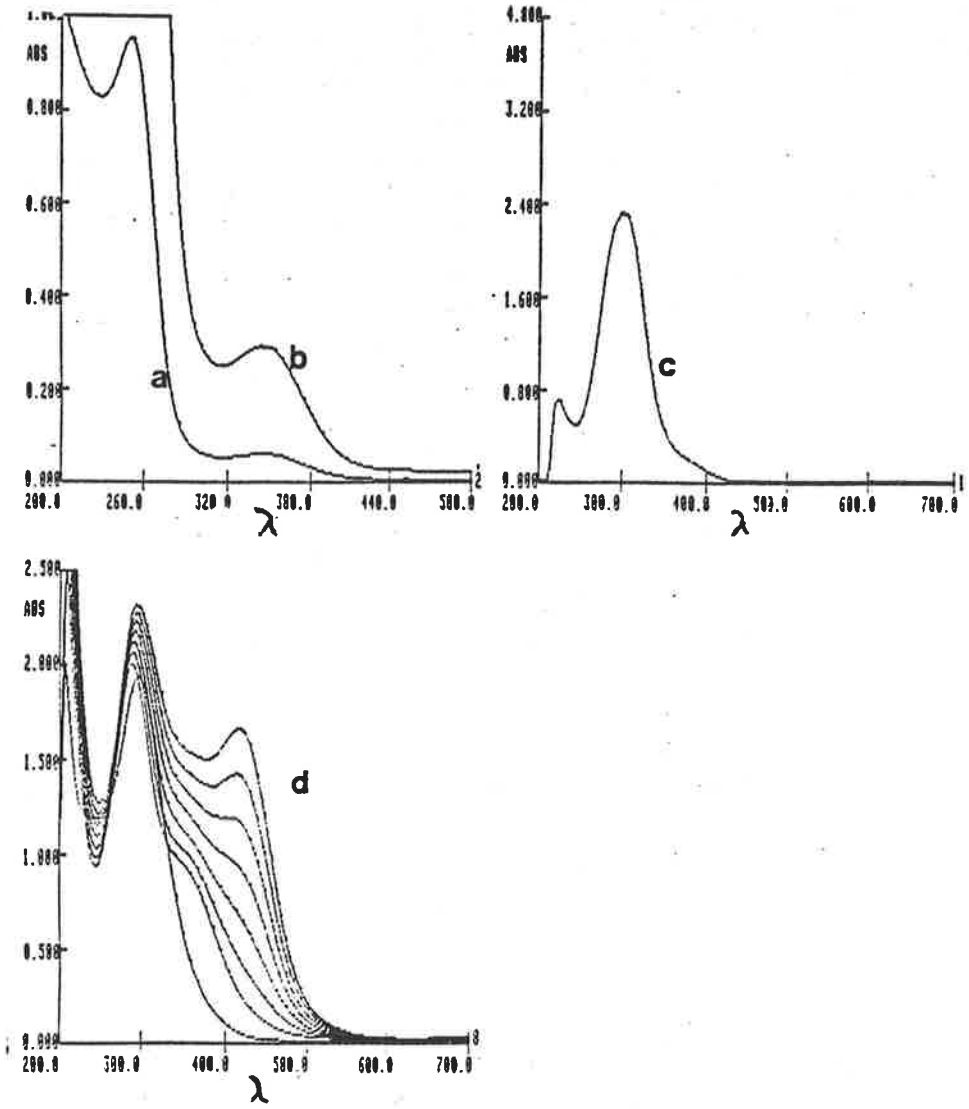

Fig. 2.1. uv/vis spectra of: (a) $[Ru(NH_3)_3(OH_2)_3]^{3+}$. $c = 4.0 \times 10^{-3}$ mol dm^{-3}, 0.2 cm cells. (b) 1.0 cm cells. (c) $[Ru(NH_3)_3(OH_2)_2(OH)]^{2+}$, 0.1 mol dm^{-3} MES buffer, $c = 1.5 \times 10^{-3}$ mol dm^{-3}, 1.0 cm cells. (d) $[Ru(NH_3)_3(OH_2)(OH)_2]^{+}$, $c = 1.1 \times 10^{-3}$ mol dm^{-3}, spectra recorded at 1 hour intervals, 1.0 cm cells.

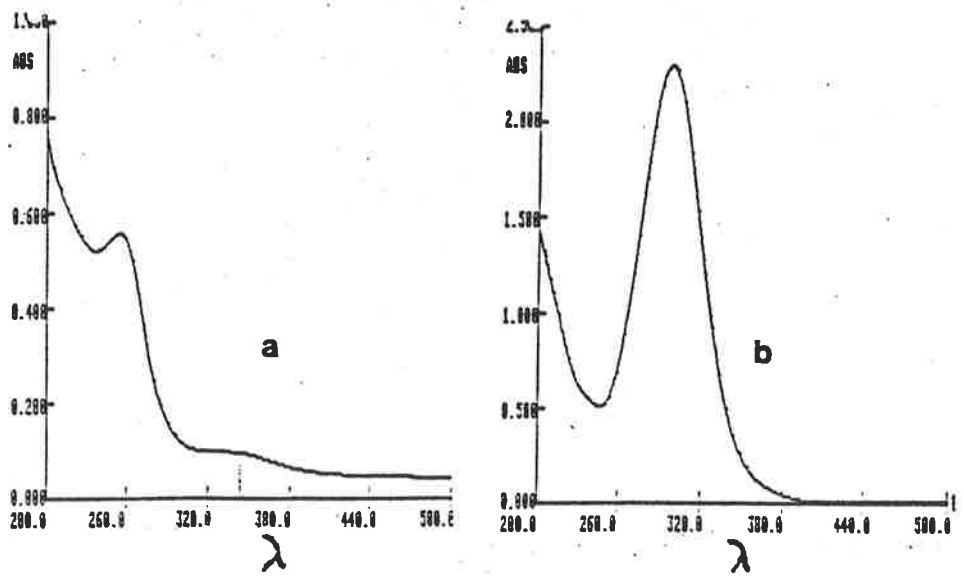

Fig. 2.2. uv/vis spectra of: (a) $[Ru(NH_3)_4(OH_2)_2]^{3+}$. c = 5.0 x 10^{-4} mol dm^{-3}, 1.0 cm cells. (c) $[Ru(NH_3)_4(OH_2)(OH)]^{2+}$, pH 6.5, c = 1.2 x 10^{-3} mol dm^{-3}, 1.0 cm cells.

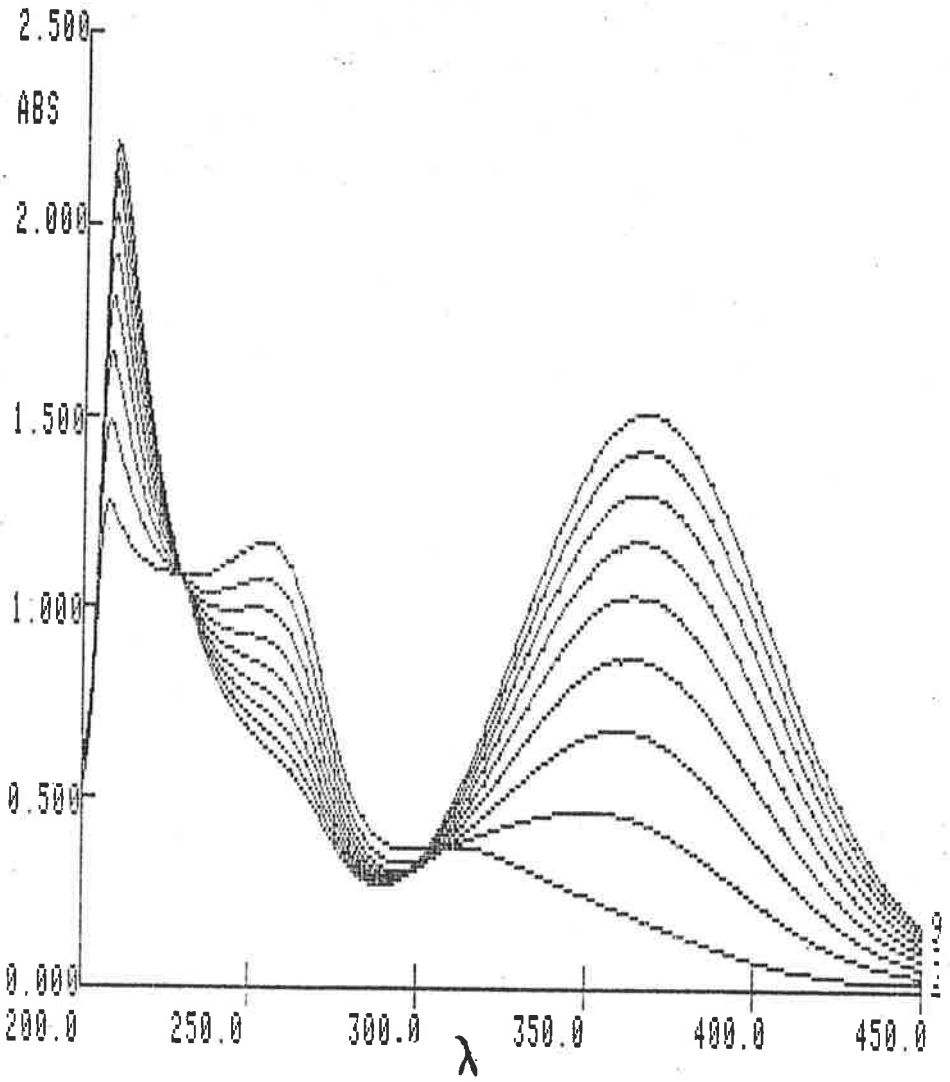

Fig. 2.3. uv/vis spectrum of $[Ru(NH_3)_3(OH_2)_3]^{3+}$ in methanol. $c = 1.0 \times 10^{-3}$ mol.dm^{-3}, 1.0 cm cells.

than one from an aqua ligand. Given their low molar absorptivities, the lower energy absorptions are probably due to d-d transistions. It can be seen from the data in Table 2.1 that, in both acid and base, the spectra of the penta-, tetra- and triammine complexes are similar, and are relatively insensitive to the distribution between ammine and aqua ligands. In the case of complexes containing at least one hydroxo ligand, the spectra are almost identical regardless of the number of ammine ligands. This probably arises because the better electron donating ability of the hydroxo ligand tends to override subtle variations in the donating abilities of the aqua and ammine ligands. Similarly, the ruthenium(II) complexes have spectra in which λ_{max} values are virtually identical, regardless of the distribution between ammine and aqua ligands, due to the smaller crystal field splitting of the Ru(II) ion compared with the Ru(III) ion. It would appear that, as is the case with pK_a values, the oxidation state of the ruthenium centre is the major determinant of the features of the spectrum.

The band assigned to a LMCT absorption in the spectrum of the complex after solvolysis in methanol is at lower energy than the bands in the hydroxo complexes. This is surprising because it would be expected that this band would be at higher energy than the comparable bands in the aqua complexes, because methanol is not as good an electron donor as water. One explanation is that the band is due to LMCT from a coordinated methoxo ion. This explanation was supported by the observation that the yellow colour of the complex in methanol (10 cm^3 left standing for 24 hours) faded significantly when three drops of methanesulphonic acid were added to the solution. In the spectrum of the resulting solution, the peak at 420 nm had disappeared, being replaced by a broad shoulder at 265 nm. This peak probably represents a combination of the absorptions at 251 nm in the original complex and the transient peak seen at 305 nm in methanol. It is possible that the slow appearance of the third absorption in the spectrum in methanol is due to the formation of a methoxo complex, perhaps with the last coordinated aqua/hydroxo ligand on the complex providing the base necessary to deprotonate the methanol.

2.5. Electrochemical Studies.

2.5.1. Tetraamminediaquaruthenium(III). At a freshly-polished glassy carbon electrode, cyclic voltammograms of aqueous solutions of $[Ru(NH_3)_4(OH_2)_2]^{3+}$ consisted of a single, quasi-reversible wave due to the Ru(III)/Ru(II) redox couple.(Fig.2.4) The $E_{1/2}$ potential of the wave was in the region -0.10v to -0.60V, and was dependent on pH. (Fig. 2.5.) e.g. in 0.1 mol dm^{-3} $HClO_4$, $E_{1/2} = -0.14$ V, in accord with previous measurements, and at pH 5, $E_{1/2} = -0.20$ V. These data, along with electrochemical data for other ammine aqua ruthenium complexes are displayed in Table 2.2. The regions of pH-dependence were as follows:

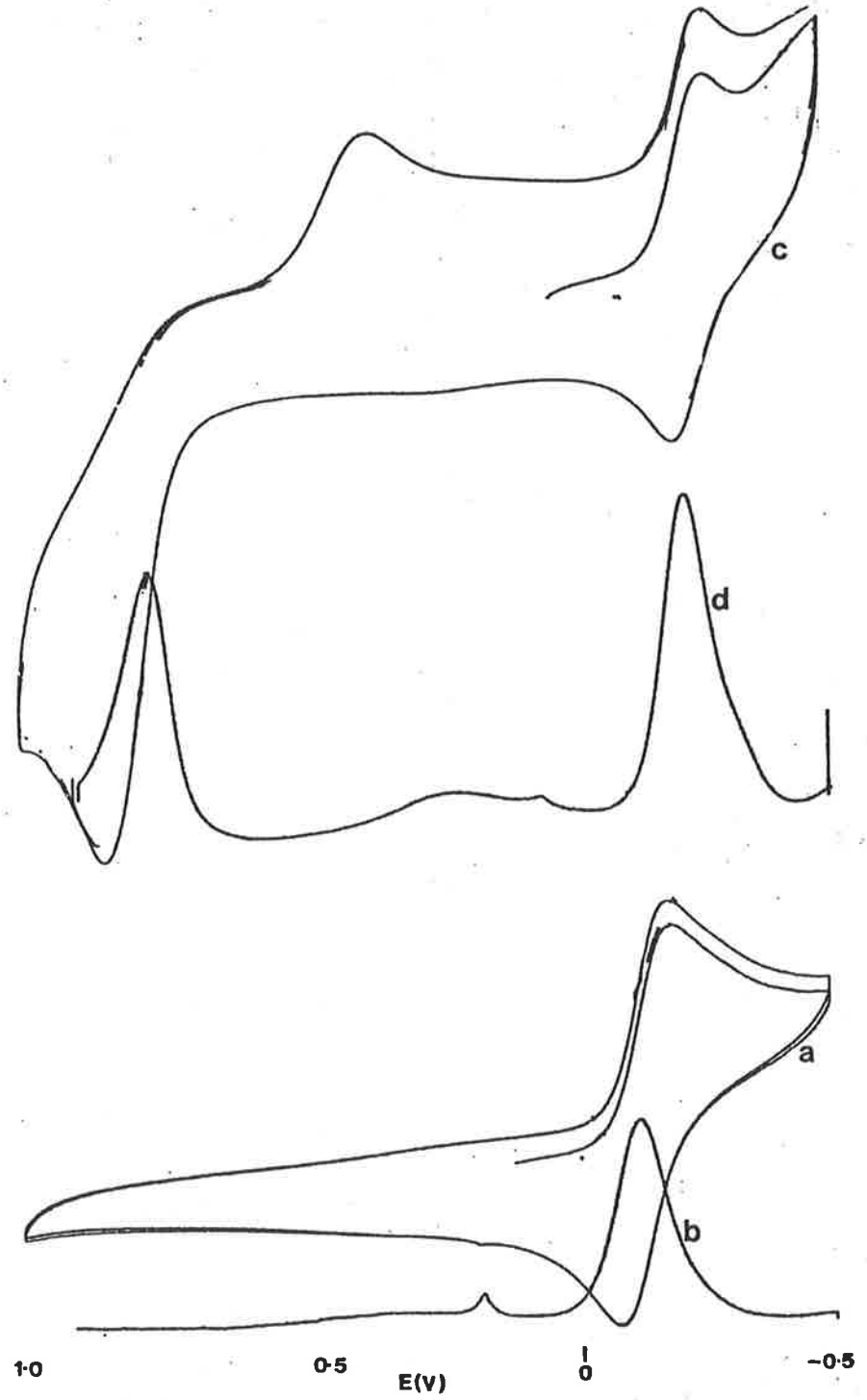

Fig. 2.4. Voltammograms of $[Ru(NH_3)_4(OH_2)_2]^{3+}$ in 0.08 mol dm^{-3} HTFMS. (a) Cyclic voltammogram at an unactivated G.C.E. (b) Differential pulse voltammogram at an unactivated G.C.E. (c) Cyclic voltammogram at an activated G.C.E. (d) Differential pulse voltammogram at an activated G.C.E.

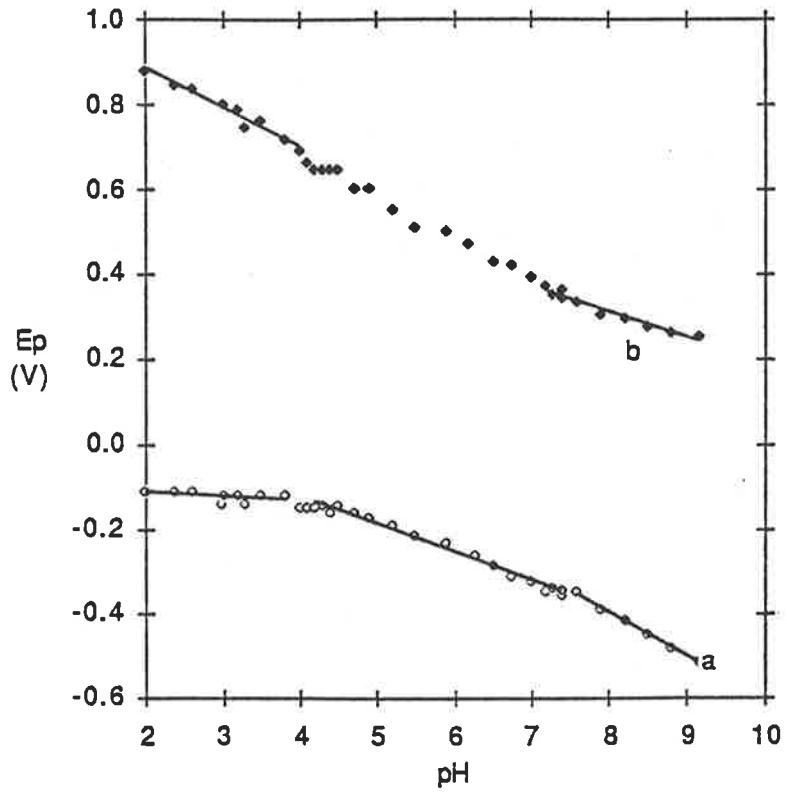

Fig. 2.5. Pourbaix diagrams for tetraamminediaquaruthenium couples. (a) Ru(III)/Ru(II) couple. (b) Ru(IV)/Ru(III) couple.

2<pH<3.8, $E_{1/2} \propto -7$ mV/pH; 4.2<pH<7.4, $E_{1/2} \propto -66$ mV/pH; 7.6<pH<9.2, $E_{1/2} \propto -107$ mV/pH. The latter two pH-dependent regions are consistent with the existence of proton-coupled electron transfer reactions involving one and two protons per electron respectively. The voltammetric wave can be assigned to the following series of redox couples:

2.0<pH<3.8

$$[Ru(NH_3)_4(OH_2)_2]^{3+} + e^- \rightleftharpoons [Ru(NH_3)_4(OH_2)_2]^{2+} \quad (2.9)$$

4.2<pH< 7.4

$$[Ru(NH_3)_4(OH_2)(OH)]^{2+} + e^- + H^+ \rightleftharpoons [Ru(NH_3)_4(OH_2)_2]^{2+} \quad (2.10)$$

7.6<pH<9.2

$$[Ru(NH_3)_4(OH)_2]^{+} + e^- + 2H^+ \rightleftharpoons [Ru(NH_3)_4(OH_2)_2]^{2+} \quad (2.11)$$

The boundaries of the pH-dependent regions are in general agreement with the pK_a values quoted above. The formation of a Ru(II) complex in the same state of protonation over the entire pH range is consistent with the expectation that the pK_a of that species would be similar to that of $[Ru(NH_3)_5OH_2]^{2+}$, which has been found previously to be 12.3 under similar conditions of ionic strength. [19b]

Couple	$E_{1/2}$(V vs SCE)	Reference
$[Ru(NH_3)_3(OH_2)_3]^{3+/2+}$	−0.10	This work
$[Ru(NH_3)_3(OH_2)_2(OH)]^{2+/+}$	−0.19[a]	"
$[Ru(NH_3)_4(OH_2)_2]^{3+/2+}$	−0.14	
$[Ru(NH_3)_4(OH_2)(OH)]^{2+/+}$	−0.20[a]	"
$[Ru(NH_3)_5(OH_2)]^{3+/2+}$	−0.16	19b
$[Ru(NH_3)_5(OH)]^{2+/+}$	−0.48[b]	18
$[Ru(NH_3)_6]^{3+/2+}$	−0.19	19b
$[Ru(OH_2)_6]^{3+/2+}$	−0.07	"

Table 2.2. Redox potentials of ammine aqua ruthenium complexes.(a) pH = 5. (b) 0.1 mol dm^{-3} NaOH.

At activated glassy carbon electrodes [22], additional waves could be observed at positive potentials. By cyclic voltammetry, these waves appeared as irreversible waves, barely discernible from the solvent oxidation wave. (Fig. 2.4) The wave observed on the anodic scan was much better resolved than that on the cathodic scan, and so the waves were attributed to oxidation of $[Ru(NH_3)_4(OH_2)_2]^{3+}$. The use of Differential Pulse Voltammetry facilitated the resolution of these waves into distinct peaks, as also shown in Fig.2.4. The potential of the peak designated as A was pH-dependent as follows:

$2<pH<4.0$, $E_{1/2} \propto -117$ mV/pH; $4<pH<7.0$, $E_{1/2} \propto -93$ mV/pH; $7.2<pH<9.2$, $E_{1/2} \propto -63$ mV/pH. At pH = 5, Ep = +0.60. These experimental data are displayed in Fig.2.5, and are consistent with the redox reactions proposed as follows:

$2<pH<4$

$$[Ru(NH_3)_4(OH_2)(O)]^{2+} + e^- + 2H^+ \rightleftharpoons [Ru(NH_3)_4(OH_2)_2]^{3+} \qquad (2.12)$$

$7.2<pH<9.2$

$$[Ru(NH_3)_4(OH)(O)]^{+} + e^- + H^+ \rightleftharpoons [Ru(NH_3)_4(OH)_2]^{+} \qquad (2.13)$$

The pH dependence below 4 is consistent with the pK_a value of the Ru(III) complex reported above, and with the behaviour of $[Ru(NH_3)_5(OH_2)]^{3+}$ at an activated electrode under similar conditions. [23] An acid-base dissociation of the Ru(IV) is also implied by these couples, and from the graph it is apparent that the pK_a is about 6.3. There is no other evidence for this acid-base dissociation, but if it did not occur the electron transfer reaction below pH 7 would be accompanied by an intramolecular rearrangement of protons and the peak potential would be independent of pH. As a consequence of this, in the region pH 4 to pH 7, there must be two different regions of pH dependence, involving one proton per electron between pH 4 and pH 6.3, and two protons per electron betwen pH 6.3 and pH 7. Because of the scatter of the experimental points (possibly due to the interaction of phosphate buffer with the complexes), it was not possible to observe these two different pH-dependent regions.

Further reaction of the oxidized species was indicated by the appearance of several DPV peaks at potentials greater than those attributed to the Ru(IV)/Ru(III) couple. When the DPV was scanned from this region of high positive potential, an additional peak was observed, at a potential slightly less positive than that for the Ru(IV)/Ru(III) couple. This peak may be due to the reduction of one of the species produced by further reaction of the Ru(IV) species.

2.5.2. Triamminetriaquaruthenium(III) At freshly-polished glassy carbon or gold electrodes, aqueous solutions of $[Ru(NH_3)_3(OH_2)_3]^{3+}$ exhibited quasi-reversible electrochemical behaviour, with a single wave evident at negative potentials. (Fig. 2.6) The $E_{1/2}$ potential was pH dependent,

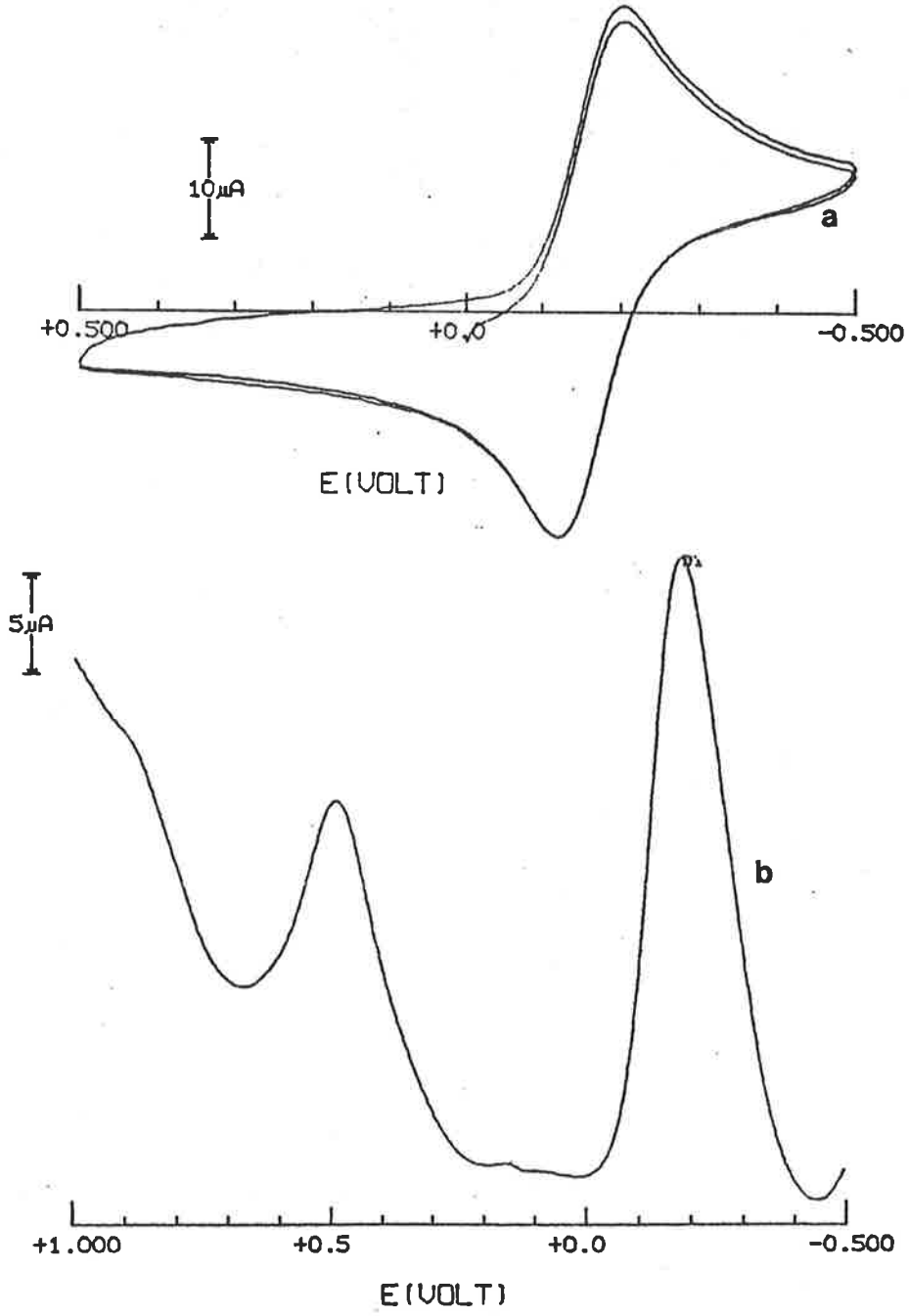

Fig. 2.6. Voltammograms of $[Ru(NH_3)_3(OH_2)_2(OH)]^{2+}$ at pH 5. (a) Cyclic voltammogram at an unactivated G.C.E. (b) Differential pulse voltammogram at an activated G.C.E.

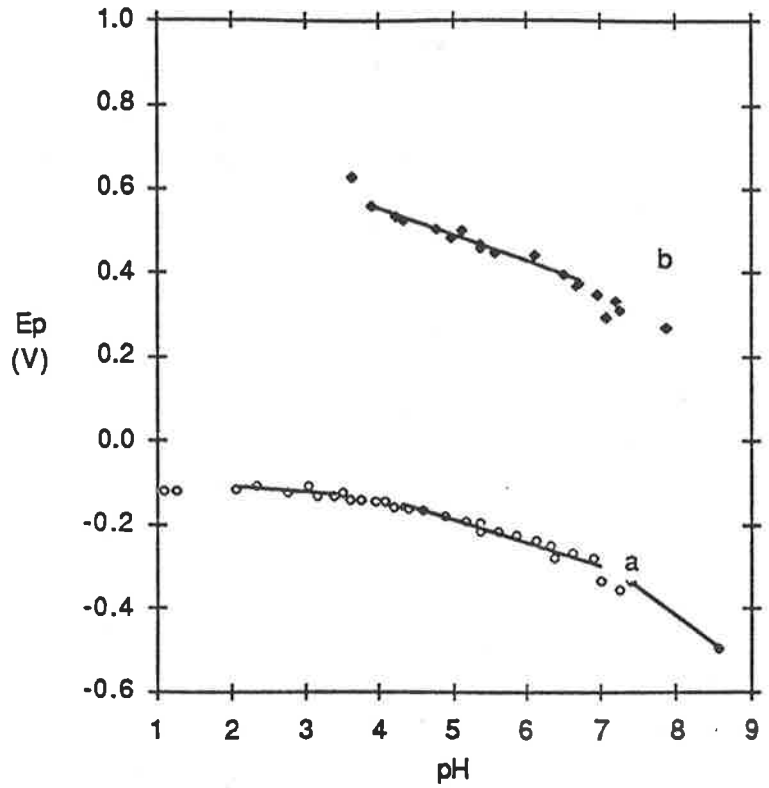

Fig. 2.7. Pourbaix diagrams for triaamminetraquaruthenium couples. (a) Ru(III)/Ru(II) couple. (b) Ru(IV)/Ru(III) couple.

as follows:

2.0<pH<3.4, $E_{1/2} \propto -4$mV/pH; 4.4<pH<7.0, $E_{1/2} \propto -57$mv/pH; 7.3<pH<8.6, $E_{1/2} \propto -118$mV/pH. The Pourbaix diagram is shown in Fig.2.7. At pH 1.5, $E_{1/2} = -0.10$ V, and at pH 5, $E_{1/2} = -0.19$ V. Similar data for other ammine aqua ruthenium complexes are displayed in Table 2.2. The latter two pH-dependecies are consistent with electron transfer coupled to the transfer of one and two protons respectively. Over the pH ranges scanned, the wave was assigned to the following couples:

2.0<pH<3.4

$$[Ru(NH_3)_3(OH_2)_3]^{3+} + e^- \rightleftharpoons [Ru(NH_3)_3(OH_2)_3]^{2+} \quad (2.14)$$

4.4<pH<7.0

$$[Ru(NH_3)_3(OH_2)_2(OH)]^{2+} + e^- + H^+ \rightleftharpoons [Ru(NH_3)_3(OH_2)_3]^{2+} \quad (2.15)$$

7.3<pH<8.6

$$[Ru(NH_3)_3(OH_2)(OH)_2]^{+} + e^- + 2H^+ \rightleftharpoons [Ru(NH_3)_3(OH_2)_3]^{2+} \quad (2.16)$$

These results are in agreement with the pK_a values reported above. Again, although the compound has not been isolated, the pK_a of $[Ru(NH_3)_3(OH_2)_3]^{2+}$ is expected to be about 12, similar to that of $[Ru(NH_3)_5OH_2]^{2+}$.

When the electrochemical experiment was conducted using an activated glassy carbon electrode, an additional wave was observed at positive potentials. The CV peaks for this wave were poorly resolved, indicating the presence of an irreversible electron transfer process, but on an anodic DPV scan, the peak could be seen quite readily, as shown in Fig. 2.6. At pH 5, the potential at which this peak occurred was +0.49 V, and over the range 3.9<pH<6.7, the potential had a pH dependence of –63mV/pH. Outside of this pH range, the peak was not sufficiently well-resolved to allow analysis of its pH dependence. At low pH values, the peak merged with that of the solvent decomposition, and at high pH values chemical reactions occurred in the solution which gave rise to extra peaks at potentials more negative than that due to the Ru(III)/Ru(II) couple. These reactions were possibly related to the reactions which were observed at high pH in the spectrophotometric studies. The DPV peak was assigned to the following redox reaction:

3.9<pH<6.7

$$[Ru(NH_3)_3(OH_2)(O)]^{2+} + e^- + H^+ \rightleftharpoons [Ru(NH_3)_3(OH_2)_2(OH)]^{2+} \quad (2.17)$$

A cathodic DPV scan over the potential range of interest revealed the presence of a small peak at approximately +0.30V, which corresponded to a CV wave at this potential which became more pronounced with repeated scanning. This additional wave probably arose from the accumulation of

the products of reaction of the initial oxidation product.

2.5.3. Discussion. Electrochemical studies of $[Ru(NH_3)_3(OH_2)_3]^{3+}$ and *cis* $[Ru(NH_3)_4(OH_2)_2]^{3+}$ revealed Ru(III)/Ru(II) couples which are pH dependent, consistent with the measured pK_a values of the compounds, andsimilar to those in the penta- and *trans* tetraammine analogues. The general trend in $E_{1/2}$ values with the decreasing number of ammine ligands (shown in Table 2.2.) is believed to reflect the greater ligand field strength of ammonia compared with water. In the absence of π-interactions, electron transfer becomes less favourable when there are more ammine ligands present, because more CFSE is lost on reduction. [19b] Electrochemistry affords a better appreciation of the differences in ligand field strength than uv/vis spectroscopy, where the variations in absorption maxima are minimal, as noted in Section 2.4.

The ability of $[Ru(NH_3)_3(OH_2)_3]^{3+}$ and *cis* $[Ru(NH_3)_4(OH_2)_2]^{3+}$ to undergo electrochemical oxidation via proton-coupled electron transfer is analogous to the pentaammineaqua case, which was described recently. [23] In these three cases, the proposal that the Ru(IV) species contains the $Ru{=}O^{2+}$ group is supported by the pH-dependence of the peak potential. In other systems, such as aquapolypyridyl complexes [24] and aqua complexes containing macrocyclic tertiary ammine ligands [25], there is further evidence for the existence of the $Ru{=}O^{2+}$ group in mononuclear complexes, because the complexes have been isolated and their spectra and crystal structures determined.

The evidence for the existence of mononuclear $Ru{=}O^{2+}$ complexes is based on the assumption that a pH dependence of –59 mV/pH is due to the transfer of one electron coupled with the transfer of one proton. However, there is the possibility that the electron transfers could involve two protons and only half an electron per ruthenium ion. This was reported to be the case when Ru(Hedta)(OH_2) was oxidized to yield an oxo-bridged dimer. [26] It was not possible to perform coulometric experiments to confirm that the electron transfers observed voltammetrically involved one electron per ruthenium ion, but the observation that the voltammetric peak heights were approximately the same for the $[Ru(NH_3)_5(OH_2)]^{3+}/[Ru(NH_3)_5(OH_2)]^{2+}$ and the $[Ru(NH_3)_5(O)]^{2+}/[Ru(NH_3)_5(OH_2)]^{3+}$ implies that this is so [23], and this proposal also provides the simplest explanation for the electrochemical results.

A notable difference between the results obtained for the triammine complex and those for other complexes referred to above is the irreversible nature of the oxidation of the triammine complex. This irreversibility may be indicative that the oxidation of the complex at the electrode is kinetically slow. Such an effect was also reported for the electrochemical oxidation of the complexes $[Ru(bpy)_2(OH_2)_2]^{3+}$, $[Ru(trpy)(bpy)(OH_2)]^{3+}$ and $[Ru(bpy)_2(py)(OH_2)]^{3+}$ at unactivated electrodes. [24, 27] In the case of the first of these complexes, activation of the electrode proved

to be kinetically favourable and the reversibility of the electrode reaction was improved. [22] The mechanisms by which the activation process is believed to enhance the electrode process were discussed in Chapter 1. However, in the present case, the reversibility of the electrode process is very poor, even when an activated electrode is used. Hence, it would appear that the oxidation of $[Ru(NH_3)_3(OH_2)_3]^{3+}$ and *cis* $[Ru(NH_3)_4(OH_2)_2]^{3+}$ at the glassy carbon electrode is extremely slow, indeed.

Another possible cause of the irreversibility is the decomposition of the oxidized species. There is evidence in the DPV experiments on both the tetraammine and triammine complexes that there is some reaction of the Ru(IV) complex. Poon and co-workers have suggested that the redox chemistry of amineruthenium complexes is usually complicated by the oxidative dehydrogenation of coordinated primary and secondary amines. [28] Other workers have proposed that the dehydrogenation is associated with imine formation involving internal electron transfer between the ligands and Ru(IV). It was found that the oxidation of 2(aminomethyl)pyridine coordinated to $Ru(bpy)_2^{4+}$ (which is a step in the oxidation of 2(aminomethyl)pyridine in $[Ru(bpy)_2(ampy)]^{4+}$) has a relatively large rate constant for the proton/electron transfer reaction, with k of the order of 10^2 at 20^0C. [29] It would seem likely that this reaction could also occur when ammonia is coordinated and, so, any $[Ru(NH_3)_3(OH_2)_2(O)]^{2+}$ formed in solution by chemical or electrochemical means would decompose rapidly. It is interesting to note, however, that other workers have been able to isolate the Ru(VI) complex, *trans* $[Ru(NH_3)_4(O)_2]^{2+}$, from a reaction involving RuO_4, without the complicating effects of the dehydrogenation reaction. [30] Furthermore, in an initial report, it has been noted that $[Ru(NH_3)_5(OH_2)]^{3+}$ and $[Ru(NH_3)_5Cl]^{2+}$ show two reversible oxidations at a coated graphite electrode and can be oxidized by Ce^{4+} to give a Ru(V) complex which is a catalyst for the oxidation of water to oxygen. [31]

Attempts were made to achieve the chemical oxidation of $[Ru(NH_3)_3(OH_2)_3]^{3+}$. To this end, a buffered solution of $[Ru(NH_3)_3(OH_2)_3]^{3+}$ was treated with a stoichiometric amount of hydrogen peroxide at 50^oC. After about fifteen minutes, the reaction mixture had a dark brown colour. A CV of the reaction mixture did not contain any electrochemical waves which could be attributed to a redox couple associated with $[Ru(NH_3)_3(OH_2)_3]^{3+}$. Treatment of the reaction mixture with concentrated hydrochloric acid solution did not yield $Ru(NH_3)Cl_3$, which would have been the expected product if the triammine portion of the original complex was still intact. Similar dark solutions were obtained when both *cis* and *trans* $[Ru(NH_3)_4(OH_2)_2]^{3+}$ were treated with a solution of hydrogen peroxide. [32]

The potentials at which oxidations involving the $RuO^{2+}/RuOH_2^{3+}$ couples occur for the ammine complexes are slightly negative of those at which the polypyridine complexes are oxidized.

[27, 32] However, the difference in the potential of the $RuO^{2+}/RuOH_2^{3+}$ couple and the Ru^{3+}/Ru^{2+} couple is much greater in the case of the ammine complexes than in the polypyridyl complexes. The factors contributing to these effects will be discussed in Chapter 3.

2.6. Redox Chemistry

As is to be expected, from its moderate reduction potential, $[Ru(NH_3)_3(OH_2)_3]^{3+}$ is readily reduced by chemical means to $[Ru(NH_3)_3(OH_2)_3]^{2+}$. Amalgamated zinc or hydrogen over platinum black are suitable reducing reagents. During the reduction, the course of the reaction can be followed by Sampled Current Polarography. The uv/vis spectrum of the golden-yellow solution (in 1 mol dm^{-3} H_2SO_4) could be determined when the reaction was shown, by SCP, to be substantially complete. The main features of the spectrum are listed in Table 2.1, as are those of the pentaammine and tetraammine analogues. The spectrum is displayed in Fig. 2.8, and it can be seen that the spectrum is very similar to the other ammineaqua complexes of ruthenium(II) which have been isolated. It was not possible to isolate the Ru(II) species, but studies could be performed on samples of the complex generated *in situ*.

When $[Ru(NH_3)_3(OH_2)_3]^{2+}$ was formed in acidic solution, in the presence of perchlorate ion, it was found that the perchlorate could be reduced to chloride. The formation of chloride was indicated by a positive $Ag^+/AgCl$ test. The redox reaction would be:

$$8[Ru(NH_3)_3(OH_2)_3]^{2+} + ClO_4^- \longrightarrow 8[Ru(NH_3)_3(OH_2)_3]^{3+} + Cl^- + 4H_2O \quad \textbf{(2.18)}$$

Previous workers have shown that $[Ru(NH_3)_5OH_2]^{2+}$ and $[Ru(OH_2)_6]^{2+}$ are also capable of reducing perchlorate, with chlorate being the initial product. [33, 34] However, in the hexaaqua system, small amounts of $[Ru(OH_2)Cl]^+$ were also found, consistent with the further reduction of lower oxidation states of chlorine. It has been proposed [35] that, in the pentaammine case, the reaction is:

$$[Ru(NH_3)_5OH_2]^{2+} + ClO_4^- \longrightarrow [Ru(NH_3)_5(O)]^{2+} + ClO_3^- + H_2O \quad \textbf{(2.19)}$$

but the Ru(IV) species was not observed due to rapid reaction with excess Ru(II) ions. i.e.

$$Ru(IV) + Ru(II) \longrightarrow 2Ru(III) \quad \textbf{(2.20)}$$

The ability of $[Ru(NH_3)_3(OH_2)_3]^{2+}$ to reduce perchlorate was first manifested during attempts at bulk electrolytic reduction of $[Ru(NH_3)_3(OH_2)_3]^{3+}$. It was found that the current did not decay exponentially, but reached a steady-state value much higher than expected of a solution in which all the oxidized form had been reduced. This is consistent with the electrocatalytic reduction of the perchlorate ion in the supporting electrolyte.

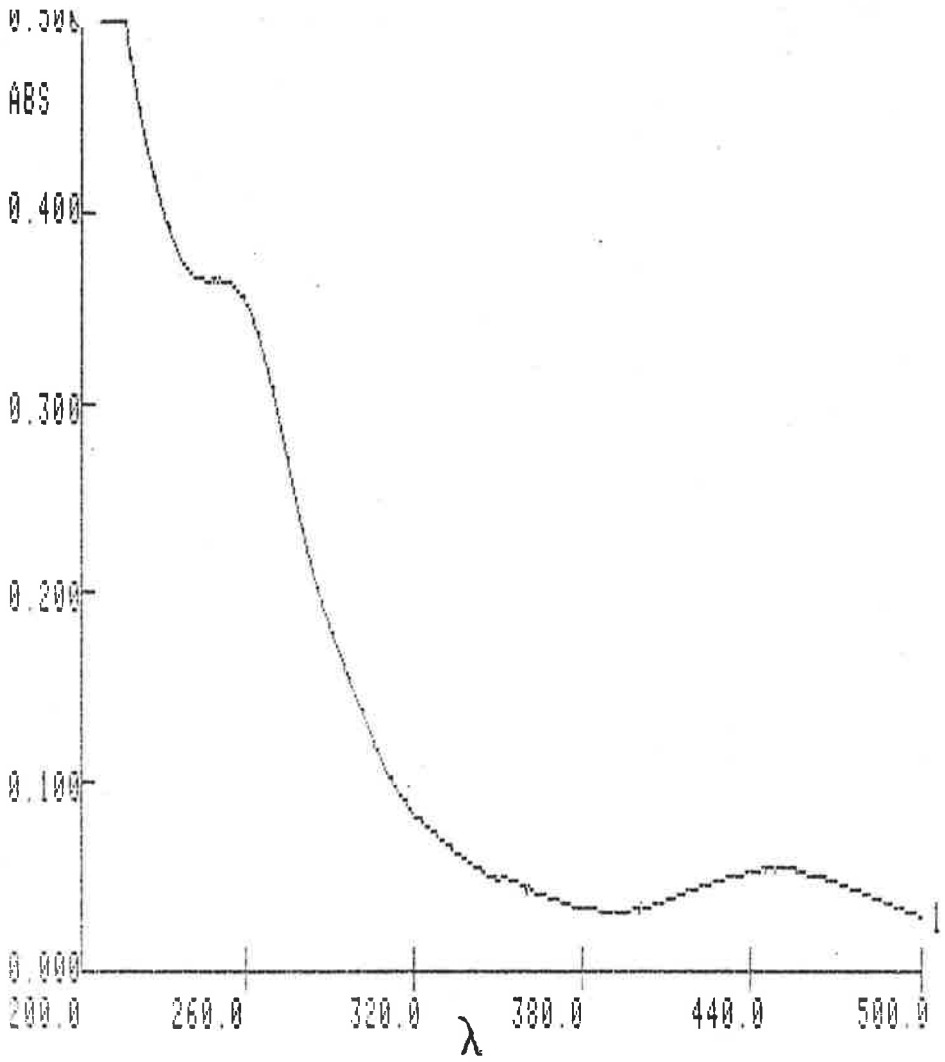

Fig. 2.8. uv/vis spectrum of: (a) $[Ru(NH_3)_3(OH_2)_3]^{2+}$. $c = 4.0 \times 10^{-3}$ mol dm^{-3}, 1.0 cm cells.

Reduction of perchlorate by the Ru(II) complex was relatively slow on the CV time-scale. This is consistent with the small rate constants found for the reactions involving $[Ru(NH_3)_5OH_2]^{2+}$ and $[Ru(OH_2)_6]^{2+}$. [33 , 34] Though the peak separation of the Ru(III)/Ru(II) wave in the CV was large, this was not due to the use of sodium perchlorate as a supporting electrolyte . The peak separation value obtained in the presence of sodium methanesulphonate was almost identical with that in the presence of perchlorate, implying that the large peak separation is due to slow electron transfer kinetics.

When the chemical reduction of $[Ru(NH_3)_3(OH_2)_3]^{3+}$ was performed at pH >7, formation of an intense blue colour in the solution was observed. This blue colour was reminiscent of those observed in the mixed oxidation state chloroammine complexes of ruthenium [15a], sugesting that the blue complex was a mixed oxidation state complex,with the ruthenium centres bridged by hydroxide ions (conveniently referred to as {RuII/RuIII}). It is proposed that the reaction involves the reaction of the Ru(II) complex formed by reduction with the unreacted Ru(III) complex. i.e.

$$[Ru(NH_3)_3(OH_2)_3]^{2+} + [Ru(NH_3)_3(OH_2)(OH)_2]^{+} \longrightarrow \{RuII/RuIII\} \qquad \textbf{(2.21)}$$

In agreement with this, a blue colour was observed in the solution which resulted from the addition of a mildly acidic aqueous solution of $[Ru(NH_3)_3(OH_2)_3]^{2+}$ (formed by H_2/Pt black reduction) to an equivalent aliquot of $[Ru(NH_3)_3(OH_2)(OH)_2]^{+}$ in degassed solution at pH 8. The blue colour was evident after the mixture was stirred under argon for about 15 minutes. The spectrum of this solution was very similar to that obtained from the blue solutions generated by reduction of $[Ru(NH_3)_3(OH_2)(OH)_2]^{3+}$ in basic solution.

Attempts were made to determine the uv/vis spectrum of {RuII/RuIII}, but interpretation of the spectra obtained proved difficult. The spectrum of a sample of {RuII/RuIII} is shown in Fig. 2.9. The difficulty in interpretation arises because the true nature of the peaks at shorter wavelengths is not certain. The peak at 590 nm is a feature unique to the blue solutions, but those between 200 nm and 300 nm may be due to either unreacted $[Ru(NH_3)_3(OH_2)(OH)_2]^{+}$, $[Ru(NH_3)_3(OH_2)_3]^{2+}$, or to high energy transitions in {RuII/RuIII}. However, assuming the peaks at 295 nm and 365 nm are due to unreacted Ru(III), an estimate of ε at 590 nm was made, and found to be betwen 8×10^3 and 11×10^3. This is approximately twice the value observed for ε_{580} in $Ru_2Cl_3(NH_3)_6^{2+}$. [34] The spectrum of this latter compound consists of the high-intensity band at 580 nm and two lower intensity bands in the region 250 nm to 350 nm (Fig.2.9). If similar short wavelength bands are present in the spectrum of {RuII/RuIII}, they cannot be differentiated from bands of either $[Ru(NH_3)_3(OH_2)(OH)_2]^{+}$ or $[Ru(NH_3)_3(OH_2)_3]^{2+}$.

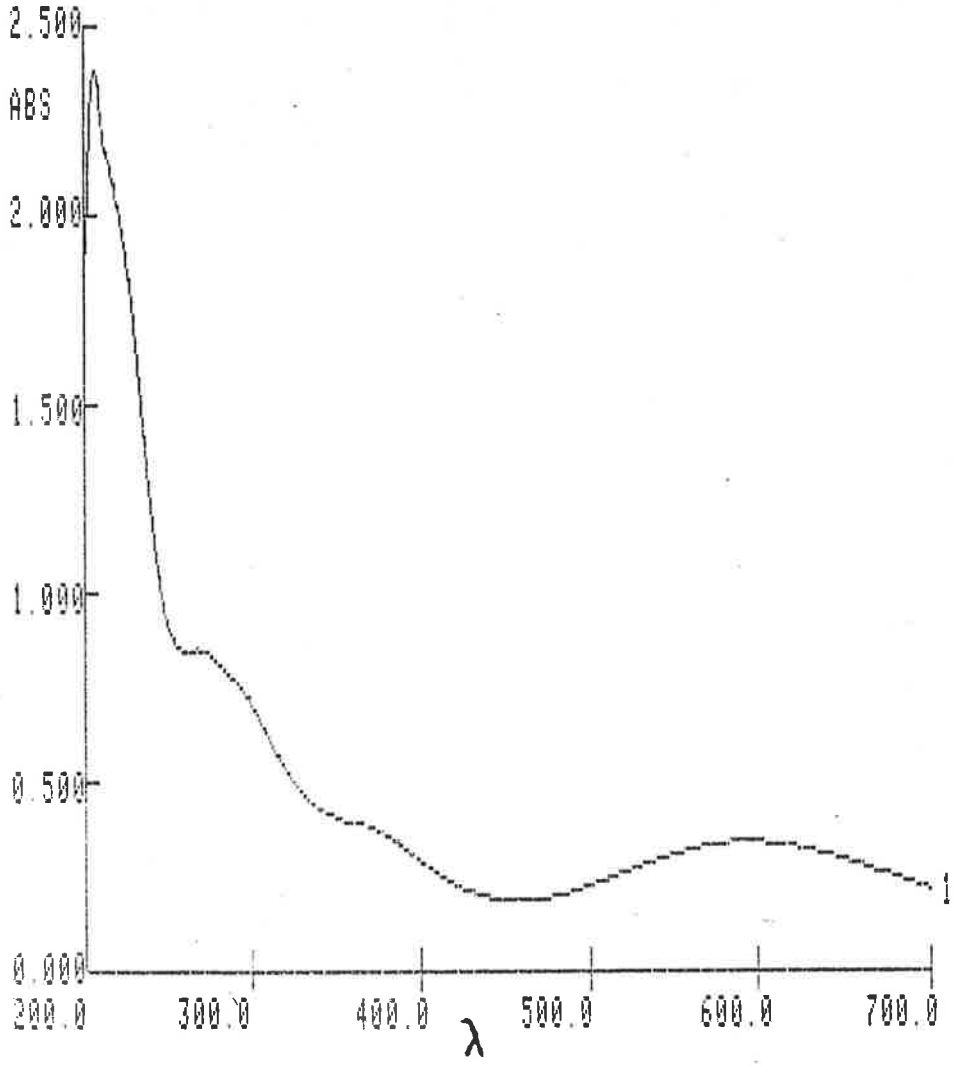

Fig. 2.9. uv/vis spectrum of the blue mixed-oxidation state species.

When the blue solutions were exposed to oxygen or acidified, the blue colour faded to a pale yellow. Because no blue colour was observed if the reaction was performed at pH <7, it is apparent that at least two hydroxyl groups must be present on the Ru(III) ion in order for the bridged species to form.

The blue solutions showed identical cyclic voltammograms, regardless of the method by which the solutions were made. Two waves are visible in the voltammogram (Fig 2.10), one reversible and one irreversible. The reversible wave, A ($E_{1/2}$ = –0.50 V), is consistent with the presence of either or both of $[Ru^{III}(NH_3)_3(OH_2)(OH)_2]^+$ or $[Ru^{II}(NH_3)_3(OH_2)_3]^{2+}$ in the solution, as the $E_{1/2}$ potential is the same as that of the III/II couple for these compounds at pH 8. By commencing the cathodic scan at potentials at which the first of those two compounds is stable, {RuII/RuIII} is oxidized. The irreversible wave, B, (E_{pa} = –0.22 V) was assigned to the oxidation of {RuII/RuIII}. The EC shape of this wave is indicative that the oxidized form decomposes quite rapidly to the mononuclear Ru(III) complex. As the cyclic experiment was continued, more of this complex formed in solution, giving rise to a higher peak current at –0.59 V. The cyclic voltammogram was determined at scan rates of up to 2 V sec^{-1}, but the cathodic peak associated with peak B could not be observed. It was thus concluded that the decomposition of di-Ru(III) complex occurred very rapidly compared with the electron transfer reaction, according to reaction 2.22, with k_1 being large.

$$\{RuII/RuIII\} + e^- \rightleftharpoons \{RuIII/RuIII\} \xrightarrow{k_1} 2Ru(III) \qquad (2.22)$$

As a comparison, voltammograms of $Ru_2Cl_3(NH_3)_6^{2+}$ contained a reversible oxidation wave at +0.32 V. [36] This is considerably more positive than the potential at which {RuII/RuIII} is oxidized, confirming the observation that {RuII/RuIII} was less stable to oxidation than $Ru_2Cl_3(NH_3)_6^{2+}$.

If the reduction of $[Ru(NH_3)_3(OH_2)(OH)_2]^+$ at high pH was allowed to continue, the blue colour slowly faded, and $[Ru(NH_3)_3(OH_2)_3]^{2+}$ was formed almost quantitatively. Thus, it is apparent that the blue species, {RuII/RuIII}, is only a transisent in the reduction of $[Ru(NH_3)_3(OH_2)(OH)_2]^+$. For this reason, {RuII/RuIII} could not be isolated and its spectrum could only be determined semi-quantitatively.

2.7. Electrochemistry in Organic Solvents.

Solutions of $[Ru(NH_3)_3(OH_2)_3]^{3+}$ in organic solvents acquired intense colours upon standing. Such colour changes were indicative of replacement of the aqua ligands by solvent molecules. Except for methanol, the solvents generally had high ultraviolet cut-off wavelengths, so that uv/vis spectroscopy was not the appropriate method by whch to study the solvolysis reactions. Consequently, the CV of $[Ru(NH_3)_3(OH_2)_3]^{3+}$ was studied in the solvents methanol, acetone,

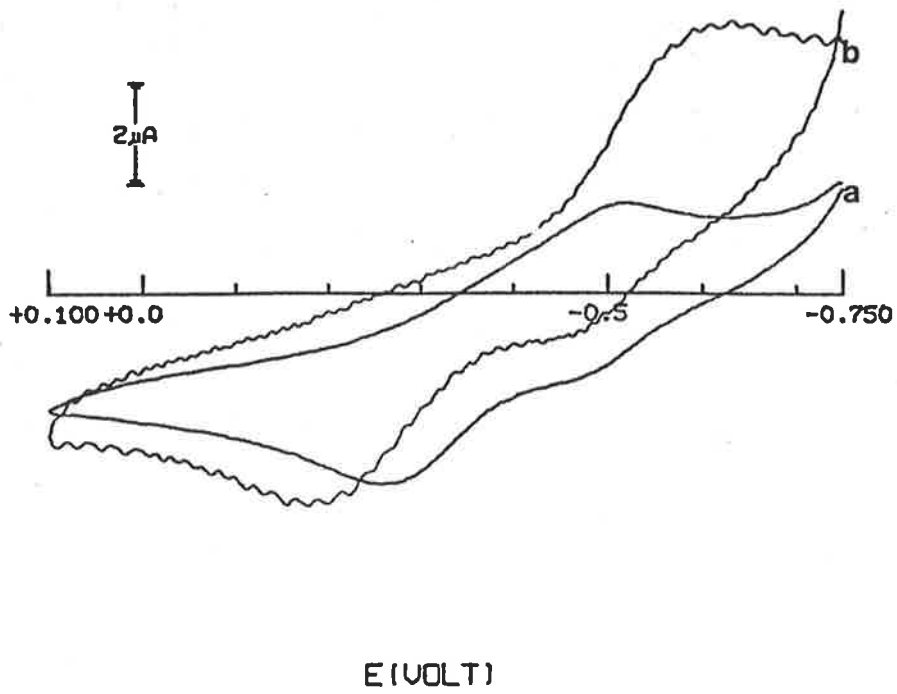

Fig. 2.10. Cyclic voltammograms of the blue mixed-oxidation state species. (a) scan rate = 100 mV sec^{-1}. (b) scan rate = 2000 mV sec^{-1}.

acetonitrile and dimethylsulphoxide. The voltammograms obtained are displayed in Fig. 2.11 and the main features of the voltammograms are listed in Table 2.3.

2.8.1. Methanol. The CV of $[Ru(NH_3)_3(OH_2)_3]^{3+}$ in methanol consisted of one reversible wave and one irreversible wave. (Fig 2.11a) The $E_{1/2}$ potentials for these peaks were estimated, from DPV, to be –0.18 V and –0.33 V. The reversible wave is consistent with the presence of $[Ru(NH_3)_3(OH_2)_3]^{3+}$ or $[Ru(NH_3)_3(OH_2)_2(OH)]^{2+}$. The irreversible wave had the characteristic shape of an EC mechanism of electron transfer followed by chemical reaction. This is consistent with the presence of a complex, $[Ru(NH_3)_3(OH_2)_{(3-n)}(MeOH)_n]^{3+}$, prior to electron transfer,

Couple	$E_{1/2}$(V vs SCE)	Reference
$[Ru(NH_3)_3(MeOH)_n(OH_2)_{3-n}]^{3+/2+}$	–0.33[a]	This work
$[Ru(NH_3)_3(MeCN)(OH_2)_2]^{3+/2+}$	+0.24	"
$[Ru(NH_3)_3(MeCN)_2(OH_2)]^{3+/2+}$	+0.60	"
$[Ru(NH_3)_3(MeCN)_3]^{3+/2+}$	+0.95	"
$[Ru(NH_3)_5(MeCN)]^{3+/2+}$	+0.19	4
$[Ru(NH_3)_3(DMSO)(OH_2)_2]^{3+/2+}$	+0.43	This work
$[Ru(NH_3)_5(DMSO)]^{3+/2+}$	+0.76	19a
$[Ru(NH_3)_3(\sigma\ acetone)_n(OH_2)_{3-n}]^{3+/2+}$	+0.04[a]	This work
$[Ru(NH_3)_3(\pi\ acetone)_n(OH_2)_{3-n}]^{3+/2+}$	+0.40, +0.57[b]	"
$[Ru(NH_3)_5(\pi\ acetone)]^{3+/2+}$	+0.75[b]	41

Table 2.3. Redox potentials of solvolyzed ammine aqua ruthenium complexes. (a) cathodic peak only. (b) anodic peak only.

followed by rapid hydrolysis of the analogous Ru(II) species. This proposal is consistent with the uv/vis spectrum after a short time, where it was observed that some degree of solvolysis occurred quite rapidly. No attempt was made to measure the voltammogram of solutions after a long time. That hydrolysis of $[Ru(NH_3)_3(OH_2)_{(3-n)}(MeOH)_n]^{2+}$ occurs in very low concentrations of water, as indicated by the EC shape of the wave, suggests that the methanol ligand is much better suited to the stabilization of the higher oxidation state than the lower.

2.8.2. Acetonitrile. The CV of $[Ru(NH_3)_3(OH_2)_3]^{3+}$ in acetonitrile consisted of several reversible waves with $E_{1/2}$ values of +0.24 V, +0.60 V and +0.95 V, in addition to a cathodic peak at –0.15 V. (Fig 2.11b) The shape of this cathodic peak is also characteristic of an EC mechanism, and the potential at which it occurs is indicative of the reduction of $[Ru(NH_3)_3(OH_2)_3]^{3+}$. Operation of the EC mechanism is evidence of fairly rapid solvolysis of the Ru(II) species. It is proposed that the

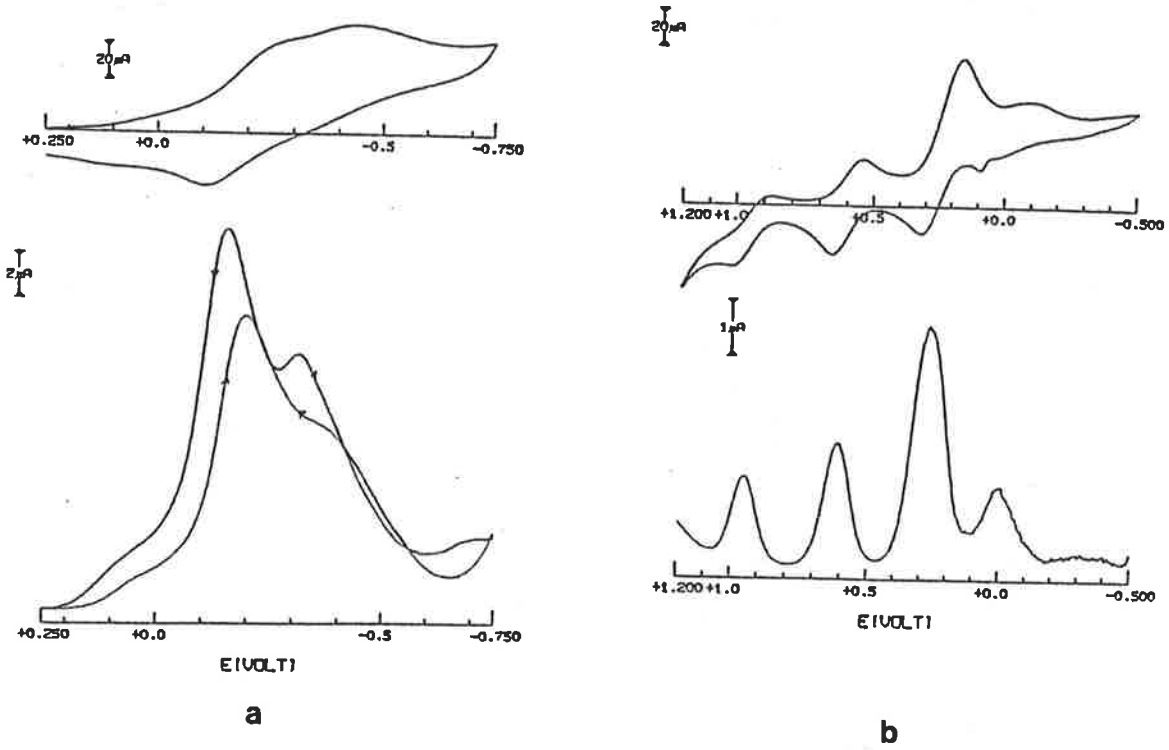

Fig. 2.11. Voltammograms of $[Ru(NH_3)_3(OH_2)_3]^{3+}$ in organic solvents. (a) Cyclic voltammogram and differential pulse voltammogram in methanol. (b) Cyclic voltammogram and differential pulse voltammogram in acetonitrile.

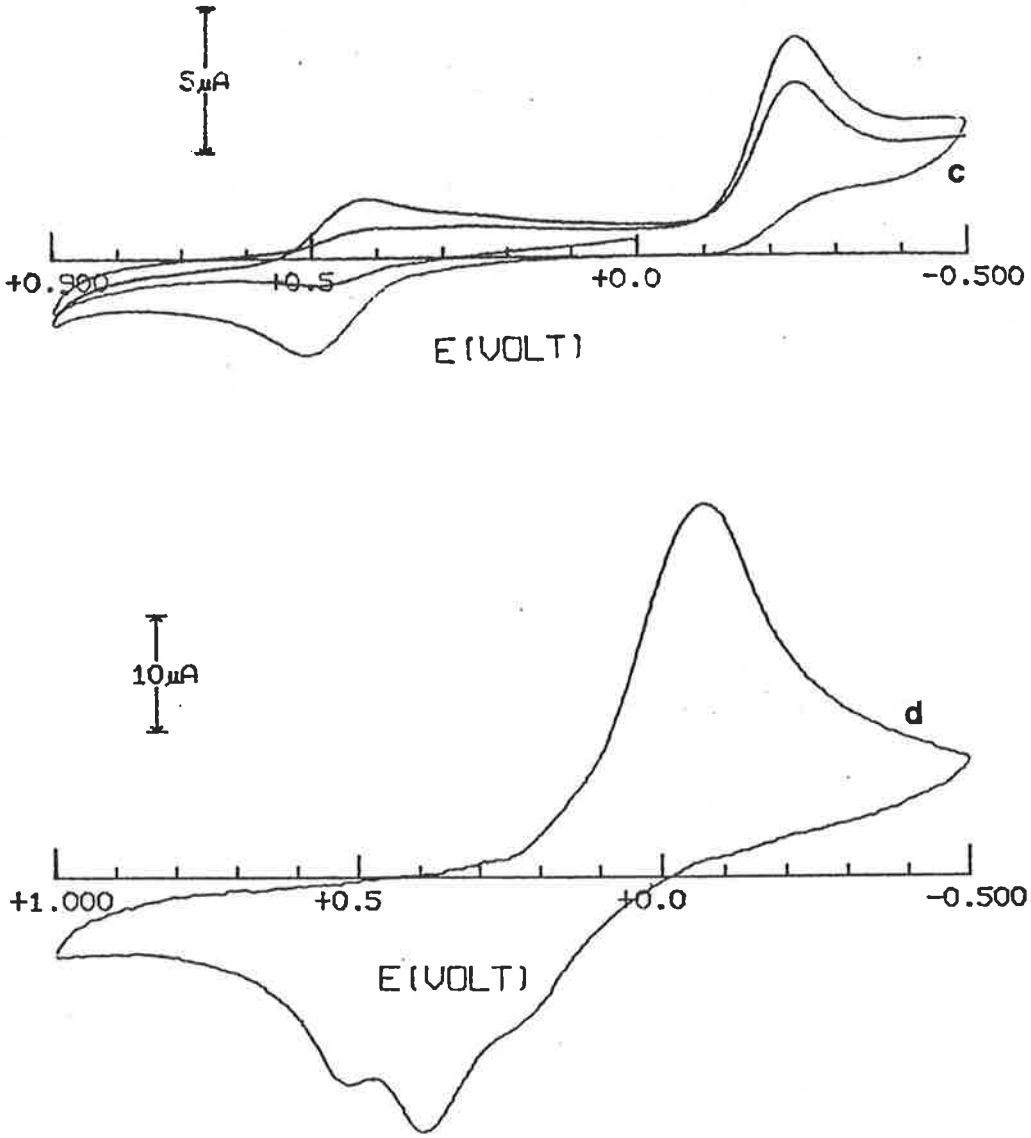

Fig. 2.11.(cont.) (c) Cyclic voltammogram in dimethylsulphoxside. (d) Cyclic voltammogram in acetone.

three reversible waves are due to the presence of the mono, bis and tris acetonitrile complexes respectively. The $E_{1/2}$ potential of the wave assigned to the mono substituted complex is similar to the value of +0.19 V previously reported for reduction of $[Ru(NH_3)_5NCMe]^{3+}$. [4] Over a period of time, the peak currents of the more positive waves increased, and those of the less positive decreased, indicative of the progressive formation of the higher substitution products by a slow substitution process involving the Ru(III) complex. It is apparent, therefore, that the reduction of the Ru(III) complex catalyzes solvolysis by acetonitrile, but that the rate of substitution on the Ru(III) complex is still appreciable.

2.8.3. Dimethylsulphoxide. In DMSO, and at low scan rates, the CV of $[Ru(NH_3)_3(OH_2)_3]^{3+}$ consisted of a cathodic EC-type peak at –0.25 V and a reversible wave at $E_{1/2}$ = +0.43 V. (Fig. 2.11c) At very high scan rates ($v > 1$ V sec^{-1}) the peak at –0.25 V was resolved into a quasi-reversible wave with peak separation of at least 185 mV. In aqueous DMSO mixtures, the $E_{1/2}$ of this wave is pH-dependent and occurs in the appropriate region for the various aqua/hydroxo complexes. In DMSO/0.1 mol dm^{-3} $MeSO_3H$ (60/40), the cathodic peak is at the same potential as that due to reduction of $[Ru(NH_3)_3(OH_2)_3]^{3+}$. Operation of an EC mechanism is evidence that solvolysis of $[Ru(NH_3)_3(OH_2)_3]^{2+}$ by DMSO occurs relatively rapidly, in a manner similar to that described above for solvolysis by acetonitrile.

The positive $E_{1/2}$ potential for the DMSO complex is indicative of a π-bonded ligand, possibly involving coordination through the sulphur atom. Such is the case with the complexes, $[Ru(NH_3)_5DMSO]^{2+}$, $[Ru(DMSO)_3Cl_3]^-$ and $[Ru(DMSO)_4Cl_2]$, for which the crystal structures have been determined. [37-39] It has been concluded that up to three DMSO ligands can adopt the S-bound form around Ru(II). In cases where there are more than three, there will be a mixture of S-bound and O-bound ligands. The $E_{1/2}$ potential for $[Ru(NH_3)_5DMSO]^{2+}$ is +0.76 V. [19a] On the basis of this information, it may be concluded that S-bound DMSO is a very strong π-acceptor ligand. The more moderate $E_{1/2}$ potential of the triammine complex, compared with the pentaammine, is perhaps due to the ability of the aqua ligands to provide electron density to the electron-deficient ruthenium centre by π-donation from the second non-bonding pair of electrons on the oxygen atom. The contribution to the electron density at the metal centre from the aqua ligands thus compensates for the strong electron-withdrawing ability of the DMSO.

2.8.4. Acetone. The cyclic voltammogram of $[Ru(NH_3)_3(OH_2)_3]^{3+}$ in acetone (Fig. 2.11d) consisted of a single cathodic peak at a more positive potential (E_p = +0.04 V) than that exhibited by the complex in aqueous acid, and two anodic peaks at positive potentials. (E_p = +0.40 V and +0.53 V respectively) The addition of aqueous base or acid (to give 60/40 acetone/water) resulted in the

cathodic peak occurring at still more positive potentials, suggesting strongly that there is σ-bonded acetone with no water in the coordination sphere, when 100% acetone is used. The peak potentials of the anodic waves are characteristic of a product involving a π-bonded species and the EC shape of the voltammogram is indicative of the occurrence of some chemical reaction after the electron transfer steps. The existence of multiple anodic peaks in the CV of the triammine ruthenium complex is attributable to the presence of species with different numbers of π-bonded acetone ligands.

Similar behaviour has been observed previously in the electrochemistry of $[Ru(NH_3)_5acetone]^{3+/2+}$ and $[Os(NH_3)_5acetone]^{3+/2+}$. [40, 41] Lay has suggested that the coordinated acetone flips from an O-bound, η^1 form to a π-bonded, η^2 form after reduction from the +3 oxidation state to the +2 state, with subsequent flipping back to the original form after oxidation to the +3 state. This proposal was supported by a crystal structure determination of $[Os(NH_3)_5acetone]^{2+}$, which showed the acetone ligand to be present in the η^2 form. [41] $[Ru(NH_3)_5acetone]^{3+}$ has not been investigated, but the Ru(II) species has been found to be a useful synthetic intermediate. [42]

If one accepts the hypothesis about the various coordination modes of the acetone in the two oxidation states, it is apparent that the Ru(II) ion is stabilized by the π-bonded, η^2 acetone ligand, and the Ru(III) ion is stabilized by the η^1, O-bound ligand. This is in contrast to the situation applying in DMSO, where the S-bound form is favoured by both oxidation states.

2.8.5. Conclusion. From the above results, it is apparent that acetonitrile and dimethylsulphoxide are strong electron accepting ligands, and that their coordination to the ruthenium centre is more rapid when Ru(II) is involved. Conversely, methanol is an electron donating ligand, and its coordination to the ruthenium centre is favoured by the presence of Ru(III). Acetone is capable of acting as either an electron acceptor or donor, and can coordinate through either the oxygen atom or through side-on coordination of the carbonyl group.

REFERENCES

(1) (a) K. Gleu, K. Rehm, *Z. Anorg. Allgem. Chem.*, **227**, 237(1936). (b) *ibid*, **235**, 352(1938). (c) K. Gleu, W. Breuhl, *Z. Anorg. Allgem. Chem.*, **237**, 335(1938)

(2) J. A. Broomhead, F. Basolo, R. G. Pearson, *Inorg. Chem.*, **3**, 826(1964)

(3) G. M. Bryant, J. E. Fergusson, *Aust. J. Chem.*, **24**, 441(1971)

(4) T. Matsubara, P. Ford, *Inorg. Chem.*, **15**, 1107(1976)

(5) C. K. Poon, S. S. Kwong, C. M. Che, Y. P. Kan, *J. Chem. Soc., Dalton Trans,* 1457(**1982**)

(6) D. M. Stanbury, D. Goswick, H. Taube, *Inorg. Chem.*, **22**, 1975(1983)

(7) J. A. Broomhead, L. Kane-Maguire, *Inorg. Chem.*, **10**, 85(1971)

(8) J. A. Stritar, H. Taube, *Inorg. Chem.*, **8**, 2281(1969)

(9) R. E. Clarke, P. C. Ford, *Inorg. Chem.*, **9**, 227(1970)

(10) P. Ford, De F. P. Rudd, R. Gaunder, H. Taube, *J. Amer. Chem. Soc.*, **90**, 1187(1968)

(11) P. C. Ford, C. Sutton, *Inorg. Chem.*, **8**, 1544(1969)

(12) M. Farraggi, A. Feder, *Inorg. Chem.*, **12**, 236(1973)

(13) D. E. Harrison, H. Taube, *J. Amer. Chem. Soc.*, **89**, 5706(1967)

(14) (a) C. M. Elson, I. J. Itzkovitch, J. A. Page, *Can. J. Chem.*, **48**, 1639(1970). (b) L. A. P. Kane-Maguire, *J. Inorg. Nucl. Chem.*, **33**, 3964(1971)

(15) (a) F. Bottomley, S. B. Tong, *Can. J. Chem.*, **49**, 3739(1971). (b) F. Bottomley, *Can. J. Chem.*, **55**, 2788(1977)

(16) B. Anderes, S. T. Collins, D. K. Lavallee, *Inorg. Chem.*, **23**, 2201(1984)

(17) N. Dixon, H. J. Lancaster, G. A. Lawrence, A. M. Sargeson, *Inorg. Chem.*, **20**, 470(1981)

(18) T. Eliades, P. Reinsalu, R. O. Harris, *Can. J. Chem.*, **47**, 3823(1969)

(19) (a) C. G. Kuehn, H. Taube, *J. Amer. Chem. Soc.*, **98**, 689(1976). (b) H. S. Lim,

B. J. Barclay, F. C. Anson, *Inorg. Chem.*, **11**, 1460(1972)

(20) W. P. Griffith, *The Chemistry of the Rarer Platinum Metals*, Interscience, London, **1967**, p166

(21) Z. Harzion, G. Navon, *Inorg. Chem.*, **19**, 2236(1980)

(22) G. E. Cabaniss, A. A. Diamantis, W. R. Murphy, L. W. Linton, T. J. Meyer, *J. Amer. Chem. Soc.*, **107**, 1845(1985)

(23) A. A. Diamantis, W. R. Murphy, T. J. Meyer, *Inorg. Chem.*, **23**, 3230(1984)

(24) K. J. Takeuchi, M. S. Thompson, D. W. Pipes, T. J. Meyer, *Inorg. Chem.*, **23**, 1845(1984), and references therein.

(25) C. M. Che, K. Y. Wong, W. H, Leong, C. K. Poon, *Inorg. Chem.*, **25**, 345(1986) and references therein.

(26) R. B. Baar, F. C. Anson, *J. Electroanal. Chem.*, **187**, 265(1985)

(27) K. J. Takeuchi, G. J. Samuels, S. W. Gersten, J. A. Gilbert, T. J. Meyer, *Inorg. Chem.*, **22**, 1407(1983)

(28) C. M. Che, K. Y. Wong, C. K. Poon, *Inorg. Chem.*, **24**, 1601(1985)

(29) (a) M. J. Ridd, F. R. Keene, *J. Amer. Chem. Soc.*, **103**, 5733(1981). (b) P. A. Adcock, F. R. Keene, R. S. Smythe, M. R. Snow, *Inorg. Chem.*, **23**, 236(1984)

(30) W. P. Griffith, D. Pawson, *J. Chem. Soc., Dalton Trans,* 1315(**1973**)

(31) R. Ramaraj, A. Kira, M. Kaneko, . *J. Chem. Soc., Chem. Comm.*, 227(**1987**)

(32) K, J, Yakeuchi, M. S. Thompson, D. W. Pipes, T. J. Meyer, *Inorg. Chem.*, **23**, 1845(1984)

(33) T. W. Kallen, J. Earley, *Inorg. Chem.*, **10**, 1152(1971)

(34) J. F. Endicott, H. Taube, *J. Amer. Chem. Soc.*, **84**, 4984(1962)

(35) H. Taube, *private communication.*

(36) E. E. Mercer, L. W. Gray, *J. Amer. Chem. Soc.*, **94**, 6426(1972)

(37) F. C. Marsh, G. Fergusson, *Can. J. Chem.*, **49**, 3590(1971)

(38) R. S. McMillan, A. Mercer, B. R. James, J. Trotter, *J. Chem. Soc., Dalton Trans,* 1006(**1975**)

(39) A. Mercer, J. Trotter, *J. Chem. Soc., Dalton Trans,* 2480(**1975**)

(40) P. A. Lay, *private communication.*

(41) W. D. Harman, D. P. Fairlie, H. Taube, *J. Amer. Chem. Soc.*, **108**, 8223(1986)

(42) J. A. Baumann, T. J. Meyer, *Inorg. Chem.*, **19**, 345(1980), and references therein.

Chapter 3.

SUBSTITUTED TRIAMMINERUTHENIUM COMPLEXES.

3.1. Introduction.

The substitution reactions of ruthenium(II) and ruthenium(III) ammine complexes have been of much interest for the past two decades, and the subject has been reviewed by Ford and, more recently, by Seddon. [1, 2] Hitherto, such reactions have been confined to the pentaammine and tetraammine groups of complexes, with spectral and electrochemical studies providing information about bonding, electron transfer reactions and substitution mechanisms. Much work has been done involving the use of analogous series of complexes where groups of ligands with various organic substituents (for example, substituted pyridines [3], and a range of carboxylate anions [4]) have been introduced into the coordination sphere. These series of complexes have been particularly useful in making comparisons between Ru(II) and other d^6 ions such as Co(III), and between Ru(III) and other d^5 ions such as Fe(III).

An important consideration when discussing substitution reactions on ammineruthenium complexes is the relative lability of the +2 and +3 oxidation states towards substitution. Most substitution reactions on Ru(II) and Ru(III) proceed via a dissociative mechanism so that, generally, Ru(II) is more labile than Ru(III). [5] This phenomenon is illustrated by reaction 3.1. For n = 2, the rate constant, $k_1 = 9\ sec^{-1}$ (at 298K) [6], but when n = 3, $k_1 = 2.1 \times 10^{-4}\ sec^{-1}$ (at 327K and $[Cl^-] = 0.1\ mol\ dm^{-3}$). [7]

$$[Ru(NH_3)_5H_2O]^{n+} + Cl^- \xrightarrow{k_1} [Ru(NH_3)_5Cl]^{(n-1)+} + H_2O \quad \textbf{(3.1)}$$

The traditional precursors to substituted complexes have been the haloammine complexes of ruthenium(III) and one usual synthetic procedure has been to remove the halide ion from the solution by precipitating it as its silver salt. This results in a solution of $[Ru(NH_3)_5H_2O]^{3+}$. Though this complex is relatively inert to substitution, the substitution reaction can be catalyzed by the presence of a small amount of the Ru(II) analogue, formed *in situ* by the action of amalgated zinc or some other reductant. Stritar and Taube first made use of this sequence in the synthesis of pentaammine carboxylato complexes. [4] The preparative reaction scheme was:

$$[Ru(NH_3)_5(OH_2)]^{3+} + Zn(Hg) \longrightarrow [Ru(NH_3)_5OH_2]^{2+}$$

$$[Ru(NH_3)_5(OH_2)]^{2+} + RCO_2H/RCO_2^- \longrightarrow [Ru(NH_3)_5(RCO_2)]^{+}$$

$$[Ru(NH_3)_5(RCO_2)]^{+} + O_2 \longrightarrow [Ru(NH_3)_5(RCO_2)]^{2+} \quad \textbf{(3.2)}$$

If the reaction solution is degassed prior to the addition of the reductant, a ruthenium(II) complex can be obtained, especially when the ligand is a good π-acceptor.

A modification of the above procedure is to introduce the reductant directly to a solution of the haloammine complex and ligand. The hydrolysis of the haloammineruthenium(II) complex is quite rapid and, once the substitution reaction is complete, the product can be isolated, halide free, by the addition of a precipitating agent, such as $NaClO_4$ or NH_4PF_6. Using these procedures, it has been possible to prepare ammineruthenium complexes containing ligands such as carboxylates [4], organonitriles [8], aromatic nitrogen heterocycles [3, 9], carbon monoxide [10] and dinitrogen. [11]

There is a trend away from the use of the perchlorate, hexafluorophosphate and tetrafluoroborate as non-coordinating anions. Perchlorate is prone to violent decomposition, and is also readily reduced. [12] This second feature of its chemistry means that perchlorate can be troublesome when present in electrochemical experiments. The fluorophosphate and fluoroborate ions are susceptible to hydrolysis, leading to the formation of fluoride ion in aqueous solutions. The sulphonate ions, e.g. methanesulphonate and trifluoromethanesulphonate, are finding favour because of their stability and poor coordinating ability. Trifluoromethanesulphonate is especially favoured because of its solubility in a wide range of organic solvents. [12]

The above procedures work well when the ligand is soluble in water, but complications arise when it is not. A convenient procedure in this case is to replace water with an organic solvent in which the precursor complex and ligand are soluble. It has been shown that acetone will replace the aqua ligand in $[Ru(NH_3)_5(OH_2)]^{2+}$, and the coordinated acetone may then be replaced by some other ligand. [11, 12] Similarly, it has been shown that the acid hydrolysis of $[Ru(NH_3)_5Cl]^{3+}$ in anhydrous HTFMS results in the formation of a labile product, $[Ru(NH_3)_5TFMS](TFMS)_2$, which is soluble in a range of organic solvents. [13, 14] TFMS is a very weak ligand and is readily replaced by almost any neutral ligand. Examples of this include replacement by water-insoluble organonitriles, pyridine, formamide and methanol.

The substitution reactions of ruthenium ammine complexes have been paralleled by the preparation of complexes of Ru(II) and (III) containing pentadentate edta as the major ligand. [15 - 17] Ligand substitution on ions in both oxidation states appeared to be enhanced by the action of the pendant arm of the edta ligand, through its ability to hydrogen bond with the aqua ligand. [15] Variation of the ligand was shown to affect the properties of the complexes in the same trends as in the substituted ammine complexes.

With the availability of $[Ru(NH_3)_3(OH_2)_3]^{3+}$, it was proposed to study the substitution reactions of bidentate ligands with this ammineruthenium complex. Substitution on the tetraammineruthenium ions has lead to a range of complexes which also contain bidentate ligands, and to studies of their spectra and electrochemistry. This new complex offers the scope to vary the coordination sphere about the ruthenium centre while leaving the ammine and aqua ligands intact. Thus, in addition to the conventional spectral and electrochemical studies, it was possible to study the effect of the non-ammine ligand on the acid/base properties of the coordinated water, as well as the proton-coupled oxidation of the $RuOH_2^{3+}$ group to the $Ru{=}O^{2+}$ group. There was also the possibility of studying complexes of the type $[Ru(NH_3)_3L_3]^{n+}$ where L may be varied from π-acceptors to π- or σ–donors, as in the cases of $[Ru(NH_3)_5L]^{n+}$ and $[Ru(NH_3)_4L_2]^{n+}$ complexes.

3.2. Ruthenium(III) Complexes.

3.2.1. Preparation of Complexes. The solvolysis of $[Ru(NH_3)_3(OH_2)_3]^{3+}$ by alcohols was discussed in Chapter 2. In alcoholic solutions, $[Ru(NH_3)_3(OH_2)_3]^{3+}$ reacted with uninegative, bidentate ligands, in the presence of lithium acetate to give a series of complexes, $[Ru(NH_3)_3(LL)(OH_2)]^{2+}$ (LL = acac, dpm, hna, oxine, bzac, dbm, and sal). The progress of the reaction could be monitored voltammetrically by adding samples of the reaction mixture to aliquots of 0.1 mol dm^3 $MeSO_3H$, in which the $[Ru(NH_3)_3(OH_2)_3]^{3+/2+}$ couple had a DPV peak at –0.09 V. During the course of the reaction, the peak current at this potential decreased, with the concomitant increase in the peak current of a peak at more negative potentials. The reaction mixtures containing the diketonate ligands were purple, and with the other ligands they were green.

The complexes containing the first three ligands were isolated as their dithionate salts after the solvent had been removed from the reaction mixture, and the resulting residue treated with dilute dithionic acid. $[Ru(NH_3)_3(oxine)(OH_2)](TFMS)_2$ was isolated by an analogous method, using 3 mol dm^{-3} HTFMS instead of dithionic acid. In this case the reaction yield was low, because there was a tendency for the acid to protonate the ligand, giving $[Ru(NH_3)_3(OH_2)_3](TFMS)_3$ as a product. Attempts were made to isolate the oxine complex as a dithionate and *p*-toluenesulphonate salt, but without success.

The ligands, bzac, dbm, and sal all reacted with $[Ru(NH_3)_3(OH_2)_3]^{3+}$ under the same conditions, but it was not possible to isolate the products by the addition of precipitating agents to the reaction mixture. When reaction mixtures containing bzac and dbm came in contact with aqueous solutions, a white precipitate was observed which was identified as the free ligand. It is not certain whether the ligand was precipitated because of the decomposition of the product, or because there was still some unreacted ligand in solution. If the white precipitate was filtered from the aqueous solution, the purple colour of the reaction mixture was still evident, and that the filtrate

contained very little of the starting material was apparent from DPV analysis of the solution. The filtrate of the bzac reaction mixture contained a species with a DPV peak at –0.28 V in acid solution. From a comparison with the DPV of $[Ru(NH_3)_3(acac)(OH_2)]^{2+}$, and knowing the difference between the $E_{1/2}$ values of $Ru(acac)_3$ (–0.67 V vs Ag/AgCl), $Ru(bzac)_3$ (–0.55 V)and $Ru(dbm)_3$ (–0.42 V), it was possible to identify the species in the solution as the desired product. Similarly, the electrochemistry of $Ru[(NH_3)_3(sal)(OH_2)]^{2+}$ was studied by adding aliquots of the ethanolic reaction mixture to the electrochemical medium.

$[Ru(NH_3)_3(C_2O_4)(OH_2)]_2(S_2O_6)$ was prepared by an adaptation of the procedure of Stritar and Taube for the preparation of ammine carboxylate complexes. [4] $[Ru(NH_3)_3(OH_2)_3]^{3+}$was reduced for a short time by hydrogen over platinum black in the presence of an equimolar amount of an oxalate buffer solution. After the reduction was stopped, the resulting red Ru(II) solution was heated at 50°C in the air for a period of time until the colour had changed to yellow. The solvent was then evaporated, and the product precipitated by the addition of a dilute solution of dithionic acid.

Examples of substituted ammine ruthenium complexes with these ligands are rare. The preparation of ammine carboxylate complexes has been discussed briefly above, and $[Ru(NH_3)_4(C_2O_4)]_2(S_2O_6)$ has been used as a synthetic intermediate for some time. [19] $[Ru(en)_2(C_2O_4)]^+$ exists in salts with a variety of anions. [20] Recently, interest has been shown in the chemistry of tetraammine diketonate complexes, such as $[Ru(NH_3)_4(acac)](TFMS)_2$ [21], and the complex $[Ru(H_2edta)(acac)]$ has also been reported. [17] A series of tris(diketonate)ruthenium(III) complexes has been studied, as referred to in Chapter 1, and the tris(oxalate) complex, $Ru(C_2O_4)_3^{3-}$, is also known. [18, 22] Hydroxynaphthaldehyde is an analogue of salicylaldehyde, a well-known ligand, which has been used as a ligand in a series of bis(chelate)(diene)ruthenium(II) complexes, as has 8-hydroxyquinoline. [23]

3.2.2. Electronic Spectra. The uv/vis spectra of the Ru(III) complexes all contained LMCT bands, and the spectra of the complexes with uninegative ligands also contained bands attributable to intra-ligand absorptions. The LMCT bands arise from transitions between the p_π ligand orbitals and the vacancy in a t_{2g} orbital of the d^5 metal centre. [24] The spectra of the complexes prepared are displayed in Fig. 3.1, and the main features are listed in Table 3.1, together with those of some related Ru(III) complexes.

All the spectra were pH dependent, reflecting the acidity of the coordinated water molecule. The intra-ligand bands were relatively insensitive to changes in pH, but the charge transfer bands were strongly influenced by changes in pH. In the hydroxo complexes, the charge transfer bands of the complexes with uninegative ligands were at higher energy than in the aqua complexes. The

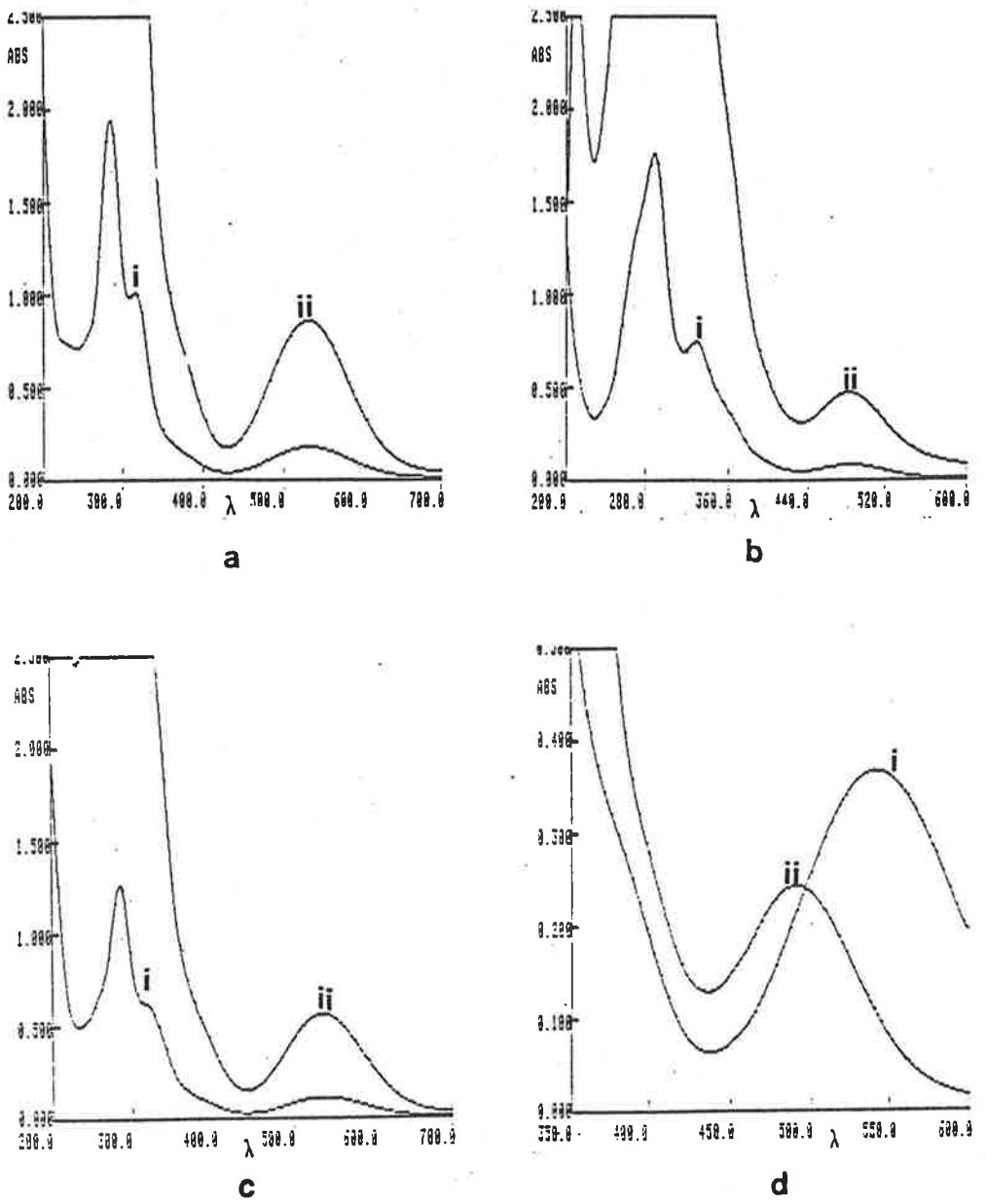

Fig. 3.1. uv/vis spectra of substituted triammineaquaruthenium(III) complexes. Unless stated otherwise, solution is 0.02 mol dm^{-3} in buffer and 0.1 mol dm^{-3} $NaMeSO_3$, and (i) 0.2 cm cells, (ii) 1.0 cm cells. (a) $[Ru(NH_3)_3(acac)(OH_2)]^{2+}$, c = 1.4 x 10^{-3} mol dm^{-3}. (b) $[Ru(NH_3)_3(acac)(OH)]^{+}$, c = 1.1 x 10^{-3} mol dm^{-3}. (c) $[Ru(NH_3)_3(dpm)(OH_2)]^{2+}$, c = 8.4 x 10^{-4} mol dm^{-3}. (d) i $[Ru(NH_3)_3(dpm)(OH_2)]^{2+}$, c = 4.6 x 10^{-4} mol dm^{-3}, 0.2 cm cells. ii $[Ru(NH_3)_3(dpm)(OH)]^{+}$, c = 4.4x 10^{-4} mol dm^{-3}, 0.2 cm cells.

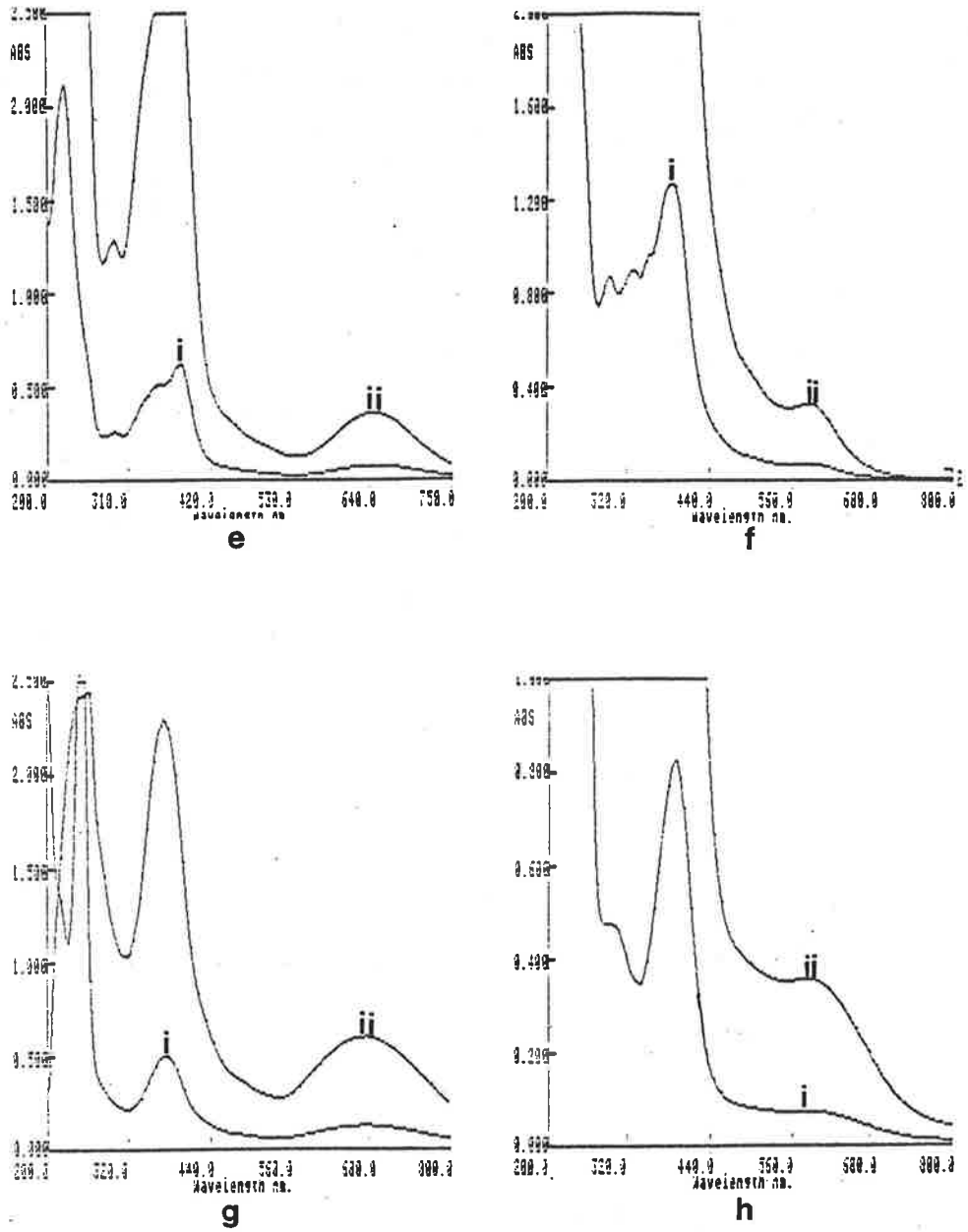

Fig. 3.1.(cont.) (e) $[Ru(NH_3)_3(hna)(OH_2)]^{2+}$, c = 2.7 x 10^{-4} mol dm^{-3}.
(f) $[Ru(NH_3)_3(hna)(OH)]^{+}$, c = 5.6 x 10^{-4} mol dm^{-3}. (g) $[Ru(NH_3)_3(oxine)(OH_2)]^{2+}$, c = 6.2 x 10^{-4} mol dm^{-3}. (h) $[Ru(NH_3)_3(oxine)(OH)]^{+}$, c = 8.2 x 10^{-4} mol dm^{-3}.

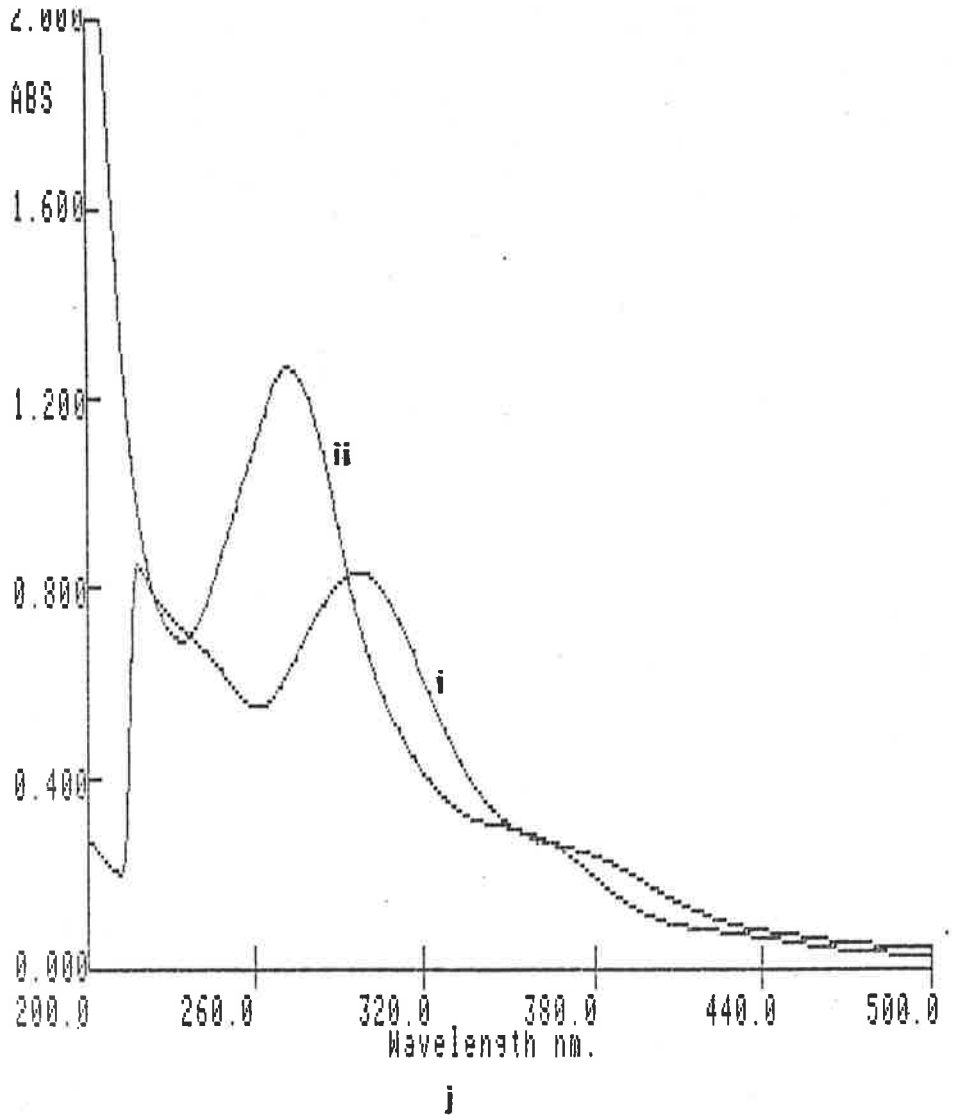

Fig. 3.1.(cont.) (j) i $[Ru(NH_3)_3(C_2O_4)(OH)]$, c = 1.2 x 10^{-3} mol dm^{-3},
ii $[Ru(NH_3)_3(C_2O_4)(OH_2)]^+$, c = 1.1 x 10^{-3} mol dm^{-3}.

LL	$RuA_3L_2(OH_2)^{n+a}$	$RuA_3L_2(OH)^{(n-1)+b}$	*cis* $RuA_4L_2^{2+}$	$Ru(LL)_3$
acac	284(7.46) 314(3.86) 529(0.66)	284(7.5) 314(3.9) 481(0.43)	281(9.59)[c] 320(5.13) 537(1.48)	272(22)[d] 347(10) 504(2.5)
dpm	284(7.52) 310sh(4) 538(0.73)	284(7.5) 310sh(4) 491(0.56)		
hna	222(39.5) 289(4.82) 377(11.6) 643(1.32)	 292(7.4),326(7.64) 384(10.8) 580(0.55)		
oxine	251(28.0) 373(4.05) 674(0.99)	251(20.6) 373(4.34) 561(0.46)		
C_2O_4	271(1.61) 350sh(.5)	297(1.15) 380sh(.5)	287(3.01)[e]	288(.32)[f] 375(.35) 490(.028) 631(.011)

Table 3.1. uv/vis spectra of substituted ammineruthenium(III) complexes. λ in nm(ε x 10^{-3} mol^{-1} dm^3 cm^{-1}). (a) in 0.1 M $MeSO_3H$. (b) 0.02 M borate buffer, 0.1 M $MeSO_3Na$, pH 10. (c) Reference 21, 0.1 M phosphate buffer, pH 3. (d) Reference 18, CH_2Cl_2 solution. (e) Reference 24, 0.1 M p-toluenesulphonic acid. (f) Reference 22.

shift in the absorption occurs because the energy of the partially filled t_{2g} orbital is increased, due to the strongly π-donating character of the OH^- ligand compared with the H_2O ligand. Assuming that the energy of the ligand orbitals is unaffected by the deprotonation of the aqua ligand, the energy of the LMCT transition must be increased. The spectrum of $[Ru(NH_3)_3(acac)(OH_2)]^{2+}$, with the LMCT band at 529 nm, is similar to that of $[Ru(NH_3)_4(acac)]^{2+}$, from whence the assignment of the band to a LMCT comes. [21] This is further evidence of the similarity of the spectra of ruthenium complexes with varying proportions of ammine and aqua ligands.

In the spectrum of $[Ru(NH_3)_3(C_2O_4)(OH_2)]^+$, the LMCT band was at 271 nm and in $[Ru(NH_3)_3(C_2O_4)(OH)]$ it was at 297 nm. That the energy of the absorption is lower in the hydroxo complex implies that the LMCT transition involves the coordinated H_2O/OH^- group and not the bidentate ligand. Similar effects are observed in the spectra of the ammine aqua/hydroxo complexes reported in Chapter 2, where the spectra have an absorption at about 295 nm when there is coordinated OH^-. Because OH^- is a better π-donor ligand than H_2O, the donor orbitals are at higher energy, and so the energy of the transition to the Ru t_{2g} orbital is lowered. The LMCT band in $[Ru(NH_3)_4(C_2O_4)]^+$ occurs at 287 nm. [24] By analogy with the spectrum of $[Ru(NH_3)_5(CH_3CO_2)]^{2+}$, this band can be assigned to a LMCT from the carboxylate ligand. [25] Thus, in $[Ru(NH_3)_3(C_2O_4)(OH_2)]^+$, theLMCT from the oxalate ligand probably occurs in the same region, but is masked by the charge ransfer from OH^-.

3.2.3. Vibrational Spectra. The vibrational spectra of the complexes were recorded as nujol mulls on KBr discs. The presence of vibrations attributable to the ligands was confirmation that the ligands were coordinated. The ligand bands were assigned by reference to the previously recorded spectra of similar complexes. [26]

In all cases there were absorptions attributable to the OH and NH stretching vibrations. In the spectrum of $[Ru(NH_3)_3(C_2O_4)(OH_2)]_2(S_2O_6).H_2O$, the (υ)OH mode was evident from the presence of two relatively sharp bands at 3480 and 3750 cm^{-1}, and in $[Ru(NH_3)_3(acac)(OH_2)](S_2O_6).H_2O$ there were analagous bands at 3450 and 3670 cm^{-1}, which were broadened due to the interaction between the coordinated water and lattice water. In the spectra of the other complexes, this interaction was more dominant, with the (υ)OH bands being evident as a single broad absorption at about 3500 cm^{-1}. For all the complexes, there were two or three bands between 3190 and 3300 cm^{-1}, attributable to the υ(NH) mode; a broad band between 1620 and 1640 cm^{-1}, attributable to the δ_d(NH) mode and several bands between 1250 and 1350 cm^{-1}, attributable to the δ_s(NH) mode. Though ammine complexes are also expected to show absorptions between 950 and 590 cm^{-1}, due to the rocking vibrations [47a], these bands were obscured by bands due to ligand or anion vibrations.

The spectra of the diketonate complexes contained bands attributable to the combination of the (υ)C=O and (υ)C=C vibrations. These were at 1500, 1570 and 1588 cm^{-1} for the acac complex, at 1530 and 1540 cm^{-1} for the dpm complex, and at 1526 and 1565 cm^{-1} for the hna complex. In the spectrum of $[Ru(NH_3)_3(C_2O_4)(OH_2)]_2(S_2O_6).H_2O$, there were (υ)C=O absorptions at 1635, 1670, 1700 and 1705 cm^{-1}.

The spectra of those complexes with an aromatic moiety in the ligand had absorptions between 1500 and 1600 cm^{-1} due to ring-expansion vibrations.

3.2.4. Acid-Base Properties. The pK_a for the dissociation of a proton from the aqua ligand in each complex, according to reaction 3.3, was measured spectrophotometrically, using the molar absorptivities at the absorption maxima in acid and base solutions.

$$[Ru(NH_3)_3(LL)(OH_2)]^{n+} \rightleftharpoons [Ru(NH_3)_3(LL)(OH_2)]^{(n-1)+} + H^+ \qquad (3.3)$$

The pK_a values determined are listed in Table 3.2. It can be seen that the coordination of a negatively charged ligand to the triammineaquaruthenium(III) group causes an increase of 2 to 3 units in the pK_a compared with that of $[Ru(NH_3)_3(OH_2)_3]^{3+}$ at 3.77.

This increase in pK_a can be explained in terms of the increase in electron density on the Ru(III) centre brought about by the σ- and π-donation from the ligand to the metal centre. The pK_a of water is decreased on coordination because of the ability of the electron deficient metal centre to stabilize the negative charge induced by proton dissociation. If the electron density at the metal centre is increased by the replacement of one of the other ligands by a stronger electron donor, then the pK_a of the coordinated water will increase because the metal centre has lost some of its ability to stabilize the negative charge. Thus, the pK_a of a complex in a series of aqua complexes may be considered to be a measure of the electron donating ability of the substituting ligand. Thus, it can be concluded that, for the complexes prepared here, the electron donating ability of the ligands increases in the order: $C_2O_4 \approx$ hna < sal < bzac < oxine <acac < dpm.

3.2.5. The Electrochemistry of $[Ru(NH_3)_3(LL)(OH_2)]^{2+}$ Complexes. The electrochemistry of the Ru(III) complexes was studied in aqueous buffer solutions at glassy carbon electrodes. At freshly polished electrodes, all the complexes showed a reversible reduction wave in the CV at negative potentials. The potential at which this wave occurred was pH dependent, and the $E_{1/2}$ potentials for the complexes at pH 3 are listed in Table 3.2, together with those of some similar complexes. At anodically activated electrodes, in addition to the reduction wave in the CV (which tended to have a larger peak separation than at unactivated electrodes), there was also an irreversible wave visible at positive potentials. On an anodic DPV scan, it was possible to resolve this wave into a distinct peak with a peak current equal to, at best, 3/4 of that due to the +3/+2 wave. The potential of this second

L	$E_{1/2}(III/II)^a$	$E_p(IV/III)^b$	pK_a
acac	−0.32	+0.57	6.1(±.1)[c] 6.1[d]
dpm	−0.41	+0.56	6.5(±.1)[c] 6.6[d]
bzac	−0.30[e]		5.9[d]
sal	−0.27[e]		5.8[d]
hna	−0.26	+0.73	5.7(±.1)[c] 5.8[d]
oxine	−0.31	+0.61	6.0(±.1)[c] 5.9[d]
C_2O_4	−0.32	+0.42[f]	5.7(±.1)[c] 5.8[d]
$(H_2O)_2$	−0.12	+0.49	3.77(±.04)
cis $RuA_4L_2^{2+}$ **or** ***cis*** $RuA_4L_2^{+}$			
acac	−0.38[g]	+1.04[i]	
C_2O_4	−0.33[h]		

Table 3.2. Redox potentials and pK_a values for substituted triammine aquo and tetraammine complexes of Ru(III) (Potentials vs SCE; 0.2 M buffer, 0.1 M $MeSO_3Na$). (a) pH = 3. (b) pH = 5. (c) spectral measurement. (d) from Pourbaix diagram. (e) compound not isolated, in situ measurement. (f) pH = 6.2. (g) Reference 21, 0.1 M phosphate buffer. (h) Reference 31, pH 3, triflate buffer. (i) Reference 18a, in CH_2Cl_2, 0.1 M $(Bu)_4NBF_4$, potential corrected to SCE scale.

peak was also pH dependent. However, when the scan direction was reversed, to give a cathodic scan, the peak was very poorly resolved, even at slow scan rates. This result is indicative that the oxidation was irreversible.

For $[Ru(NH_3)_3(acac)(OH_2)]^{2+}$, the voltammograms of which are shown in Fig. 3.2, the $E_{1/2}$ potential of the +3/+2 wave was –0.32 V at pH 3, and was independent of pH in the range 2.6 <pH<5.0. In the range 7.6<pH<9.0, from the Pourbaix diagram (Fig. 3.3) the pH dependence for this wave was –55 mV/pH, which is very close to the predicted value of –59 mV/pH for a one electron transfer reaction coupled with the transfer of one proton. The electrochemical wave can, therefore, be assigned to the reactions 3.4 and 3.5.

2.6<pH<5.3

$$[Ru(NH_3)_3(acac)(OH_2)]^{2+} + e^- \rightleftharpoons [Ru(NH_3)_3(acac)(OH_2)]^{+} \quad \textbf{(3.4)}$$

7.6<pH<9.0

$$[Ru(NH_3)_3(acac)(OH)]^{+} + e^- + H^+ \rightleftharpoons [Ru(NH_3)_3(acac)(OH_2)]^{+} \quad \textbf{(3.5)}$$

The intersection of the two lines in the Pourbaix diagram corresponds to a pK_a value of 6.1, which is in close agreement with the value determined spectroscopically.

The $E_{1/2}$ for the reduction in acid solution is about 60 mV less negative than $E_{1/2}$ for the $[Ru(NH_3)_4(acac)]^{2+/+}$ couple, recently reported as –0.38 V in 0.1 mol dm^{-3} phosphate buffer. [21] In Chapter 2, it was shown that the substitution of an aqua ligand on a metal complex by an ammine ligand leads to a decrease in the $E_{1/2}$ of approximately 20 mV. Also, it has been shown recently that the $E_{1/2}$ of a redox couple involving a ruthenium complex can be affected by the concentration of phosphate buffer in the solution. [27] An increase in the phosphate buffer concentration from 0.01 mol dm^{-3} to 0.1 mol dm^{-3} caused a decrease in the $E_{1/2}$ of the $Ru(NH_3)_6^{3+/2+}$ couple by approximately 40 mV, and was attributed to the formation of labile ion pairs. The combined effects of the extra ammine ligand and the phosphate ion in solution are probably responsible for the relatively large difference in the $E_{1/2}$ values of the triammineaqua and pentaammine pentanedionate complexes. There was no evidence to suggest that the acac ligand in $[Ru(NH_3)_3(acac)(OH_2)]^{2+}$ was protonated at low pH, as was observed in the electrochemical studies on $[Ru(NH_3)_4(acac)]^{2+}$. [21]

The Pourbaix diagram for the peak at positive potentials is also displayed in Fig. 3.3. At low pH, the positive peak became less well resolved, a phenomenon which was observed when activated glassy carbon electrodes were used to study the oxidation of $[Ru(NH_3)_5(OH_2)]^{3+}$. [28] Furthermore, at high pH, the peak was also less easily resolved because of its merging with the solvent oxidation wave. However, over a limited range, it was possible to observe electrochemical

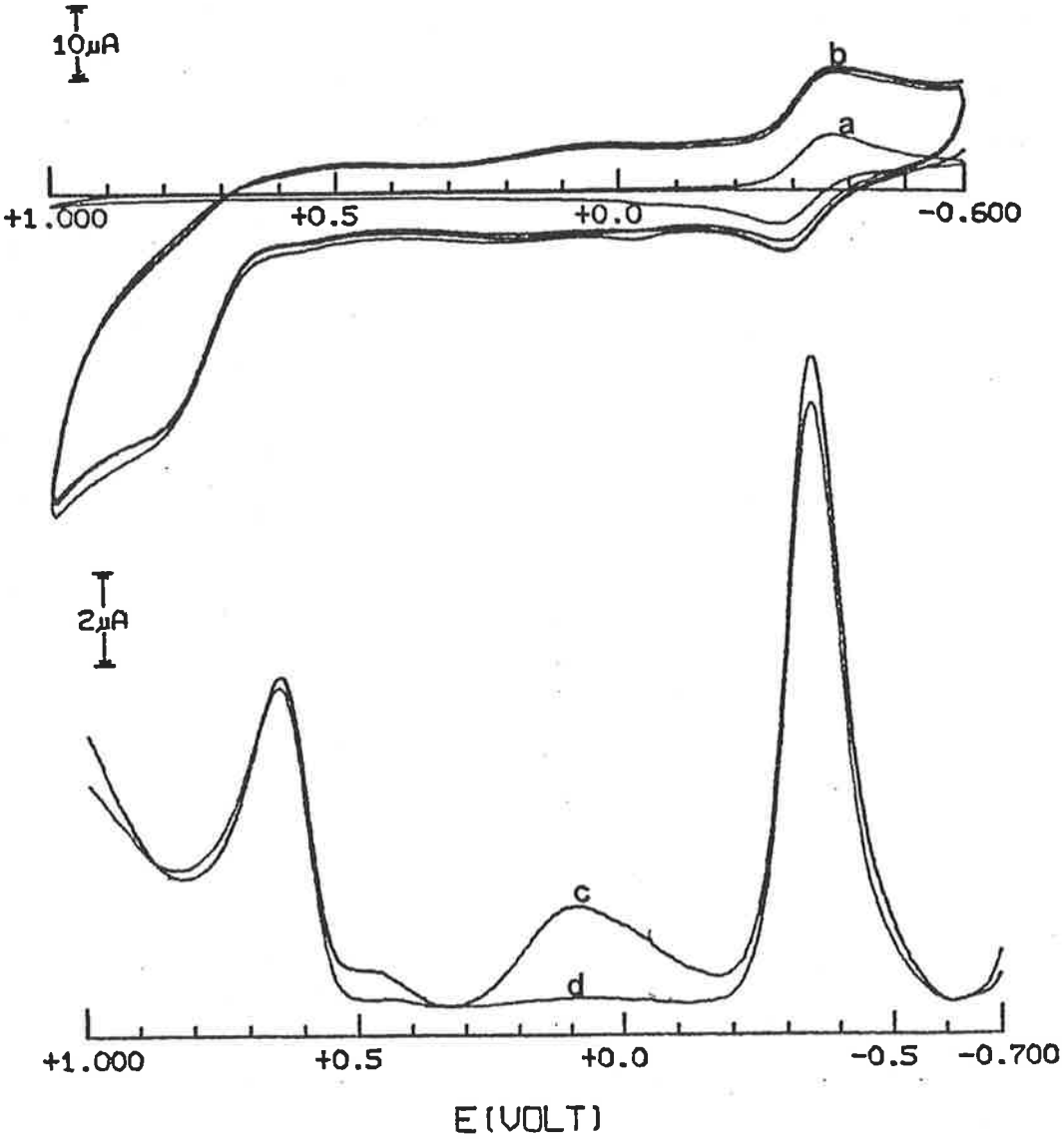

Fig. 3.2. Voltammograms of $[Ru(NH_3)_3(acac)(OH_2)]^{2+}$ at pH 4. (a) Cyclic voltammogram at an unactivated G.C.E. (b) Cyclic voltammogram at an activated G.C.E. (c) Differential pulse voltammogram at an activated G.C.E. (d) Differential pulse voltammogram at an activated G.C.E., corrected for background current.

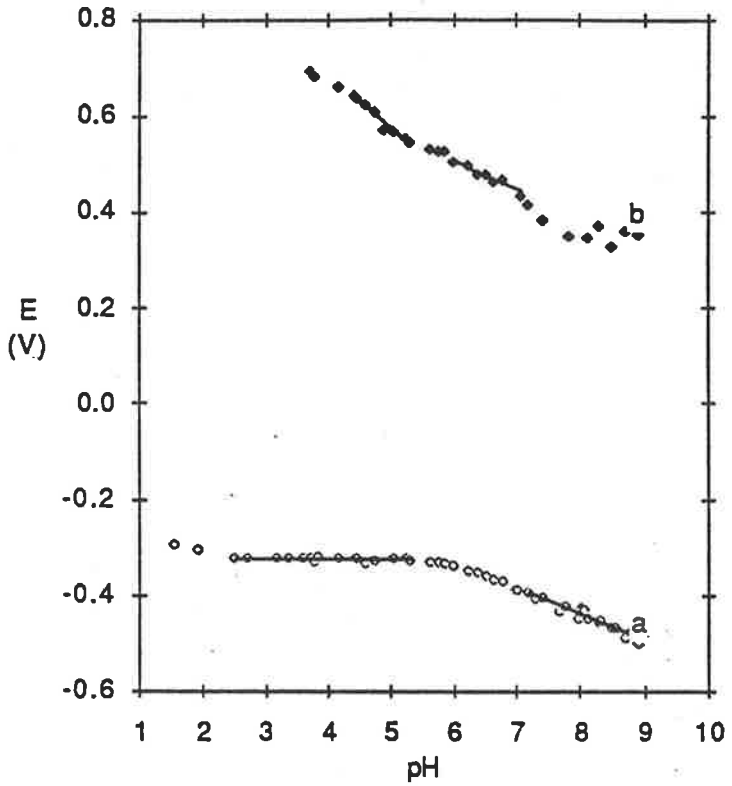

Fig. 3.3. Pourbaix diagrams for $[Ru(NH_3)_3(acac)(OH_2)]$ redox couples. (a) Ru(III)/Ru(II) couple. (b) Ru(IV)/Ru(III) couple.

behaviour consistent with the presence of a $RuO^{2+}/RuOH_2^{3+}$ couple. In the range, 4.4<pH<5.3, the pH dependence was –112 mV/pH, close to the ideal value for two proton/one electron transfer, and between pH 6.0 and 6.7, the slope was –57 mV/pH. These results are consistent with the following reactions.

4.4<pH<5.3

$$[Ru(NH_3)_3(acac)(O)]^+ + e^- + 2H^+ \rightleftharpoons [Ru(NH_3)_3(acac)(OH_2)]^{2+} \quad \textbf{(3.6)}$$

6.0<pH<6.7

$$[Ru(NH_3)_3(acac)(O)]^+ + e^- + H^+ \rightleftharpoons [Ru(NH_3)_3(acac)(OH)]^+ \quad \textbf{(3.7)}$$

The intersection of the two lines in the Pourbaix diagram is at slightly less than the spectroscopically determined pK_a value of the Ru(III) complex.

For $[Ru(NH_3)_3(dpm)(OH_2)]^{2+}$, the voltammograms of which are shown in Fig. 3.4., the $E_{1/2}$ potential of the +3/+2 wave was –0.41 V at pH 3, and was independent of pH in the range 3.4 <pH<5.4. From the Pourbaix diagram (Fig. 3.5), above pH 7.7, the pH dependence for this wave was –57 mV/pH, which is close to the ideal value of –59 mV/pH for a one proton/one electron transfer. The electrochemical wave can, therefore, be assigned to the reactions 3.8 and 3.9.

3.4<pH<5.4

$$[Ru(NH_3)_3(dpm)(OH_2)]^{2+} + e^- \rightleftharpoons [Ru(NH_3)_3(dpm)(OH_2)]^+ \quad \textbf{(3.8)}$$

7.7<pH<9.1

$$[Ru(NH_3)_3(dpm)(OH)]^+ + e^- + H^+ \rightleftharpoons [Ru(NH_3)_3(dpm)(OH_2)]^+ \quad \textbf{(3.9)}$$

The intersection of the two lines in the Pourbaix diagram lies between pH 6.5 and 6.6, which is in agreement with the pK_a value determined spectroscopically.

The Pourbaix diagram for the peak at positive potentials is also displayed in Fig. 3.5. The pH range over which reliable measurements could be made was limited by the same factors as those which were operating in the DPV experiments on $[Ru(NH_3)_3(acac)(OH_2)]^{2+}$, but to a greater extent than in the first case. Again, it was possible to observe electrochemical behaviour consistent with the presence of a $RuO^{2+}/RuOH^{2+}$ couple. Between pH 7.4 and 9.0, the pH dependence was –56 mV/pH. This is consistent with the following reaction.

7.4<pH<9.0

$$[Ru(NH_3)_3(dpm)(O)]^+ + e^- + H^+ \rightleftharpoons [Ru(NH_3)_3(dpm)(OH)]^+ \quad \textbf{(3.10)}$$

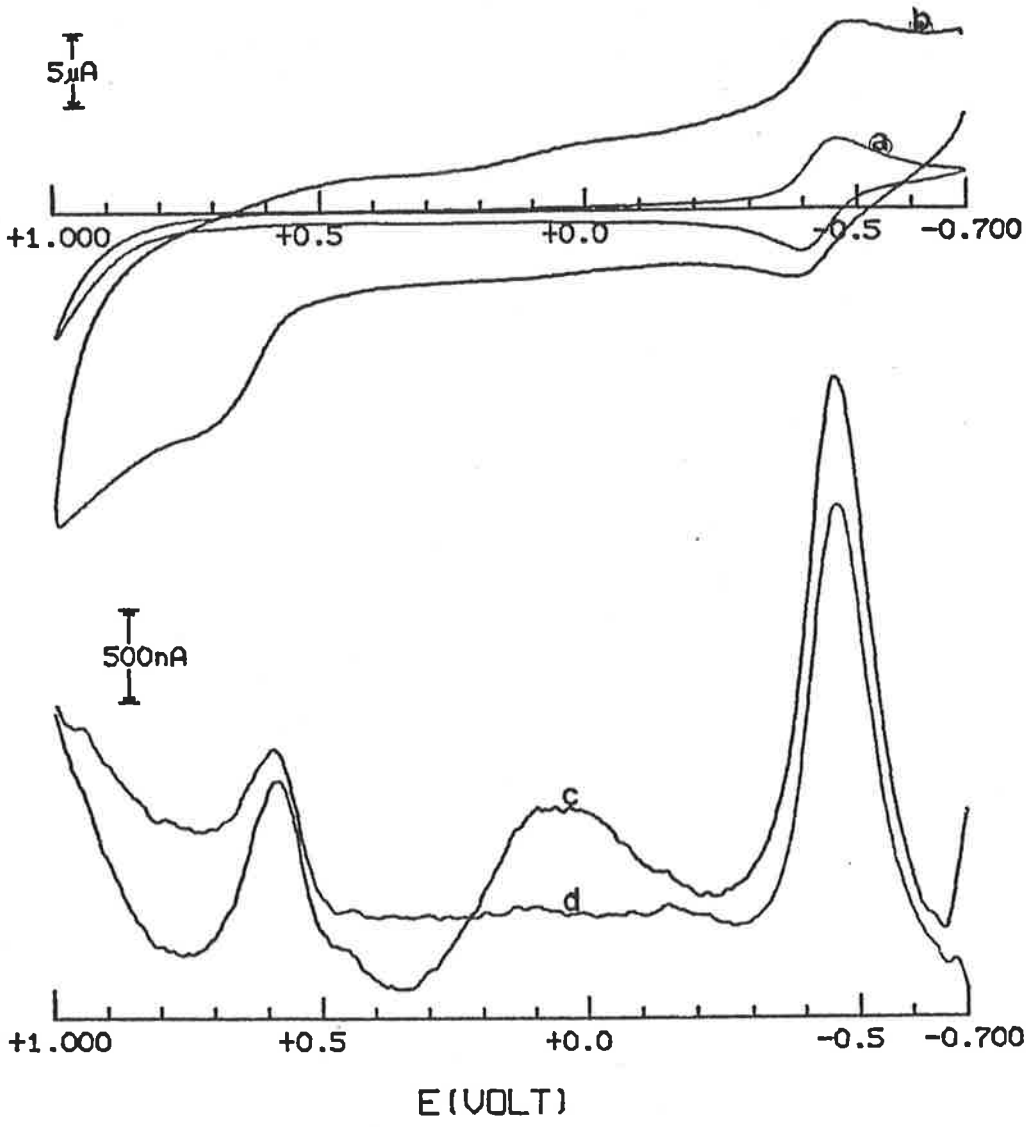

Fig. 3.4. Voltammograms of $[Ru(NH_3)_3(dpm)(OH_2)]^{2+}$ at pH 4.5. (a) Cyclic voltammogram at an unactivated G.C.E. (b) Cyclic voltammogram at an activated G.C.E. (c) Differential pulse voltammogram at an activated G.C.E. (d) Differential pulse voltammogram at an activated G.C.E., corrected for background current.

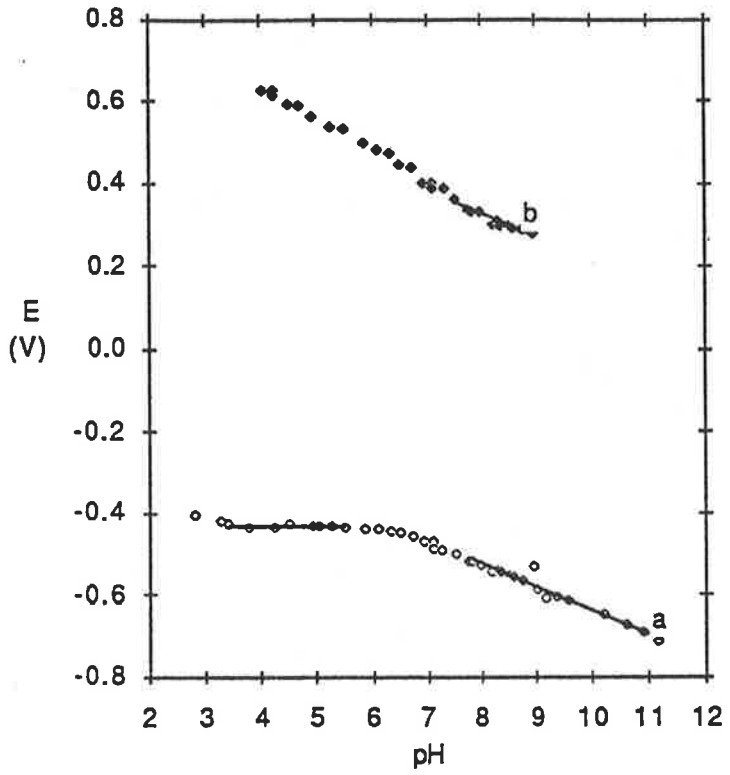

Fig. 3.5. Pourbaix diagrams for $[Ru(NH_3)_3(dpm)(OH_2)]$ redox couples. (a) Ru(III)/Ru(II) couple. (b) Ru(IV)/Ru(III) couple.

In the Differential Pulse Voltammogram of $[Ru(NH_3)_3(dpm)(OH_2)]^{2+}$ at the activated electrode, a broad peak at approximately +0.05 V was distinguishable, in addition to the peaks assigned to the $Ru^{3+/2+}$ and $RuO^{2+}/RuOH^{2+}$ couples. This peak is believed to be due to some electrochemical process involving the solvent and the activated electrode. When an instrumental background correction procedure was applied, this broad peak was no longer evident in the voltammogram.

The voltammograms of $[Ru(NH_3)_3(hna)(OH_2)]^{2+}$ are shown in Fig. 3.6. The CV appears poorly resolved because of the operation of a normalization process in the instrumental display. The display is normalized so that the point on the curve with the highest current is at the highest point possible in the display. In this case, the "tail" due to the solvent oxidation wave has the highest current so that the $Ru^{3+/2+}$ wave appears poorly resolved. The wave due to the $RuO^{2+}/RuOH_2^{3+}$ couple is evident in the CV as a shoulder to the solvent oxidation wave. In the DPV, this peak is better resolved. The Pourbaix diagram for these voltammograms, shown in Fig. 3.7, is consistent with the pH dependence of the two electrochemical processes being similar to those discussed above.

For the $Ru^{3+/2+}$ CV wave, the $E_{1/2}$ value at pH 3 was –0.26 V, and independent of pH below pH 4.6. Above pH 6.6, this wave varied with pH to the extent of –56 mV/pH. These results are indicative of the following redox processes.

pH<4.6

$$[Ru(NH_3)_3(hna)(OH_2)]^{2+} + e^- \rightleftharpoons [Ru(NH_3)_3(hna)(OH_2)]^{+} \quad \textbf{(3.11)}$$

pH>6.6

$$[Ru(NH_3)_3(hna)(OH)]^{+} + e^- + H^+ \rightleftharpoons [Ru(NH_3)_3(hna)(OH_2)]^{+} \quad \textbf{(3.12)}$$

For the $RuO^{2+}/RuOH_2^{3+}$ peak, the peak potential was +0.75 V at pH 5, and +0.37 V at pH 8. Between pH 4.8 and 5.6, the pH dependence was –114 mV/pH, and above 6.3 it was –59 mV/pH. This corresponds to the reactions 3.13 and 3.14.

4.8<pH<5.6

$$[Ru(NH_3)_3(hna)(O)]^{+} + e^- + 2H^+ \rightleftharpoons [Ru(NH_3)_3(hna)(OH_2)]^{2+} \quad \textbf{(3.13)}$$

pH>6.3

$$[Ru(NH_3)_3(hna)(O)]^{+} + e^- + H^+ \rightleftharpoons [Ru(NH_3)_3(hna)(OH)]^{+} \quad \textbf{(3.14)}$$

The intersection of the lines in the Pourbaix diagram was at pH 5.8 for the $Ru^{3+/2+}$ wave, and at 6.0 for the $RuO^{2+}/RuOH_2^{3+}$ peak, both of which are close to the spectroscopically determined pK_a value of 5.7, though somewhat higher.

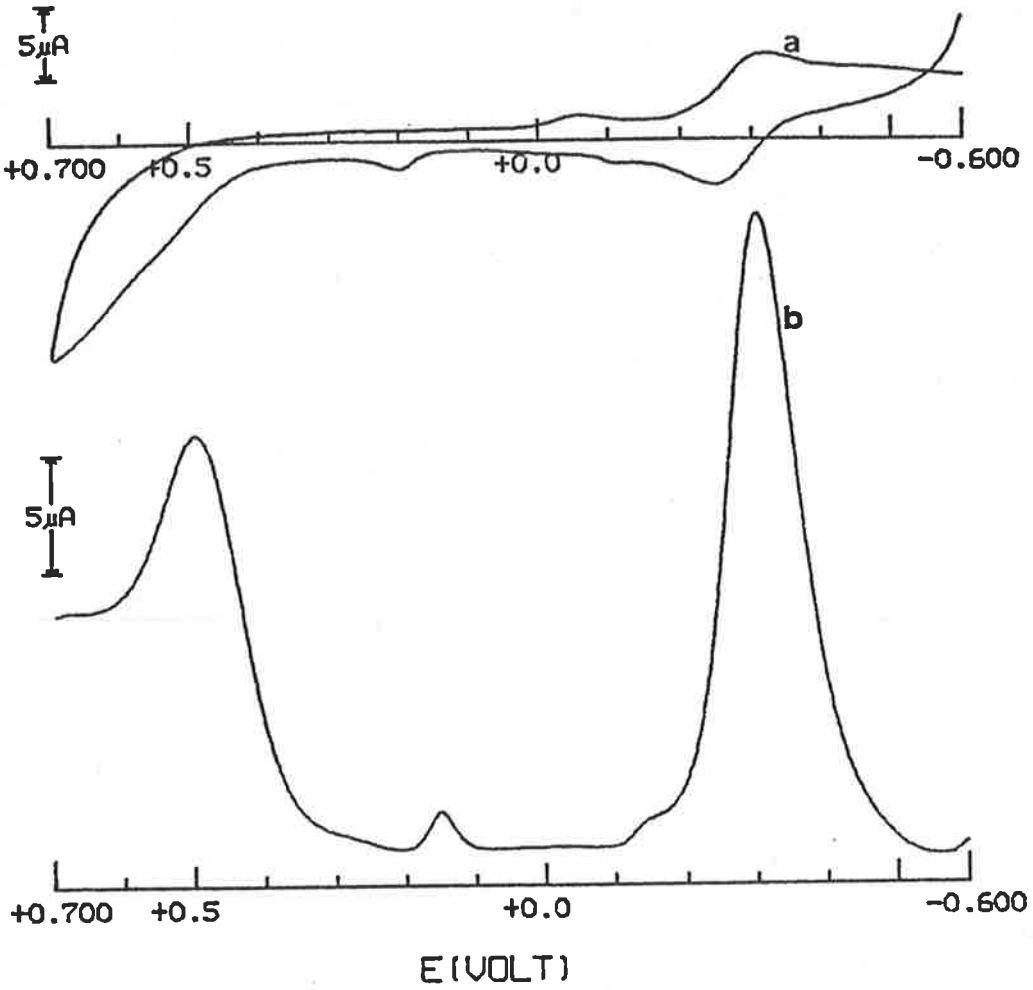

Fig. 3.6. Voltammograms of $[Ru(NH_3)_3(hna)(OH_2)]^+$ at pH 6.1. (a) Cyclic voltammogram at an activated G.C.E. (b) Differential pulse voltammogram at an activated G.C.E.

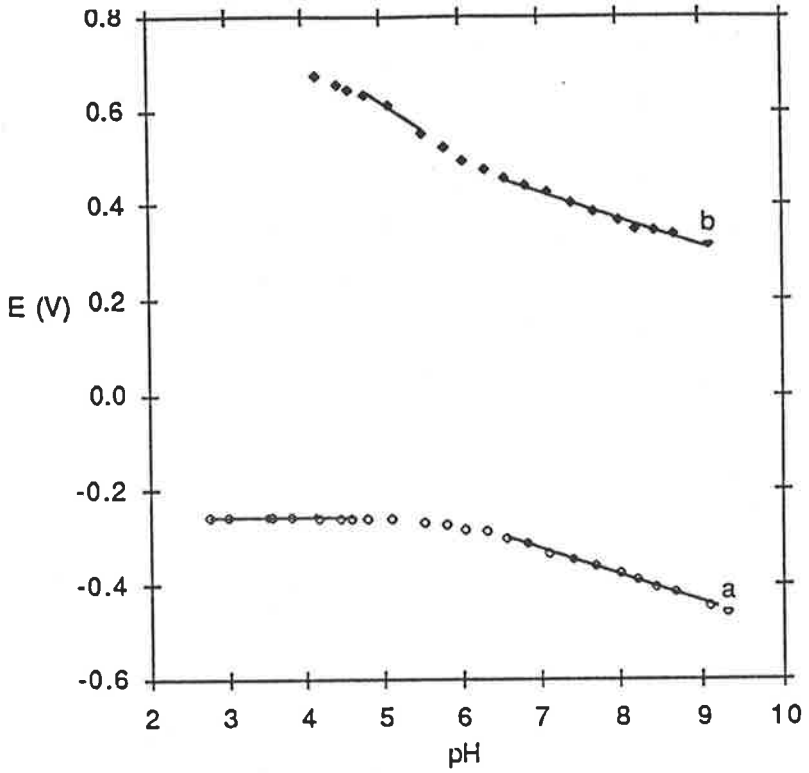

Fig. 3.7. Pourbaix diagrams for $[Ru(NH_3)_3(hna)(OH_2)]$ redox couples. (a) Ru(III)/Ru(II) couple. (b) Ru(IV)/Ru(III) couple.

The voltammograms of $[Ru(NH_3)_3(oxine)(OH_2)]^{2+}$ are shown in Fig. 3.8. The CV again appears poorly resolved because of the normalization process in the instrumental display and, once again, the wave due to the $RuO^{2+}/RuOH_2^{3+}$ couple is evident in the CV as a shoulder to the solvent oxidation wave. In the DPV, this peak is better resolved. The Pourbaix diagram for these voltammograms, shown in Fig. 3.9, reveals that the pH dependence of the two electrochemical processes is similar to those discussed above.

For the $Ru^{3+/2+}$ CV wave, the $E_{1/2}$ potential at pH 3 was –0.31 V, and independent of pH below pH 5.3. Above pH 6.2, this wave varied with pH to the extent of –56 mV/pH. These results are indicative of the following redox processes:

pH<5.3

$$[Ru(NH_3)_3(oxine)(OH_2)]^{2+} + e^- \rightleftharpoons [Ru(NH_3)_3(oxine)(OH_2)]^{+} \quad \textbf{(3.15)}$$

pH>6.2

$$[Ru(NH_3)_3(oxine)(OH)]^{+} + e^- + H^+ \rightleftharpoons [Ru(NH_3)_3(oxine)(OH_2)]^{+} \quad \textbf{(3.16)}$$

For the $RuO^{2+}/RuOH_2^{3+}$ peak, the peak potential was +0.61 V at pH 5, and +0.37 V at pH 8. Between pH 5 and 6, the pH dependence was –113 mV/pH, and above 6.6 it was –53 mV/pH. This corresponds to the reactions 3.17 and 3.18.

5<pH<6

$$[Ru(NH_3)_3(oxine)(O)]^{+} + e^- + 2H^+ \rightleftharpoons [Ru(NH_3)_3(oxine)(OH_2)]^{2+} \quad \textbf{(3.17)}$$

pH>6.6

$$[Ru(NH_3)_3(oxine)(O)]^{+} + e^- + H^+ \rightleftharpoons [Ru(NH_3)_3(oxine)(OH)]^{+} \quad \textbf{(3.18)}$$

The intersection of the lines in the Pourbaix diagram was at pH 6.2 for the $Ru^{3+/2+}$ wave, and at 6.3 for the $RuO^{2+}/RuOH_2^{3+}$ peak, both of which are close to the spectroscopically determined pK_a value of 6.0, though somewhat higher.

The complexes $[Ru(NH_3)_3(bzac)(OH_2)]^{2+}$ and $[Ru(NH_3)_3(sal)(OH_2)]^{2+}$ were not isolated as solid samples, but the CV reduction wave for each species was studied using solution samples withdrawn from the reaction mixtures. The Pourbaix diagrams are shown as Fig. 3.10 and 3.11. The behaviour of the two complexes at activated glassy carbon electrodes was not studied.

For $[Ru(NH_3)_3(bzac)(OH_2)]^{2+}$ the $E_{1/2}$ potential was –0.30 V at pH 3, and independent of pH between pH 5.4 and 3.0 Between pH 6 and 8, $E_{1/2}$ varied by –60 mV/pH. The intersection of the two lines in the Pourbaix diagram yields a pK_a value of 5.9. These results are consistent with the redox couples 3.19 and 3.20.

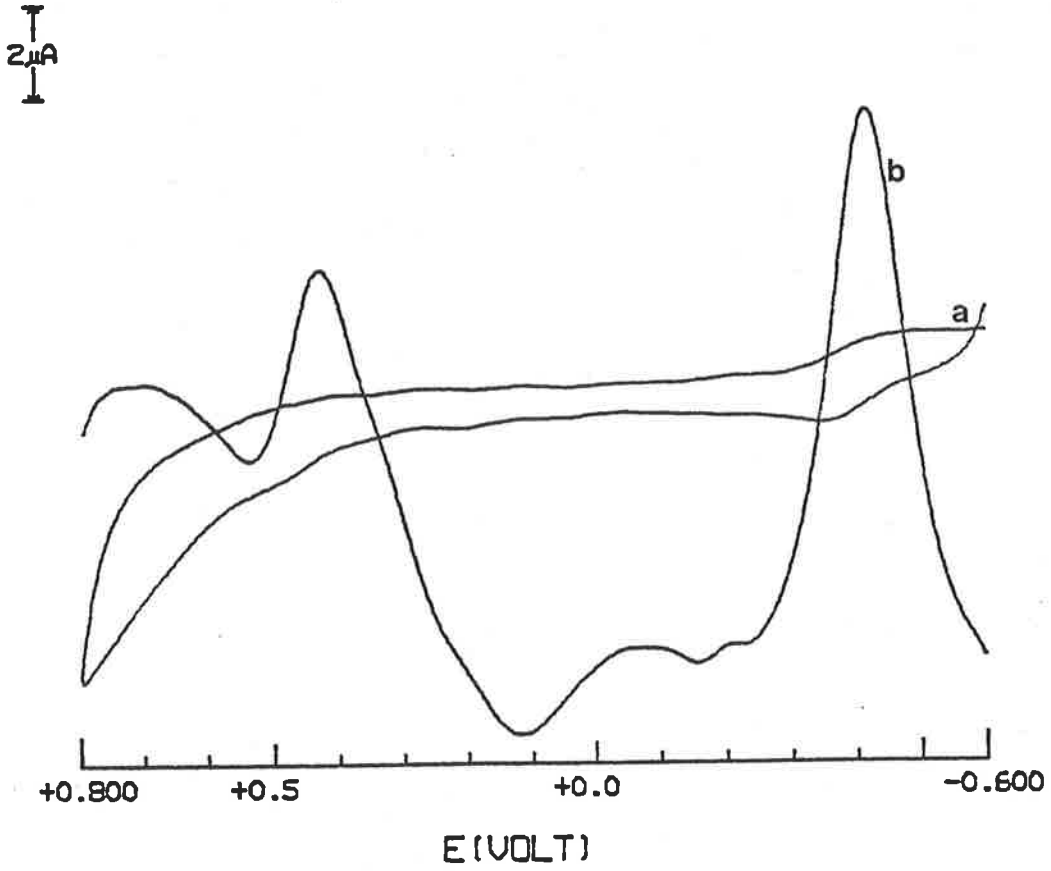

Fig. 3.8. Voltammograms of $[Ru(NH_3)_3(oxine)(OH_2)]^+$ at pH 7.0. (a) Cyclic voltammogram at an activated G.C.E. (b) Differential pulse voltammogram at an activated G.C.E.

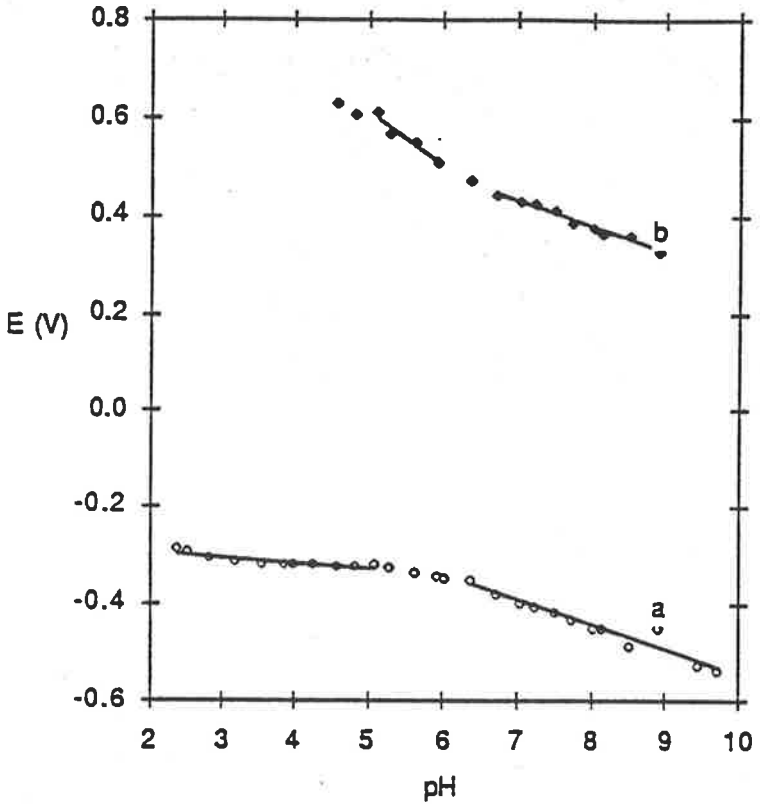

Fig. 3.9. Pourbaix diagrams for [$Ru(NH_3)_3(oxine)(OH_2)$] redox couples. (a) Ru(III)/Ru(II) couple. (b) Ru(IV)/Ru(III) couple.

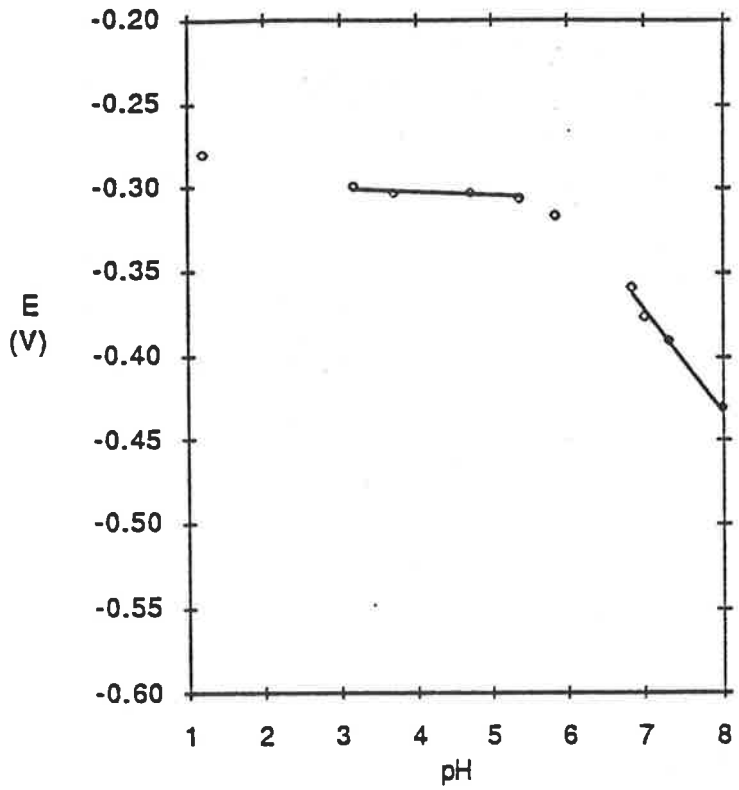

Fig. 3.10. Pourbaix diagram for the Ru(III)/Ru(II) redox couple of $[Ru(NH_3)_3(bzac)(OH_2)]^{2+}$.

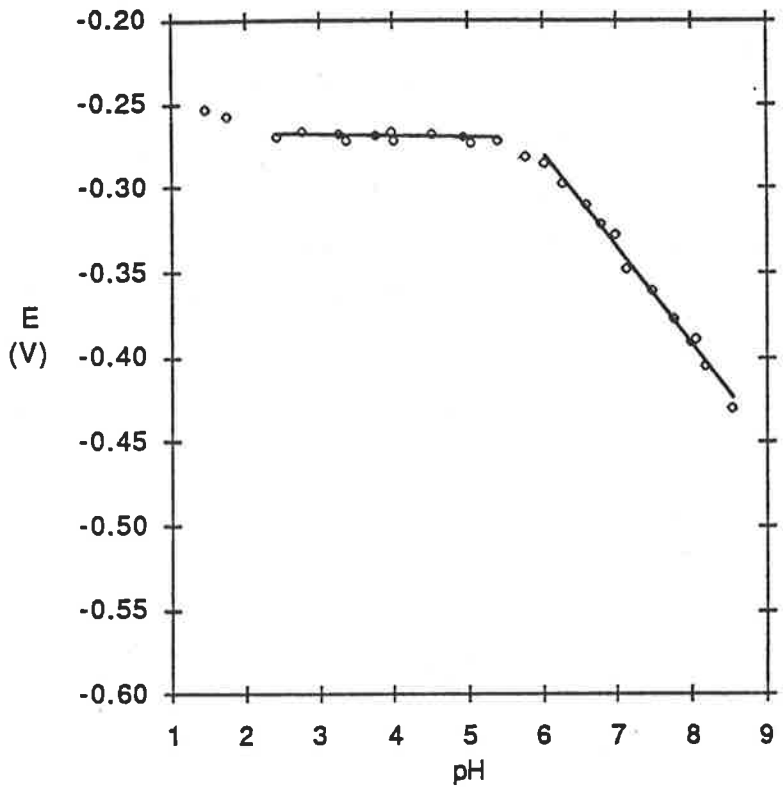

Fig. 3.11. Pourbaix diagram for the Ru(III)/Ru(II) redox couple of $[Ru(NH_3)_3(sal)(CH_2)]^{2+}$.

3.0<pH<5.4

$$[Ru(NH_3)_3(bzac)(OH_2)]^{2+} + e^- \rightleftharpoons [Ru(NH_3)_3(bzac)(OH_2)]^+ \quad \textbf{(3.19)}$$

6.0<pH<8.0

$$[Ru(NH_3)_3(bzac)(OH)]^+ + e^- + H^+ \rightleftharpoons [Ru(NH_3)_3(bzac)(OH_2)]^+ \quad \textbf{(3.20)}$$

For $[Ru(NH_3)_3(sal)(OH_2)]^{2+}$ the $E_{1/2}$ potential was –0.27 V at pH 3, and independent of pH between pH 5.4 and 2.4. Above pH 6, $E_{1/2}$ varied by –56 mV/pH. The intersection of the two lines in the Pourbaix diagram yields a pK_a value of 5.8. These results are consistent with the redox couples 3.21 and 3.22.

2.4<pH<5.4

$$[Ru(NH_3)_3(sal)(OH_2)]^{2+} + e^- \rightleftharpoons [Ru(NH_3)_3(sal)(OH_2)]^+ \quad \textbf{(3.21)}$$

pH>6.0

$$[Ru(NH_3)_3(sal)(OH)]^+ + e^- + H^+ \rightleftharpoons [Ru(NH_3)_3(sal)(OH_2)]^+ \quad \textbf{(3.22)}$$

3.2.6. The Electrochemistry of $[Ru(NH_3)_3(C_2O_4)(OH_2)]^+$. The electrochemistry of $[Ru(NH_3)_3(C_2O_4)(OH_2)]^+$ was also studied in aqueous buffer solutions at glassy carbon electrodes. It was possible to observe a reversible $Ru^{3+/2+}$ wave in the CV at negative potentials. The behaviour of this wave was identical at freshly polished and anodically activated electrodes (Fig. 3.12). At pH 3, the $E_{1/2}$ potential of this wave was –0.32 V and was independent of pH in the range pH 5.0 to pH 2.6. Between pH 7 and pH 9, the pH dependence for this wave was –59 mV/pH (Fig. 3.13). These results are consistent with the existence of two redox couples shown below. The intersection of the two lines in the Pourbaix diagram, at pH =5.8, is in close agreement with the spectroscopically determined pK_a value of 5.7.

2.6<pH<5.0

$$[Ru(NH_3)_3(C_2O_4)(OH_2)]^+ + e^- \rightleftharpoons [Ru(NH_3)_3(C_2O_4)(OH_2)] \quad \textbf{(3.23)}$$

7.0<pH<9.0

$$[Ru(NH_3)_3(C_2O_4)(OH)] + e^- + H^+ \rightleftharpoons [Ru(NH_3)_3(C_2O_4)(OH_2)] \quad \textbf{(3.24)}$$

The $E_{1/2}$ potential of $[Ru(NH_3)_3(C_2O_4)(OH_2)]^+$ at pH 3 is very close to that of $[Ru(NH_3)_4(C_2O_4)]^+$ [31], as can be seen from the data in Table 3.2. The difference in the two values is much smaller than in the case of the pentanedionate complexes, probably because there was no phosphate ion effect in the electrochemical studies on $[Ru(NH_3)_4(C_2O_4)]^+$.

An electrochemical wave due to the oxidation of $[Ru(NH_3)_3(C_2O_4)(OH_2)]^+$ could be observed at both freshly polished and anodically activated electrodes (Fig 3.12). At very slow scan rates (10 -

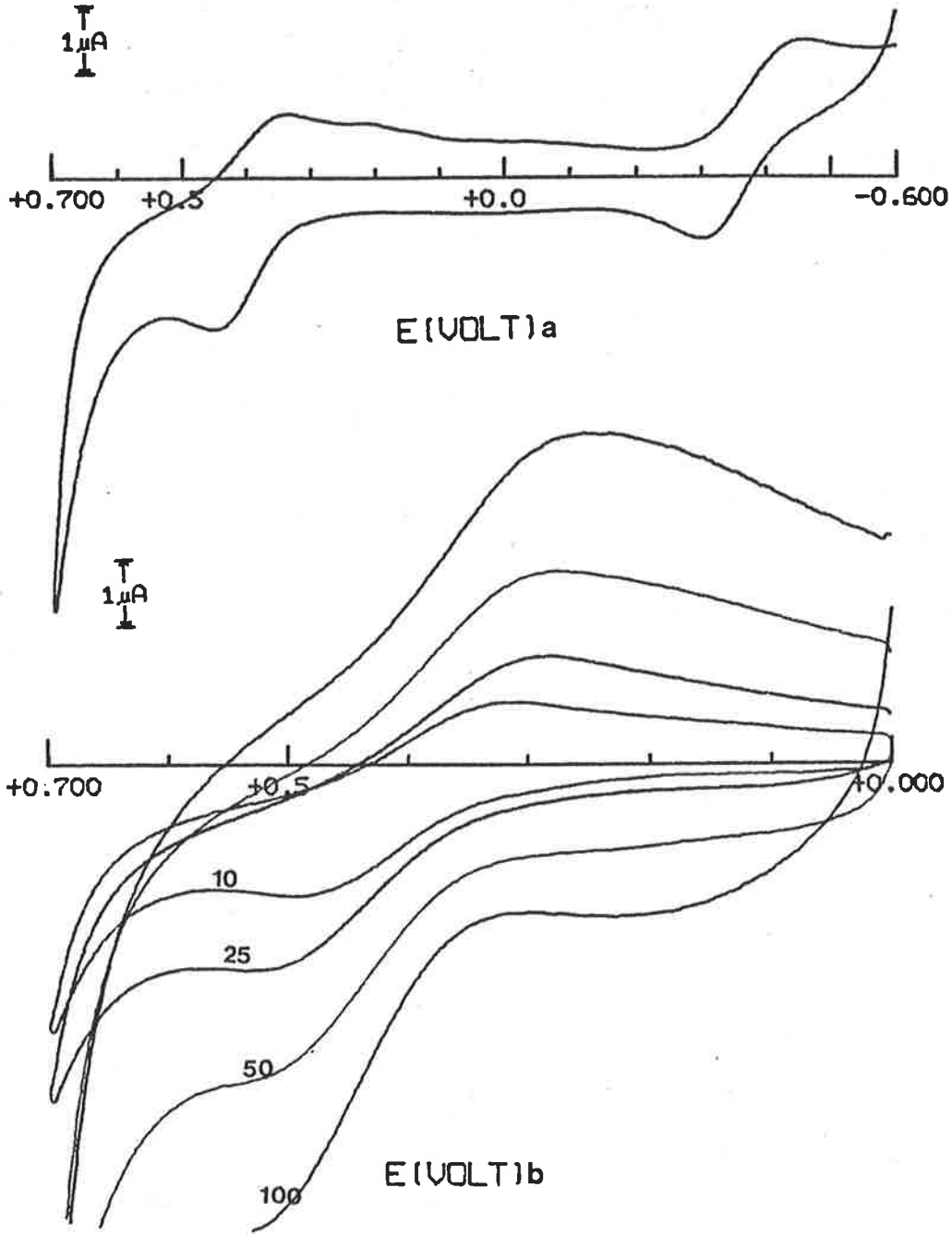

Fig. 3.12. Cyclic voltammograms of $[Ru(NH_3)_3(C_2O_4)(OH_2)]$ at pH 6.1, at a freshly-polished G.C.E. (a) Full potential scan. (b) Voltammograms at variable scan rate (mV sec^{-1}).

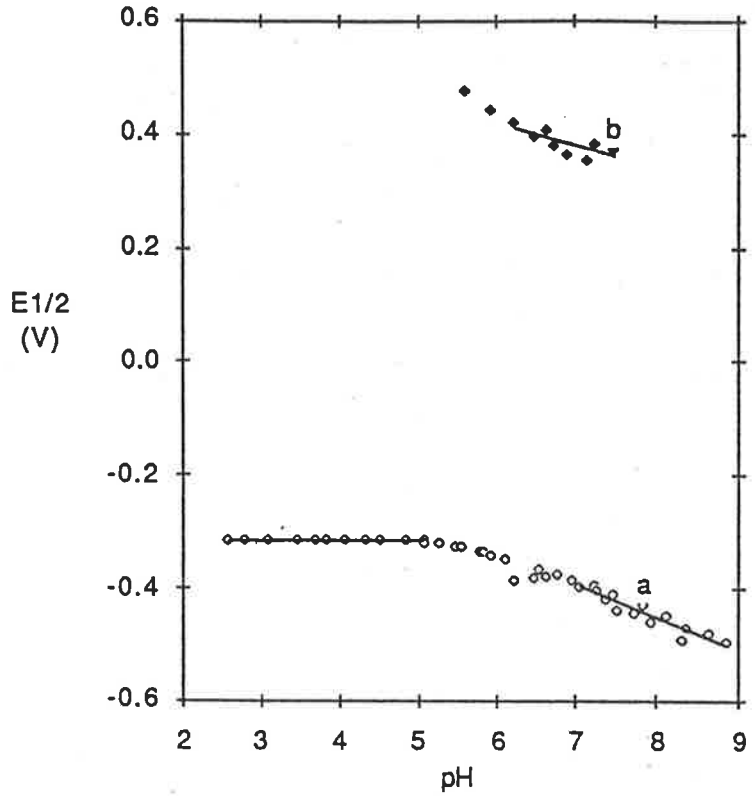

Fig. 3.13. Pourbaix diagrams for $[Ru(NH_3)_3(C_2O_4)(OH_2)]$ redox couples. (a) Ru(III)/Ru(II) couple. (b) Ru(IV)/Ru(III) couple.

25 mV sec^{-1}), it was possible to observe a quasi-reversible wave at neutral to high pH. At higher scan rates, and at lower pH, this wave broadened and merged with the solvent oxidation wave. In the Pourbaix diagram for this wave (Fig. 3.13), $E_{1/2}$ and the cathodic peak potential varied by –71 mV/pH above pH 6. The anodic peak potential remained almost constant with increasing pH because of the merging of this peak with the solvent oxidation wave. However, that the cathodic wave is well defined in this range, and its pH dependence is reasonably close to the ideal for a one proton/one electron transfer, is evidence that $[Ru(NH_3)_3(C_2O_4)(OH)]$ undergoes oxidation according to 3.25.

pH>6.0

$$[Ru(NH_3)_3(C_2O_4)(O)] + e^- + H^+ \rightleftharpoons [Ru(NH_3)_3(C_2O_4)(OH)] \quad \textbf{(3.25)}$$

When the electrochemical oxidation was performed at an activated electrode, there was no improvement in the resolution of Ru^{4+}/Ru^{3+} CV wave over that when a freshly polished electrode is used at low scan rates. The behaviour of the DPV peak was quite unusual. As the pH of the solution was increased, the pH dependence of the peak increased. Thus, at pH 4 the pH dependence was –41 mV/pH, while at pH 8 it was –150 mV/pH. This behaviour is the opposite to what would be expected if the DPV peak was due to the redox couple 3.25. It is apparent that the activated electrode affected the oxidation of $[Ru(NH_3)_3(C_2O_4)(OH_2)]^+$ in a manner different from the other examples where the activation procedure was used. One possible explanation is that, at high pH, the oxidation process was also involving the ammine NH groups. It has been shown previously that at high pH, an activated electrode can be used to observe the proton-coupled oxidation of $[Ru(NH_3)_6]^{3+}$. [27] If this same process was operating in the present case, then the pH dependence of the electrochemical oxidation would be much higher than anticipated.

The chemical oxidation of $[Ru(NH_3)_3(C_2O_4)(OH_2)]^+$ was attempted. However, when a solution of the complex, buffered at pH 7, reacted with hydrogen peroxide solution, a dark brown colour was observed in the solution, indicative of oxidative decomposition, as occurred with $[Ru(NH_3)_3(OH_2)_3]^{3+}$ and *cis* $[Ru(NH_3)_4(OH_2)_2]^{3+}$. [29]

3.2.7. Discussion of Electrochemical Results. The existence of well-behaved, pH dependent CV waves for the $[Ru(NH_3)_3(LL)(OH_2)]^{2+/+}$ couples is in agreement with what was to be expected from consideration of the ammine aqua complexes referred to in Chapter 2, and from the behaviour of substituted edta complexes of ruthenium(III). [17] As noted above, there are few examples of bidentate, uninegative ammine ruthenium(III) complexes with which these results may be compared. The similarity in the $E_{1/2}$ potentials of $[Ru(NH_3)_3(acac)(OH_2)]^{2+}$ and $[Ru(NH_3)_4(acac)]^{2+}$has already been noted. All the substituted ammineaqua ruthenium(III) complexes have $Ru^{3+/2+}$ couples with $E_{1/2}$ potentials more negative than that of

$[Ru(NH_3)_3(OH_2)_3]^{3+}$. This reflects the electron donating ability of the ligands used, as was also evident from the comparison of pK_a values. The reduction potentials were more negative because the donation of electron density into the metal orbitals by the ligands makes the addition of an electron by electrochemical reduction less energetically favourable.

The relative order of the electron donating ability, as illustrated by reduction potential, is dpm>acac>oxine>bzac>sal>hna. The same ranking for the diketonate ligands, dpm, acac and bzac, was found for the reduction of $Ru(diketonate)_3$ complexes. [18, 30] Similarly, in a series of vanadium complexes with benzolyhydrazone ligands, $\{R=N\text{-}N\text{-}C(O)Ph\}^{2-}$, the reduction potentials of the V(IV) complexes varied with R in the same order. [31]

The existence of a $RuO^{2+}/RuOH_2^{3+}$ couple in the electrochemistry of the substituted ammineaqua ruthenium(III) complexes is also to be expected on the basis of comparison with the ammineaqua complexes reported in Chapter 2, and also by comparison with the substituted aquaruthenium 2+ and 3+ complexes referred to in Chapter 1. It is apparent from the data in Table 3.3 that the Ru(IV)/Ru(III) couples occur over a smaller range of potentials than the Ru(III)/Ru(II) couples and that, in the absence of π-backbonding, the difference in the potentials of the Ru(IV)/Ru(III) couple and the Ru(III)/Ru(II) couple is within the range 0.6 V - 0.8 V. The small range over which the Ru(IV)/Ru(III) couples occur has been noted by other authors, and this has been attributed to the similar σ-donor properties of the ammine and polypyridyl ligands, while the large range of potentials for the Ru(III)/Ru(II) couples was attributed to the effect of the $d_{\pi\text{-}\pi^*}$ interaction in the Ru(II) state. [28] These present results lead to the conclusion that it is not only the σ-donor properties of the co-ligands, but the overall electron donating ability which determines the potential of the proton-coupled oxidation of Ru(III). The potentials for the oxidation of the two polypyridyl complexes listed in the table are indicative that, perhaps, the π-acceptor ability of the ligands has some impact on the oxidation. In similar comparitive studies, it was found that, for a large range of $Ru(diketonate)_3$ complexes, there was a relatively constant difference between the reduction and oxidation potentials. [18, 30]

There is now, also, an apparent trend in the stability of the oxoruthenium(IV) complexes. On a voltammetric scale, the substituted triammineoxoruthenium complexes with the uninegative ligands are less stable than the triamminetriaqua, which, it has already been noted, is less stable than the pentaammine complex, the polypyridyl complexes and the macrocyclic tertiary amine complexes. [28, 29, 32, 33] A possible explanation for this trend is that the π-donating ability of the O^{2-} ligand, when combined with that of the bidentate, uninegative ligands, is too great to be accomodated on a Ru(IV) centre. In previous cases where the $RuO^{2+}/RuOH_2^{3+}$ couple has been observed, the other ligands have been either σ-donors, as in the case of $[Ru(NH_3)_3(OH_2)_3]^{3+}$, $[Ru(NH_3)_5(OH_2)]^{3+}$ [28a]

{M}	E(III/II)[a]	E(IV/III)[b]	ΔE(V)	Reference
$\{Ru(NH_3)_3acac\}^c$	−0.39	+0.45	.84	This work
$\{Ru(NH_3)_3C_2O_4\}^c$	−0.41	+0.37	.78	"
$\{Ru(NH_3)_3hna\}^c$	−0.32	+0.43	.75	"
$\{Ru(NH_3)_3(OH_2)_2\}^d$	−0.19	+0.49	.68	"
$\{Ru(NH_3)_4(OH_2)\}^d$	−0.20	+0.60	.80	"
$\{Ru(NH_3)_5\}^e$	−0.21	+0.41	.62	28
{Ru(trpy)(bpy)}[f]	+0.48	+0.61	.13	32
$\{Ru(bpy)_2(OH_2)\}^g$	+0.53	+0.76	.23	33

Table 3.3. Potentials (V vs SCE) of Ru(IV) and Ru(III) couples involving proton-coupled electron transfer. (a) $\{M\}OH + e^- + H^+ \rightleftharpoons \{M\}OH_2$. (b) $\{M\}=O + e^- + H^+ \rightleftharpoons \{M\}OH$. (c) pH = 7. (d) pH = 5. (e) pH = 4.72. (f) pH =7. (g) pH =4.

and *trans* $[Ru(tmc)(OH_2)(O)]^{2+}$ [29], or σ-donor/π-acceptor ligands as in the case of $[Ru(trpy)(bpy)(O)]^{2+}$ [32] and *cis* $[Ru(bpy)_2(OH_2)(O)]^{2+}$. [33] In these latter cases, there was not any great competition to the O^{2-} ligand from other π-donors. It would appear, therefore, that the inclusion of a π-donor ligand in the coordination sphere destabilizes the Ru^{IV}=O group and possibly favours the formation of Ru(V) complexes. This destabilization process probably competes with the oxidative dehydrogenation reaction for the decomposition of the Ru(IV) complex.

Support for this proposal can be found in a report of oxovanadium complexes containing tridentate, dinegative ligands. [34] It was found that, with dinegative ligands having O-N-O donor atoms, and for which stable $V^{IV}(L)_2$ complexes could be obtained, V(IV) complexes of the type, $[V(L)(O)]_2$, were very readily oxidized to the corresponding V(V) complexes. It seems likely, therefore, that this effect is also important in determining the stability of the oxoruthenium(IV) complexes.

That it was possible to observe a quasi-reversible proton-coupled Ru^{4+}/Ru^{3+} wave in the oxalate complex supports the arguments used concerning the π-donating ligands destabilizing the Ru^{IV}=O species. The pK_a of $[Ru(NH_3)_3(C_2O_4)(OH_2)]^+$ implies that the oxalate ion is not a good π-donor ligand because, despite being a dinegative ligand, the pK_a value of the complex is the same as that of the hna complex, which is only a uninegative ligand. Clearly then, the electron-donor properties of the oxalate ion are not sufficiently strong to interfere with the stabilization of the Ru(IV) complex by the oxo ligand.

3.2. 8. Comparison of $E_{1/2}$ with pK_a. In discussing the pK_a values and $E_{1/2}$ potentials of the substituted triammine complexes it was stated that both depended on the electron donating ability of the particular ligand. It might be expected that, if the same ligand effects are operating in determining both quantities, there would be a good correlation between them. In Fig. 3.14 the $E_{1/2}$ potentials for the complexes under consideration are plotted against pK_a. It can be seen from the diagram that there is a linear relationship between $E_{1/2}$ at pH 3 and pK_a for the six complexes with uninegative, bidentate ligands.

It can also be noticed that the $E_{1/2}$ potential of $[Ru(NH_3)_3(C_2O_4)(OH_2)]^+$ is more negative than would be predicted from consideration of its pK_a. However this apparent anomaly should not be regarded as serious, because there are several possible reasons why the comparison of the oxalate complex with the others should not be valid. The oxalate complex differs from the others in at least three respects. The oxalate ligand is dinegative whereas the ligands in the other complexes are uninegative. The metal ligand ring is 5-membered rather than 6-membered as in the case of the complexes with the uninegative ligands. Thus there may be additional steric factors to be

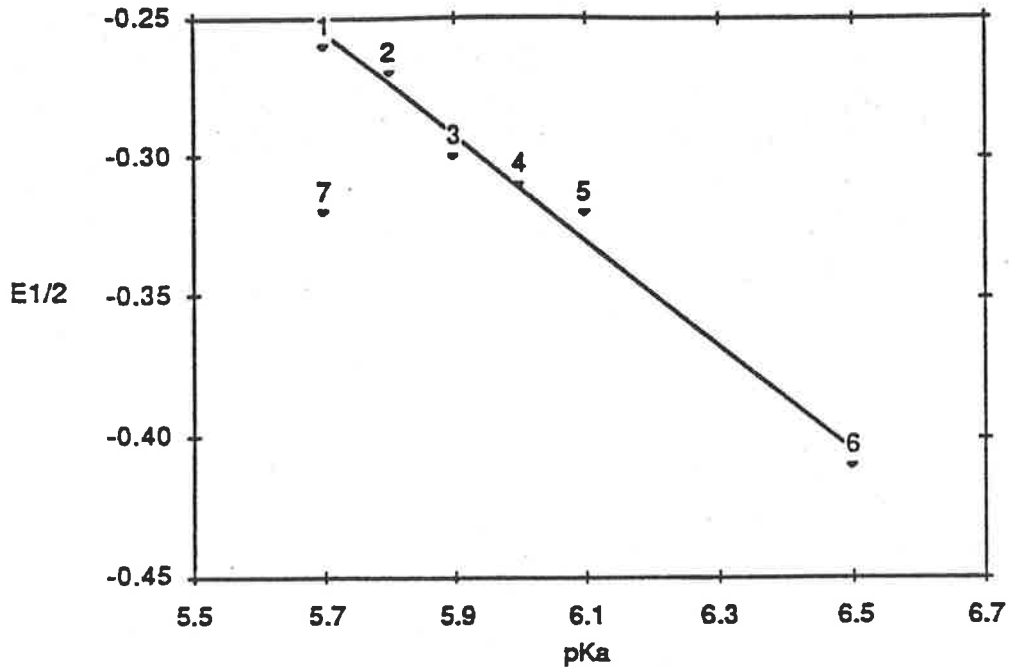

Fig. 3.14. Graph of $E_{1/2}$ at pH 3 vs pK_a for substituted triammineaqua ruthenium(III) complexes. (1) L = hna. (2) L = sal. (3) L = bzac. (4) L = oxine. (5) L = acac. (6) L = dpm. (7) L = C_2O_4.

considered. Finally, the dissociation of a proton from the Ru(III) aqua complex or reduction to Ru(II) results in a neutral species in solution, whereas the other complexes retain a single positive charge after both these reactions. It is likely that there will be differences in the solvation of these complexes because of this factor, and so comparisons between the oxalate complex and the other Ru(III) complexes must be made with care.

3.2.9. Electrolytic Reduction of Ru(III) Complexes. The complexes $[Ru(NH_3)_3(C_2O_4)(OH_2)]^+$, $[Ru(NH_3)_3(oxine)(OH_2)]^{2+}$ and $[Ru(NH_3)_3(hna)(OH_2)]^{2+}$ were reduced at a mercury pool cathode in a 0.1 mol dm^{-3} methanesulphonic acid solution. The reduction potential was chosen to be 150 mV cathodic of the $E_{1/2}$ determined by CV. The solutions were degassed with either argon or nitrogen gas, and in the latter case, there was no evidence of the formation of a dinitrogen complex with any of the reduced species. Reduction with amalgamated zinc produced the same results as electrolytic reduction.

When $[Ru(NH_3)_3(C_2O_4)(OH_2)]^+$ was reduced, the initial yellow colour of the solution faded to almost colourless. After about 45 minutes, at which time a charge equal to 0.8 electron per ruthenium had been passed, and the electrolytic current had decayed to a steady state, a CV of the solution contained a single wave with $E_{1/2} = -0.10$ V, consistent with the presence of $[Ru(NH_3)_3(OH_2)_3]^{3+}$. The identity of the product was confimed by the uv/vis spectrum, which was the same as for fresh samples of $[Ru(NH_3)_3(OH_2)_3]^{3+}$ under similar conditions.

The hydrolysis of the oxalate complex was to be expected given the lability of the carboxylate ligand in other Ru(II) ammine complexes. [4] Clearly, though the CV of $[Ru(NH_3)_3(C_2O_4)(OH_2)]^+$ is reversible at moderate scan rates (25 - 100 mV sec^{-1}), on a longer time scale the hydrolysis reaction is able to occur to an appreciable extent.

During the initial stage of the reduction of $[Ru(NH_3)_3(hna)(OH_2)]^{2+}$, the green colour of the original complex was quickly replaced by a purple colour. The purple species was very unstable to oxidation, decomposing to the original complex if the reduction was halted momentarily, or if a sample was removed from the reduction cell to allow determination of its uv/vis spectrum. If the reduction was allowed to continue, over a period of about 45 minutes, the purple colour faded to yellow, and the total charge which had passed when the current reached a steady state was equivalent to more than two electrons per ruthenium. There was no current flow if, at this stage, an oxidizing potential was applied to the cell. A CV of the yellow solution contained a single, irreversible wave, with a cathodic peak potential of –0.28 V. It is apparent that the Ru(II) complex, which is the initial reduction product, is capable of accepting further electrons, possibly into the π system of the ligand, and that the resulting species is not capable of undergoing electrochemical oxidation.

When $[Ru(NH_3)_3(oxine)(OH_2)]^{2+}$ was reduced, the initial green colour was gradually replaced by a golden-brown colour. A CV of the reduced solution showed that the golden-brown species was $[Ru(NH_3)_3(oxine)(OH_2)]^{+}$ and if the solution was exposed to the air, the green colour returned.

It was possible to determine a semi-quantitative uv/vis spectrum of the Ru(II) complex. As the reduction reaction proceeded, the bands at 250 nm, 370 nm and 674 nm in the uv/vis spectrum of $[Ru(NH_3)_3(oxine)(OH_2)]^{2+}$ were replaced by bands at 235 nm and 465 nm, with isosbestic points at 242, 265, 335 and 400 nm (Fig. 3.15.) The estimated molar absorptivities were $\varepsilon_{235} = 3 \times 10^4$ and $\varepsilon_{465} = 6 \times 10^3$. It was a little surprising that these intra-ligand bands were so greatly affected by the reduction of Ru(III) to Ru(II), because it would be expected that the reduction would not have a great effect on the energy of the ligand orbitals. However, similar spectral changes have been noted during the electrolytic reduction of $Ru(dbm)_3$ to $Ru(dbm)_3^-$. [18]

3.2.10. Description of the Crystal Structure of $[Ru(NH_3)_3(acac)(OH_2)](S_2O_6).2H_2O$. Cubic crystals of $[Ru(NH_3)_3(acac)(OH_2)](S_2O_6).2H_2O$ were obtained from the synthesis reaction mixture after ethanol had been added to a solution of the reaction product in dilute dithionic acid. The crystal structure was determined by Dr. E. R. T. Tiekink, and is shown in Fig. 3.16, which also shows the atomic numbering scheme employed. The bond lengths and angles are listed in Tables 3.4 and 3.5, which follow Fig. 3.16.

The structure comprises an almost perfectly octahedral arrangement of donor atoms about the ruthenium ion. All the bond angles are close to either 90 or 180 degrees. The ammine ligands occupy one face of the octahedron, as is the case in the precursor complex, $Ru(NH_3)_3Cl_3$. [35]

The average length of Ru-N bonds for the ammine ligands *trans* to acac is 2.111 Å, which is slightly shorter than the average Ru-N distance in $Ru(NH_3)_3Cl_3$ (2.121 Å) [35], and slightly longer than the average length in $[Ru(NH_3)_6](BF_4)_3$ (2.104 Å). [36] The comparison with the structure of $Ru(NH_3)_3Cl_3$ must be treated cautiously, due to the presence of extensive hydrogen bonding in that complex. The slight increase in the Ru-N distance in the acac complex, compared with the hexaammine, is probably due to the lower charge on the ruthenium ion. The Ru-N bond which is *trans* to the the aqua ligand is slightly shorter than the others, being 2.046(11) Å. This is possibly due to the lesser competition, between the ammine and aqua ligand for the same metal orbital, than between the ammine ligands and the anionic acac ligand.

The Ru-O bond distance to the aqua ligand is 2.058(10) Å, which is longer than the average Ru-O distance (2.029 Å) in $[Ru(OH_2)_6](pTS)_3$ [37], possibly due to the lower charge on the ruthenium centre. The average Ru-O distance between the metal and the acac ligand is 2.004 Å, which is very close to average Ru-O distance in $Ru(acac)_3$ (2.00 Å). [38] The aqua ligand was

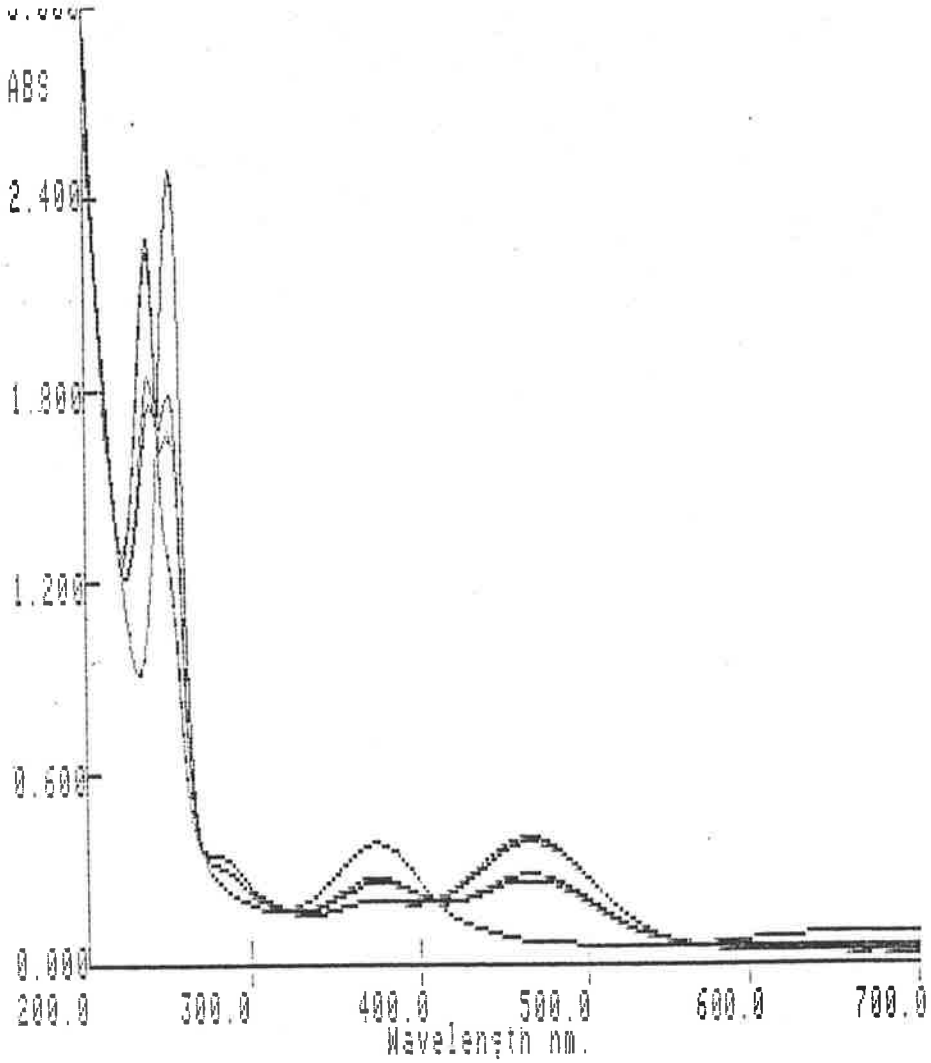

Fig. 3.15. uv/vis spectra of $[Ru(NH_3)_3(oxine)(OH_2)]^{2+}$ under conditions of reductive electrolysis.

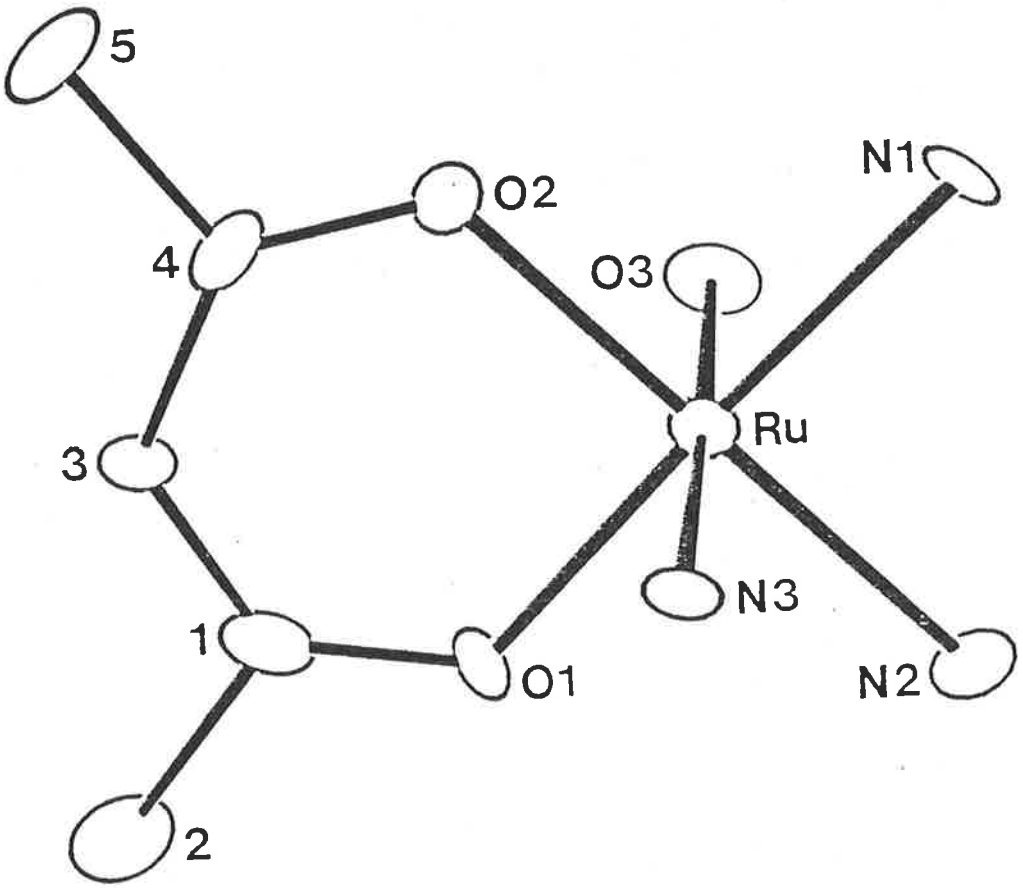

Fig. 3.16. X-ray crystal structure of $[Ru(NH_3)_3(acac)(OH_2)]S_2O_6.2H_2O$.

Atoms	Distance	Atoms	Distance
Ru–O(1)	1.995(11)	Ru–O(2)	2.013(12)
Ru–N(1)	2.097(14)	Ru–N(2)	2.124(15)
Ru–N(3)	2.046(11)	Ru–O(3)	2.058(10)
C(1)–O(1)	1.26(3)	C(4)–O(2)	1.27(2)
C(1)–C(2)	1.54(3)	C(1)–C(3)	1.40(3)
C(3)–C(4)	1.38(2)	C(4)–C(5)	1.49(2)
S(1)–O(4)	1.45(1)	S(1)–O(5)	1.46(1)
S(1)–O(6)	1.43(1)	S(2)–O(7)	1.46(1)
S(2)–O(8)	1.45(1)	S(2)–O(9)	1.44(1)
S(1)–S(2)	2.127(6)		

Table. 3.4. Bond lengths in $[Ru(NH_3)_3(acac)(OH_2)]S_2O_6.2H_2O$.

O(1)–Ru–O(2)	93.9(5)	O(1)–Ru–O(3)	90.7(5)
O(1)–Ru–N(1)	178.1(6)	O(1)–Ru–N(2)	87.4(6)
O(1)–Ru–N(3)	88.4(6)	O(2)–Ru–O(3)	90.8(5)
O(2)–Ru–N(1)	88.0(6)	O(2)–Ru–N(2)	177.3(5)
O(2)–Ru–N(3)	87.8(5)	O(3)–Ru–N(1)	89.1(5)
O(3)–Ru–N(2)	91.5(5)	O(3)–Ru–N(3)	178.2(5)
N(1)–Ru–N(2)	90.7(5)	N(1)–Ru–N(3)	91.8(5)
N(2)–Ru–N(3)	89.9(5)		
Ru–O(1)–C(1)	122(2)	Ru–O(2)–C(4)	124(2)
O(1)–C(1)–C(2)	117(2)	O(2)–C(4)–C(3)	125(2)
C(3)–C(1)–O(1)	128(2)	C(5)–C(4)–O(2)	116(2)
C(2)–C(1)–C(3)	114(2)	C(3)–C(4)–C(5)	119(2)
S(2)–S(1)–O(4)	103.9(5)	S(2)–S(1)–O(5)	104.0(6)
S(2)–S(1)–O(6)	105.2(6)	O(4)–S(1)–O(5)	113.8(9)
O(4)–S(1)–O(6)	113.5(8)	O(5)–S(1)–O(6)	114.9(8)
S(1)–S(2)–O(7)	104.2(6)	S(1)–S(2)–O(8)	104.8(6)
S(1)–S(2)–O(9)	103.2(5)	O(7)–S(2)–O(8)	113.4(9)
O(7)–S(2)–O(9)	116.4(10)	O(8)–S(2)–O(9)	113.1(8)

Table. 3.5. Bond angles in $[Ru(NH_3)_3(acac)(OH_2)]S_2O_6.2H_2O$.

involved in significant hydrogen bonding contacts with the dithionate anion, with the O-O' distances being 2.64 and 2.67 Å.

3.3. Ruthenium(II) Complexes.

3.3.1. Preparation of Complexes. In aqueous solution, $[Ru(NH_3)_3(OH_2)_3]^{2+}$ reacted with π-acceptor ligands to give brightly coloured solutions of the substituted ammine complexes. $[Ru(NH_3)_3(OH_2)_3]^{2+}$ was either generated prior to reaction with the ligand by reduction of $[Ru(NH_3)_3(OH_2)_3]^{3+}$ with hydrogen over platinum black, or by reduction of the Ru(III) complex by amalgamated zinc or hydrogen over platinum black in the presence of the ligand. The latter procedure causes a lowering of the pH, which assists the reactions through the dissolution of some protonated ligands in the aqueous solvent. Solutions of $[Ru(NH_3)_3(OH_2)_3]^{2+}$ had a distinctive golden colour which changed when ligands were added to the solution. The progress of the reactions could be monitored voltammetrically using 100 µl samples of the reaction mixture in aliquots of 0.1 mol dm^{-3} $MeSO_3H$. In this medium, the $[Ru(NH_3)_3(OH_2)_3]^{3+/2+}$ couple had a DPV peak at approximately –0.15 V (on an anodic scan). The peak current at this potential could be seen to decrease during the course of the reaction, with the concomitant appearance of a peak at positive potentials. If the ligand was to be added to a solution of the pre-reduced complex, SCP was used to show that reduction was substantially complete before the ligand was added.

When the ligand was 1,10-phenanthroline, the reaction involved stirring a solution of $[Ru(NH_3)_3(OH_2)_3]^{2+}$ with 1 molar equivalent of the ligand at room temperature for periods of up to 4 hours, at which time DPV showed the substitution reaction to be substantially complete. At this stage, the reaction mixture was an intense red-coloured solution from which $[Ru(NH_3)_3(phen)(OH_2)](PF_6)_2$ could be isolated after addition of excess NH_4PF_6. However, when the ligand was 2,2'-bipyridine, reaction under similar conditions resulted in the isolation of $[Ru(NH_3)_2(bpy)_2](PF_6)_2$. The identity of this product was verified by microanalysis and comparison of its uv/vis spectrum with that reported for this complex in the literature. [39]

The possibility of obtaining $[Ru(NH_3)_3(bpy)(OH_2)]^{3+}$, in order to study its reduction, was investigated. The reaction betwen bpy and $[Ru(NH_3)_3(OH_2)_3]^{3+}$ in ethanol was monitored voltammetrically. Using DPV, it was possible to observe the appearance of $[Ru(NH_3)_2(bpy)_2]^{3+}$ (E_p = +0.62 V) while there were still appreciable amounts of $[Ru(NH_3)_3(OH_2)_3]^{3+}$ in solution. The mono bpy complex could be identified by the presence of a DPV peak at +0.24 V, which is close to the $E_{1/2}$ potential of the $[Ru(NH_3)_4(bpy)]^{3+/2+}$ couple. [40] When phen was used, however, there was no evidence of the formation of $[Ru(NH_3)_2(phen)_2]^{3+}$ until about 10 hours had elapsed, by which time there was no evidence of any significant amounts of $[Ru(NH_3)_3(OH_2)_3]^{3+}$ in solution. It is apparent that the reaction of bpy with $[Ru(NH_3)_3(bpy)(OH_2)]^{3+}$ proceeds more readily than the

reaction of bpy with $[Ru(NH_3)_3(OH_2)_3]^{3+}$, whereas there is no such complication in the reaction between phen and $[Ru(NH_3)_3(OH_2)_3]^{3+}$.

$[Ru(NH_3)_3(OH_2)_3]^{2+}$reacted with one molar equivalent of 2(aminomethyl)pyridine, to give $[Ru(NH_3)_3(ampy)(OH_2)]^{2+}$, the PF_6^-salt of which precipitated from the reaction mixture as a canary yellow solid after the addition of NH_4PF_6. Solutions and solid samples of this complex were unstable, even when stored in the freezer compartment of the refrigerator. On standing overnight, the yellow samples turned red. DPV analysis of the red samples revealed that, in addition to a peak at +0.03 V, which was characteristic of the fresh sample, there was an additional peak at +0.38 V. If $NaClO_4$ was used as the precipitating agent in the reaction, the red colour formed immediately in the reaction mixture. This led to the conclusion that the change in colour was due to an oxidation reaction, in this latter case by the ClO_4^- ion. It has been reported previously that $[Ru(NH_3)_4(ampy)_2]^{2+}$ undergoes a ligand-based oxidation, resulting in the formation of a red-coloured 2-iminomethylpyridine complex. [40] A similar reaction has also been observed in the case of $[Ru(bpy)_2(ampy)]^{2+}$. [41] That the red compound was the result of oxidation and not due to the substitution of a second ampy ligand on the Ru(II) centre is supported by consideration of its $E_{1/2}$ potential. The $E_{1/2}$ potential of *cis* $[Ru(NH_3)_4(py)_2]^{2+}$ is +0.26 V [42], and it would be expected that a bis ampy complex would have a DPV peak near this value. That this is less than the oxidation potential of the red compound implies that the imine portion of the iminomethylpyridine ligand is a better π-acceptor than a second pyridine molecule.

$[Ru(NH_3)_3(MeCN)_3]^{2+}$ was formed by reaction of $[Ru(NH_3)_3(OH_2)_3]^{2+}$ with acetonitrile. $[Ru(NH_3)_3(OH_2)_3]^{3+}$ was reduced by amalgamated zinc in degassed 0.01 mol dm^{-3} HTFMS solution in the presence of excess ligand for 4.5 hours. After filtering the resultant canary yellow solution, a pale yellow solid could be precipitated by the addition of NH_4PF_6. The chloride and bromide salts were then obtained by dissolving the PF_6^- salt in butanone and adding an excess of the appropriate tetra(n-butyl)ammonium halide salt to the solution. When $[Ru(NH_3)_3(OH_2)_3]^{2+}$ reacted with two eqivalents of benzonitrile (PhCN), the solid isolated after the addition of excess NH_4PF_6 contained a mixture of three compounds in the ratio 1:10:1, as shown by the relative heights of the DPV peaks. The potentials of the three peaks (+0.25 V, +0.64 V and +0.95 V) were indicative of a mixture of the mono, bis and tris cyanobenzene complexes. The $E_{1/2}$ values for $[Ru(NH_3)_5(PhCN)]^{2+}$ and *cis* $[Ru(NH_3)_4(PhCN)_2]^{2+}$ are, +0.27 V and +0.63 V, respectively [42], implying that the major component in the mixture was the bis(cyanobenzene) complex. It is apparent from this result that the presence of an aqua group in the coordination sphere of the Ru(II) ion will readily allow the substitution of an organonitrile ligand, even when there are already two such ligands attached to the metal centre.

When $[Ru(NH_3)_3(OH_2)_3]^{2+}$, formed by reduction of $[Ru(NH_3)_3(OH_2)_3]^{3+}$ by amalgamated zinc in a pyridinium methanesulphonate buffer, reacted with the excess pyridine it was possible to isolate $[Ru(NH_3)_3(py)_3]^{2+}$ as its ClO_4^- or PF_6^- salt by the addition of an appropriate precipitating agent. The golden yellow perchlorate salt was recrystallized from hot methanol. Attempts to isolate the bis pyridine complex were unsuccessful, resulting in the formation of at least a small amount of the tris pyridine complex in all cases. This is similar to the results obtained for the attempted synthesis of the bis benzonitrile complex.

3.3.2. Electronic Spectra. The uv/vis spectra of the Ru(II) complexes all contained intense MLCT bands, and bands attributable to intra-ligand absorptions. The MLCT bands arise from transitions between the filled t_{2g} orbitals of Ru(II) and the empty π^* orbitals of the ligand. The main features of the spectra of the complexes prepared, together with those of some related ruthenium complexes, are given in Table 3.6.

The uv/vis spectrum of $[Ru(NH_3)_3(phen)(OH_2)]^{2+}$ (shown in Fig. 3.17) was pH dependent, as was to be expected given the presence of the aqua ligand. (The pK_a of the complex was found, by pH titration, to be 10.6(± 0.1)). In 0.1 mol dm^{-3} $MeSO_3H$, the charge transfer band was observed at 470 nm ($\varepsilon = 4.01 \times 10^3$), while the intra ligand bands were observed at 222 nm ($\varepsilon = 3.85 \times 10^4$) and 265 nm ($\varepsilon = 3.22 \times 10^4$). In NaOH solution, the charge transfer band was observed at 490 nm($\varepsilon = 2.95 \times 10^3$) and the intraligand bands were at the same wavelength, but with increased intensities ($\varepsilon_{222} = 4.84 \times 10^4$, $\varepsilon_{265} = 4.37 \times 10^4$). The colour of the solution changed quite rapidly after the addition of the base to the complex, indicating that the complex was unstable in NaOH solution, possibly due to aerial oxidation. If the NaOH solution was degassed with argon prior to adding it to the solid sample, the colour change was much slower and it was posssible to determine the spectrum within an hour. The spectrum in acid solution is very similar to that reported for $[Ru(NH_3)_4(phen)]^{2+}$. [43]

It is apparent from the shift in the MLCT band that the replacement of the aqua ligand with a hydroxo ligand raises the energy of the highest occupied metal–based orbital, so that the transition to the lowest lying π^* orbital is of lower energy, consistent with HO^- being a stronger π-donor ligand than H_2O.

The spectrum of $[Ru(NH_3)_2(bpy)_2]^{2+}$ was close to that previously reported for this complex. [39] The spectrum of the prepared sample contained two charge transfer bands, at 349 nm ($\varepsilon = 7.35 \times 10^3$) and 488 nm ($\varepsilon = 9.10 \times 10^3$), compared with 350 nm ($\varepsilon = 8.02 \times 10^3$) and 495 nm ($\varepsilon = 9.34 \times 10^3$) in the previously determined spectrum. These absorptions are also comparable with the two charge transfer bands in $[Ru(NH_3)_4(bpy)]^{2+}$. [40] The molar absorptivities of the intra-ligand absorptions are diagnostic of the of the number of bpy ligands present in the complex, being

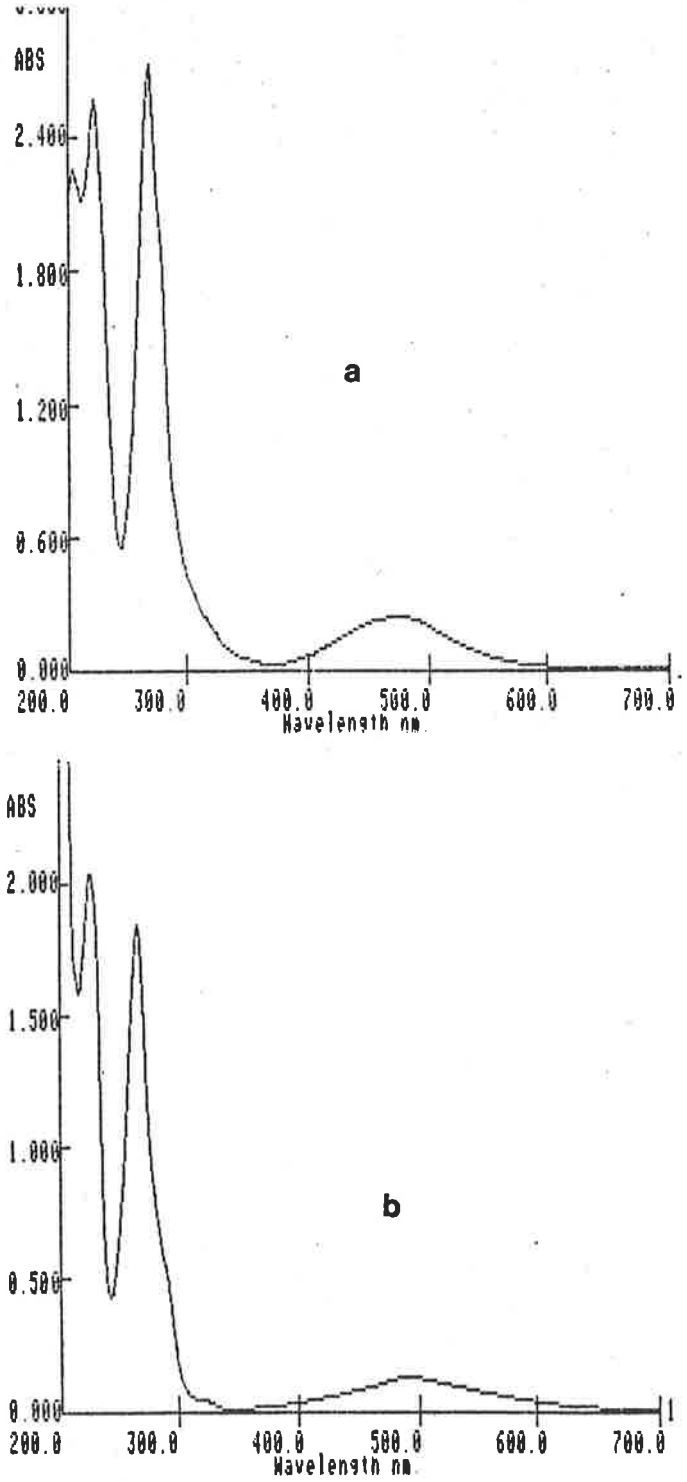

Fig. 3.17. uv/vis spectrum of: (a) $[Ru(NH_3)_3(phen)(OH_2)]^{2+}$, c = 6.7 x 10^{-4} mol dm^{-3} in 0.1 mol dm^{-3} $MeSO_3H$, 0.2 cm cells. (b) $[Ru(NH_3)_3(phen)(OH)]^{+}$, c = 4.2 x 10^{-4} mol dm^{-3} in 0.1 mol dm^{-3} NaOH, 0.2 cm cells.

L	$RuA_3L_3^{2+}$	$RuA_3L_2(OH_2)^{2+}$	*cis* $RuA_4L_2^{2+}$	RuA_5L^{2+}
MeCN	240(>20)[a,b] 332(0.25)			229(15.5)[c] 332(0.25)
py	244(17.6)[b] 350sh(12) 393(18.0)		245(7.24)[d] 378sh(6.46) 410(7.94)	244(4.57)[e] 407(7.76)
ampy		251(8.73)[b] 400(3.17)	248(6.3)[f] 414(5.8)	
phen		220(38.5)[b] 265(32.2) 470(4.01)	265(35)[g] 471(6.7)	
bpy	243(20.4)[b,h] 291(57.4) 349(7.35) 488(9.10)	244(21.8)[h,i] 292(58.8) 350(8.02) 495(9.34)	244(10)[f] 294(32) 367(5.7) 523(3.5)	
		$RuA_3L_2(OH)^+$		
phen		222(48.4)[b] 265(43.7) 490(2.95)		

Table 3.6. uv/vis spectra of ruthenium(II) complexes with π-acceptor ligands. (a) λ in nm(ε x 10^{-3} cm mol dm^{-3}). (b) This work. (c) Reference 7. (d) Reference 8. (e) Reference 3. (f) Reference 40. (g) Reference 43. (h) Spectrum is that of $[RuA_2(bpy)_2]^{2+}$. (i) Reference 39.

approximately proportional to the number of ligands. In $[Ru(NH_3)_4(bpy)]^{2+}$ the molar absorptivities of the intra-ligand bands are $\varepsilon_{244} = 1.0 \times 10^4$ and $\varepsilon_{294} = 3.2 \times 10^4$ which are approximately half the values observed for the intra-ligand bands in $[Ru(NH_3)_2(bpy)_2]^{2+}$, $\varepsilon_{244} = 2.1 \times 10^4$ and $\varepsilon_{292} = 5.8 \times 10^4$.

In the bpy and phen complexes reported here, the intra-ligand bands are at lower energy than the corresponding bands in the free ligand. This shift is normally observed in the spectra of such complexes and is ascribed to the effect of the positive charge on the energy levels of the ligand. [39] A similar shift is also observed when the free ligands are protonated. [44]

In the spectrum of $[Ru(NH_3)_3(ampy)(H_2O)]^{2+}$ a single intra-ligand absorption was observed at 251 nm ($\varepsilon = 8.73 \times 10^3$), and the MLCT band was at 400 nm ($\varepsilon = 3.17 \times 10^3$). These bands are similar to those observed in $[Ru(NH_3)_4(ampy)]^{2+}$ and $[Ru(NH_3)_5(py)]^{2+}$. [40,3]

In the case of $[Ru(NH_3)_3(py)_3]^{2+}$, the absorption bands were at wavelengths similar to those in $[Ru(NH_3)_5(py)]^{2+}$ (Fig. 3.18) The intra-ligand band was at 244 nm ($\varepsilon = 1.76 \times 10^4$) and the MLCT band was at 393 nm ($\varepsilon = 1.2 \times 10^4$). In addition, there is a shoulder to the charge transfer band, at 350 nm ($\varepsilon = 1.8 \times 10^4$). This spectrum compares well with those of the *cis* and *trans* isomers of $[Ru(NH_3)_4(py)_2]^{2+}$. [8] The *trans* isomer has a single MLCT band at 423 nm ($\varepsilon = 1.66 \times 10^4$), while the *cis* isomer shows a MLCT band similar to the tris pyridine complex, with a peak at 410 nm ($\varepsilon = 7.94 \times 10^3$) and a shoulder at 375 nm ($\varepsilon = 6.45 \times 10^3$). It has been shown that two independent MLCT transitions may be expected for the tetraammine complexes, but that the higher energy band is not observed unless there is some distortion to the ligand arrangement. [45] A ligand field treatment of the orbital energies in *cis* MX_3Y_3 complexes has shown that $[Ru(NH_3)_3(py)_3]^{2+}$ would be expected to have only one MLCT band. [46] However, if there is some distortion of the coordination sphere, then the degeneracy of the t_2 orbitals would be lifted, somewhat, so that a second transition to the ligand π^* orbital may become apparent. Given the presence of 3 pyridine ligands in a facial arrangement, it is quite possible that there would be some distortion.

The spectrum of $[Ru(NH_3)_3(MeCN)_3]^{2+}$ consisted of a single absorption band at 332 nm ($\varepsilon = 2.53 \times 10^2$) assigned to a MLCT. There was also a band at 240 nm with $\varepsilon > 2 \times 10^4$. This is comparable with the spectrum of $[Ru(NH_3)_5(MeCN)]^{2+}$. [7] The presence of a single MLCT implies that there is very little distortion of coordination sphere, which might be expected, given the small bulk of the acetonitrile molecule compared with the pyridine molecule.

3.3.3. Vibrational Spectra. The vibrational spectra of the complexes were recorded as nujol mulls on KBr plates. The presence of ligand vibration bands in the spectra served as confirmation that the ligands were coordinated. In the complexes containing aromatic heterocycle ligands, there

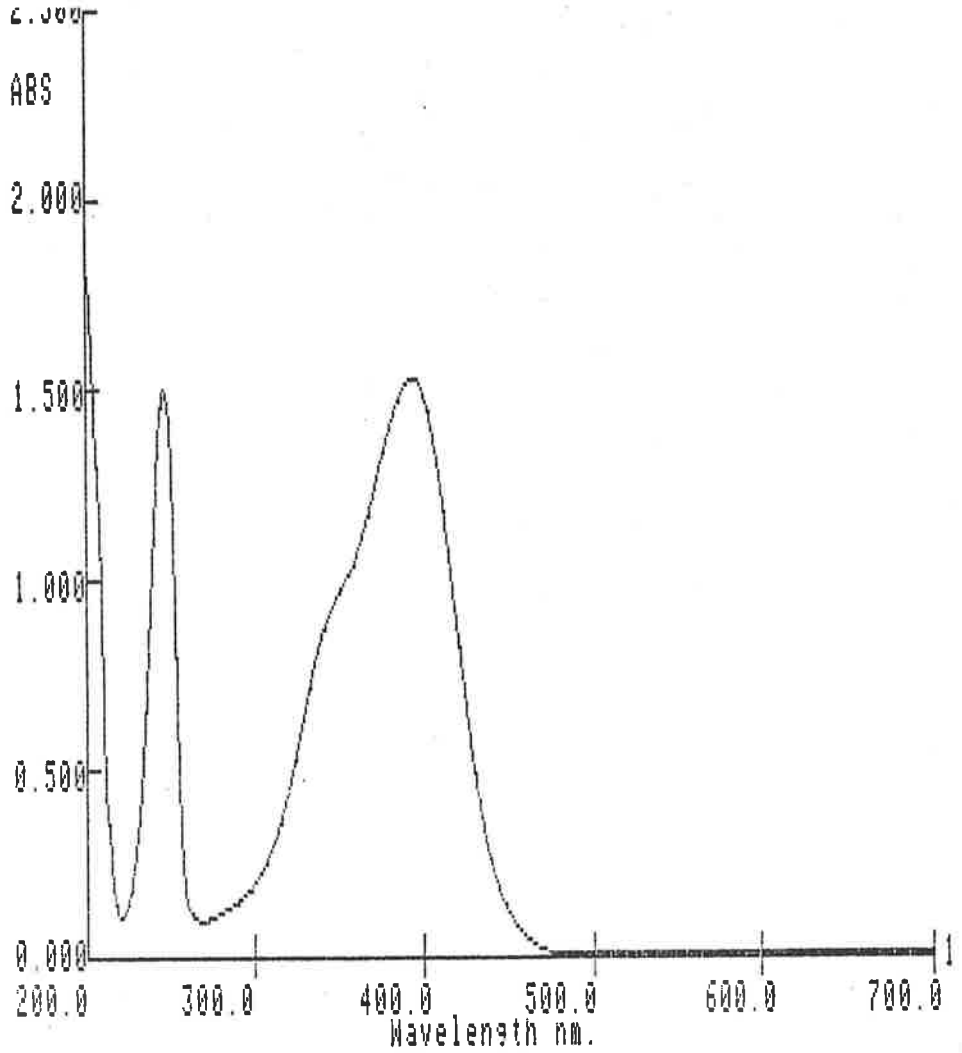

Fig. 3.18. uv/vis spectrum of $[Ru(NH_3)_3(py)_3]^{2+}$, c = 4.2 x 10^{-4} mol dm^{-3} in 0.1 mol dm^{-3} $MeSO_3H$

were multiple absorptions in the regions 1600 -1620 cm^{-1}, 1500 - 1600 cm^{-1} and 1400 -1500 cm^{-1} attributable to ring vibrations. Additionally, there were absorptions between 600 and 750 cm^{-1} due to the C-H out of plane deformations of the aromatic rings.

In all cases there were absorptions attributable to the NH groups of the ammine ligands. These were found in three regions of the spectrum: two or three bands between 3200 and 3350 cm^{-1}, attributable to the υ(NH) mode; a broad band between 1620 and 1640 cm^{-1}, attributable to the δ_d(NH) mode and several bands between 1250 and 1350 cm^{-1}, attributable to the δ_s(NH) mode. Though ammine complexes are also expected to show absorptions between 950 and 590 cm^{-1}, due to NH rocking vibrations [47a], these bands were obscured by bands due to ligand or anion vibrations. When the anion was PF_6^-, the υ(NH) bands were very sharp, because of specific hydrogen binding between the anion and the ammine ligands. In the spectrum of $[Ru(NH_3)_3(MeCN)_3]Cl_2.2H_20$ the υ(NH) bands are very broad because of hydrogen bonding between the molecules of lattice water and the ammine ligands. It was not possible to reliably assign the υ(RuN) absorption bands because these are usually very weak and occur close to the lower limit of the accessible range in KBr plates. [47b].

The spectrum of $[Ru(NH_3)_3(phen)(OH_2)](PF_6)_2$ showed strong bands at 3600 cm^{-1} and 3670 cm^{-1} due to the υ(OH) mode of the coordinated water. A strong absorption 1630 cm^{-1}, due to δ_d(NH) and an aromatic ring vibration, obscured any possible δ_d(OH) bands, nor was it possible to locate any Ru–O absorptions, for the reasons outlined above for the υ(RuN) bands.

In the spectrum of $[Ru(NH_3)_3(MeCN)_3]Cl_2.2H_20$ there were three bands attributable to the υ(CN) mode. Two were evident as sharp peaks at 2262 cm^{-1} and 2278 cm^{-1}. The lower energy peak was about twice as intense as that at higher energy. These bands were assigned to the E and A_1 mode vibrations, respectively, by comparison with the spectra of *fac* $M(CO)_3$ complexes. [48a] The third band was evident as a shoulder at 2266 cm^{-1}. Group theory predicts that a molecule of C_{3v} symmetry, such as $[Ru(NH_3)_3(MeCN)_3]^{2+}$, would have two ir active absorptions due to υ(CN), but anisotropy in the environment of the complex will cause slight splitting of the E mode. [48b] In the spectrum of the PF_6^- salt, there was a single peak at 2285 cm^{-1} and for the Br^- salt, the peak was at 2272 cm^{-1}. The anion dependence of the stretching frequency is due to polarization effects of the anion. Anions positively polarize the hydrogens of the ammine ligands, allowing greater electron release to the ruthenium and thence to the ligand π^* orbitals. The smaller the anion radius the greater is the electron release and the lower the vibration frequency. [49] It seems possible that with the Br^- and PF_6^- ions the intensity of the A_1 mode vibration is lowered to the

extent that it is not visible in the spectrum. A similar effect has been noted in the ir spectra of dinitrogen complexes, where the intensity of the absorption decreased as its energy increased. [50]

The υ(CN) band in free acetonitrile is seen at 2254 cm^{-1}, and, for $[Ru(NH_3)_5(MeCN)]^{2+}$, the energy of the υ(CN) band is modified by coordination, but is also dependent on the anion. For the Cl^-, Br^- and PF_6^- salts the bands are at 2237, 2238 and 2277 cm^{-1}, respectively. [49] It has been noted previously that, for the pentaammine complexes, the energy of the υ(CN) vibration is lowered in Ru(II) complexes, and increased in Ru(III) complexes, reflecting the strength of π-backbonding in the binding of the nitrile group to the Ru(II) centre and the effect of σ–donation to the Ru(III) centre. [1] That the υ(CN) frequency is greater in the triammine tris(acetonitrile) complex than in the free ligand is probably due to a combination of effects. The presence of only 3 σ–donating NH_3 groups means that the π-backbonding ability of the triammine Ru(II) centre will be less than that of the pentaammine. Secondly, what π-donation does occur is spread over three π-accepting ligands instead of only one. The end result is that because of reduced π-donation to each nitrile ligand, the σ– contribution is predominant, as in the case of Ru(III) complexes, and there is an increase in the frequency of the υ(CN) vibration. This explanation is borne out by the frequencies of the υ(CN) vibrations in a series of tris(phosphine) tris(acetonitrile) Ru(II) complexes, where the presence of the weakly σ–donating/π-accepting phosphine ligands causes the υ(CN) frequencies in the complexes to be higher than in the free ligand. [51]

3.3.4. Electrochemical Studies. The electrochemistry of the Ru(II) complexes was studied in aqueous solution at a freshly polished glassy carbon electrode. All the complexes showed a reversible or quasi-reversible oxidation wave at potentials greater than zero in 0.1 mol dm^{-3} methanesulphonic acid. The $E_{1/2}$ potentials of these complexes are listed in Table 3.7, along with those of similar ruthenium complexes.

The $E_{1/2}$ potential for the $[Ru(NH_3)_3(phen)(OH_2)]^{3+/2+}$ couple was pH dependent, due to the presence of the aqua ligand. In 0.1 mol dm^{-3} acid, $E_{1/2}$ = +0.26 V. At pH 8, $E_{1/2}$ = –0.02 V, and at pH 12, $E_{1/2}$ = –0.23 V. The cyclic voltammograms at pH 1 and pH 8 are shown in Fig. 3.19. The $E_{1/2}$ potential in acid solution is similar to that for the $[Ru(NH_3)_4(phen)]^{3+/2+}$ couple. [43] The Pourbaix diagram showed three distinct regions of pH dependence (Fig. 3.20). Below pH 3 and above pH 11.5, the $E_{1/2}$ potential was independent of pH, and betweeen pH 4 and pH 11, the slope of the graph of was –62 mV/pH. These results can be summarized in the redox couples shown as reactions 3.26 to 3.28.

1<pH<3

$$[Ru(NH_3)_3(phen)(OH_2)]^{3+} + e^- \rightleftharpoons [Ru(NH_3)_3(phen)(OH_2)]^{2+} \quad \textbf{(3.26)}$$

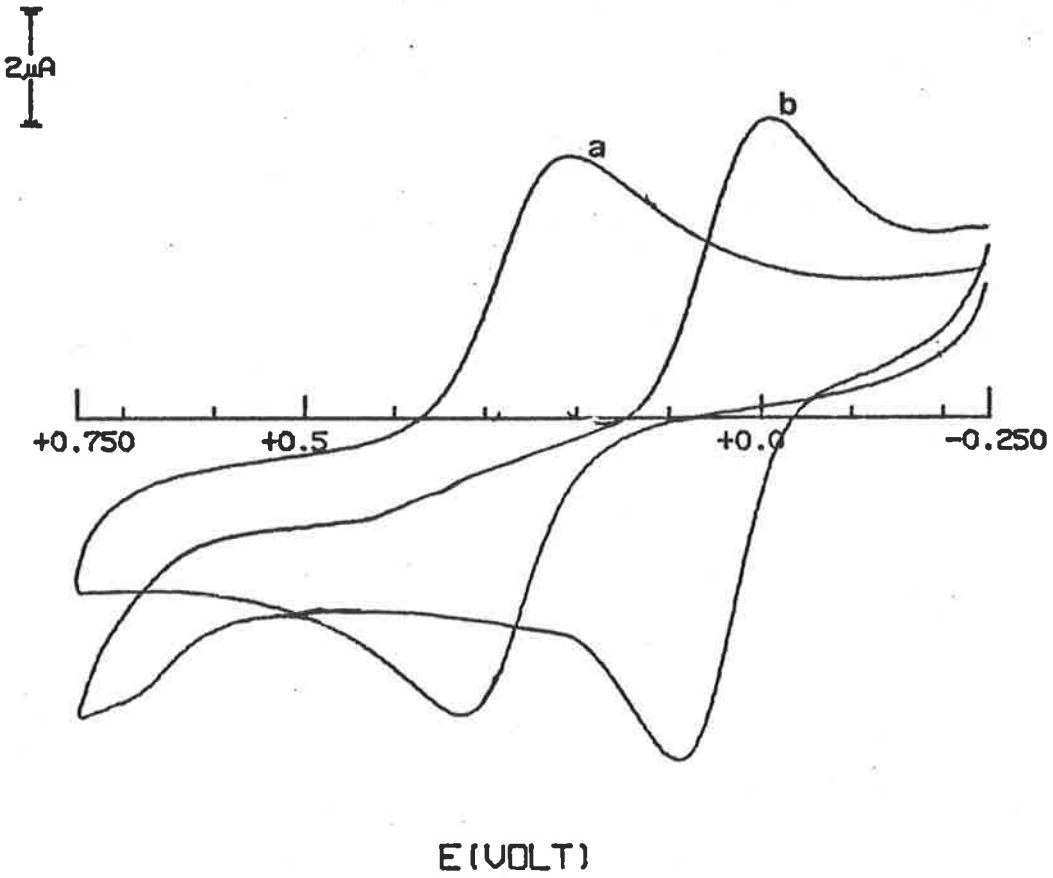

Fig. 3.19. Cyclic voltammograms of $[Ru(NH_3)_3(phen)(OH_2)]^{2+}$. (a) in 0.1 mol dm^{-3} $MeSO_3H$. (b) pH 8.0.

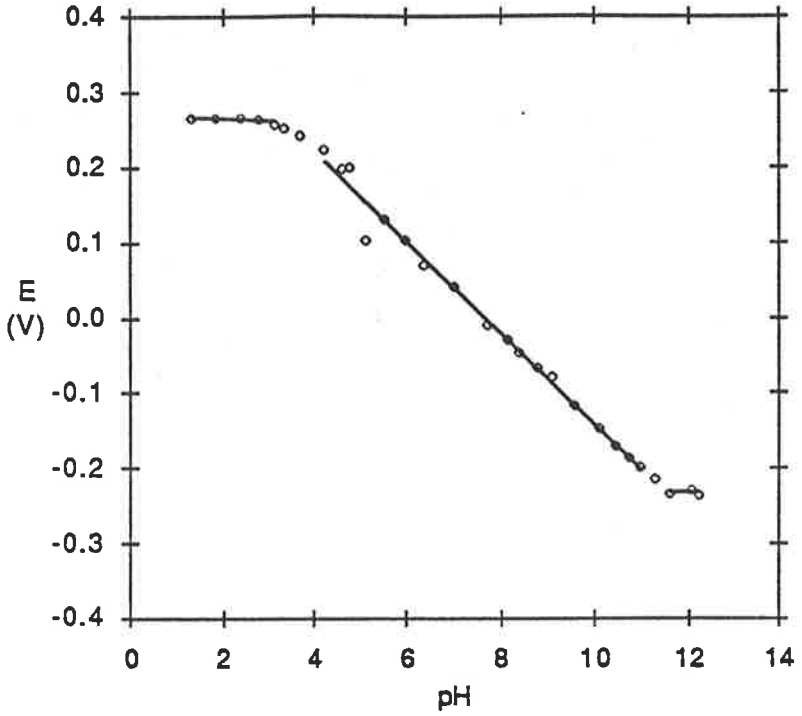

Fig. 3.20. Pourbaix diagram for the Ru(III)/Ru(II) redox couple of $[Ru(NH_3)_3(phen)(OH_2)]^{2+}$.

L	RuA_3L_3	$RuA_3L_2(OH_2)$	*cis* RuA_4L_2	RuA_5L
MeCN	+0.87[a]			+0.18[b]
PhCN	+0.95[a,f]	+0.64[a,f]	+0.63[b]	+0.24[b]
py	+0.48[a]		+0.26[b]	+0.06[b]
ampy		+0.04[a]	+0.05[c]	
bpy	+0.62[a,g] +0.65[e,g]	+0.27[a,f]	+0.27[c]	
phen		+0.26(pH2)[a] +0.04(pH7) -0.23(pH12)	+0.29[d]	

Table 3.7. $E_{1/2}$ potentials of the Ru(III)/Ru(II) couples for complexes with π-acceptor ligands. (a) This work. (b) Reference 42. (c) Reference 40. (d) Reference 43. (e) Reference 53. (f) Compound present in a mixture of substitution products. (g) The complex is $[Ru(NH_3)_2(bpy)_2]^{2+}$.

4<pH<11

$$[Ru(NH_3)_3(phen)(OH)]^{2+} + e^- + H^+ \rightleftharpoons [Ru(NH_3)_3(phen)(OH_2)]^{2+} \quad \textbf{(3.27)}$$

pH>11.5

$$[Ru(NH_3)_3(phen)(OH)]^{2+} + e^- \rightleftharpoons [Ru(NH_3)_3(phen)(OH)]^{+} \quad \textbf{(3.28)}$$

From the intercepts of the lines on the Pourbaix diagram, it can be seen that, in a solution of ionic strength 0.1, the pK_a of the aqua ligand on the Ru(III) complex is about 3.5, and the pK_a of the aqua ligand on the Ru(II) complex is about 11.4. Because the pK_a value is dependent upon the ionic stength of the solution [54], this pK_a is comparable with the pK_a of the Ru(II) complex in water (10.6). The estimated pK_a of the Ru(III) complex is higher than that of $[Ru(terpy)(bpy)(H_2O)]^{3+}$ (1.7) and $[Ru(bpy)_2(py)(H_2O)]^{3+}$ (0.85). [32, 52]. It is expected that the complexes with the equivalent of five pyridine rings in their coordination spheres would have lower pK_a values due to the cumulative electron accepting properties of the pyridine rings in the ligands.

The $E_{1/2}$ potential for the oxidation of freshly prepared $[Ru(NH_3)_3(ampy)(H_2O)]^{2+}$ was also pH dependent. In 0.1 mol dm^{-3} acid, $E_{1/2}$ = +0.04 V, and at pH 8, $E_{1/2}$ = –0.20 V. The $E_{1/2}$ potential in acid solution is very similar to that of $[Ru(NH_3)_5(py)]^{2+}$. [42] The Pourbaix diagram is shown in Fig. 3.21, and between pH 4.5 and pH 8, the slope of the graph is –58 mV/pH, indicative of a one electron/one proton electron transfer. This corresponds to the redox couples shown in 3.29 and 3.30.

3<pH

$$[Ru(NH_3)_3(ampy)(H_2O)]^{3+} + e^- \rightleftharpoons [Ru(NH_3)_3(ampy)(H_2O)]^{2+} \quad \textbf{(3.29)}$$

4.5<pH<8

$$[Ru(NH_3)_3(ampy)(OH)]^{2+} + e^- + H^+ \rightleftharpoons [Ru(NH_3)_3(ampy)(H_2O)]^{2+} \quad \textbf{(3.30)}$$

From the intercepts of the lines in the Pourbaix diagram, it is apparent that the pK_a for the Ru(III) complex is approximately 4.

The cyclic voltammogram of $[Ru(NH_3)_3(py)_3]^{2+}$ consisted of a single quasi reversible wave with $E_{1/2}$ = +0.48 V. At a scan rate of 25 mV sec^{-1}, the peak separation, ΔE_p, = 72 mV, while at 900 mV sec^{-1}, ΔE_p = 126 mV. The $E_{1/2}$ potential is approximately mid way between the value for *cis* $[Ru(NH_3)_4(py)_2]^{3+/2+}$ (+0.26 V) and $[Ru(NH_3)_2(bpy)_2]^{3+/2+}$ (+0.65 V). [42, 53] With the $E_{1/2}$ potential for $[Ru(NH_3)_5(py)]^{3+/2+}$ being +0.06 V [42], it is apparent that replacement of an ammine ligand by a pyridine ligand causes an increase in the oxidation potential of the ruthenium complex of approximately 0.2 V.

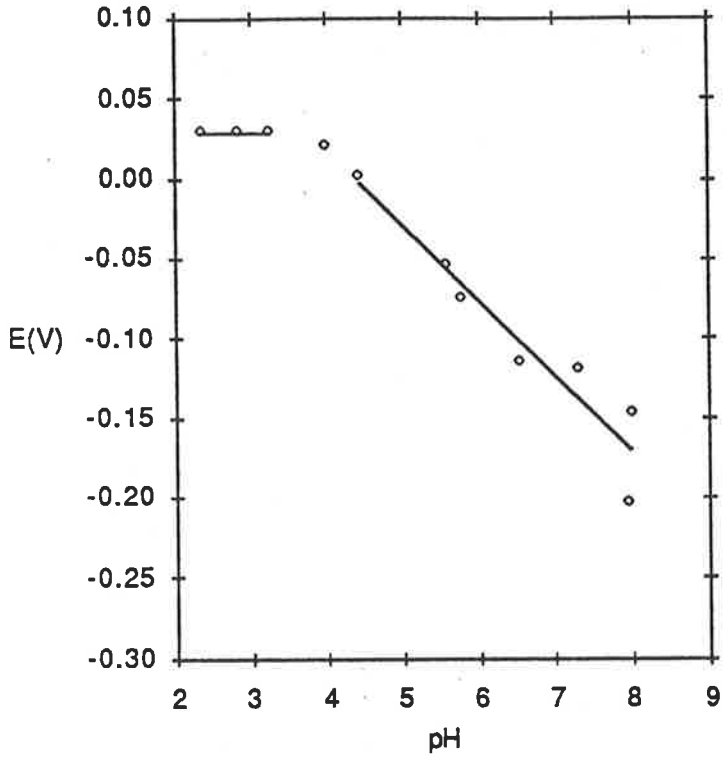

Fig. 3.21. Pourbaix diagram for the Ru(III)/Ru(II) redox couple of $[Ru(NH_3)_3(ampy)(OH_2)]^{2+}$.

From a comparison of the $E_{1/2}$ potentials of the previously known polypyridyl and pyridine complexes with those reported here, it is apparent that the effect on the metal centre of substitution by multiple pyridine rings is additive. This is similar to the effect already noted in the uv/vis spectrum, where the molar absorptivity of the intra-ligand bands is roughly proportional to the number of pyridine rings in the coordination sphere.

The cyclic voltammogram of $[Ru(NH_3)_3(MeCN)_3]^{2+}$ consisted of a quasi-reversible wave with $E_{1/2}$ = +0.87 V. The peak separation was highly dependent on the scan rate. (Fig. 3.22) At 25 mV sec^{-1}, ΔE_p = 72 mV, while at 900 mV sec^{-1}, ΔE_p = 261 mV. The $E_{1/2}$ potential for the $[Ru(NH_3)_3(MeCN)_3]^{3+/2+}$ couple in aqueous solution is less positive than that measured in acetonitrile (see Section 2.8.2). This is probably arises due to the existence of the liquid junction potential between the aqueous calomel electrode and the acetonitrile solvent.

3.4. Triammine(tripod)ruthenium(II) Complexes.

3.4.1. Introduction. The triamminetriaquaruthenium ions contain labile ligands (i.e. H_2O) in a facial arrangement. The preceding sections have described the substitution of these ligands by mono- and bidentate ligands, and it was considered useful to examine the substitution of the three aqua ligands by tridentate ligands capable of assuming a facial arrangement in octahedral geometry. Keene and co-workers have previously shown that tripodal, tris(pyridyl) ligands (py_3X, where X is a group or atom connected to the *ortho* position of each pyridine ring) are capable of occupying one face of an octahedral complex. [55-58] Apart from their ability to assume a facial arrangement of donor atoms, these ligands are also of interest because of the opportunity offered by the triammine(tripod)ruthenium(II) complexes to further examine the effects of the ligand combination of 3 σ-donors and 3-π acceptors, and to further study the additivity of the effects on the metal centre of multiple pyridine rings.

3.4.2. Preparation of the Complexes. In aqueous solution the tripodal ligands, tris(pyridyl)methanol, tris(pyridyl)methane and tris(pyridyl)amine, reacted with $[Ru(NH_3)_3(OH_2)_3]^{2+}$ to give bright yellow solutions of $[Ru(NH_3)_3(tripod)]^{2+}$. $[Ru(NH_3)_3(OH_2)_3]^{2+}$ was generated in situ by hydrogen reduction of $[Ru(NH_3)_3(OH_2)_3]^{3+}$. The complexes could be isolated as solids by the addition of excess NH_4PF_6 to the reaction mixture. If the reaction mixtures came in contact with air before the solids were precipitated, a dark green colour was seen to form, indicative of possible partial oxidation of the product.

The compounds were converted to the bromide salts by the addition of excess tetra(n-butyl)ammonium bromide to a solution of the PF_6^- salt in butanone. The bromide salts were then recrystallized from hot methanol.

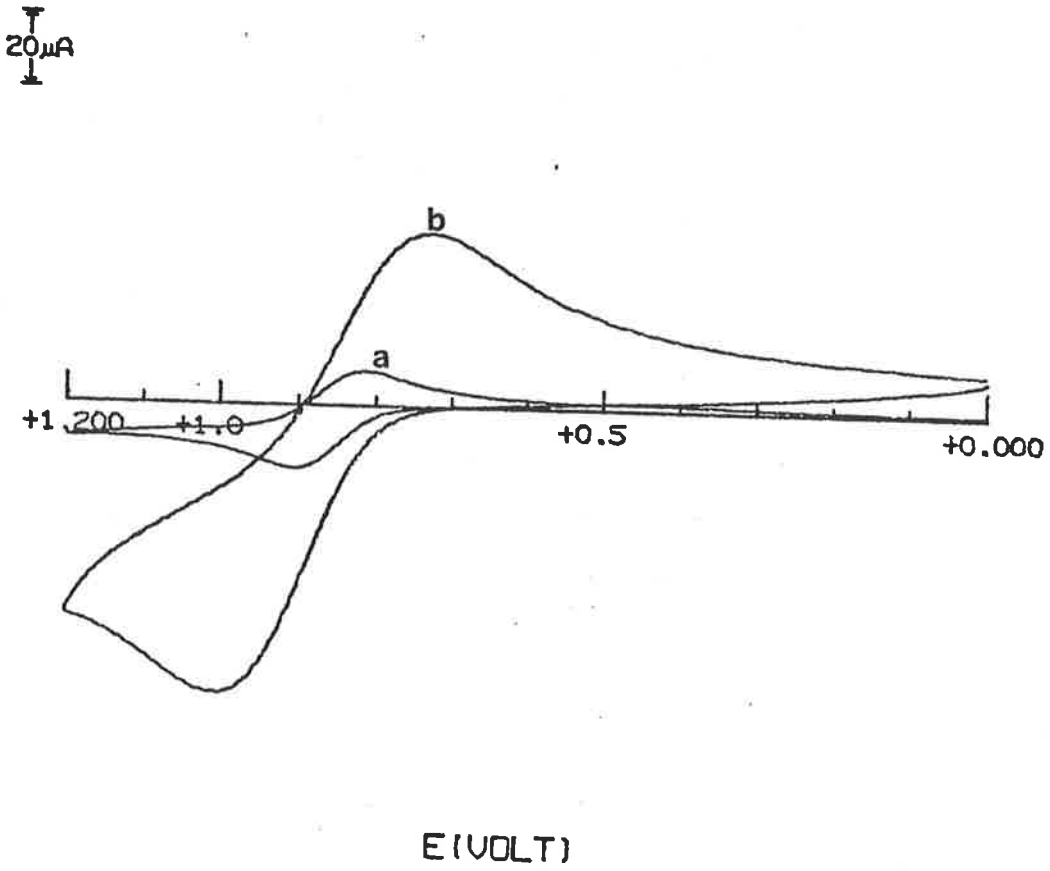

Fig. 3.22. Cyclic voltammogramsof $[Ru(NH_3)_3(MeCN)_3]^{2+}$ in 0.1 mol dm^{-3} $MeSO_3H$. (a) 100 mV sec^{-1}. (b) 900 mV sec^{-1}.

In both $[Ru(NH_3)_3\{(py)_3CH\}]^{2+}$ and $[Ru(NH_3)_3\{(py)_3N\}]^{2+}$ the ligands are believed to be coordinated through the three pyridyl nitrogen atoms, in a facial arrangement (N, N', N''). A crystal structure determination has revealed that the ligand, $(py)_3COH$ is coordinated through two pyridyl rings and the oxygen atom of the alcohol group (N, N', O). In the complex, $[Ru\{(py)_3COH)\}_2]^{2+}$, both modes of coordination are observed. [56]

Attempts were made to prepare the complex with tris(pyridyl)phosphine as the tripod ligand, but DPV analysis of the reaction mixture indicated the formation of at least two species in the reaction. No attempt was made to refine the reaction conditions to give the required complex as the sole product.

3.4.3. Electronic Spectra. As with the Ru(II) complexes reported above, the uv/vis spectra of the three complexes with tripod ligands all contained bands attributable to intra-ligand absorptions and to MLCT. The spectra are displayed in Fig. 3.23 and the main features are listed in Table 3.8, where they are compared with the spectra of some $Ru(tripod)_2^{2+}$ complexes prepared previously. [56, 57]

The spectra of $[Ru(NH_3)_3\{(py)_3CH\}]^{2+}$ and $[Ru(NH_3)_3\{(py)_3N\}]^{2+}$ are similar. The MLCT bands are at 369 and 415 nm for tripod = $(py)_3CH$ and at 367 and 414 nm for tripod = $(py)_3N$. The intra-ligand bands are at 249 and 280 nm in both cases but, of these, the lower energy band is only evident as a shoulder in the spectrum of $[Ru(NH_3)_3\{(py)_3CH\}]^{2+}$. The MLCT bands are similar in energy and intensity to those in the spectra of $[Ru(NH_3)_3(py)_3]^{2+}$, $[Ru(NH_3)_4(py)_2]^{2+}$ [8] and the $Ru(tripod)_2^{2+}$ complexes, but no intra–ligand bands were quoted for the last examples. [57] It was noted, when discussing the spectrum of $[Ru(NH_3)_3(py)_3]^{2+}$, that complexes of C_{3v} symmetry would be expected to show only one MLCT band unless there was some distortion of the coordination sphere. The presence of two distinct MLCT peaks suggests that there is a larger degree of distortion in these two complexes, than in the tris(pyridine) complex. It is not surprising that there should be some distortion of the coordination sphere in this case, because the three pyridyl rings are subject to the rigidity constraints imposed by the bond to the bridgehead group.

The spectrum of $[Ru(NH_3)_3\{(py)_3COH\}]^{2+}$, shown in Fig. 3.24, was expected to be pH dependent, due to the presence of a weakly acidic -OH group on the ligand. In 0.1 mol dm^{-3} $MeSO_3H$, the intra-ligand bands were present at 260 nm and at 240 nm (shoulder), and at pH 8, the band at 240 was resolved into a peak, and the lower energy band was at 265 nm. The expected MLCT bands were evident as weak shoulders at 350 ($\varepsilon = 1.5 \times 10^3$) and 415 nm ($\varepsilon = 4.5 \times 10^2$) in acid solution, and in base there was a shoulder at 350 nm. The intra-ligand bands are comparable to those in the spectra of $[Ru\{(py)_3COH\}_2]^{2+}$, which has one peak at 246 nm when the -OH group is protonated, and one peak at 253 nm when the O-H group is deprotonated. [56] However, the MLCT absorptions are surprising. The energy at which they occur is comparable with the energy of

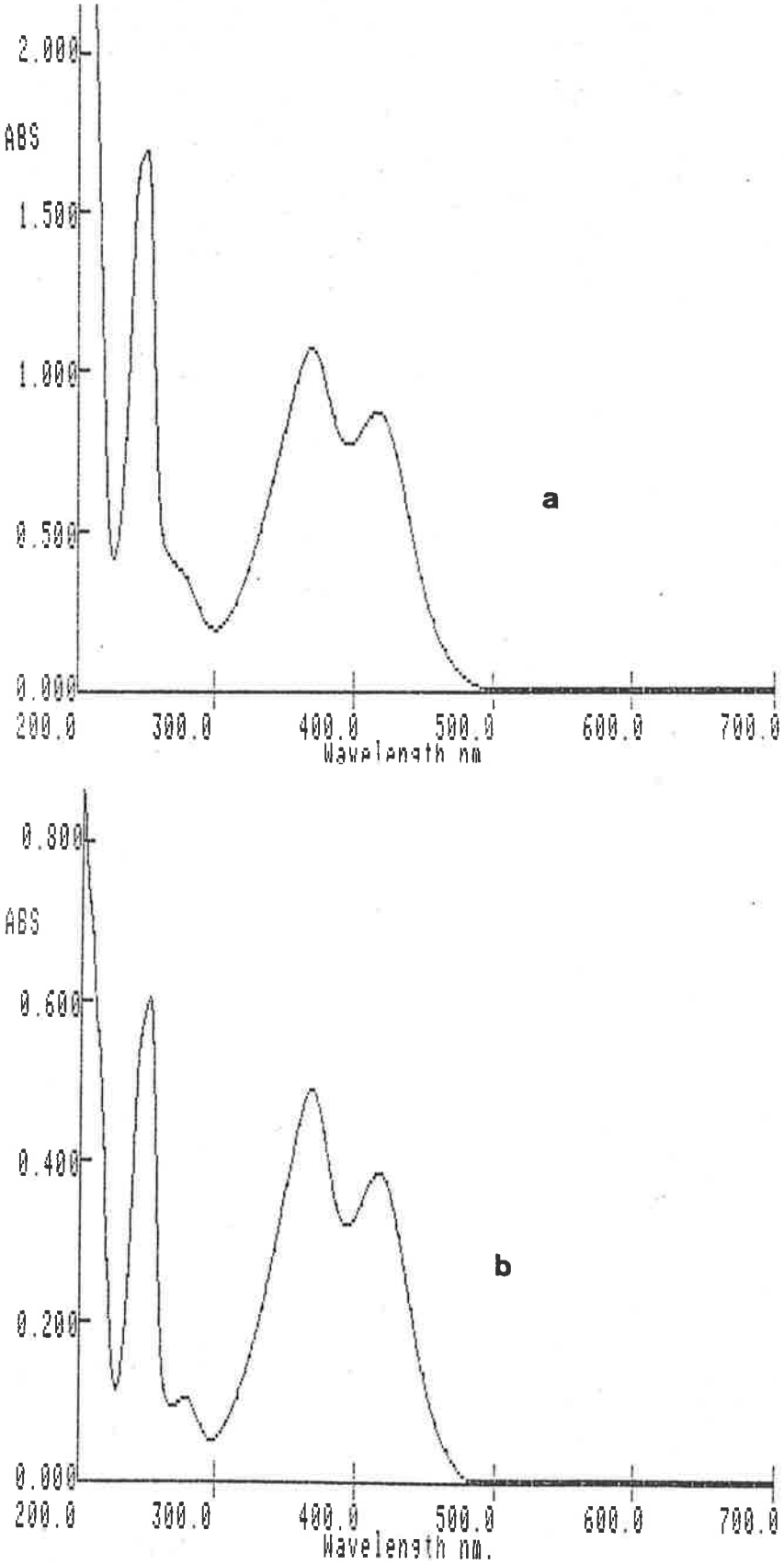

Fig. 3.23. uv/vis spectra of: (a) $[Ru(NH_3)_3\{(py)_3CH\}]^{2+}$ in 0.1 mol dm^{-3} $MeSO_3H$. $c = 5.9 \times 10^{-4}$ mol dm^{-3}, 0.2 cm cells. (b) $[Ru(NH_3)_3\{(py)_3N\}]^{2+}$ in 0.1 mol dm^{-3} $MeSO_3H$. $c = 1.9 \times 10^{-4}$ mol dm^{-3}, 0.2 cm cells.

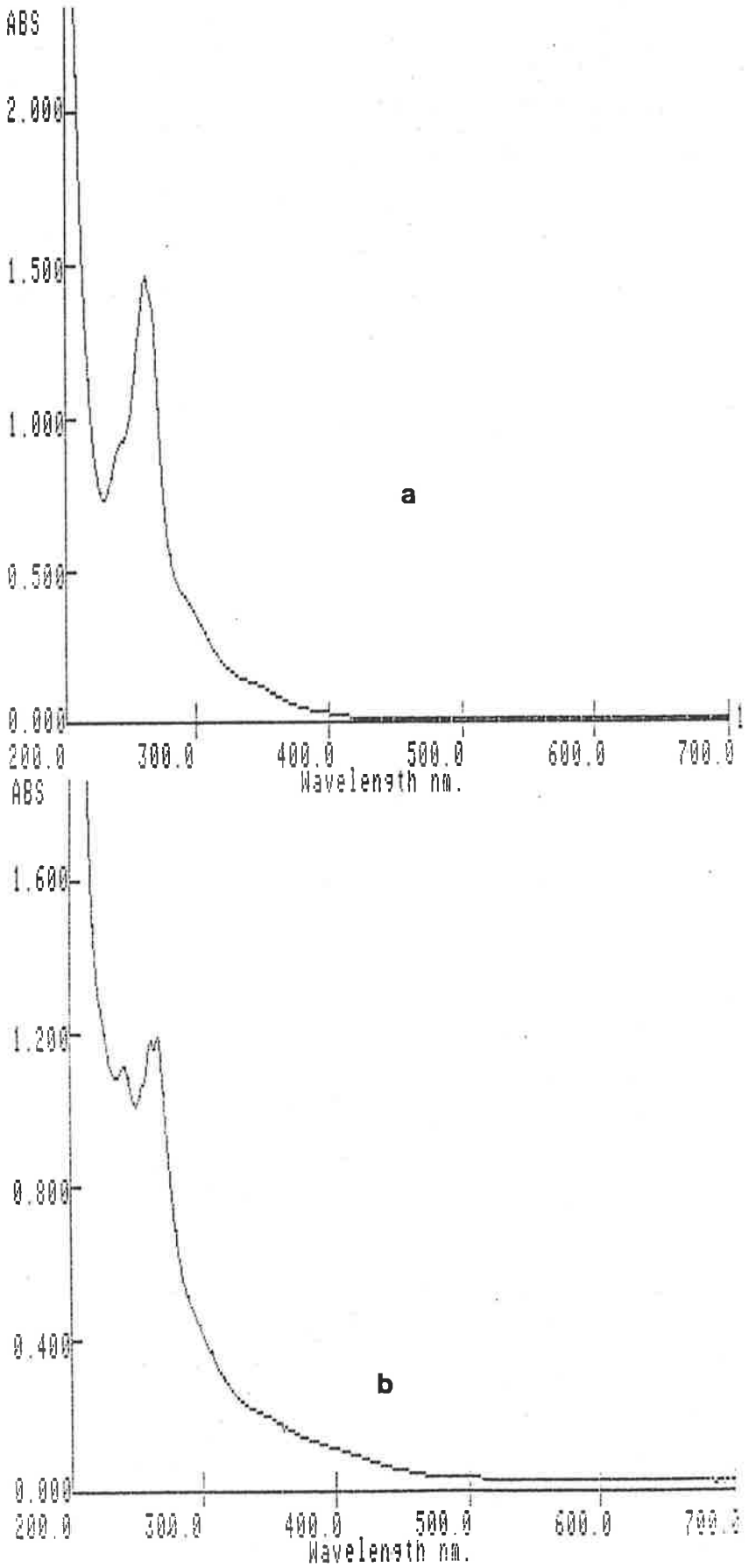

Fig. 3.24. uv/vis spectra of: (a) $[Ru(NH_3)_3\{(py)_3COH\}]^{2+}$ in 0.1 mol dm^{-3} $MeSO_3H$. $c = 5.0 \times 10^{-4}$ mol dm^{-3}, 0.2 cm cells. (b) $[Ru(NH_3)_3\{(py)_3CO\}]^{+}$ in 0.1 mol dm^{-3} NaOH. $c = 3.8 \times 10^{-4}$ mol dm^{-3}, 0.2 cm cells.

	$RuA_3(tripod)^{2+}$		$Ru(tripod)_2^{2+}$	
Tripod	$\lambda(\varepsilon \times 10^{-3})$	$E_{1/2}$	$\lambda(\varepsilon \times 10^{-3})$	$E_{1/2}$
$(py)_3COH$	240sh(8.9)[a,b] 260(14.3) 350sh(1.5) 415(.45)	+0.07[b]	246(30.6)[c] 415(24.7)	+0.40[d]
$(py)_3CO^-$	240(14.5)[b] 265(15.5) 350sh(2.5)	-0.09[b]	253(30.5)[c] 432(27.8)	+0.25[e]
$(py)_3CH$	249(14.3)[b] 280sh(2.5) 369(9.06) 415(7.34	+0.50[b]	350[f] 405	+1.27[g]
$(py)_3N$	249(15.7)[b] 280(2.6) 367(12.7) 414(10.0)	+0.57[b]	340[f] 400	+1.35[g]

Table 3.8. uv/vis spectra and $E_{1/2}$ (oxidation) potentials of Ru(II) tripod complexes. (a) λ in nm. (b) This work, 0.1 M $MeSO_3H$ (acid solution), 0.02 M TRIS buffer, 0.1 M $MeSO_3Na$ (base solution), pH 8. (c) Reference 56. (d)vs SSCE, 0.05 M H_2SO_4, glassy carbon electrode, 100 mV sec^{-1}. (e) 0.05M TRIS, 0.1M KNO_3. (f) Intra-ligand bands and ε not quoted. Reference 57. (g) vs SSCE, MeCN solution, Pt electrode, Reference 57.

the MLCT in $[Ru\{(py)_3COH\}_2]^{2+}$ and the other two triammine complexes, but there seems to be no explanation for their low intensity. The intensities of the MLCT bands in both the protonated and deprotonated forms of $[Ru\{(py)_3COH\}_2]^{2+}$ are comparable to that of the intra-ligand bands ($\varepsilon \approx 3 \times 10^4$), and suggest that both of the ligands are involved in the transitions. [56] There are some structural differences between $[Ru(NH_3)_3\{(py)_3COH\}]^{2+}$ and $[Ru\{(py)_3COH\}_2]^{2+}$, as described below, but it is unlikely that these are the cause of the low intensity of the MLCT.

3.4.3. Vibrational Spectra. The ir spectra of the salts of the three complexes contained three sharp bands in the 3200 - 3360 cm^{-1} due to specific hydrogen bonding between the NH_3 groups and the PF_6^- anion. The presence of a weak, broad band at 3650 cm^{-1} in the spectrum of $[Ru(NH_3)_3(py)_3COH)](PF_6)_2$ was indicative of the presence of the C–OH group. The remainder of the spectrum, in each case, was consistent with the presence of the ligand.

3.4.5. Electrochemical Studies. In 0.1 mol dm^{-3} $MeSO_3H$ solution, at a glassy carbon electrode, the three complexes had reversible CV waves due to the $[Ru(NH_3)_3(tripod)]^{3+/2+}$ couple. The $E_{1/2}$ values are listed in Table 3.8, where they are compared with those of the bis(tripod) complexes. The CV of the complex with $(py)_3COH$ is pH dependent, because of the presence of the –OH group ligand. (Fig. 3.25.) In acid solution, where the complex form is $[Ru(NH_3)_3\{(py)_3COH\}]^{2+}$, $E_{1/2}$ is +0.07 V. At pH 8, where the complex exists as $[Ru(NH_3)_3\{(py)_3CO\}]^{+}$, $E_{1/2}$ is –0.09 V. The pK_a of $[Ru\{(py)_3COH\}_2]^{2+}$ is 3.78 (in 0.1 M KNO_3), compared with a value of 7.2 for the coordinated 2–pyridinemethanol in $[Ru(bpy)_2(pyCH_2OH)]^{2+}$. [56] The higher acidity of coordinated tris(2-pyridyl)methanol was attributed to steric strain within the tripod ligand. A decrease in $E_{1/2}$ potential of +0.16 V over the pH range 1 to 8 is consistent with a pK_a comparable to that of $[Ru\{(py)_3COH\}_2]^{2+}$.

The $E_{1/2}$ potentials for the $[Ru(NH_3)_3(tripod)]^{3+/2+}$ couples are all less positive than those for the corresponding bis (tripod) complexes. This reflects the difference between the π-acceptor properties of the three extra pyridyl rings in the bis(tripod) complexes and the σ–donor properties of the ammine ligands in the triammine complexes. The $E_{1/2}$ potentials for complexes involving $(py)_3COH$ as a ligand are less positive than those for $[Ru(NH_3)_3\{(py)_3CH\}]^{2+}$and $[Ru(NH_3)_3\{(py)_3N\}]^{2+}$, because of the σ–donor ability of the -OH group, and the presence of only two π-accepting pyridyl groups in the coordination sphere when the ligand is in the (N, N', O) mode. For $[Ru(NH_3)_3\{(py)_3CH\}]^{2+}$ and $[Ru(NH_3)_3\{(py)_3N\}]^{2+}$, the $E_{1/2}$ potentials are more positive than that of $[Ru(NH_3)_3(py)_3]^{2+}$, indicating that the rigid configuration of three pyridine rings leads to better π-acceptor ability than the non-bridged configuration of pyridine rings.

3.4.6 Description of the Crystal Structure of $[Ru(NH_3)_3\{(py)_3COH\}]Br_2$. Crystals of $[Ru(NH_3)_3\{(py)_3COH\}]Br_2$ were obtained as orange rectangular blocks from methanol by vapour

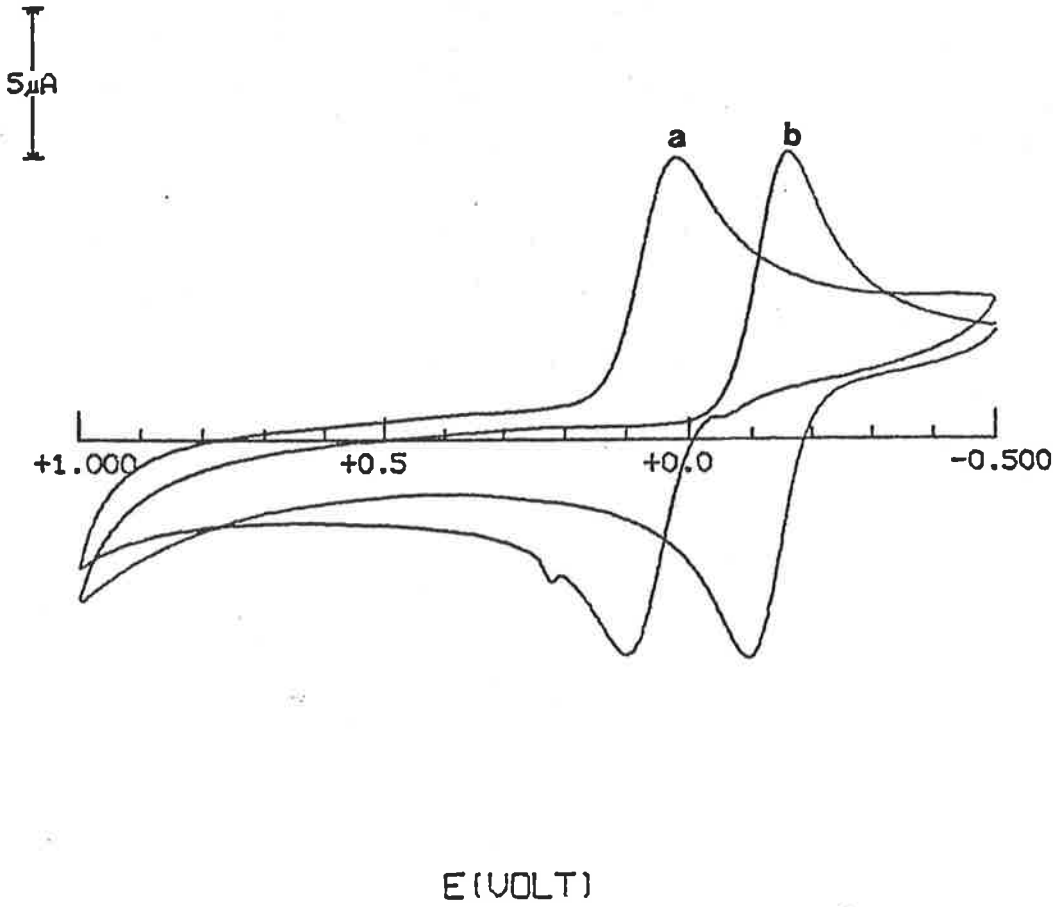

Fig. 3.25. Cyclic voltammograms of: (a) $[Ru(NH_3)_3\{(py)_3COH\}]^{2+}$ in 0.1 mol dm^{-3} $MeSO_3H$. (b) $[Ru(NH_3)_3\{(py)_3CO\}]^{+}$, pH 8.0, TRIS buffer.

diffusion of acetone. The crystal structure was determined by Dr. E. R. T. Tiekink, and is shown in Fig. 3.26., which also shows the atomic numbering scheme employed. The bond lengths and angles are listed in Tables 3.9 and 3.10, which follow Fig. 3.26.

The crystal structure comprises a distorted octahedron, with the ammine ligands arranged facially, and the tripod ligand, coordinated in the (N, N', O) mode, also ocupying one face. The bond angles between Ru and the donor atoms of the tripod ligand are all less than 90°, indicating a small ligand bite. As a consequence, the angles between the atoms *trans* to each other are less than 180°, indicating that the steric constraints of the tripod ligand prevent the donor atoms from occupying the apical positions of a regular octahedron. The bond angles between Ru and the ammine N atoms are close to 90°, indicating that the facial arrangement of the ammines is nearly regular.

The Ru-N bond lengths for the ammine ligands are between 2.124 Å and 2.132 Å. These bond lengths are shorter than those of the Ru-N bonds in $[Ru(NH_3)_6]I_2$, where the the average length is 2.144 Å. [36] This shortening of the bonds can be attributed to the co-operative effects operating between the σ–donor ammine ligands and the π-acceptor pyridyl rings, whereby the π-acceptor character of the pyridyl rings reduces the competition between the ammine and pyridyl N-donor atoms for the metal d orbital The same effect is seen in nitrosyl complexes when the ligand *trans* to the NO ligand is not a π-acceptor. [59] The pyridyl Ru-N bond lengths are 2.065(4) Å and 2.053(4) Å, which are very close to the average Ru-N bond length of 2.053(6) Å in $[Ru\{(py)_3COH\}_2]^{2+}$ [56] and 2.056 Å in $[Ru(bpy)_3]^{2+}$[60], indicating that the π-backbonding to the pyridyl rings of the tripod ligands is similar to that of other polypyridyl ligands.

The Ru-O bond length in $[Ru(NH_3)_3\{(py)_3COH\}]^{2+}$ is 1.963(3) Å, which is shorter than the average Ru-O bond length in $[Ru(H_2O)_6](pTS)_2$ (2.12(2) Å). [37] In $[Ru\{(py)_3COH\}_2]^{2+}$, the Ru-O bond distance is 2.111(4) Å, which is longer than the average Ru-N bond distance in that compound. [56]

The distortion of the coordination sphere is a feature of the (N, N' O) coordination mode, and probably arises because the distance between the bridgehead carbon atom and the O-donor atom (1.439 Å) is much less than the distance between the bridgehead carbon atom and the pyridyl N-donor atoms (2.382 Å and 2.388 Å). In the structure of $[Co\{(py)_3COH\}_2]^{3+}$, where both ligands coordinate in the (N, N' N") mode, the six nitrogen atoms are arranged in almost perfect octahedral geometry [55], and in $[Ru\{(py)_3CH\}_2]^{2+}$, where only the (N, N' N") mode is possible, the bond angles and distances, while not as regular as in the case of the cobalt complex, are much closer to those of a regular octahedron than in the (N, N', O) tris(pyridyl)methanol complexes. [58]

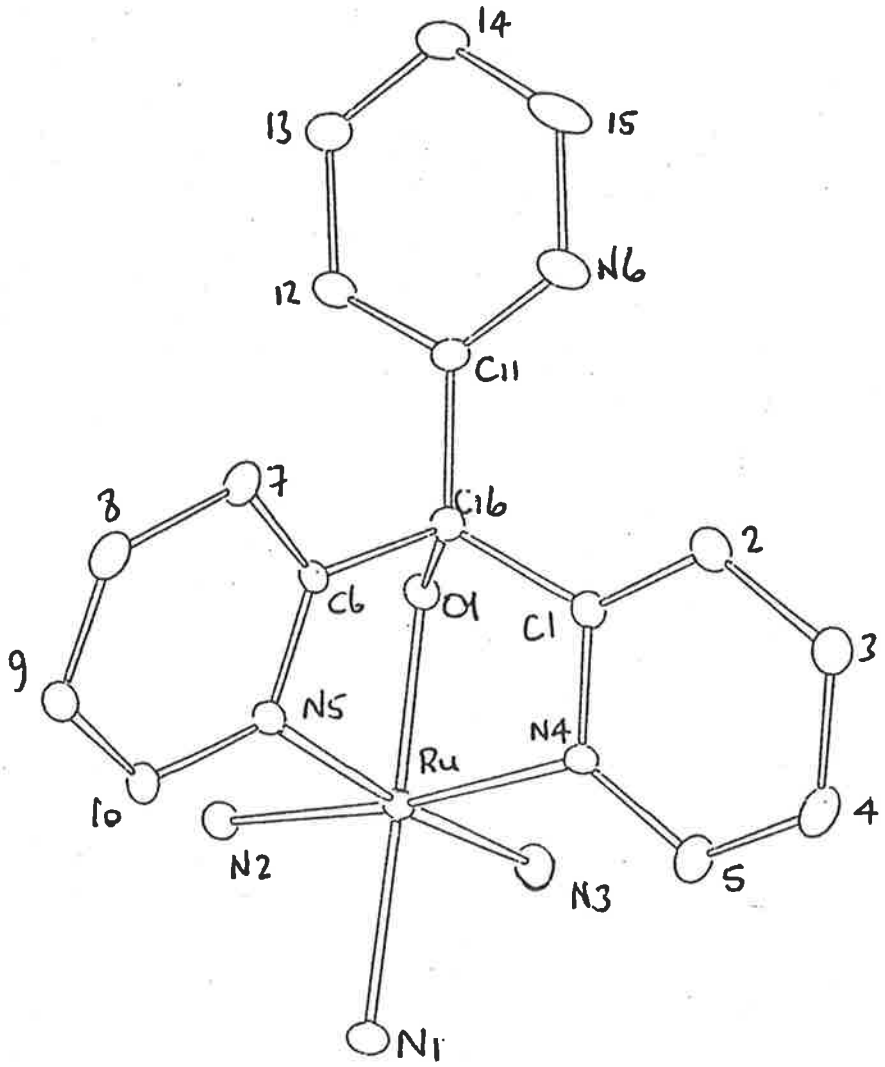

Fig. 3.26. X-ray crystal structure of $[Ru(NH_3)_3((py)_3COH)]Br_2$.

N(1)	--- Ru	2.124(5)	N(2)	--- Ru	2.124(4)
N(3)	--- Ru	2.132(5)	N(4)	--- Ru	2.065(4)
N(5)	--- Ru	2.053(4)	O(1)	--- Ru	1.963(3)
C(1)	--- N(4)	1.350(7)	C(5)	--- N(4)	1.333(7)
C(6)	--- N(5)	1.341(7)	C(10)	--- N(5)	1.354(7)
C(11)	--- N(6)	1.321(7)	C(15)	--- N(6)	1.343(9)
C(16)	--- O(1)	1.439(6)	C(2)	--- C(1)	1.365(8)
C(16)	--- C(1)	1.546(7)	C(3)	--- C(2)	1.395(9)
C(4)	--- C(3)	1.383(9)	C(5)	--- C(4)	1.365(8)
C(7)	--- C(6)	1.406(7)	C(16)	--- C(6)	1.527(7)
C(8)	--- C(7)	1.398(7)	C(9)	--- C(8)	1.356(9)
C(10)	--- C(9)	1.378(9)	C(12)	--- C(11)	1.369(8)
C(16)	--- C(11)	1.518(7)	C(13)	--- C(12)	1.380(8)
C(14)	--- C(13)	1.361(9)	C(15)	--- C(14)	1.359(10)

Table. 3.9. Bond lengths in $[Ru(NH_3)_3\{(py)_3COH\}]Br_2$.

N(2)	- Ru	- N(1)	88.5(2)	N(3)	- Ru	- N(1)	90.2(2)
N(3)	- Ru	- N(2)	88.6(2)	N(4)	- Ru	- N(1)	98.1(2)
N(4)	- Ru	- N(2)	173.2(2)	N(4)	- Ru	- N(3)	92.8(2)
N(5)	- Ru	- N(1)	95.2(2)	N(5)	- Ru	- N(2)	93.4(2)
N(5)	- Ru	- N(3)	174.3(2)	N(5)	- Ru	- N(4)	84.5(2)
O(1)	- Ru	- N(1)	174.3(2)	O(1)	- Ru	- N(2)	94.1(2)
O(1)	- Ru	- N(3)	94.9(2)	O(1)	- Ru	- N(4)	79.2(2)
O(1)	- Ru	- N(5)	79.6(2)	C(6)	- Ru	- N(1)	118.4(2)
C(6)	- Ru	- N(2)	105.2(2)	C(6)	- Ru	- N(3)	148.0(2)
C(6)	- Ru	- N(4)	70.3(2)	C(6)	- Ru	- N(5)	26.4(2)
C(6)	- Ru	- O(1)	56.0(1)	C(16)	- Ru	- N(1)	143.5(2)
C(16)	- Ru	- N(2)	115.4(2)	C(16)	- Ru	- N(3)	116.0(2)
C(16)	- Ru	- N(4)	58.0(2)	C(16)	- Ru	- N(5)	58.3(2)
C(16)	- Ru	- O(1)	31.0(1)	C(16)	- Ru	- C(6)	32.0(1)
C(1)	- N(4)	- Ru	112.0(3)	C(5)	- N(4)	- Ru	128.0(4)
C(5)	- N(4)	- C(1)	120.0(4)	C(6)	- N(5)	- Ru	110.8(3)
C(10)	- N(5)	- Ru	129.9(4)	C(10)	- N(5)	- C(6)	119.3(5)
C(15)	- N(6)	- C(11)	117.6(6)	C(16)	- O(1)	- Ru	104.3(3)
C(2)	- C(1)	- N(4)	121.1(5)	C(16)	- C(1)	- N(4)	110.5(4)
C(16)	- C(1)	- C(2)	128.4(5)	C(3)	- C(2)	- C(1)	118.7(6)
C(4)	- C(3)	- C(2)	119.6(6)	C(5)	- C(4)	- C(3)	118.3(6)
C(4)	- C(5)	- N(4)	122.2(6)	N(5)	- C(6)	- Ru	42.8(2)
C(7)	- C(6)	- Ru	164.8(4)	C(7)	- C(6)	- N(5)	122.0(5)
C(16)	- C(6)	- Ru	69.8(3)	C(16)	- C(6)	- N(5)	112.6(4)
C(16)	- C(6)	- C(7)	125.4(5)	C(8)	- C(7)	- C(6)	117.3(5)
C(9)	- C(8)	- C(7)	120.0(5)	C(10)	- C(9)	- C(8)	120.2(5)
C(9)	- C(10)	- N(5)	121.1(5)	C(12)	- C(11)	- N(6)	121.3(5)
C(16)	- C(11)	- N(6)	120.1(5)	C(16)	- C(11)	- C(12)	118.5(5)
C(13)	- C(12)	- C(11)	120.7(5)	C(14)	- C(13)	- C(12)	118.0(6)
C(15)	- C(14)	- C(13)	118.2(6)	C(14)	- C(15)	- N(6)	124.1(6)
O(1)	- C(16)	- Ru	44.6(2)	C(1)	- C(16)	- Ru	79.4(3)
C(1)	- C(16)	- O(1)	105.6(4)	C(6)	- C(16)	- Ru	78.2(3)
C(6)	- C(16)	- O(1)	106.2(4)	C(6)	- C(16)	- C(1)	103.7(4)
C(11)	- C(16)	- Ru	153.3(3)	C(11)	- C(16)	- O(1)	109.1(4)
C(11)	- C(16)	- C(1)	119.8(4)	C(11)	- C(16)	- C(6)	111.5(4)

Table. 3.10. Bond angles in $[Ru(NH_3)_3\{(py)_3COH\}]Br_2$.

Similar distortions about the (N, N', O) ligand are also apparent in the structure of $Ru\{(py)_3COH\}_2]^{2+}$, but, in that case, the deviations from regular geometry are greater, with the N-Ru-O angles being 76.2° and 77.2° compared with 79.6° and 79.2° for the triammine complex. [56] The bond angles between Ru and the donor atoms of the (N, N', N") ligand are closer to 90° than those of the (N, N', O) ligand, and are almost comparable with the bond angles betwen Ru and the ammine ligands in the triammine complex.

A notable difference between the structures of $[Ru(NH_3)_3\{(py)_3COH\}]^{2+}$ and $Ru\{(py)_3COH\}_2]^{2+}$ is the Ru-O distance. In the triammine complex this bond is shorter than the Ru-N bonds, and also shorter than the average bond length in $[Ru(H_2O)_6](pTS)_2$. [37] However, in the bis(tripod) complex, the Ru-O bond length is greater than any of the Ru-N bond lengths, and longer than the same bond in $[Ru(NH_3)_3\{(py)_3COH\}]^{2+}$. [67] It would, perhaps, be expected that the effect of five pyridine rings on the Ru(II) centre would be to make it more like a Ru(III) ion, but this would tend to shorten the Ru-O bond.

Another diference between the structures of the two tris(pyridyl) methanol complexes is the orientation of the uncoordinated pyridyl ring. In $Ru\{(py)_3COH\}_2]^{2+}$ the planes of the three pyridine rings of the (N, N', O) ligand are aligned at 120° and the uncordinated ring is almost coplanar with the ring trans to the coordinated OH group. [56] However, in $[Ru(NH_3)_3\{(py)_3COH\}]^{2+}$, the uncoordinated pyridine ring lies perpendicular to the line intersecting the planes of the other two rings of the (N, N', O) ligand. This may, in some way, contribute to the low intensity of the MLCT bands, but this seems unlikely, because this arrangement of the rings reduces the overall symmetry of the complex, which would be expected to result in more intense uv/vis absorptions.

3.5 Conclusions.

It has been possible to synthesize a series of substituted triammine complexes of ruthenium(III) and ruthenium(II) having ligands which range from strong π-donors to strong π-acceptors. The stabilization of the two oxidation states by the various ligands fits in with the pattern which had previously been established for the ruthenium penta- and tetraamine and edta complexes.

The substituted triammineaqua ruthenium(III) and ruthenium (II) complexes show pH-dependent reductions and oxidations which are consistent with the pK_a of the coordinated water in each case. There is a linear relationship between the reduction potential of the aqua complex and the pK_a of the Ru(III) complexes containing uninegative, bidentate ligands. At high pH, the $E_{1/2}$ for the Ru^{3+}/Ru^{2+} couple is more negative than that at low pH, because of the greater π-donating character of the OH^- ligand compared with the H_2O ligand. At low pH, the $E_{1/2}$ for the Ru^{3+}/Ru^{2+}

couple is very similar to that for the same couple in the penta- and tetraammine complexes with the same ligands, confirming the conclusion that the electron-donating properties of the aqua and ammine ligands are similar. It was possible to achieve electrochemical reduction of some of the Ru(III) complexes, but reaction of the reduced species with dinitrogen did not yield substituted triammine dinitrogen complexes.

It is apparent that π-donor ligands destabilize the Ru^{IV}=O group, but that π-donation from the oxalate ligand is sufficiently weak to allow the observation of a quasi-reversible Ru^{IV}=O/Ru^{III}OH couple.

The uv/vis spectra contain the LMCT bands expected for Ru(III) complexes with σ- and π-donor ligands, and the MLCT bands expected for Ru(II) complexes with π-acceptor ligands. The spectra of the complexes containing the aqua ligand are pH dependent, reflecting the effect of the differing π-donating abilities of the hydroxo and aqua ligands. At low pH, the spectra are very similar to those of the penta- and tetraammine complexes with the same ligands. In most spectra there were also intra-ligand bands, with their intensity roughly proportional to the number of such ligands present in the complex.

Crystal structure determinations show that the facial arrangement of ammine ligands which is present in $Ru(NH_3)_3Cl_3$ is retained in the substituted triammine complexes. The ruthenium(III) complex with acac as the ligand had a regular octahedral arrangement, but the ruthenium(II) complex with $(py)_3COH$ as the ligand was considerably distorted due to the coordination through the OH group and two pyridyl nitrogen atoms.

REFERENCES.

(1) P. C. Ford, *Coord. Chem. Rev.*, **5**, 75(1970)

(2) E. A. Seddon, K. R. Seddon, "The Chemistry of Ruthenium", Elsevier, Amsterdam, 1984.

(3) P. Ford, De F. P. Rudd, R. Gaunder, H. Taube, *J. Amer. Chem. Soc.*, **90**, 1187(1968)

(4) J. A. Stritar, H. Taube, *Inorg. Chem.*, **8**, 2281(1969)

(5) T. Matsubara, C. Creutz, *Inorg. Chem.*, **18**, 1856(1979)

(6) G. N. Coleman, J. W. Cresler, F. A. Shirley, J. R. Kuempel, *Inorg. Chem.*, **12**, 1036(1973)

(7) J. A. Broomhead, L. Kane-Maguire, *Inorg. Chem.*, **10**, 85(1971)

(8) R. E. Clarke, P. C. Ford, *Inorg. Chem.*, **9**, 227(1970)

(9) P. C. Ford, C. Sutton, *Inorg. Chem.*, **8**, 1544(1969)

(10) A. D. Allen, T. Eliades, R. O. Harris, P. Reinsalu, *Can. J. Chem.*, **47**, 1605(1969)

(11) D. E. Harrison, H. Taube, *J. Amer. Chem. Soc.*, **89**, 5706(1967)

(12) (a) N. E. Dixon, G. A. Lawrence, P. A. Lay, A. M. Sargeson, *Inorg. Chem.*, **23**, 2940(1984). (b) G. A. Lawrence, *Chem. Rev.*, **86**, 17(1986)

(13) R. W. Callahan, G. M. Brown, T. J. Meyer, *Inorg. Chem.*, **19**, 1443(1975)

(14) J. A. Baumann, T. J. Meyer, *Inorg. Chem.*, **19**, 345(1980)

(15) B. Anderes, S. T. Collins, D. K. Lavallee, *Inorg. Chem.*, **23**, 2201(1984)

(16) A. A. Diamantis, J. V. Dubrawski, *Inorg. Chem.*, **20**, 1142(1981)

(17) A. A. Diamantis, J. V. Dubrawski, *Inorg. Chem.*, **22**, 1934(1983)

(18) (a) G. A. Heath, K. R. Seddon. J. B. A. F. Smeulders, *Unpublished results.* (b) A. Endo, K. Shimizu, G. P. Sato, *Chem. Lett.*, 581(**1985**), and references therein.

(19) S. Pell, J. N. Armor, *Inorg. Chem.*, **12**, 873(1973)

(20) J. A. Broomhead, L. Kane-Maguire, *J. Chem. Soc., A,* 546(**1967**)

(21) R. Sahai, A. K. Kabisatpathy, J. D. Peterson, *Inorg. Chim. Acta,* **115**, L33(1986)

(22) R. W. Olliff, A. L. Odell, *J. Chem. Soc.*, 2417(**1964**)

(23) J. Powell, *J, Organomet. Chem.*, **65**, 89(1974)

(24) F. Ige, F. Ojo, O. Olubuyide, *Inorg. Chem.*, **20**, 1757(1981)

(25) S. W. Lin, A. F. Schreiner, *Inorg. Chim. Acta,* **5**, 290(1971)

(26) K. Nakamoto, "Infrared and Raman Spectra of Inorganic and Coordination Compounds." (3rd Ed.) J. Wiley & Sons, New York, 1978.

(27) R. T. Jones, Honours Report, The University of Adelaide, 1986.

(28) (a) A. A. Diamantis, W. R. Murphy, T. J. Meyer, *Inorg. Chem.*, **23**, 3230(1984). (b) A. A. Diamantis, *priv. comm.*

(29) C. M. Che, K-Y. Wong, C-K. Poon, *Inorg. Chem.*, **24**, 1797(1985)

(30) Y. Takeuchi, A. Endo. K. Shimizu, G. P. Sato, *J. Electroanal. Chem.*, **185**, 185(1985)

(31) Md. A. Salam, Ph. D. Thesis, The University of Adelaide, 1986.

(32) K. J. Takeuchi, M. S. Thompson, D. W. Pipes, T. J. Meyer, *Inorg. Chem.*, **23**, 1845(1984)

(33) K. J. Takeuchi, G. Samuels, S. W. Gersten, J. A. Gilbert, T. J. Meyer, *Inorg. Chem.*, **22**, 1407(1983)

(34) A. A. Diamantis, J. M. Frederiksen, Md. A. Salam, M. R. Snow, E. R. T. Tiekink, *Aust. J. Chem.*, **39**, 1081(1986)

(35) F. Bottomley, *Can. J. Chem.*, **55**, 2788(1977)

(36) H. C. Stynes, J. A. Ibers, *Inorg. Chem.*, **10**, 2304(1971)

(37) P. Bernhard, H-B. Burgi, J. Hauser, H. Lehman, A. Ludi, *Inorg. Chem.*, **21**, 3936(1982)

(38) G. K-J. Chao, R. L. Sime, R. J. Sime, *Acta. Crystallogr., Sect. B.*, **29**, 2845(1973)

(39) G. M. Bryant, J. E. Fergusson, H. K. J. Powell, *Aust. J. Chem.*, **24**, 257(1971)

(40) V. E. Alvarez, R. J. Allen, T. Matsubara, P. C. Ford, *J. Amer. Chem. Soc.*, **96**, 7686(1974)

(41) M. J. Ridd, F. R. Keene, *J. Amer. Chem. Soc.*, **103**, 5733(1981)

(42) T. Matsubara, P. C. Ford, *Inorg. Chem.*, **15**, 1107(1976)

(43) G. N. Brown, N. Sutin, *J. Amer. Chem. Soc.*, **101**, 883(1979)

(44) W. R. McWhinnie, J. D. Miller, *Adv. Inorg. Chem. Radiochem.*, **12**, 135(1969)

(45) A. B. P. Lever, "Inorganic Electronic Spectroscopy", (2^{nd} Ed), Elsevier, New York, 1984, p337

(46) R. Krishnamurthy, W. B. Schaap, *J. Chem. Ed.*, 46, 799(1969)

(47) K. Nakamoto, "Infrared and Raman Spectra of Inorganic and Coordination Compounds" (3^{rd}Ed.), J. Wiley & Sons, New York, 1978. (a) p197. (b) p199

(48) P. S. Braterman "Metal Carbonyl Spectra", Academic Press, London, 1975. (a)p214. (b) p46

(49) J. Chatt, G. J. Leigh, N. Thankarajan, *J. Chem. Soc., A*, 3168(**1971**)

(50) D. J. Darensbourg, *Inorg. Chem.*, **11**, 1436(1972), and references therein.

(51) R. H. Crabtree, A. J. Pearman, *J. Organomet. Chem.*, **157**,335(1978)

(52) B. A. Moyer, T. J. Meyer, *J. Amer. Chem. Soc.*, **100**, 360(1978)

(53) G. M. Brown, T. R. Weaver, F. R. Keene, T. J. Meyer, *Inorg. Chem.*, **15**, 190(1976)

(54) H, S. Lim, B. J. Barclay, F. C. Anson, *Inorg. Chem.*, **11**, 1460(1972)

(55) D. J. Szalda, F. R. Keene, *Inorg. Chem.*, **25**, 2795(1986)

(56) F. R. Keene, D. J. Szalda, T. A. Wilson, *Inorg. Chem.*, in press

(57) F. R. Keene, P. J. Stephenson, unpublished results.

(58) F. R. Keene, P. J. Stephenson, M. R. Snow, E. R. T. Tiekink, unpublished results.

(59) F. Bottomley, *Coord. Chem. Rev.*, **26**, 7(1978)

(60) D. P. Rillema, O. S. Jones, H. A. Levy, *J. Chem. Soc., Chem., Comm.*, 849(1979)

Chapter 4.

RUTHENIUM COMPLEXES WITH TRIDENTATE LIGANDS.

4.1. Introduction.

In Chapter 1, the stabilization of the +4 oxidation state of ruthenium was discussed, and it was shown that this oxidation state was favoured by complexes having ligands capable of strong π-donation. One of the ligands discussed in this context was the oxo (O^{2-}) ligand, and the work described in Chapters 2 and 3 has shown that the Ru(IV) oxidation state can be obtained in solution by proton-coupled electrochemical oxidation. The pH dependence of the proton-coupled oxidations was evidence that the oxo group was being formed on the Ru(IV) centre. The irreversibility of the voltammetric waves indicated that the Ru(IV) species were unstable, probably due to the effects of the other ligands.

Other workers in this laboratory have shown that dinegative, tridentate ligands derived from Schiff's bases are capable of eliminating the oxo ligand from the $V{=}O^{2+}$ group, and stabilizing the +4 oxidation state of vanadium. [1-3] The ligands formed by the reaction between aroyl hydrazines and ß-diketones, have been known for some time [4], and are capable of forming complexes of the type, $M(tridentate)_2$, with a variety of metal ions. Crystallographic studies have shown that the ligands retain their planar form upon coordination, resulting in geometries ranging from trigonal prismatic to meridional octahedra. Examples of these complexes include $V(acacBH)_2$*, $Ti(bzacBH)_2$ and $Ti(acacBH)_2$ [3] and $Mn(salDHP)_2$. [5] Other tridentate, dinegative ligands with O-N-O donor atoms can be formed by using 2-hydroxy aromatic carbonyl compounds instead of diketones, or by using 2-hydroxy amines instead of aroylhydrazines. There are potentially four classes of ligand available, using various combinations of the two component parts, as shown in Fig. 4.1.

The oxo (O^{2-}) group is almost ubiquitous in vanadium(IV) complexes, and this is due to its ability to stabilze the V^{4+} ion by p_π-d_π donation. [6] The ability of the dinegative, tridentate ligands to replace the oxo ligand in vanadium(IV) complexes is strong evidence that their π-donor abilities are comparable to that of the oxo group. Given the ease with which the tridentate ligands are able to replace the oxo group, and the ability of the oxo group to stabilize Ru(IV), it was considered likely that the dinegative, tridentate ligands would also be useful in stabilizing the Ru(IV) ion.

*Refer to the list of abbreviations.

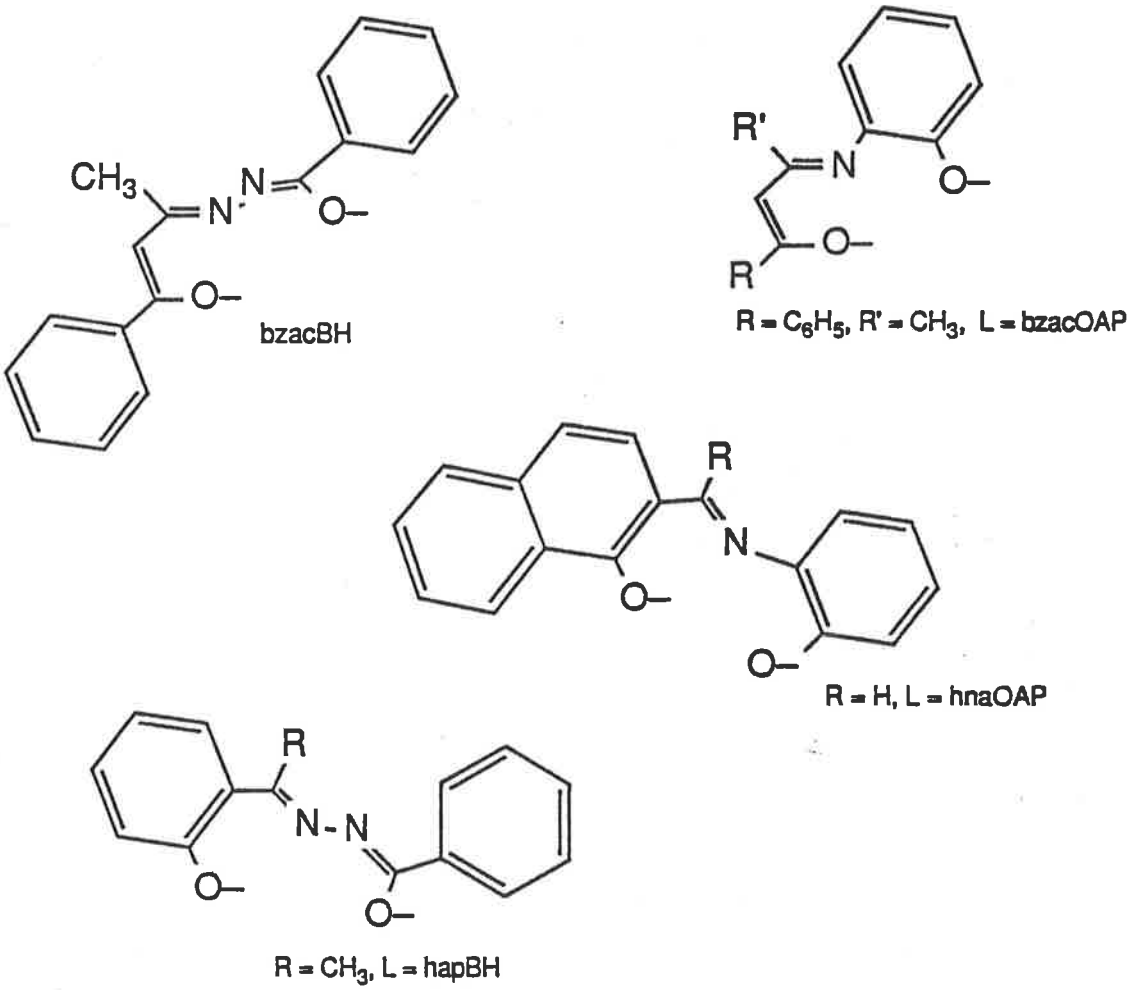

Fig. 4.1. Some examples of tridentate ligands.

4.2. Preparation of bis-(Tridentate) Ruthenium Complexes.

$RuCl_3.3H_2O$ reacted with two molar equivalents of the protonated ligand, LH_2, in refluxing ethanol, in the presence of four molar equivalents of base. After about four hours the solution was allowed to cool, sometimes at –10°C overnight, and a dark microcrystalline solid could be filtered from the reaction mixture. The base used was either lithium acetate or triethylamine. When the ligand was hnaBH, the product from the reaction where triethylamine was used as the base was much more soluble in ethanol and chloroform than the product from the reaction using lithium acetate. However, no differences could be detected from microanalysis or electrochemical behaviour.

In the synthesis of the vanadium(IV) bis-(tridentate) complexes, it was necessary to maintain an oxygen free atmosphere in order to prevent the oxidation of some reaction intermediates. If air was allowed in to the reaction mixture, complexes of the type, $[\{VO(L)_2\}_2O]$, were obtained. [1, 7] The reaction between $RuCl_3$ and the ligands in the presence of air was expected to favour oxidation of the Ru(III), and it was expected that the Ru(IV) complexes would precipitate from the reaction mixture, thus precluding further oxidation.

Microanalytical results, as shown in Table 4.1, indicated that the products contained two ligand molecules per ruthenium and, except for two cases, gave closest agreement with the formulation of the complexes as $RuL_2.H_2O$. For the complex with salBH,the formulation, $Ru(salBH)_2.0.5C_2H_5OH$ was indicated, and for the complex with bzacOAP, a dimeric formulation , $Ru_2(bzacOAP)_2.H_2O$, was indicated. Although the reactions were performed in ethanol, the solvent was not dried prior to use because of the hydrated state of the ruthenium starting material. Clearly, there was water present in the reaction mixture to give rise to the presence of lattice water in the solid products.

The complex with bzacBH was moderately soluble in acetone and chloroform as well as dimethyl sulphoxide, which was the only solvent in which any of the other products had appreciable solubililty except that the complexes containing salBH and bzacOAP were not soluble in any of the common organic solvents.

$V(acacBH)_2$ can only be prepared by a template reaction between $VO(acac)_2$ and benzoylhydrazinze, because the free diketone reacts with the hydrazine to give a heterocyclic compound. [2] The preparation of $Ru(acacBH)_2$ was attempted, by the reaction of $Ru(acac)_3$ with benzoylhydrazine in refluxing ethanol. After 4 hours, $Ru(acac)_3$ was recovered, unchanged, from the reaction mixture.

Ligand.	Found.				Calculated.			
	C	H	N	Cl	C	H	N	Cl
bzacBH[a]	60.88	4.39	8.46		60.44	4.47	8.29	
bzac-pCl-BH[a]	55.16	3.70	7.51	10.31	56.08	3.79	7.52	9.52
hnaBH[a]	61.26	3.76	7.62		62.15	3.77	8.05	
hna-pCl-BH[a]	55.82	3.31	7.04	9.26	56.55	3.16	7.33	9.27
hapBH[a]	58.03	4.17	8.86		57.75	4.20	8.98	
bzacSalH[a]	56.06	4.18	7.62		57.70	4.27	7.62	
salBH[b]	57.63	3.95	9.27		57.78	4.20	8.98	
bzacOAP[c]	53.38	3.99	3.86		53.18	3.90	3.88	

Table 4.1. Comparison of micronalysis results with expected percentages for Ru(IV) complexes. (a) formulation based on $RuL_2.H_2O$. (b) formulation based on $RuL_2.0.5EtOH$. (c) formulation based on $Ru_2L_2.H_2O$

4.3. Electrochemical Studies.

The electrochemistry of ruthenium bis(tridentate) complexes was studied at a platinum electrode in DMSO solution, with 0.1 mol dm^{-3} $NaClO_4$ supporting electrolyte, and a SCE reference electrode. (Under these conditions, ferrocene was oxidized at +0.447 V.) For all but one of the complexes, it was possible to observe two quasi-reversible waves which were assigned to the Ru^{4+}/Ru^{3+} and Ru^{3+}/Ru^{2+} couples. The potential of the Ru^{3+}/Ru^{2+} couple was 1.3 V to 1.6 V more negative than that of the Ru^{4+}/Ru^{3+} couple. The $E_{1/2}$ potentials of these couples are listed in Table 4.2, along with those of some similar complexes.

Linear sweep voltammetry on stirred solutions, in the potential range of the Ru^{4+}/Ru^{3+} couples, was used to determine the ruthenium oxidation state in each complex. For the complexes with bzacBH and bzac-pCl-BH the LSV showed that there was no current at potentials more positive than $E_{1/2}$, and there was a cathodic current at potentials less positive than $E_{1/2}$ (Figs. 4.2 and 4.3). This result was evidence that these two complexes were in the Ru(IV) state. For the complexes with the ligands hnaOAP, hapBH, hnaBH and hna-pCl-BH, the LSV showed that an anodic current flowed at potentials more positive than $E_{1/2}$, and there was no current at potentials less positive than $E_{1/2}$. This result was evidence that these complexes were in the Ru(III) state. For the complex with bzacSalH, there was a small anodic current in the stirred solution voltammogram at potentials more positive than $E_{1/2}$ and a small cathodic current at potentials less positive than $E_{1/2}$. (Fig. 4.4). This was an indication that, perhaps, the product of the reaction was a mixture of oxidation states. The stirred solution voltammogram was identical for several freshly-prepared samples of the product, so it seems unlikely that there was a mixture of compounds. It may be that the product was a Ru(III) complex which reacted in the voltammetric solution to give a mixture of oxidation states.

The CV of the complex with hnaOAP consisted of a single quasi-reverisble wave with $E_{1/2}$ = +0.46 and ΔE_p = 104 mV at a scan rate of 100mV sec^{-1}. On a cathodic scan from +0.75 V, the OSWV voltammogram showed a peak at +0.57 V, which is considerably different from the $E_{1/2}$ determined from the CV. On continuing this cathodic scan multiple peaks were observed at negative potentials, with the most intense being at –1.09 V. The peak at –1.09 V was probably due to the Ru^{3+}/Ru^{2+} couple, but the limited solubility of this complex in DMSO made interpretation of the results difficult.

In addition to the two reversible waves, the cyclic voltammograms of the complexes containing bzacSalH, hapBH and hnaBH also contained a cathodic peak at approximately –0.5 V (Figs. 4.4, 4.5, 4.6). In the case of the bzacSalH complex, after the scan direction had been reversed at –1.75 V, the height of this peak was less on subsequent cathodic scans. In the voltammograms of

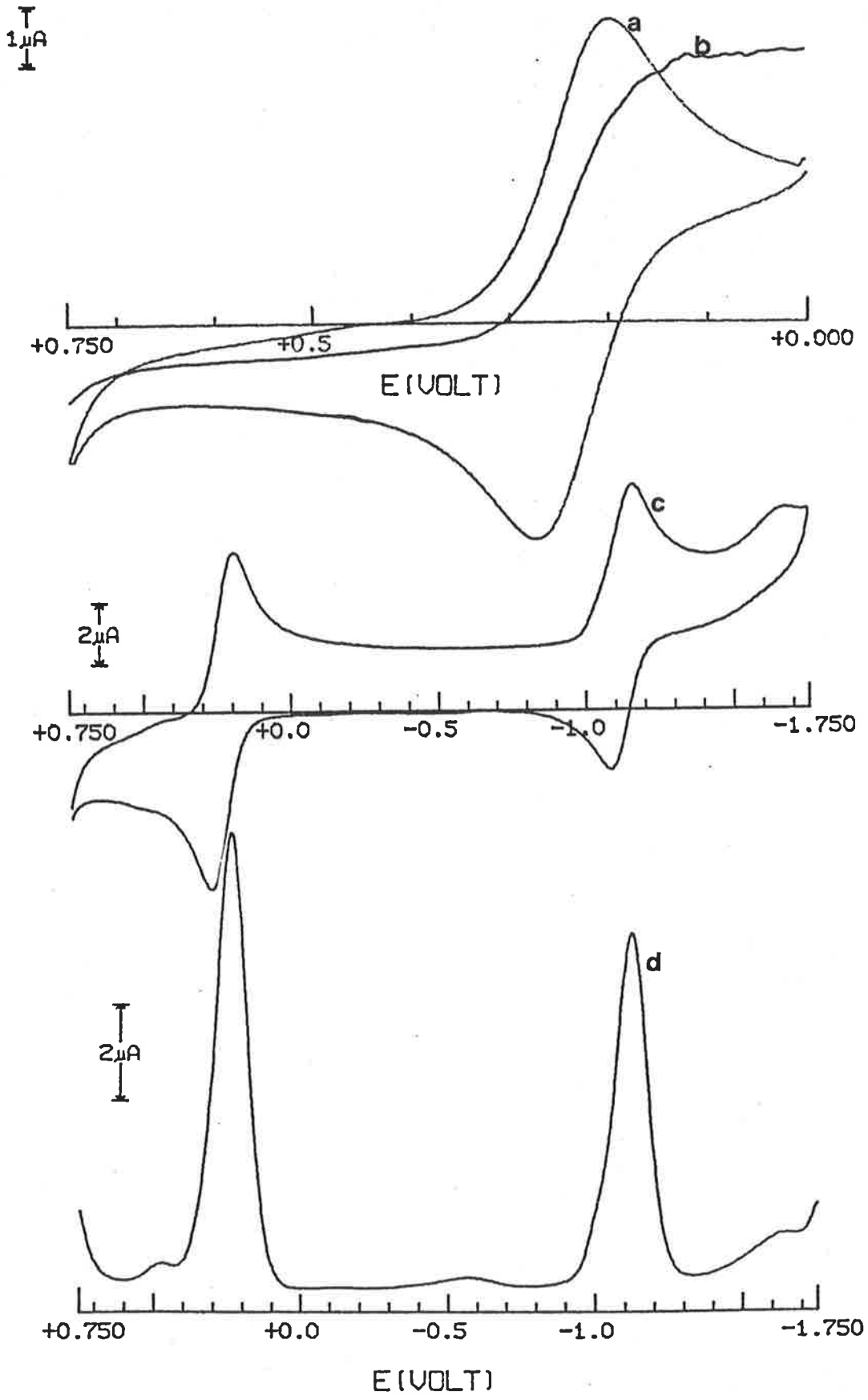

Fig. 4.2. Voltammograms of $Ru(bzacBH)_2$ in DMSO. (a) Cyclic voltammogram of the Ru^{4+}/Ru^{3+} couple. (b) Stirred solution linear sweep voltammogram of the Ru^{4+}/Ru^{3+} couple. (c) Cyclic voltammogram of the Ru^{4+}/Ru^{3+} and Ru^{3+}/Ru^{2+} couples. (d) Differential pulse voltammogram of the Ru^{4+}/Ru^{3+} and Ru^{3+}/Ru^{2+} couples.

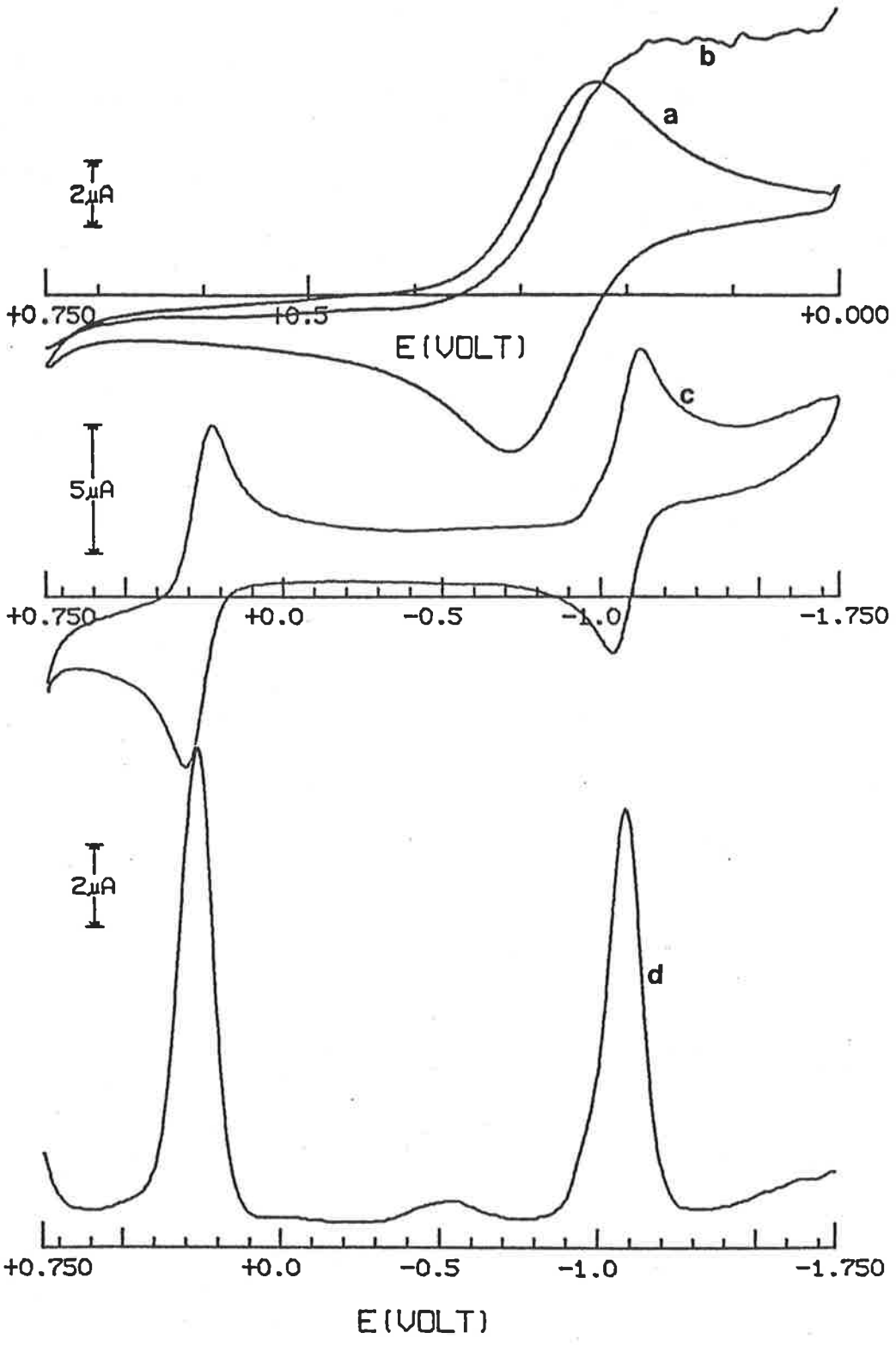

Fig. 4.3. Voltammograms of $Ru(bzac\text{-}pCl\text{-}BH)_2$ in DMSO. (a) Cyclic voltammogram of the Ru^{4+}/Ru^{3+} couple. (b) Stirred solution linear sweep voltammogram of the Ru^{4+}/Ru^{3+} couple. (c) Cyclic voltammogram of the Ru^{4+}/Ru^{3+} and Ru^{3+}/Ru^{2+} couples. (d) Differential pulse voltammogram of the Ru^{4+}/Ru^{3+} and Ru^{3+}/Ru^{2+} couples.

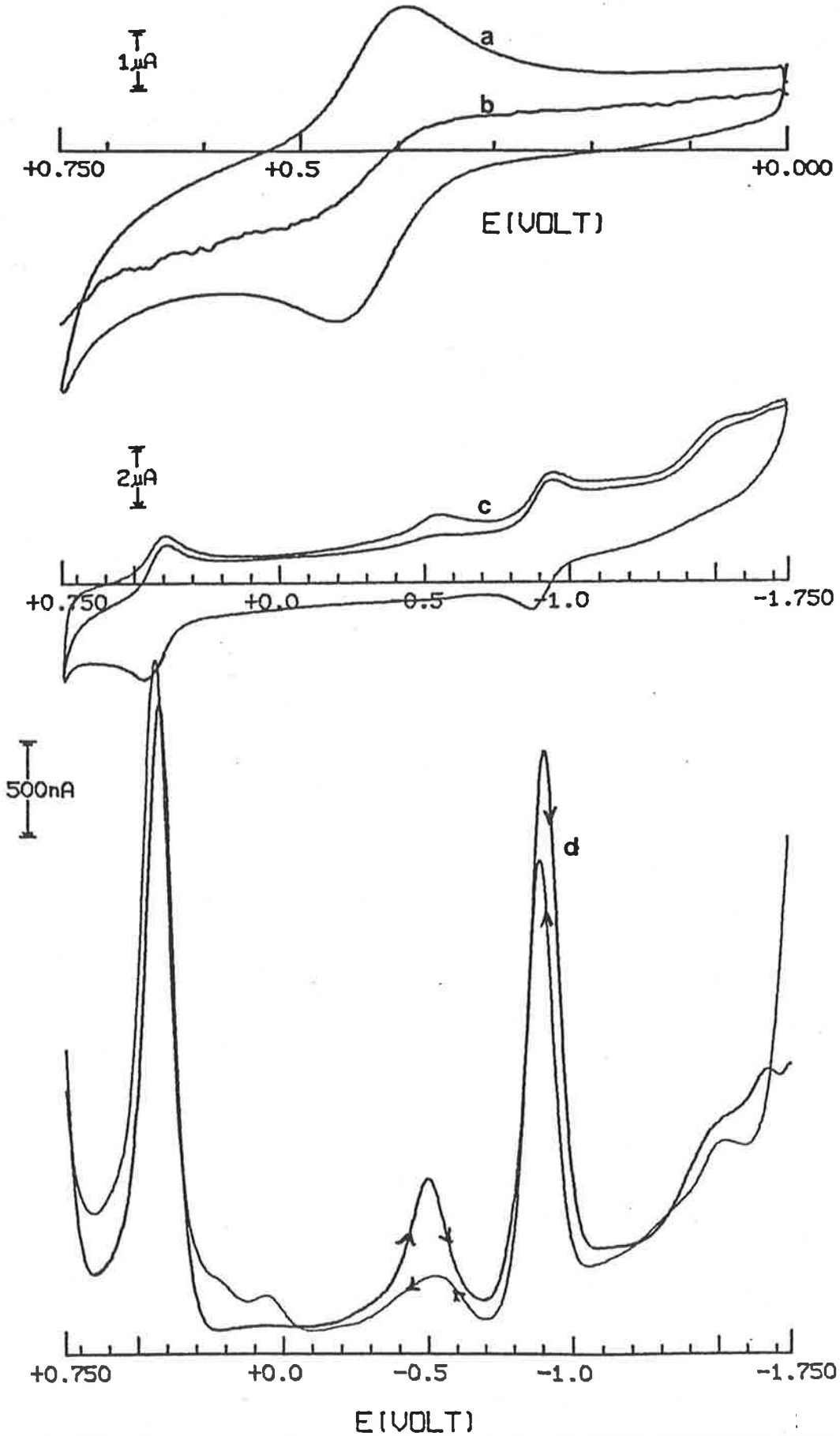

Fig. 4.4. Voltammograms of "Ru(bzacSalH)$_2$" in DMSO. (a) Cyclic voltammogram of the Ru^{4+}/Ru^{3+} couple. (b) Stirred solution linear sweep voltammogram of the Ru^{4+}/Ru^{3+} couple. (c) Cyclic voltammogram of the Ru^{4+}/Ru^{3+} and Ru^{3+}/Ru^{2+} couples. (d) Differential pulse voltammogram of the Ru^{4+}/Ru^{3+} and Ru^{3+}/Ru^{2+} couples.

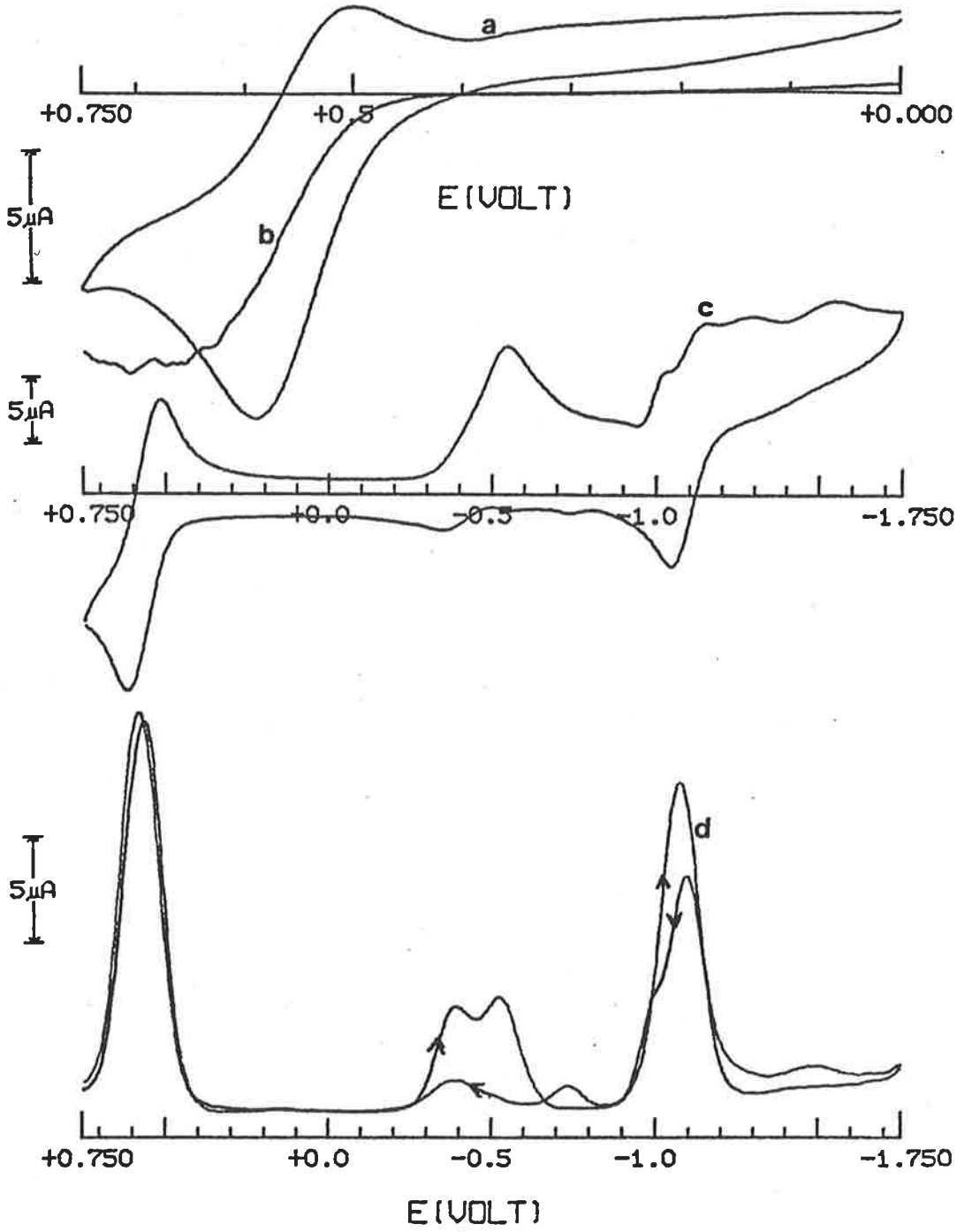

Fig. 4.5. Voltammograms of "Ru(hapBH)$_2$" in DMSO. (a) Cyclic voltammogram of the Ru^{4+}/Ru^{3+} couple. (b) Stirred solution linear sweep voltammogram of the Ru^{4+}/Ru^{3+} couple. (c) Cyclic voltammogram of the Ru^{4+}/Ru^{3+} and Ru^{3+}/Ru^{2+} couples. (d) Differential pulse voltammogram of the Ru^{4+}/Ru^{3+} and Ru^{3+}/Ru^{2+} couples.

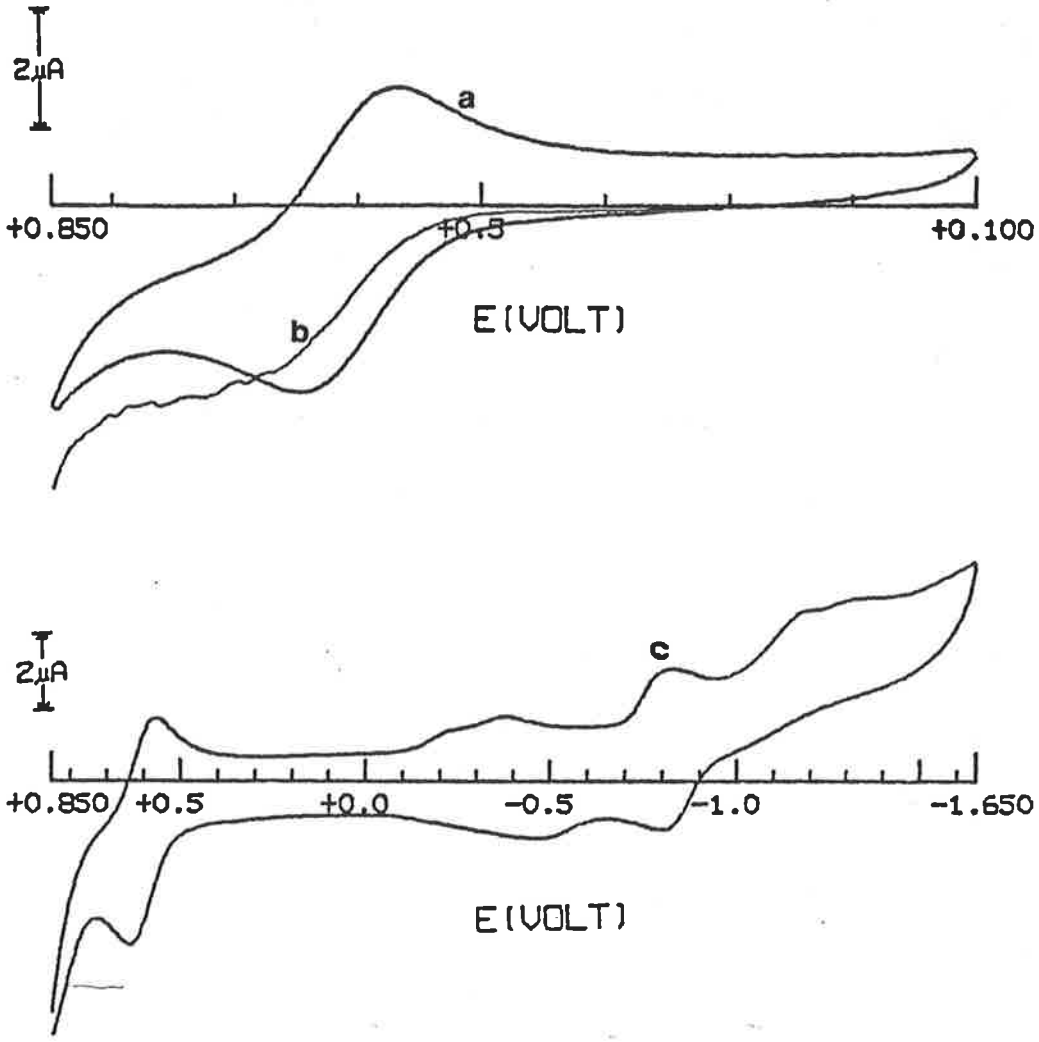

Fig. 4.6. (a) Cyclic voltammogram of the $Ru(hnaBH)_2^{0/-}$ redox couple in DMSO. (b) Stirred solution linear sweep voltammogram of the $Ru(hnaBH)_2^{0/-}$ redox couple in DMSO. (c) Cyclic voltammogram of the $Ru(hnaBH)_2^{0/-}$ and $Ru(hnaBH)_2^{-/2-}$ redox couples in DMSO.

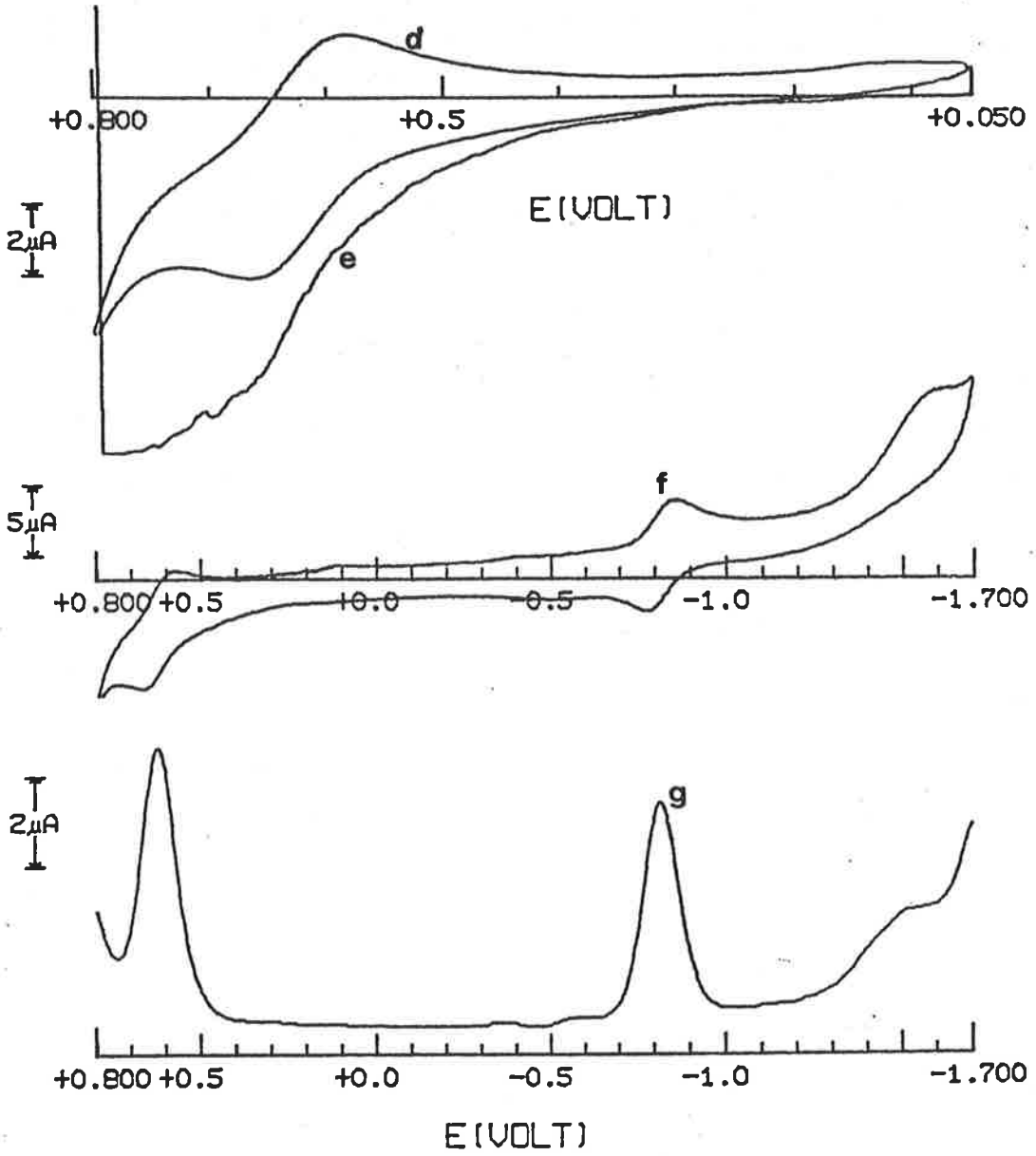

Fig. 4.6.(cont) Voltammograms of "Ru(hna-pCl-BH)$_2$" in DMSO. (d) Cyclic voltammogram of the Ru^{4+}/Ru^{3+} couple. (e) Stirred solution linear sweep voltammogram of the Ru^{4+}/Ru^{3+} couple. (f) Cyclic voltammogram of the Ru^{4+}/Ru^{3+} and Ru^{3+}/Ru^{2+} couples. (g) Differential pulse voltammogram of the Ru^{4+}/Ru^{3+} and Ru^{3+}/Ru^{2+} couples.

Complex	$E_{1/2}(\Delta Ep)^a$ IV/III	$E_{1/2}(\Delta Ep)$ III/II	$\Delta E_{1/2}$	Oxid^n State^b
$Ru(bzacBH)_2$	+0.24(80)	−1.12(74)	1.36	+4
$Ru(bzac\text{-}pCl\text{-}BH)_2$	+0.27(77)	−1.08(83)	1.35	+4
$Ru(bzacSalH)_2$	+0.43(77)	−0.91(74)	1.34	+3
$Ru(hnaOAP)_2$	+0.46(104)	−1.09^c	1.55	+3
$Ru(hapBH)_2$	+0.55(91)	−1.08^c	1.63	+3
$Ru(hnaBH)_2$	+0.62(77)	−0.85(65)	1.47	+3
$Ru(hna\text{-}pCl\text{-}BH)_2$	+0.65(98)	−0.81(74)	1.44	+3
$V(bzacBH)_2$	−0.35(90)			
$V(bzac\text{-}pCl\text{-}BH)_2$	−0.29(170)			
$V(hnaOAP)_2$	−0.21(190)	−1.68(160)	1.89	
$V(hnaBH)_2$	−0.16(80)	−1.71(90)	1.87	
$V(bzacSalH)_2$	−0.11(80)	−1.76(80)	1.87	
$Ti(bzacBH)_2$	−0.89			
$Ti(hnaBH)_2$	−0.75			
$Mn(bzacBH)_2$	+0.14			

Table 4.2. Redox potentials of M(tridentate)$_2$ complexes. Ruthenium complexes, this work, potentials vs SCE in DMSO solution. Vanadium and Titanium complexes, Reference 2, potentials vs SCE with Et_4NCl electrolyte in DMSO solution. Manganese complex, Reference 9, vs SCE with Et_4NCl electrolyte in CH_2Cl_2 solution. (a) V(mV) (b) Ruthenium oxidation state determined from stirred solution LSV. (c) $E_{1/2}$ determined from peak potential in OSWV experiment.

the hapBH and hnaBH complexes, the height of this peak was comparable to that of those assigned to the Ru^{4+}/Ru^{3+} and Ru^{3+}/Ru^{2+} couples. However, when the CV of the hnaBH complex was studied in acetone, this peak was not observed. [8] Therefore, it is apparent that this peak arises from some interaction between the complexes and the DMSO solvent. In the hapBH and hnaBH complexes, there are other cathodic peaks, at potentials more negative than the Ru^{3+}/Ru^{2+} couple which appear to be associated with this irreversible wave. The interaction between the DMSO and the complexes which gives rise to the irreversible cathodic wave is not readily identifiable. It may involve some Ru(III) species, or the inclusion of dimethylsulphoxide in the ruthenium coordination sphere.

With the exception of these irreversible cathodic waves, the electrochemistry of the RuL_2 complexes is similar to that of the vanadium and titanium complexes. [2] The data in Table 4.2 for ruthenium and vanadium complexes are plotted in Fig. 4.7. Though the number of data is small, it is apparent that there are two groups of complexes, and within each there is a consistent trend in $E_{1/2}$ potential. These two groups of complexes are those with a bzac portion in the ligand and those with a hna portion. Clearly, within groups of ligands, the electron donating ability of the ligands, as measured by $E_{1/2}$ potential, varies in the same manner for both metals.

The range of $E_{1/2}$ potentials for the M^{4+}/M^{3+} couples is very different. For ruthenium complexes, the difference between the highest and lowest $E_{1/2}$ potentials is 0.38 V, whereas for the vanadium complexes, the difference is 0.19 V . The larger range of $E_{1/2}$ values in the ruthenium complexes is probably due to the larger size of the 4d orbitals of ruthenium compared with the 3d orbitals of vanadium. Because the d orbitals are larger, there is greater overlap between them and the ligand orbitals, which means that the complex is more susceptible to changes in the ligand.

For the $M(bzacBH)_2$ complexes, the $E_{1/2}$ potentials for the M^{4+}/M^{3+} couple are plotted against the periodic core charge of the ion in Fig. 4.8, where they are compared with a similar plot for the $[MCl_6]$ complexes. [10] It can be seen that the variation of $E_{1/2}$ across the periods for the 4-d and 5-d hexachlorometallates follows a regular pattern which parallels the variation in ionization potential of the metal ions. It can also be seen that the lines for the 4-d and 5-d series are parallel. The variation of $E_{1/2}$ for the limited series of $M(bzacBH)_2$ complexes seems to follow a similar pattern. It can be assumed on the basis of Heath's results that the line for the missing 4d series of $M(bzacBH)_2$ complexes would be parrallel to that for the 3d series. Therefore, it is to be expected that the $E_{1/2}$ potential for $Ru(bzacBH)_2^{0/-}$ would lie at a slightly more positive potential than that of the $Mn(bzacBH)_2^{0/-}$ couple. Heath and co-workers also showed that the slopes of the lines across a series were ligand-dependent, being less for the hexachlorometallates than for the corresponding

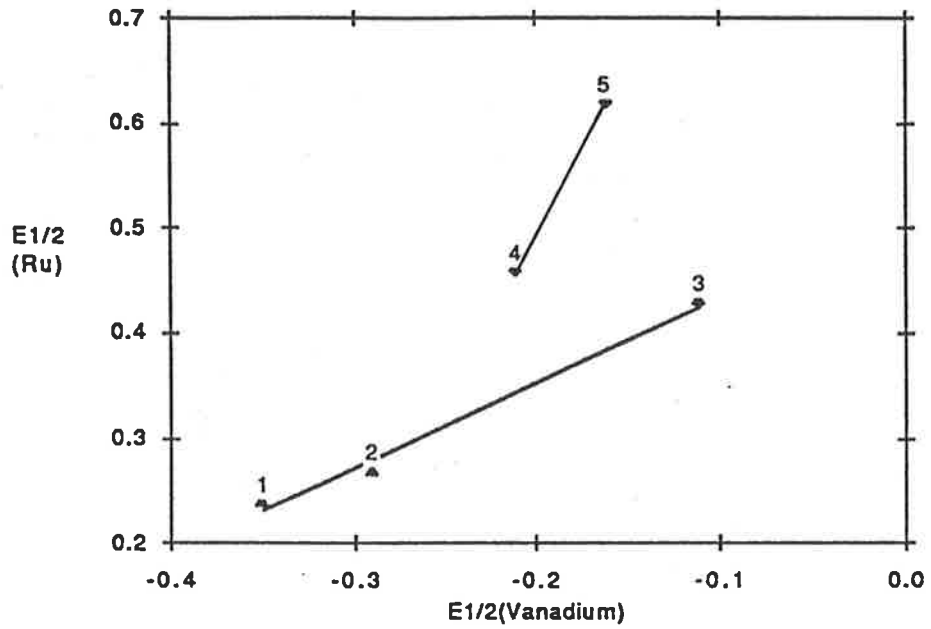

Fig. 4.7. Plot of $E_{1/2}$ for Ru(tridentate)$_2^{0/-}$ redox couples vs $E_{1/2}$ for V(tridentate)$_2^{0/-}$ redox couples. (1) L = bzacBH. (2) L = bzac-pCl-BH. (3) L = bzacSalH. (4) L = hnaBH.(5) L = hnaOAP.

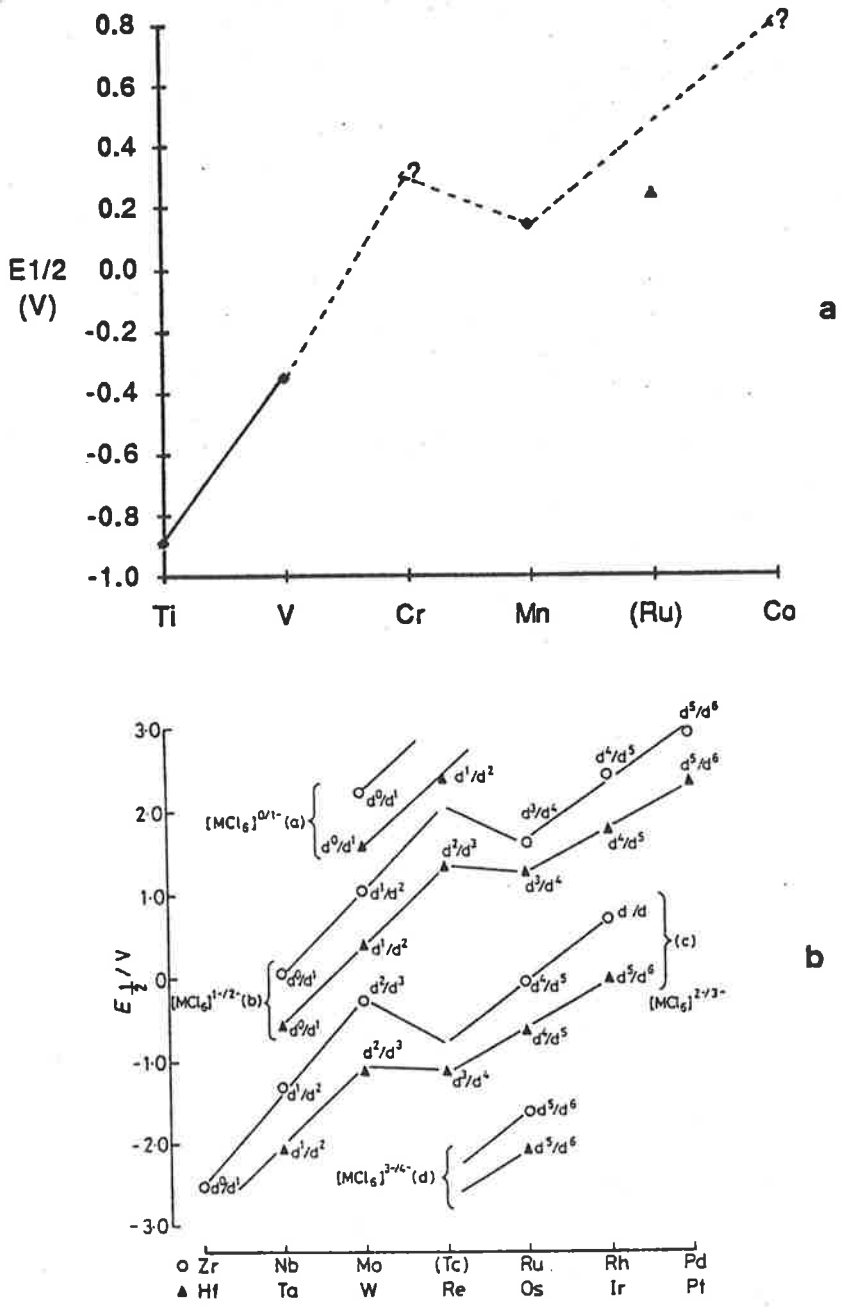

Fig. 4.8 Trends in $E_{1/2}$ potentials for: (a) $M(bzacBH)_2^{0/-}$ redox couples (points for Cr and Co estimated by extrapolation). (b) $[MCl_6]^{z/z-1}$ redox couples. [10]

fluoro complexes. [10] This can be attributed to the greater nephelauxetic effect of the chloro ligand and it is consistent with the much smaller slope involved with the limited number of $M(bzacBH)_2$ complexes.

Another feature that is common to $M(tridentate)_2$ complexes of ruthenium and vanadium is that there is a relatively constant separation of the potentials of the two redox couples for each metal. There is some uncertainty about the titanium complexes because it is not known whether the redox couples at more negative potentials are ligand- or metal-centred. For the ruthenium complexes, the potential separation between the two couples is between 1.3 V and 1.6 V, and for the vanadium complexes, the separations are between 1.6 and 1.8 V. The separations between the ruthenium couples may be compared with the potential separations of between 1.55 V and 1.9 V for the Ru/Ru^{3+} and Ru^{3+}/Ru^{2+} couples in a large number of $Ru(diketonate)_3$ complexes. [11-13] The ligand-dependence of the separation between successive couples for any one element has also been dealt with by Heath's group and was explained in terms of electron-electron correlations and the nephelauxetic effect.

In dichloromethane solution, the $E_{1/2}$ potentials for oxidation of the $Ru^{III}(diketonate)_3$ complexes were in the range +1.05 V to +1.84 V (converted to SCE scale), which is considerably greater than the potentials at which the $Ru^{III}(tridentate)_2$ complexes are oxidized. This is a reflection of the greater π-donating ability of two dinegative ligands compared with three uninegative ligands.

As noted above, the complexes with the lowest $E_{1/2}$ potentials for the Ru^{4+}/Ru^{3+} couples were isolated as Ru(IV) complexes, while those with the highest $E_{1/2}$ potentials for the Ru^{4+}/Ru^{3+} couples were isolated as Ru(III) complexes. This result is consistent with the capacities of the various ligands to stabilize higher oxidation states by π-donation. The better π-donors would be expected to favour the higher oxidation state, and to give complexes with less negative $E_{1/2}$ potentials. Given that the microanalytical results for these compounds were all consistent with the formulation of the compounds as $RuL_2.H_2O$, the question of the exact composition of these complexes becomes important. With two dinegative anions present in the compound, a ruthenium(III) complex requires the presence of a cation to maintain neutrality of charge. At first it was considered that the cation in the compound must be lithium, coming from the lithium acetate used as a base in the preparative reaction. However, this is not so. Analysis of the Ru(III) compounds showed that each contained less than 0.05% Li.

4.4. Mass Spectra.

The complexes were too involatile to allow the determination of the mass spectra by the conventional electron impact process. The mass spectra of the complexes could be obtained using Fast Atom Bombardment (FAB) mass spectrometry. In this technique, the sample under investigation is dissolved in an inert matrix, and then subjected to bombardment by a stream of high energy heavy atoms (in this case argon atoms were used). The bombardment of the sample results in the formation of positive and negative ions, which may be detected separately by changing the acceleration potential in the spectrometer from +8 kV (for positive ion spectra) to –8 kV (for negative ion spectra). There are 7 isotopes of ruthenium and their mass numbers and relative abundances are: 96(5.51%), 98(1.87%), 99(12.72%), 100(12.62%), 101(17.07%), 102(31.63%) and 104(18.58%). Complexes of ruthenium have mass spectra which show a pattern of 7 peaks, with their intensities roughly proportional to the relative abundances. The most intense peak generally corresponds to the Ru^{102} isotope. In some cases, high resolution mass spectrometry was used in order to obtain the molecular weight, and so clarify the composition of the Ru(III) complexes. In this process, the most intense peak was calibrated against a sample of caesium iodide, and its molecular weight determined, instrumentally, by comparison with a well-defined peak in the calibrant.

4.4.1. $Ru^{IV}L_2$ Complexes. The most intense peak in the molecular ion ruthenium isostope peak for $Ru(bzacBH)_2$ was at m/z = 659 amu which agrees with the molecular weight expected for $Ru^{102}(bzacBH)_2$. In the spectrum of $Ru(bzac\text{-}pCl\text{-}BH)_2$, the two most intense peaks in the molecular ion pattern were at m/z = 727 amu and m/z = 729 amu which correspond to the molecular weights of RuL_2 for the $Ru^{102}Cl^{35}Cl^{35}$ and $Ru^{102}Cl^{37}Cl^{35}$ isotopic combinations. The ruthenium isotope patterns for the two complexes were identical in both the positive ion and negative ion spectra. There were no fragmentations observed.

The complexes with the ligands salBH and bzacOAP could only be studied by mass spectrometry, because they were not sufficiently soluble in any solvent for electrochemical or spectral measurements. In the absence of any evidence to the contrary, both were assumed to be ruthenium(IV) complexes. The complex with salBH was formulated as $Ru(salBH)_2.0.5EtOH$. The mass spectrum of this compound contained a molecular ion signal with a regular ruthenium isotope pattern. The most intense peak in the pattern was at m/z = 578 amu, which corresponds to the molecular weight of $Ru^{102}(salBH)_2$.

On the basis of microanalysis, the complex with bzacOAP was formulated as $Ru_2(bzacOAP)_2$. However, the highest molecular weight fragment in the mass spectrum was at m/z = 605 amu, which is the molecular weight expected for $Ru^{102}(bzacOAP)_2$. Additionally, in this spectrum, a distinct fragmentation pattern was observed. There were two other ions having the ruthenium isotope

pattern, with the most intense peaks being at m/z = 353 amu and m/z = 338 amu. This spectrum corresponds to the following fragmentation pattern.

$$[Ru^{102}(bzacOAP)_2]^+ \longrightarrow [Ru^{102}(bzacOAP)_2 - bzacOAP]^+$$

$$m/z = 605 \qquad m/z = 353$$

$$\downarrow$$

$$[Ru^{102}(bzacOAP)_2 - bzacOAP - CH_3]^+$$

$$m/z = 338$$

This is quite strong evidence that the complex is actually $Ru(bzacOAP)_2$ and implies that the microanalytical results were inaccurate, probably due to some contamination of the sample.

4.4.2. $Ru^{III}L_2$ Complexes. The spectra of the complexes with hnaBH, hna-pCl-BH and bzacSalH were determined as both positive ion and negative ion spectra. The negative ion spectra of the three complexes all had molecular ion peaks with the expected ruthenium isotope pattern. The positive ion spectra showed a molecular ion with a peak pattern which was consistent with the overlap of two ruthenium isotope patterns, an indication that, possibly, both RuL_2^+ and $HRuL_2^+$ molecular ions were formed.

For the complex with hnaBH, the negative ion spectrum contained an isotope pattern with the maximum peak at m/z = 678 amu, which is equal to the molecular weight of the species $Ru^{102}(hnaBH)_2$. Despite the unusual isotope pattern in the positive spectrum, the most intense peak was at m/z = 679 amu. In the high resolution spectrum, this peak was found to be 679.13(±.05) amu, which is close to the value predicted for $[HRuL_2]$, 679.092 amu. It would appear that the Ru(III) species contains the two tridentate ligands, perhaps with the charge of the complex being balanced by the presence of a hydrogen ion. However, the position of this hydrogen ion is not certain, and it is also known that $[M+H]^+$ ions (where M represents the molecular ion) may be generated buring the bombardment of the sample. [14] Therefore it is not possible to conclusively assign the complex as $[HRu(hnaBH)_2]$

The spectra of the complexes with hna-pCl-BH and bzacSalh were similar to that of the hnaBH complex, with the negative ion spectra being consistent with RuL_2, and the most intense peak in the positive ion spectrum being consistent with the formulation, $[HRuL_2]$. The results of the positive ion and negative ion spectra are consistent with each other. If the formula of the complexes is $[HRuL_2]$, then, in the negative ion spectrum, it would be expected that the molecular ion which was observed would be readily generated by the loss of a proton from the complex.

4.5. Vibrational Spectra.

It was anticipated that the vibrational spectra of the complexes would confirm some of the assumptions made about their composition. In particular, the presence of lattice water would be readily indicated by the presence of the characteristic (υ)OH bands between 3300 and 3800 cm^{-1}, or the assignment of some of the complexes as $H[RuL_2]$ would be confirmed by the presence of bands characteristic of the (υ)OH mode between 3200 and 3450 cm^{-1}. The presence of strong bands between 850 and 1000 cm^{-1} would have been indicative of the possible presence of Ru=O groups [15], which would have implied that the higher oxidation state complexes were not of the type, RuL_2. The ir spectra of the complexes were recorded as nujol mulls on KBr windows and the Ru(III) complexes were also recorded in KBr pellets in the range 2500 cm^{-1} to 3600 cm^{-1}.

Generally, the spectra were similar to those of the $V^{IV}L_2$ complexes. [2] The absence of any intense bands between 850 cm^{-1} and 1000 cm^{-1} in all spectra confirmed the absence of a Ru=O bond. All the spectra contained weak broad bands centred in the range 3420 cm^{-1} to 3460 cm^{-1} providing evidence of the presence of lattice water. In the spectrum of the salBH complex, there was no evidence of the presence of ethanol in the lattice which was indicated by the microanalysis result.

In the KBr pellet spectra of some of the Ru(III) complexes there were weak absorptions in the region 3180 cm^{-1} to 3220 cm^{-1} which were assigned to a (υ)NH vibration. The aromatic (υ)CH vibrations were evident as sharp bands between 2980 cm^{-1} and 3050 cm^{-1}, so the weak bands at slightly higher energies were not due to this mode of vibration. In the vanadium(IV) complexes, V(O)(Cl)(HL), there is one uninegative, tridentate ligand. The ir spectra of these complexes showed weak, broad bands at approximately 3200 cm^{-1}, which were attributed to the (υ)NH vibration. [2] It would appear, therefore, that the 3+ charge in the Ru(III) complexes is accomodated by partial deprotonation of one of the tridentate ligands instead of double deprotonation of both of them.

4.6. Magnetic Properties.

The magnetic properties of the RuL_2 complexes were determine at a single temperature by the Gouy method. The lack of a suitable instrument prevented the determination of magnetic suscetibilities at many temperatures. The interpretation of single temperature magnetic measurements can not be conclusive because the magnetic susceptibility of a complex is proportional to the square root of the temperature at which the measurement is made. [16] However, it is possible to compare experimental results with the magnetic susceptibility of known examples. The magnetic properties of the RuL_2 complexes are presented in Table 4.3.

L	bzacBH	bzac-pCl-BH	hnaBH	hna-pCl-BH	hapBH	bzacSalH.
χ_M x 10^6 (cgs units)	117	1020	1750	1079	1510	2200
μ_{eff} (B.M.)	0.53	1.6	2.0	1.9	1.6	2.3

Table 4.3. Magnetic moments of RuL_2 complexes at 298 K.

It can be seen that the magnetic moment of $Ru(bzacBH)_2$ is considerably lower than that of any of the other complexes, and that this complex is nearly diamagnetic. In an octahedral complex, with two unpaired electrons in degenerate orbitals, the magnetic moment is expected to be 2.8 B.M. [16] The magnetic moments of a large number of mononuclear Ru(IV) complexes (which are low spin d^4complexes) are close to this value. [17] However, in a different geometry, in which the degeneracy is lifted, a d^4 complex may be diamagnetic. If the nearest empty energy level in such a complex is thermally accessible, then there may be a small magnetic moment observed, which is larger than that for a diamagnetic complex. If there is some distortion in these compounds, then some temperature dependence of the magnetic moment should be observed.

Such temperature dependence was observed indirectly by H^1 NMR spectroscopy. The spectrum of $Ru(bzacBH)_2$ was determined at 90 MHz in CD_2Cl_2 at three temperatures: 300K, 253 K and 233K. The temperature dependence of the peak at 3.88 ppm (assigned to the methyl group in the ligand) was examined. At 300 K, this line was rather broad, with $W_{1/2}$ = 12 Hz, whereas at 253 K and 233 K, $W_{1/2}$ was 3 Hz. The broadening of the line at higher temperatures can be attributed to the slight paramagnetism of the complex. The narrower line at lower temperatures implies that the magnetic moment of the complex is lower. This result reinforces the proposal of a thermal distribution of ions between low spin and high spin state.

The presence of a diamagnetic ion confirms the assignment of the complex as $Ru^{IV}(bzacBH)_2$. The stirred solution voltammetry experiment showed that this complex was in a higher oxidation state than most of the other complexes, but did not provide information about the identity of that higher oxidation state. Of the possible oxidation states, only one, Ru(IV), has an even number of d electrons as required for diamagnetism.

A similar experiment was attempted with $Ru(bzac\text{-}pCl\text{-}BH)_2$, but the complex was not sufficiently soluble in CD_2Cl_2 to allow the determination to be made. However, the complex can still be confidently assigned as Ru(IV) on the basis of the stirred solution voltammetry experiment, which showed that it is in the same oxidation state as $Ru(bzacBH)_2$. That the magnetic moment of the chloro substituted complex is higher than that of the unsubstituted must be due to a smaller

energy gap between the filled energy levels in the diamagnetic form and the next highest energy levels.

The magnetic moments of the complexes with hnaBH, hna-pCl-BH, and bzacSalH are all consistent with the presence of one unpaired electron [16], which is indicative of the complexes being low spin d^3 complexes. Though the magnetic moment of the complex with hapBH was indicative of slightly less than one unpaired electron per ruthenium ion it, too, can be assigned as Ru(III) on the basis of its similar voltammetry in the stirred solution.

4.7. Electronic Spectra.

The uv/vis spectra of $Ru(bzacBH)_2$, $Ru(bzac\text{-}pCl\text{-}BH)_2$ and the complexes with hnaBH and hna-pCl-BH in DMSO solution were recorded , as were the spectra of the protonated ligands. The concentration of the complex solutions was 2.5×10^{-4} mol dm^{-3} and of the ligand solutions was 5.0×10^{-4} mol dm^{-3}mol dm^{-3}. The spectra are displayed in Figs. 4.9 - 4.12, and the absorption maxima are listed in Table 4.4.

It can be seen that the spectra of the complexes contain absorptions which can be readily assigned to intra-ligand transitions. In addition to these absorptions, there is a fairly strong absorption in each spectrum betwen 410 nm and 445 nm, sometimes being evident as a shoulder to an intra-ligand band. This absorption is also present in the spectra of the ligands, bzacBH and bzac-pCl-BH ,in DMSO, but with a lower intensity than in the complex spectra. The spectra of these ligands in CH_2Cl_2 contained a single band, which was the same as the higher energy absorption in DMSO solution. The lower energy bands were also observed in methanol in the presence of lithium acetate, and their intensity is roughly proportional to the amount of base in solution. It is possible that there is some degree of enolization of the ligands in the presence of DMSO, so that there is some contribution to the spectrum from the enolate forms. There are two possible enol structures in each of the tridentate ligands, and the ligands present in the complexes are deprotonated at both enol sites. It has been shown for polypyridyl complexes of ruthenium(II) that the intra-ligand bands in the complex spectrum are almost identical with those in the spectrum of the protonated ligands. [18] It is possible that there exists a similar relationship between the spectra of the protonated and coordinated tridentate ligands. On this basis, the lower energy band in the spectra of the ligand can be assigned to a second intra-ligand transition of the double enol form of the ligand.

Except in the case of the complex with hna-pCl-BH, the intensities of the higher energy absorption bands in the complex spectra are approximately twice as intense as the same bands in the spectra of the free ligands. This is consistent with the presence of two tridentate ligands per

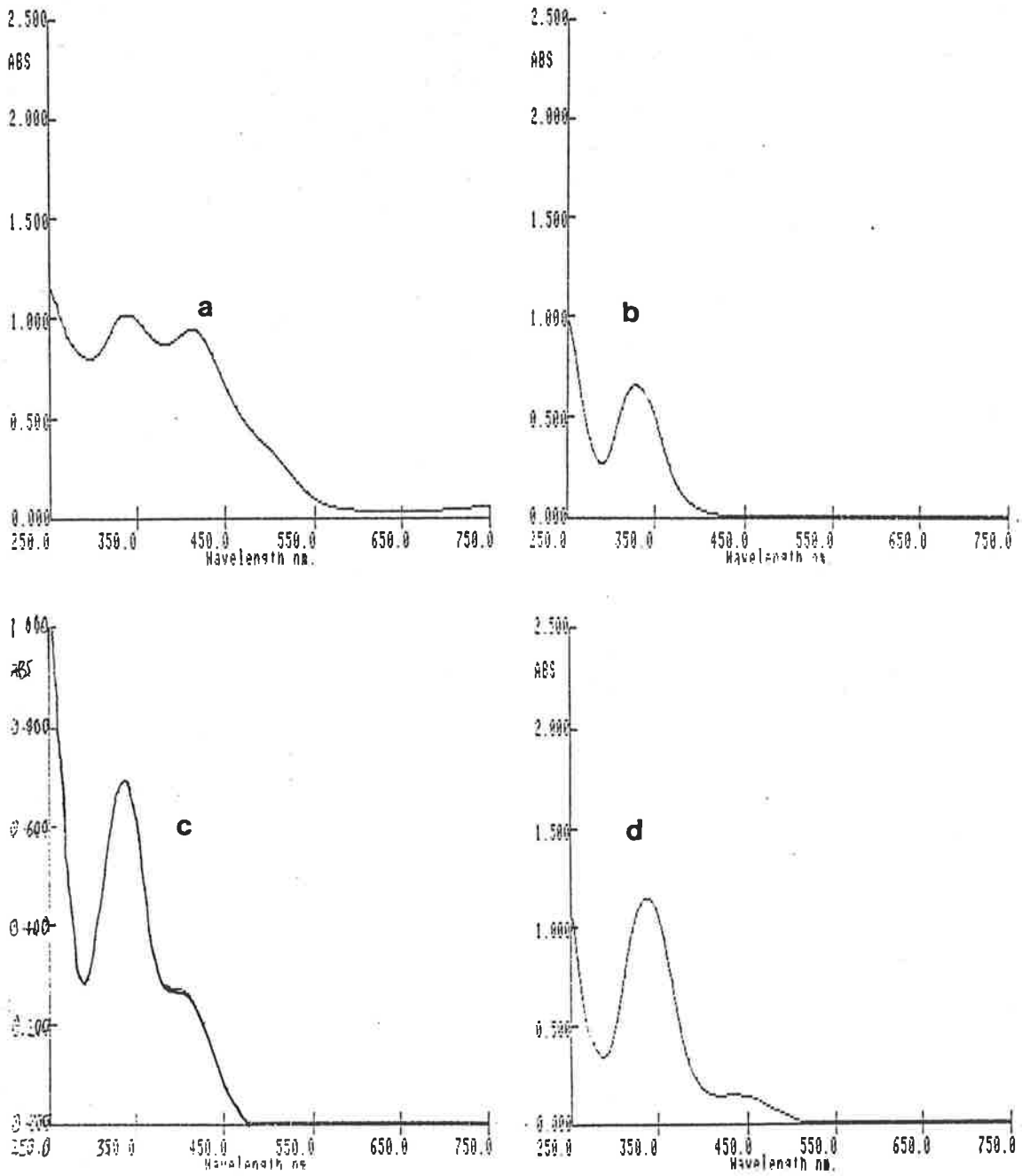

Fig. 4.9. uv/vis spectra of: (a) $Ru(bzacBH)_2$ in DMSO, c = 2.5 x 10^{-4} mol dm^{-3}. (b) $H_2bzacBH$ in CH_2Cl_2, c = 5.0 x 10^{-4} mol dm^{-3}. (c) $H_2bzacBH$ in MeOH, c = 5.0 x 10^{-4} mol dm^{-3}. (d) $H_2bzacBH$ in DMSO, c = 5.0 x 10^{-4} mol dm^{-3}.

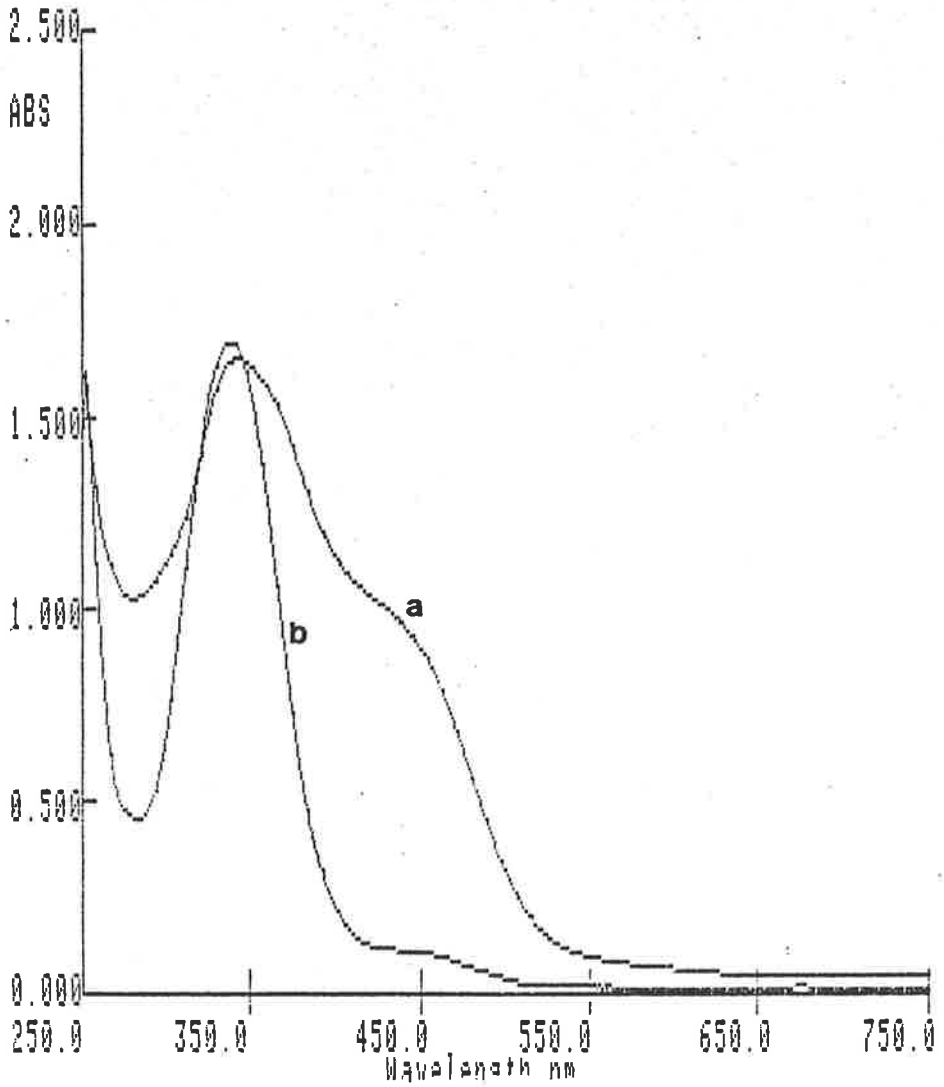

Fig. 4.10. uv/vis spectra of: (a) $Ru(bzac\text{-}pCl\text{-}BH)_2$ in DMSO, c = 2.5 x 10^{-4} mol dm^{-3}. (b) $H_2bzac\text{-}pCl\text{-}BH$ in DMSO, c = 5.0 x 10^{-4} mol dm^{-3}.

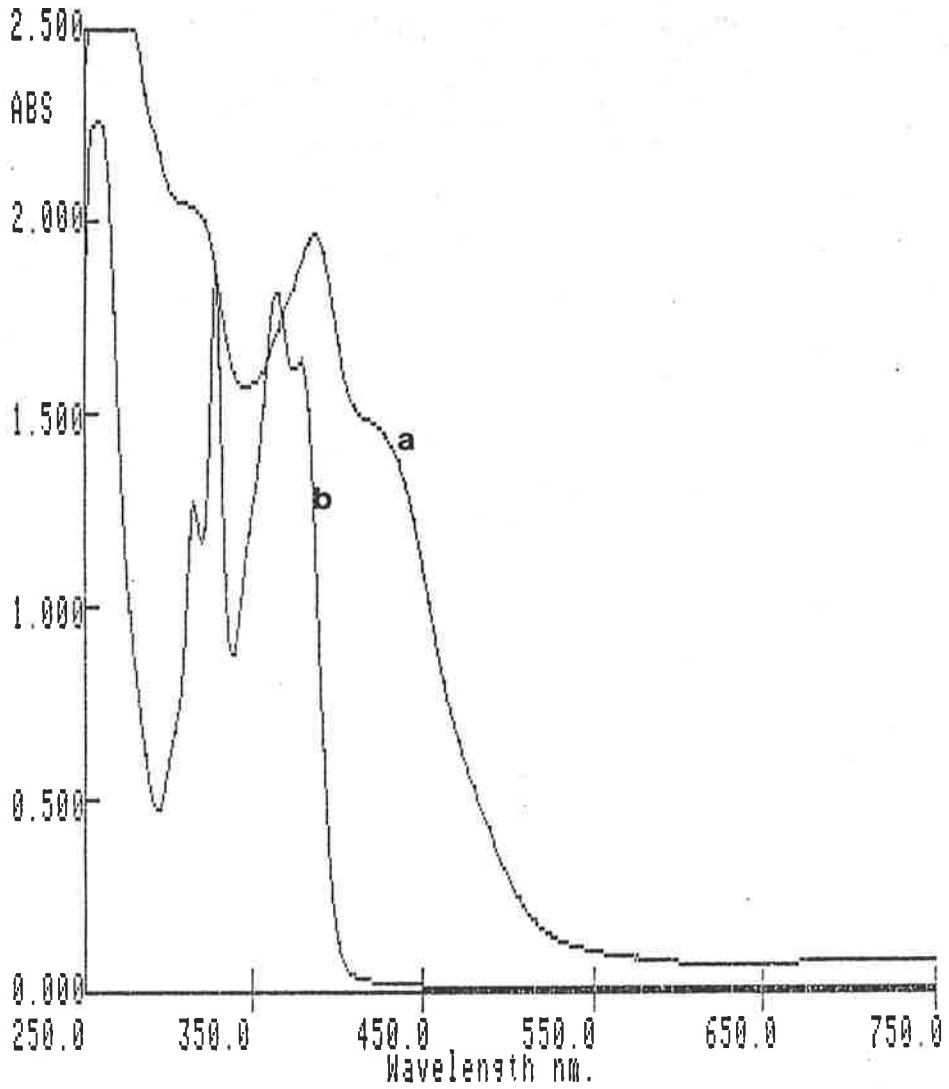

Fig. 4.11. uv/vis spectra of: (a) $Ru(hnaBH)_2$ in DMSO, c = 2.5 x 10^{-4} mol dm^{-3}.
(b) H_2hnaBH in DMSO, c = 5.0 x 10^{-4} mol dm^{-3}.

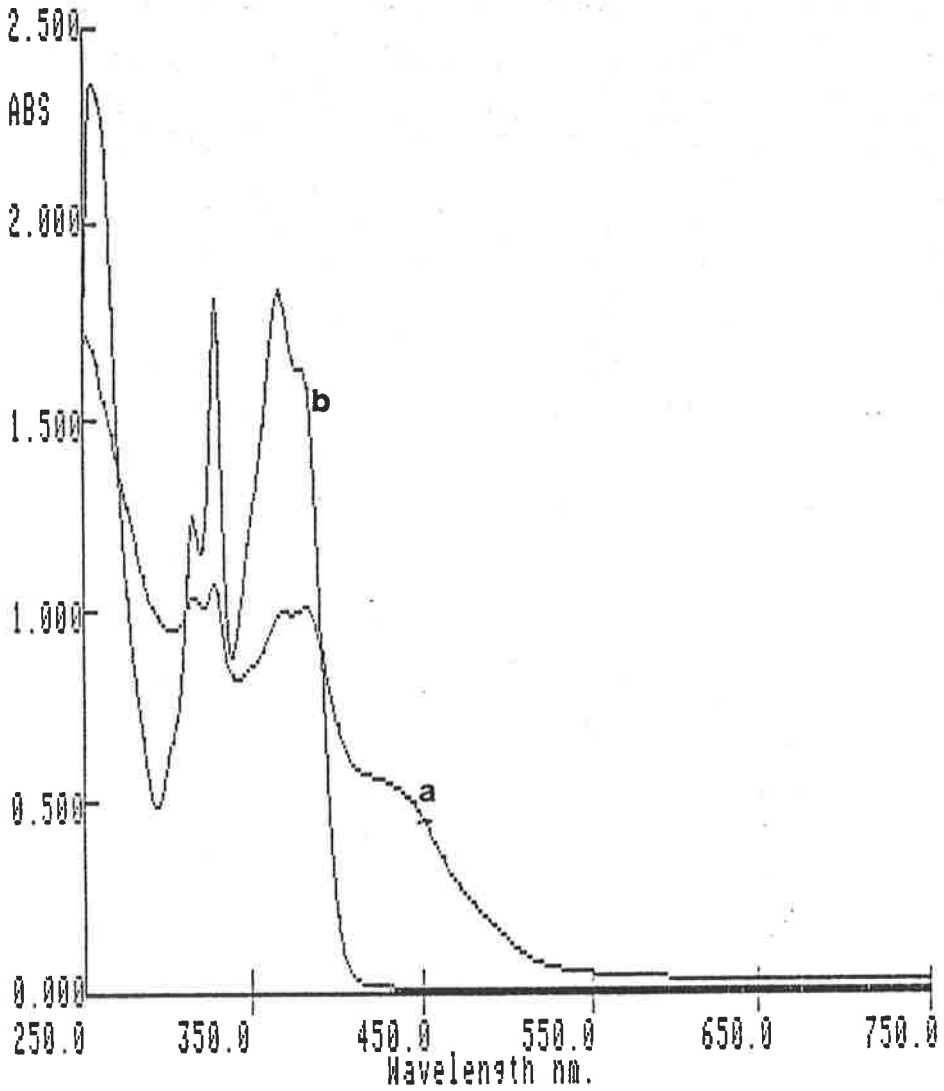

Fig. 4.12. uv/vis spectra of: (a) $Ru(hna\text{-}pCl\text{-}BH)_2$ in DMSO, $c = 2.5 \times 10^{-4}$ mol dm^{-3}. (b) $H_2hna\text{-}pCl\text{-}BH$ in DMSO, $c = 5.0 \times 10^{-4}$ mol dm^{-3}.

ruthenium. The additive properties of intra-ligand absorptions were observed in the Ru(II) polypyridyl complexes, as described in Chapter 3. In the spectrum of the complex with hna-pCl-BH, the intra-ligand bands have less than half the intensity of the same bands in the free ligand. There is no apparent explanation for this.

L	LH_2[a]	RuL_2
bzacBH	325(6.46)[b] 335(12.0)[c] 433sh(2.7)[c]	335(20.2) 412(18.7) 410sh(2.7)
bzac-pCl-BH	336(17.0) 450sh(.95)	342(33.0) 450sh(18)
hnaBH	312(12.6), 325(18.6) 362(18.1), 377(16.3)	312sh(41) 385(39.2) 440sh(26) 723(1.6)
hna-pCl-BH	313(12.3) 326(17.8) 364(18.1)	314(20.6) 326(21.6) 368(20.0) 380(20.4) 430sh(11)

Table 4.4. uv/vis spectra of RuL_2 complexes and ligands LH_2. (a) λ in nm(ε x 10^{-3} cm mol dm^{-3}). (b) in CH_2Cl_2 solution. (c) in DMSO solution.

4.8 Conclusion.

It is clear that ruthenium(IV) complexes with the dinegative tridentate ligands derived from Schiff's bases can be obtained for ligands which have sufficiently strong π-electron donating ability. Of the ligands used in this study, only bzacBH and bzac-pCl-BH are sufficiently strong π-donors to stabilize the Ru(IV) state. This is apparent from the electrochemistry of the RuL_2 complexes. The only two complexes which were identified as being Ru(IV) were $Ru(bzacBH)_2$ and $Ru(bzac\text{-}pCl\text{-}BH)_2$, which were the complexes with the lowest $E_{1/2}$ potential for the Ru^{4+}/Ru^{3+} couple. The complexes with the ligands hapBH, hnaBH, hna-pCl-BH, bzacSalH and hnaOAP were all Ru(III) complexes, and the $E_{1/2}$ potentials for Ru^{4+}/Ru^{3+} couple in these complexes were all greater than those for the Ru(IV) complexes.

There is some spectral evidence to support the formulation of the Ru(III) complexes as [Ru(L)(HL)], but the mass spectra may be subject to some interference from the positive ion generated in the spectrometer. The microanalytical results are all consistent with the formulation, $[RuL_2].H_2O$. The proposed formulation is, at best, tentative.

REFERENCES.

(1) A.A. Diamantis, M. R. Snow, J. A. Vanzo, *J. Chem. Soc., Chem. Comm.*, 264(**1976**)

(2) Md. A. Salam, Ph. D. Thesis, The Unversity of Adelaide, 1986.

(3) A.A. Diamantis, M. Manikas, Md. A. Salam, M. R. Snow, E. R. T. Tiekink, *Inorg. Chem.*, submitted for publication.

(4) H. Ohta, *Bull. Chem. Soc. Japan*, **33**, 1337(1960)

(5) D. P. Kessissoglou, W. M. Butler, V. L. Pecoraro, *J. Chem. Soc., Chem. Comm.*, 1253(**1986**)

(6) F. A. Cotton, G. Wilkinson, "Advanced Inorganic Chemistry, 4th Ed.", J. Wiley & Sons, New York, 1980, p 716.

(7) A.A. Diamantis, J. M. Frederiksen, Md. A. Salam, M. R. Snow, E. R. T. Tiekink, *Aust. J. Chem.*, **39**, 1081(1986)

(8) A.A. Diamantis, *private communication.*

(9) A.A. Diamantis, R. T. Jones, R. Keough, M. Manikas, unpublished results.

(10) G. A. Heath, K. A. Moock, D. W. A. Sharp, L. J. Yellowlees, *J. Chem. Soc., Chem. Comm.*, 1503(**1985**)

(11) G. A. Heath, K. R. Seddon. J. B. A. F. Smeulders, Unpublished results.

(12) A. Endo, K. Shimizu, G. P. Sato, *Chem. Lett.*, 581(**1985**)

(13) Y. Takeuchi, A. Endo, K. Shimizu, G. P. Sato, *J. Electroanal. Chem.*, **185**, 185(1985)

(14) M. I. Bruce, M. J. Liddell, *Appl. Organomet. Chem.*, in press.

(15) K. Nakamoto, "Infrared and Raman Spectra of Inorganic and Coordination Compounds"(3rd Ed.), J. Wiley & Sons, New York, 1978, p 115.

(16) W. G. Porterfield, "Inorganic Chemistry. A Unified Approach", Addison-Wesley, Reading, Mass. (USA), 1984, p 457.

(17) E. A. Seddon, K. R. Seddon, "The Chemistry of Ruthenium", Elsevier, Amsterdam, 1984, Chapter 7.

(18) W. R. McWhinnie, J. D. Miller, *Adv. Inorg. Chem. Radiochem.*, **12**, 135(1969)

CHAPTER 5.

DINITROGEN AND NITROSYL COMPLEXES.

5.1. Introduction.

5.1.1. Dinitrogen Complexes. Interest in the chemistry of dinitrogen complexes arose because of their potential to be used as models for the active site of the nitrogen-fixing enzyme, nitrogenase. The first dinitrogen complex to be isolated and identified as such was $[Ru(NH_3)_5N_2]^{2+}$. [1] Following this original report, there was considerable activity in the field, much of which is recorded in several review articles on the subject. [2 - 4] Though the ammineruthenium and osmium dinitrogen complexes represent only a small fraction of the total number of dinitrogen complexes synthesized, they are the only examples of dinitrogen complexes containing σ-donor ligands, and the only examples which have been studied in aqueous solution. [5]

The dinitrogen molecule, N_2, is isoelectronic with the π-acceptor ligands, carbon monoxide (CO) and cyanide (CN^-). The bonding schemes which have been used to describe the coordination of CO to transition metals have also been used to describe the bonding of the N_2 ligand. These schemes are dealt with in the review article by Sellman. [4] In a large proportion of cases, the N_2 ligand is coordinated to the metal centre in an "end on" fashion, in either a terminal or bridging mode. The existence of the dinitrogen ligand in the bridging mode is an example of the nucleophilicity of the coordinated ligand, which is reported to be comparable to, or better than, that of free dinitrogen. [6] In the "end on" configuration the ligand molecule possesses a $3\sigma_g$ orbital capable of σ-donation of electrons to the metal centre, and a $1\pi_g$ anti-bonding orbital which is unoccupied and capable of participating in π-back-bonding from the metal t_{2g} orbitals. The major difference between the bonding of CO and N_2 to transition metals lies in the differences which exist between the orbital energy levels of the two ligands. Both the HOMO and LUMO orbitals of N_2 are at a much lower energy than those of CO (–15.6 and –7 eV respectively for N_2, and –14 eV and –6 eV respectively for CO). Most metal complexes possess orbitals (*i.e.* e_g and t_{2g} orbitals) whose energies correspond better to those of the σ and π* orbitals of CO than those of the N_2 molecule. In general, carbon monoxide is both a better σ-donor and π-acceptor than N_2, hence the greater stability of coordinated CO compared with N_2. Additionally, the nature of the $3\sigma_g$ orbital of the N_2 molecule is such that most of the electron density is between the two nitrogen atoms, rather than at one atom, as is the case with CO. Thus, the major contribution to the metal N_2 bond is the π-donation to the $1\pi_g$ orbital of the ligand, whereas the metal-CO bond is a mixture of σ- and π-bonding.

The uv/vis spectra of the ruthenium ammine dinitrogen complexes contain absorptions which are characteristic of the bonding mode of the N_2 ligand. These absorptions occur at about 225 nm for terminally bound N_2 and about 265 nm for bridging N_2. [2] These absorptions are related to transitions between essentially metal-centred orbitals of T_{2g} symmetry and essentially ligand-centred orbitals.

The operation of the back-bonding to the π^* orbital of the ligand is manifest in changes to the ir absorption frequency of the N-N stretching mode. In N_2, this vibration is only Raman-active, absorbing at 2331 cm^{-1}.[7] In dinitrogen complexes, the (υ)N-N absorption is also infrared active, and the frequency of the absorption has been shown to be dependent on the anion present in the salt. For the complexes, $[Ru(NH_3)_5N_2]X_2$, (X = Cl, Br, I, BF_4, PF_6) the frequencies for (υ)N-N decrease with the decrease in the anion radius, as polarization of the metal centre by the counter ion causes electron release into the dinitrogen ligand. [8]

The tetraammineaqua dinitrogen complex, *cis* $[Ru(NH_3)_4(OH_2)N_2]^{2+}$ has been reported [9], and so has the bis(dinitrogen) complex, *cis* $[Ru(NH_3)_4(N_2)_2]^{2+}$. [10] The bis diaminoethane analogues are also known, including $[Ru(en)_2(N_2)_2]^{2+}$ [11] and $[Ru(en)_2N_3(N_2)]^+$, the only substituted amine terminal dinitrogen complex of ruthenium known. [12] With the availability of the triamminediaqua moiety it was considered possible to obtain complexes of the type, $[Ru(NH_3)_3L_2N_2]$, where L_2 represents two monodentate ligands or a bidentate ligand. It was considered that it may be possible to observe the effect of the adjacent coordination environment on the strength of the metal-N_2 bond, and on the N-N bond itself.

5.1.2. Nitrosyl Complexes. The properties of ruthenium nitrosyl complexes are of interest to this work because the nitrosyl complexes are precursors to the synthesis of analogous dinitrogen complexes. The formation of a terminal dinitrogen ligand by nucleophilic attack on a coordinated ligand offered a solution to the problem of reaction of N_2 with more than one ruthenium ion, leading to the formation of a bridged dinitrogen complex .

Ruthenium is believed to form more complexes with the nitric oxide ligand than any other element. [13] The chemistry of these ruthenium nitrosyl complexes has been reviewed by many authors. [14 - 16] The interaction between the NO molecule and a transition metal centre differs from that involving most other ligands in that the NO is formally a three-electron donor. Feltham and Enemark have descibed a scheme in which the ruthenium-nitrosyl group may be considered as a $\{RuNO\}^n$ group, where n is equal to the number of electrons in the metal d orbitals, plus the number of electrons in the π^* orbitals of the NO ligand. [16]

It is convenient to consider that the bonding interaction arises from the transfer of a single electron from NO to the metal centre. The resulting NO^+ is isoelectronic with N_2 and CO,and accepts electron density from the reduced metal ion into its π^* orbital. This scheme provides a useful basis for comparison between the nitrosyl complexes and those of other π-acid ligands.

This conventional explanation is reinforced by the substantial strengthening of the *trans* ligand-ruthenium bond which is observed in a variety of complexes, as illustrated by the shorter length of this bond compared with *cis* ligand-ruthenium bonds. [14 and references therein] The explanation is that the NO^+ ligand is a very poor σ-donor, but a very good π-acceptor. It does not compete with the *trans* ligand for the empty orbital of the ruthenium centre, and further, it assists in the σ-donation from the *trans* ligand by delocalizing the electron density into its π^* orbital.

The extent of donation of electron density from the metal d orbitals to the ligand π^* orbital can be seen in the variation of the infrared absorption frequency for the NO stretching mode. Free nitric oxide has an infrared absorption for this mode at $1840cm^{-1}$ and the nitrosyl cation, which is the formal state of the ligand, shows (υ)NO between 2150 cm^{-1} and 2400 cm^{-1}. [17] In ruthenium nitrosyl complexes, a range of frequencies is observed. Those above 1620 cm^{-1} are associated with linear M-NO groups, and those less than 1610 cm^{-1} are associated with bent M-NO groups. [18] Furthermore, it has been suggested that linear $\{MNO\}^6$ nitrosyls with (υ)NO greater than about 1850 cm^{-1} are sufficiently similar to the NO^+ formulation to render the ligand susceptible to nucleophilic attack on the nitrogen atom. [19] Bottomley has reviewed this aspect of the chemistry of nitrosyl complexes [20], and has also carried out investigations of direct relevance to the current work. When hydrazine or hydroxylamine were reacted with $[Ru(NH_3)_5NO]^{3+}$, either $[Ru(NH_3)_5N_2]^{2+}$, or a mixture of $[Ru(NH_3)_5N_2O]^{2+}$ and $[Ru(NH_3)_5N_3]^+$, were produced, depending on the reaction conditions used. [21, 22]

5.2. Preparation and Characterization of Nitrosyl Complexes.

5.2.1. $[Ru(NH_3)_3NO(Cl)_2]Cl$. Nitrosyl complexes of the triammine series could be prepared by the direct reaction of nitric oxide gas. Aqueous suspensions of $Ru(NH_3)_3Cl_3$ reacted with nitric oxide gas to yield a nitrosyl complex, $[Ru(NH_3)_3NO(Cl)_2]^+$, which precipitated from the reaction mixture as its chloride salt. The addition of ethanol to the reaction mixture increased the yield of product. Depending on the reaction conditions employed, two products were obtained. Reaction at high temperatures (up to 90°C) gave two products. The first was a red crystalline solid and the second was a pale pink powder. At lower temperatures (<40°C) formation of the crystalline solid was favoured, but with a lower overall yield.

Both products had ir absorptions characteristic of the nitrosyl ligand in the region 1800 cm^{-1} to 2000 cm^{-1}, but it was in this feature that the major difference between the two forms of the complex was apparent. In a nujol mull, the spectrum of the crystalline product had three ir absorptions in the nitrosyl region, at 1920 cm^{-1},1910 cm^{-1} and 1882 cm^{-1}, whereas the spectrum of the pink solid had a single broad band at 1850 cm^{-1}. In aqueous solution, however, the spectrum of the crystalline form contained only a single, sharp peak at 1912 cm^{-1}. Consideration of the molecular symmetry of the complex requires that there would be only one peak due to the (υ)NO mode. However, different site symmetries in the crystal structure could produce the split peaks, as also observed in the complexes, *cis* $[Ru(NH_3)_4NOCl]Cl_2$, *cis* $[Ru(NH_3)_4NOBr]Br_2$ and *cis* $[Ru(NH_3)_4NO(OH_2)_2](ClO_4)_3$. [23] On the basis of this comparison, it would seem that the two products obtained from the nitrosylation reaction are the same complex in two different solid state environments. The energy of the ir absorptions are very similar to those of previously measured nitrosyl complexes, as can be seen from the data listed in Table 5.1.

The red form of the compound was considerably more soluble in water than the pink. However, both were sufficiently soluble to allow determination of the uv/vis spectrum, and both gave the same spectrum. In water, the uv/vis spectrum changed considerably with time. Absorptions initially present at 207 nm (ε =12000) and 360 nm (ε = 100)gradually gave way to absorptions at 196 nm (ε = 12000) and 350 nm (ε =150) respectively. Additionally, there was a weak, broad band at 500 nm (ε = 30), which was unchanged over the same time span. The energy and intensity of these absorption bands are comparable to those in the *trans* tetraamine nitrosyl complexes [24], the main features of which are listed in Table 5.2. In a previous report it was proposed that the spectrum of $[Ru(NH_3)_3NOCl_2]Cl$ consisted of bands at 242 nm (ε = 2950), 343 nm (ε =80) and 490 nm (ε=120). [25] The same report contains some speculation that, in dilute aqueous solution, the form of the complex is $[Ru(NH_3)_3NOCl(OH_2)]^{2+}$. However, some of the evidence used to support this proposal is self-contradictory, so the validity of any comparison is questionable.

There is some uncertainty surrounding the nature of the transitions giving rise to these absorptions. In considering the spectra of the *trans* tetraammineruthenium nitrosyls, Schreiner and co-workers assigned the weak low energy bands to $d_\pi(Ru) \rightarrow \pi^*(NO)$ transitions with a spin-forbidden d→d component also included. The medium intensity, medium energy bands were assigned to mainly d→d transitions, and the high energy bands to ligand (Cl^-) to metal charge transfers. [24] When Pell and Armor studied the spectra of the *cis* tetraammines, they agreed with the assignments of Schreiner, but expressed reservations about the assignment of the high energy bands as due to LMCT transitions. [23] These high energy absorptions were not present in

Compound	$\upsilon(cm^{-1})$	Reference
$[Ru(NH_3)_3NO(Cl)_2]Cl_2$	1920, 1910, 1882	This work
$[Ru(NH_3)_3NO(Br)_2]Br_2$	1932, 1915, 1909, 1885	"
$[Ru(NH_3)_3(C_2O_4)NO]_2C_2O_4$	1906	"
cis $[Ru(NH_3)_4NOCl]Cl_2$	1933, 1899	23
trans $[Ru(NH_3)_4NOCl]Cl_2$	1880	"
cis $[Ru(NH_3)_4NOBr]Br_2$	1934, 1902	"
trans $[Ru(NH_3)_4NOBr]Br_2$	1870	"
cis $[Ru(NH_3)_4NO(OH_2)_2](ClO_4)_3$	1928, 1848	"
trans $[Ru(NH_3)_4NO(OH_2)_2](ClO_4)_3$	1925	"
$[Ru(NH_3)_5NO]Cl_3$	1930	35
$[Ru(NH_3)_5NO]Br_3$	1913	23

Table 5.1. Nitrosyl stretching frequencies of ruthenium nitrosyl complexes.

Compound	λ(nm)	ε(l mol^{-1} cm^{-1})	Reference
$[Ru(NH_3)_3NO(Cl)_2]^+$	207	1.21×10^4	This work
	360	1.01×10^2	
	500	3.0×10^1	
$[Ru(NH_3)_3NO(OH_2)_2]^{2+}$	196	1.23×10^4	"
	350	1.5×10^2	
	500	3.0×10^1	
$[Ru(NH_3)_3(C_2O_4)NO]^+$	225	7.5×10^3	"
	330	1.7×10^2	
	462	3.6×10^1	
cis $[Ru(NH_3)_4NO(Cl)]^{2+}$	345	1.26×10^3	23
	480	1.9×10^1	
trans $[Ru(NH_3)_4NO(Cl)]^{2+}$	245	4.2×10^3	24
	330	2.64×10^2	
	441	1.7×10^1	
cis $[Ru(NH_3)_4NO(OH_2)]^{2+}$	230(sh)	2.0×10^3	23
	325	8.7×10^1	
	435	1.6×10^1	
$[Ru(NH_3)_5NO]^{3+}$	305	5.6×10^1	25
	455	1.5×10^1	

Table 5.2. uv/vis spectra of ruthenium nitrosyl complexes.

the spectra above 200 nm, but it was thought that the LMCT might be expected at shorter wavelengths and perhaps hidden by ligand-localized transitions. This conclusion was based on a comparison of the LMCT bands in *cis* and *trans* $[Co(en)_2(Cl)Br]^+$where the band in the *cis* complex is at higher energy than in the *trans*. [26] However, Nikol'skii and co-workers considered the lowest energy bands to be d→d, with the occupied metal orbital having some Cl character when this ligand was present. The medium intensity bands were assigned to $d_\pi(Ru) \rightarrow \pi^*(NO)$ transitions. [27] This conclusion was reached after it was found that irradiation of aqueous solutions of $[RuCl_5(NO)]^{2-}$ in the medium energy absorption region resulted in replacement of NO by H_2O, implying that transitions involving NO lie there.The time dependence of the spectrum of $[Ru(NH_3)_3NO(Cl)_2]Cl$ was indicative of hydrolysis involving replacement of the chloro ligands and, in 2 mol dm^{-3} sodium chloride solution, the change in the spectrum was considerably slower. The hydrolysis of the complex in dilute aqueous solution was confirmed by the results of conductance measurements. A fresh solution of $[Ru(NH_3)_3NO(Cl)_2]Cl$ in water had a molar conductance at infinite dilution, $\Lambda^0_m = 170\ \Omega^{-1}\ cm^{-1}\ mol^{-1}\ dm^{-3}$, indicative of a 1:1 electrolyte. The same solution, 24 hours later, had $\Lambda^0_m = 371\ \Omega^{-1}\ cm^{-1}\ mol^{-1}\ dm^{-3}$, indicative of a 3:1 electrolyte.

5.2.2. $[Ru(NH_3)_3NO(Br)_2]Br$ and $[Ru(NH_3)_3NO(C_2O_4)]_2C_2O_4$. Reaction of $[Ru(NH_3)_3NO(Cl)_2]Cl$ with 4 mol dm^{-3} HBr solution resulted in the formation of $[Ru(NH_3)_3NO(Br)_2]Br$. Similarly, reaction with 3 molar equivalents of oxalic acid in the presence of lithium acetate yielded $[Ru(NH_3)_3NO(C_2O_4)]_2C_2O_4$. These compounds were characterized by elemental analysis, uv/vis spectroscopy and by comparison of their ir spectra with that of $[Ru(NH_3)_3NO(Cl)_2]Cl_2$.

The intense absorptions due to charge transfer bands from bromide to the solvent obscured any features at low wavelengths in the uv/vis spectrum of $[Ru(NH_3)_3NO(Br)_2]Br$. At higher wavelengths, the spectrum was identical to that of $[Ru(NH_3)_3NO(OH_2)_2]^{3+}$, indicative of hydrolysis of the bromo ligands. The uv/vis spectrum of $[Ru(NH_3)_3NO(C_2O_4)]^{2+}$ contained absorptions at 225 nm (ε =7500), 330 nm (ε = 170) and 462 nm (ε = 36), all characteristic of ammine nitrosyl complexes.

The ir spectrum of $[Ru(NH_3)_3NO(Br)_2]Br$ contained split peaks due to (υ)NO, similar to the chloro compound, with the peaks ocurring at 1932 cm^{-1}, 1915 cm^{-1}, 1909 cm^{-1} and 1885 cm^{-1}. The spectrum of $[Ru(NH_3)_3NO(C_2O_4)]_2C_2O_4$ contained a single peak due to (υ)NO at 1906 cm^{-1}. Because of the splitting of the (υ)NO peaks in the solid state, it is not possible to compare the vibration frequencies under different coordination environments and draw any certain conclusions.

5.2.3 Other Triammineruthenium Nitrosyl Complexes. In view of the lability of $[Ru(NH_3)_3NO(Cl)_2]Cl$ towards hydrolysis, it was considered that substitution reactions involving the replacement of chloro ligands would be relatively facile. However, only the two substituted triammine nitrosyl complexes mentioned above could be isolated and characterized. When substitution reactions were attempted with thiocyanate ion, benzonitrile and bis-1,2(diphenylphosphino)ethane the unreacted starting complex and the ligand were the only compounds obtained.

$[Ru(NH_3)_3NO(Cl)_2]Cl$ had limited solubility in refluxing ethanol, where reaction with acacH, in the presence of lithium acetate, resulted in the formation of a dark brown solution from which no solid could be isolated. $[Ru(NH_3)_3NO(Cl)_2]Cl$ could not be isolated from the reaction mixture by treatment with concentrated HCl solution. It is possible that nucleophilic attack occurred at the NO ligand , resulting in the formation of the complex, $[Ru(NH_3)_3(Cl)_2\{(O)N\text{-}C(C(O)CH_3)_2\}]$, in a manner similar to that reported for the reaction of $[RuCl(bpy)_2NO]^{2+}$ with $acac^-$. [28]

When bpy reacted with $[Ru(NH_3)_3NO(Cl)_2]Cl$ in reluxing ethanol, *trans* $[Ru(NH_3)_4NOCl]Cl_2$ was isolated in approximately 40% yield. This was apparent from the analytical results, and a comparison with the previously reported ir and uv/vis spectra. (Tables 5.1. and 5.2., respectively). [23,24] The yellow solid which resulted from the reaction of $[Ru(NH_3)_3NO(Cl)_2]Cl_2$ with ethylenediamine had an absorption at 1850 cm^{-1} in its ir spectrum, but was shown by elemental analysis to contain less than 2% carbon. This was possibly an impure form of a tetraammine complex. It is apparent from these results that extraneous reactions were occurring. It is possible that the N-donor ligands were initially bound to the ruthenium, but then underwent decomposition reactions which left the ligand N atom bound to the ruthenium centre. An alternative explanation is that, under the conditions employed (refluxing ethanol solution), the nitrosyl complex underwent a series of dismutation reactions, leading to the formation of the tetraammine complexes.

It is possible that the lack of success in forming more examples of substituted triammine nitrosyl complexes is due to the problem of finding solvents in which both $[Ru(NH_3)_3NO(Cl)_2]Cl_2$ and the organic ligands were soluble. The limited solubility of the chloride salt in organic solvents meant that rather severe conditions were required to dissolve sufficient of the complex. Those same conditions, however, apparently facilitated undesirable side reactions.

5.3. Isolation of Triammineruthenium Dinitrogen Complexes.

The isolation of terminal dinitrogen complexes of triammineruthenium was a major aim of the project. Previous work in this field gave an indication of the reactions most likely to lead to the required complexes.

Banham obtained a bridged dinitrogen complex as the product of the reaction between dinitrogen gas and a triammineaquaruthenium(II) complex, formed by heterogeneous reduction of $Ru(NH_3)_3Cl_3$ in water. [29] This is to be expected, given that nitrogen gas has a poor solubility in water and that low concentrations of N_2 favour the formation of bridged dinitrogen complexes. The formation of the bridged complex is further favoured by the ability of coordinated dinitrogen to act as a nucleophile, and the presence of two aqua ligands on the Ru(II) ion with which the bound N_2 ligand may react. Clearly, attempts to synthesize terminal dinitrogen complexes by the reaction of $[Ru(NH_3)_3(OH_2)_3]^{2+}$ with N_2 gas would result in the formation of large amounts of a bridged dinitrogen complex. Hence, a more reliable method for the synthesis of terminal dintrogen complexes was required.

The conversion of coordinated nitrosyl to terminal dintrogen was first reported by Bottomley and Crawford [21, 22] . Hydroxide ion reacted with $[Ru(NH_3)_5NO]^{3+}$ to yield a mixture of $[Ru(NH_3)_5N_2]^{2+}$ and *cis* $[RuOH(NH_3)_4NO]^{2+}$. Similarly, the reaction between hydrazine and $[Ru(NH_3)_5NO]^{3+}$ yielded $[Ru(NH_3)_5N_2]^{2+}$ in a room temperature reaction, and a mixture of $[Ru(NH_3)_5N_2O]^{2+}$ and $[Ru(NH_3)_5N_3]^{+}$ in a reaction at –23°C. [20]

In a similar way, Diamantis and Sparrow were able to show that coordinated N_2O could be converted to coordinated N_2 in the presence of a reducing agent. [30] The reducing agent could be zinc metal, hydrogen over platinum, or even $[Ru(NH_3)_5H_2O]^{2+}$.

Both these synthetic methods offered scope for obtaining terminal dinitrogen complexes without the complication of forming bridged complexes as by-products, because the dinitrogen precursor was already in the metal coordination sphere prior to the reaction.

$[Ru(NH_3)_3NO(Cl)_2]Cl$ reacted with hydrazine hydrate in either aqueous solution or methanolic suspension to give a solution containing the complex $[Ru(NH_3)_3N_2(OH_2)_2]^{2+}$. Depending on the procedure used a variety of products could be isolated. (i) Addition of an excess of ethanol to the methanolic reaction mixture resulted in the precipitation of a yellow complex, $[Ru(NH_3)_3N_2(Cl)_2]$, (ii) addition of excess NaX (X = Br, I) to aqueous reaction mixtures yielded the complexes, $[Ru(NH_3)_3N_2(X)_2]$ and (iii) addition of excess NH_4A (A = PF_6, BF_4) to aqueous reaction mixtures resulted in the isolation of the salts, $[Ru(NH_3)_3N_2(OH_2)_2]A_2$.

The presence of the terminal dinitrogen ligand was confirmed by comparison of the ir and uv/vis spectra of the products with those of other terminal dinitrogen complexes. However, it was not possible to isolate any of the terminal dinitrogen complexes as the sole reaction product. Microanalysis of the PF_6^- salt indicated that the complex contained more nitrogen than expected, and the results were consistent with the presence of one hydrazine molecule per ruthenium ion.

Coordinated hydrazine has been reported previously in ruthenium pentaammine complexes. [31] The uv/vis spectra were indicative of the presence of a small amount of the bridged dinitrogen complex, and electrochemical experiments showed evidence of some oxidation of the terminal dinitrogen complex.

An intense MLCT band was observed in the uv/vis spectrum at 222 nm. The position of this band was the same, regardless of the anion or ligand present, indicating rapid hydrolysis of the neutral complexes, similar to that which occurred with the nitrosyl complexes. The highest apparent value obtained for ε at this wavelength was 12000 dm^3 mol^{-1} cm^{-1} for $[Ru(NH_3)_3N_2(OH_2)_2]^{2+}$ as its PF_6^- salt. The spectrum, shown in Fig. 5.1, also had a small peak at 265 nm, indicative of the presence of small amount of the bridged complex. From a comparison with the spectra of other ammineruthenium dinitrogen complexes (Table 5.3), the molar absorptivity at the lower of these two wavelengths would be expected to be in the range 14000 to 18000 dm^3 mol^{-1} cm^{-1}. The spectra of the bromo and iodo complexes were obtained after the solution of the complex had been passed through an anion exchange column in the chloride form. This procedure was necessary because the intense bands due to charge transfer from halide to solvent obscured the metal-N_2 charge transfer bands. In addition to the peaks attributable to the dinitrogen complexes, there was also a shoulder at approximately 350 nm. This shoulder was probably due to absorption by a Ru(III) impurity which was identifed at a later stage. The presence of appreciable amounts of $[Ru(NH_3)_3(OH_2)_2]_2N_2^{4+}$ implied that even though the terminal dinitrogen ligand was formed from a precursor ligand, there was still the opportunity for the terminal dinitrogen complex to react with other complexes in the reaction mixture to form the bridged complex.

The CV of $[Ru(NH_3)_3N_2(OH_2)_2]^{2+}$ as its PF_6^- salt was determined in 0.1 mol dm^{-3} methanesulphonic acid. This voltammogram, shown in Fig. 5.2, contained three main features. (i) An irreversible cathodic wave with E_p = +0.84 V, (ii) a reversible wave with $E_{1/2}$ = –0.15 V, which was present on the initial cathodic scan from 0.0 V, and (iii) an increase in the peak current of the reversible wave on scanning subsequent to the scan past the oxidation at the irreversible wave. That the initial wave at –0.15 V increased after the dinitrogen complex had been oxidized implies that the reversible wave was due to the product of the decomposition reaction which occurred after the oxidation of the dinitrogen complex. It is expected that upon oxidation of the dinitrogen complex, the dinitrogen ligand would be lost because there is insufficient electron density on the Ru(III) centre to provide sufficent back-bonding to keep the dinitrogen bound. The use of scan rates of up to 2 V sec^{-1} did not reveal any sign of a cathodic peak associated with the anodic peak at +0.84 V.

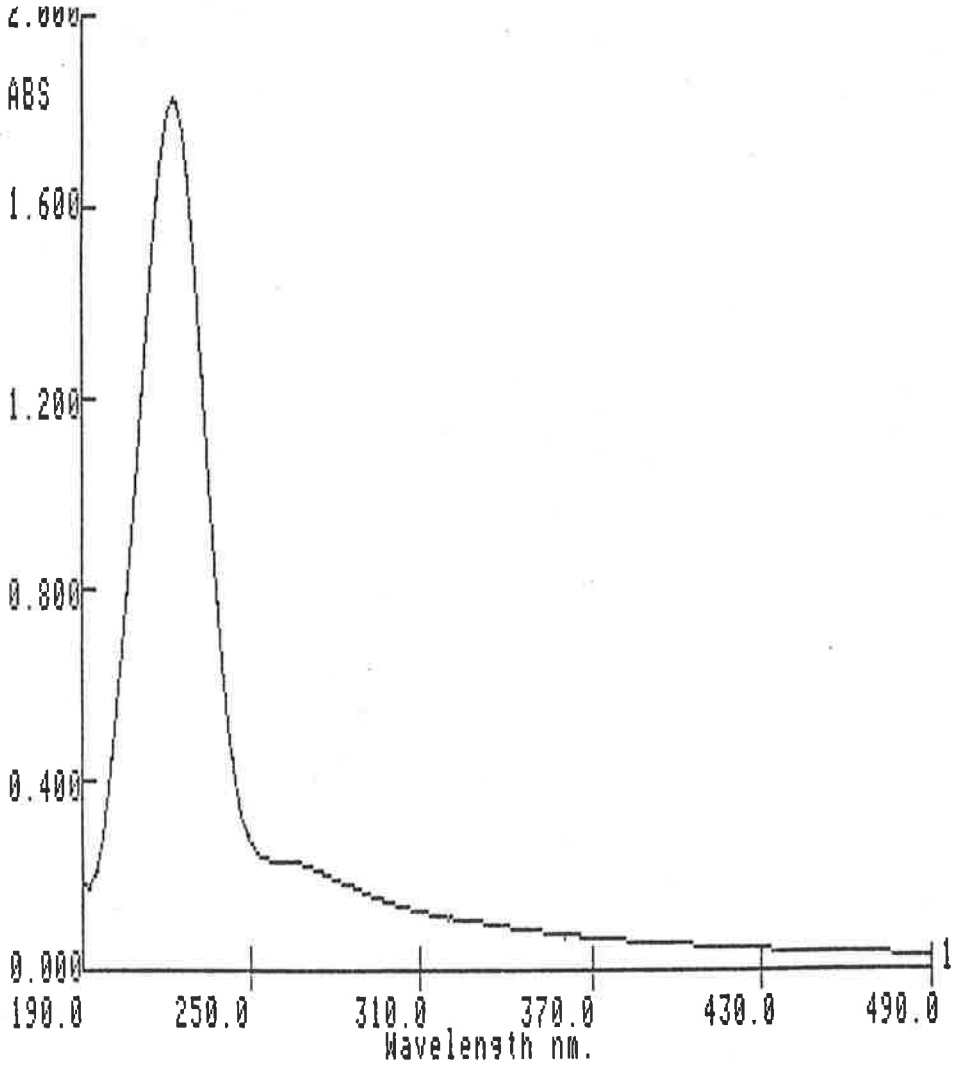

Fig. 5.1. uv/vis spectrum of $[Ru(NH_3)_3(OH_2)_2N_2]^{2+}$ in 0.1 mol dm^{-3} perchloric acid. $\varepsilon_{222} \approx 12\,000$.

Compound	λ(nm)	ε(l mol^{-1} cm^{-1})	Reference
$[Ru(NH_3)_3(OH_2)_2N_2]^{2+}$	222	1.2x 10^4 [a]	This work
$[Ru(NH_3)_3(OH_2)_2]_2N_2^{4+}$	262	4.4 x 10^4	29
cis $[Ru(NH_3)_4(OH_2)N_2]^{2+}$	222	1.74 x 10^4	9
cis $[Ru(NH_3)_4(OH_2)]_2N_2^{4+}$	262	5.0 x 10^4	"
$[Ru(NH_3)_5N_2]^{2+}$	221	1.6 x 10^4	32
$[Ru(NH_3)_5]_2N_2^{4+}$	263	4.7 x 10^4	"
$[Ru(OH_2)_5N_2]^{2+}$	218	(b)	33
$[Ru(OH_2)_5]_2N_2^{4+}$	255	5.6 x 10^4	"
$[Ru(en)_2(OH_2)N_2]^{2+}$	223	1.4 x 10^4	12
$[Ru(en)_2(OH_2)]_2N_2^{4+}$	265	4.8 x 10^4	"

Table 5.3. uv/vis spectra of ruthenium dinitrogen complexes. (a) estimate made on impure sample. (b) not measured, compound not isolated.

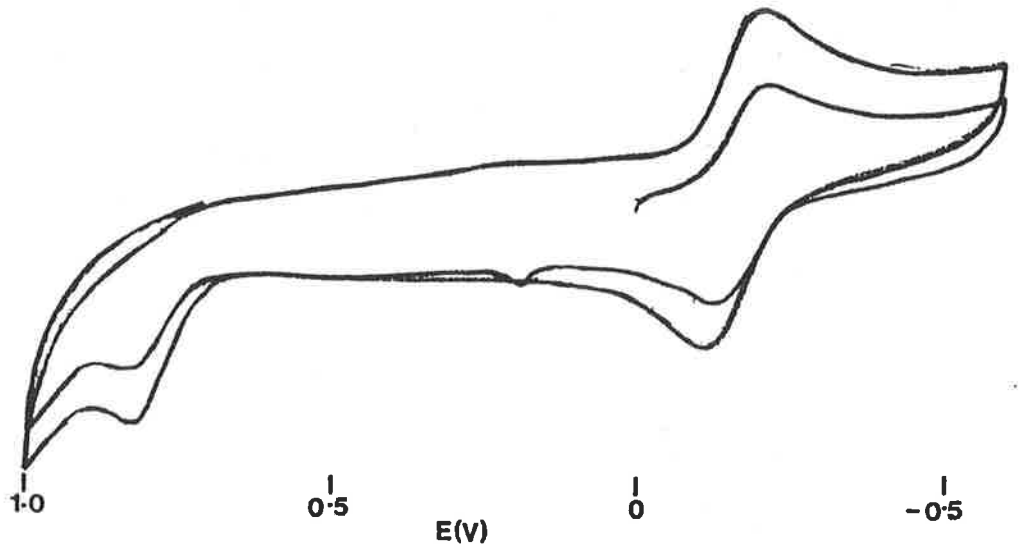

Fig. 5.2. Cyclic voltammogram of $[Ru(NH_3)_3(OH_2)_2N_2]^{2+}$ in 0.1 mol dm^{-3} perchloric acid.

There would appear to be many components in the reaction mixture capable of producing a Ru(III) species which was the same as the decomposition product of the terminal triammine dinitrogen complex. Bottomley and Crawford have shown that hydrazine is capable of oxidizing a Ru(II) complex. [22] Furthermore, $[Ru(NH_3)_5N_2O]^{2+}$, which has been identified as an intermediate in the reaction between $[Ru(NH_3)_5NO]^{3+}$ and hydrazine [20], has been shown to disproportionate to $[Ru(NH_3)_5N_2]^{2+}$ and $[Ru(NH_3)_5OH]^{2+}$. [30] Thus the presence of the decomposition product of the terminal dinitrogen complex in the isolated salts is not surprising. However, the formulation of this decomposition product is still open to speculation.

The decomposition product is not $[Ru(NH_3)_3(OH_2)_3]^{3+}$, because the $E_{1/2}$ value for its reduction (–0.15 V) is 50 mV more negative than that of the triaqua complex. If the dinitrogen complex also contains coordinated hydrazine, as implied by the microanalysis results, then it might be expected that the decomposition product after oxidation would have an $E_{1/2}$ value close to –0.14 V, which is the $E_{1/2}$ value for the redox couple *cis* $[Ru(NH_3)_4(OH_2)_2]^{3+/2+}$. A Ru(III) ammine hydrazine complex appears most likely to be the decomposition product.

The anodic peak potential in the CV is very similar to that of $[Ru(NH_3)_5N_2]^{2+}$. The electrochemistry of this complex and of $[Ru(NH_3)_4N_2(OH_2)]^{2+}$ were studied by Page and co-workers. [34] The CV of the terminal pentaammine dinitrogen complex had an anodic peak at +0.81 V, but there was no corresponding cathodic peak at scan rates up to 100 V sec^{-1}, indicating that the loss of the dinitrogen ligand from the oxidized form occurred very rapidly. In the case of the bridged pentaammine complex it was possible to observe an anodic and a cathodic peak with a peak separation of 60 mV, and $E_{1/2}$ = +0.465 V. From the voltammetric studies it was estimated that the rate constant for the decomposition of $[Ru(NH_3)_5N_2Ru(NH_3)_5]^{5+}$ to $[Ru(NH_3)_5N_2]^{2+}$ and $Ru^{III}(NH_3)_5X$ was 0.1 sec^{-1}. When these oxidation potentials are compared with the $E_{1/2}$ values for the $[Ru(NH_3)_3(OH_2)_3]^{3+/2+}$ and $[Ru(NH_3)_5(OH_2)]^{3+/2+}$ couples, it can be seen that the dintrogen ligand greatly stabilizes the Ru(II) centre towards oxidation, although the bridged complexes are more readily oxidized than than are the terminal complexes. The electrochemistry of $[Os(NH_3)_5N_2]^{2+}$, was also studied by Page , and it was found that the CV wave was reversible, and had an oxidation potential less positive than that of the ruthenium analogue. The rate constant measured for the decomposition of $[Os(NH_3)_5N_2]^{3+}$ to $Os^{III}(NH_3)_5X$ and N_2 was 0.02 sec^{-1}

Different techniques were used in further attempts to obtain the terminal dinitrogen complex in a pure form. The method of Diamantis and Sparrow [30] was used, whereby N_2O gas was bubbled through a solution of $[Ru(NH_3)_3(OH_2)_3]^{3+}$ in the presence of a reducing agent (amalgamated zinc). It was hoped that in this reaction there would not be the opportunity for the dinitrogen complex to oxidize. However, while the oxidative decomposition of the terminal dinitrogen complex might not

have been occurring in this case, there were still appreciable amounts of the bridged complex formed, so this approach was not pursued further.

Similarly, attempts were made to isolate the terminal complex from a high pressure reaction in a solution containing a precipitating agent (e.g. NH_4PF_6) It was intended that the high pressure conditions would increase the concentration of nitrogen gas in the reaction solution, thus favouring formation of the terminal complex. The presence of the excess of precipitating anion was expected to result in the precipitation of the dinitrogen complex upon formation, and so prevent further reaction to give the bridged dinitrogen complex. However, to precipitate the complex immediately upon formation requires a high concentration of the ruthenium precursor in solution, a condition which favours the formation of the bridged species. Again, appreciable amounts of the bridged complex were formed in this reaction.

In the ir spectra, the N_2 stretching frequency was dependent on the anion present in the dinitrogen complex or its salt. The values for $(\upsilon)N_2$ are listed in Table 5.4, and it can be seen that the variation in stretching frequency parallels that observed in terminal pentaammine dinitrogenruthenium salts. [8]

X =	Cl	Br	I	BF_4	PF_6
$Ru(NH_3)_3X_2N_2$ [a]	2112	2118	2122	2145	2164
$[Ru(NH_3)_5N_2]X_2$ [b]	2092	2109	2120	2142	2167

Table 5.4. Frequencies of N-N stretching mode in dinitrogen complexes, in cm^{-1}. (a) The anion may be present as a counter ion to a cationic aqua complex or as a coordinated lignad. (b) Reference 8.

This effect involves interaction between the anion and the ammine ligands, whereby the release of electron density into the dinitrogen ligand from the metal centre is increased when the metal centre is polarized to a greater extent by an anion of smaller radius. [8]

5.4. Conclusion.

It was possible to synthesize terminal dintrogen complexes of triammineruthenium(II), but it was found that other reactions occur in the reaction solution which lead to the formation of impurities in the form of the bridged dinitrogen complex and the product of oxidative decomposition of the terminal dinitrogen complex. The synthesis of a range of substituted triamminenitrosylruthenium complexes was hindered by the insolubility of the parent complex,

$[Ru(NH_3)_3NO(Cl)_2]Cl$, in the organic solvents in which the various ligands were soluble, and by the reaction of some ligands with this complex to yield tetraamminenitrosylruthenium complexes.

REFERENCES

(1) A. D. Allen, C. V. Senoff, *Chem. Commun.*, 621(**1965**)

(2) J. Chatt, J. R. Dilworth, R. L. Richards, *Chem. Rev.*, **78**, 589(1978)

(3) A. D. Allen, F. Bottomley, *Acc. Chem. Res.*, **1**, 360(1968)

(4) D. Sellman, *Angew. Chem., Intl. Ed.*, **13**, 639(1974)

(5) A. A. Diamantis, J. V. Dubrawski, *Inorg. Chem.*, **20**, 1142(1981)

(6) I. J. Itzkovich, J. A. Page, *Can. J. Chem.*,**46**, 2743(1968)

(7) F. A. Cotton, G. Wilkinson, "Advanced Inorganic Chemistry", 3rd Ed., J. Wiley & Sons, New York, 1972, p710

(8) J. Chatt, G. J. Leigh, N. Thankarajan, *J. Chem. Soc., A.*, 3169(**1971**)

(9) (a)C. M. Elson, I. J. Itzkovitch, J. A. Page, *Can. J. Chem.*,**48**, 1639(1970). (b)L. A. P. Kane-Maguire, *J. Inorg. Nucl. Chem.*, **33**, 3964((1971)

(10) J. E. Fergusson, J. L. Love, *Chem. Commun.*, 399(**1969**)

(11) L. A. P. Kane-Maguire, P. S. Sheridan, F. Basolo, R. G. Pearson, *J. Amer. Chem. Soc.*, **92**, 5865(1970)

(12) L. A. P. Kane-Maguire, P. S. Sheridan, F. Basolo, *Inorg. Synth.*, **12**, 23(1970)

(13) W. P. Griffith, "*The Chemistry of the Rarer Platinum Metals*", Interscience, London, 1967

(14) F. Bottomley, *Coord. Chem. Rev.*, **26**, 7(1978)

(15) B. F. G. Johnson, J. A. M^{c}Leverty, *Progr. Inorg. Chem.*, **7**, 277(1966)

(16) J. H. Enemark, R. D. Feltham, *Coord. Chem. Rev.*, **13**, 339(1974)

(17) F. A. Cotton, G. Wilkinson, "Advanced Inorganic Chemistry", 3rd Ed., J. Wiley & Sons, New York, 1972, p356

(18) B. L. Haymore, J. A. Ibers, *Inorg. Chem.*, **14**, 3060(1975)

(19) R. W. Adams, J. Chatt. N. E. Hooper, G. J. Leigh, *J. Chem. Soc., Dalton Trans.*, 1125(**1977**)

(20) F. Bottomley, *Acc. Chem. Res.*, **11**, 158(1978)

(21) F. Bottomley, J. R. Crawford, *Chem. Commun.*, 200(**1971**)

(22) F. Bottomley, J. R. Crawford, *J. Amer. Chem. Soc.*, **94**, 9092(1972)

(23) S. Pell, J. N. Armor, *Inorg. Chem.*, **12**, 873(1973)

(24) A. F. Schreiner, S. W. Lim, P. J. Hauser, E. A. Hopcus, D. J. Hamm, J. D.Gunter, *Inorg. Chem.*, **11**, 880(1972)

(25) N. M. Sinitsin, A. A. Svetlov, N. B. Brikova, *Koord. Khim.*, **3**, 593(1977)

(26) K. Nakamoto, J. Fujita, M. Kobayaski, R. Tuschida, *J. Chem. Phys.*, **27**, 439(1957)

(27) A. B. Nikol'skii, A. M. Popov, I. V. Vasilevskii, *Soviet J. Coord. Chem.*, **2**, 508(1976)

(28) M. Mukaida, M. Yanida, T. Nomura, *Bull. Chem. Soc. Japan,* **50**, 3053(1977)

(29) P. W. Banham, Honours Thesis, The University of Adelaide, 1980

(30) A. A. Diamantis, G. J., Sparrow, *Chem. Commun.*, 469(**1969**)

(31) J. Chatt, R. L. Richards, J. E. Fergusson, J. L. Love, *Chem. Commun.*, 1522(**1968**)

(32) D. E. Harrison, H. Taube, *Science*, **159**, 320(1968)

(33) C. Creutz, H. Taube, *Inorg. Chem.*, **10**, 2664(1971)

(34) C. M. Elson, J. Gulens, I. J. Itzkovitch, J. A. Page, *J. Chem. Soc., D.*, 875(**1970**)

(35) M. B. Fairey, R. J. Irving, *Spectrochim. Acta*, **22**, 359(1966)

Chapter 6.

EXPERIMENTAL.

6.1. Materials.

6.1.1. Preparative Materials. Ruthenium trichloride trihydrate was purchased from Johnson Matthey Ltd.

Trifluoromethanesulphonic acid, ammonium hexafluorophosphate, 2,2,6,6-tetramethylhepta-3,5-dione (dipivaloylmethane), 2(aminomethyl)pyridine and 2-hydroxynaphthaldeyde (Tech) were obtained from Aldrich Chemicals.

Methanesulphonic acid (techn. 70% aqueous solution), tetra(n-butyl)ammonium bromide (purum) and 1-phenylbuta-1,3-dione (purum) were obtained from Fluka AG.

Silver carbonate, sodium perchlorate and penta-2,4,-dione were obtained from BDH chemicals as Analar reagents.

The tridentate ligands were prepared by literature methods by Dr. Md. A. Salam. [1] The tripodal ligands were supplied by Dr. F. R. Keene, having been prepared by literature methods. [2, 3]

All other materials used in preparative work were reagent grade chemicals.

Micranalyses were performed by the Canadian Microanalytical Service, Ltd.

6.1.2. Electrochemical Materials. Glassy carbon rod was obtained from Atomergic Chemicals. High purity water was obtained by treating deionized water in a Millipore Milli-Q™ water purification system. The water was passed through activated charcoal, cation and anion exchange columns and then through an Organex™ cartridge.

Sodium methanesulphonate was prepared by the neutralization of methanesulphonic acid by an equimolar amount of sodium carbonate (AR, Univar Chemicals). The sodium methanesulphonate was twice recrystallized from water/ethanol before use. Sodium perchlorate was used as received.

The solvents dimethylsulphoxide, methanol and acetone were BDH Analar grade. Acetonitrile was Waters Associates Liquid Chromatography grade.

High purity argon, nitrogen and hydrogen and medical grade nitrous oxide were obtained from Commonwealth Industrial Gases Ltd. Nitric oxide was obtained from Matheson Gas Products. The

argon was passed through a purging column containing an acid solution of chromous ion, followed by a water scrubber to dissolve traces of acid.

The materials used to prepare the buffer solutions were all analytical grade reagents. The buffers used and their pH ranges were: chloroacetate, 2<pH<4; phthalate, 3<pH<5; acetate, 3.5<pH<5.5; MES, 5<pH<7; phosphate, 5<pH<7; TRIS, 7<pH<9; borate, 9<pH<11. The pH of the electrochemical solutions was adjusted by the dropwise addition of 0.1 mol dm^{-3} sodium hydroxide or methanesulphonic acid. The solution pH was measured using an Activon combined pH electrode connected to an Orion Research 701A digital pH meter.

Alumina slurries for electrode polishing were obtained from Buehler. Diamond pastes for electrode polishing were obtained from Hyprez, and were used with a Buehler extender oil. Platinum electrodes were polished on a Microcloth™ polishing pad (Buehler), and glassy carbon electrodes were polished on a Texmet™ polishing pad (Buehler).

6.2. Instruments.

Electrochemical experiments were performed with either of two combinations of instruments. (1)A Princeton Applied Research 174 potentiostat and a Pine Instruments RDE 3 potentiostat connected to a Hewlet Packard 7015 B X-Y recorder. (2)A Bioanalytical Systems BAS 100 electrochemical analyser connected to an Amust P88-2 digital printer and a Houston Instruments HIPLOT DMP40 digital plotter. Sampled Current Polarography experiments were performed using a locally made dropping mercury electrode attached to the BAS 100.

Electronic spectra were recorded on a Varian DMS 100 uv/visible spectrophotometer connected to a Epson MX-80 digital printer. Infrared spectra were recorded on a Perkin Elmer 683 Infrared spectrophotometer. NMR spectra were recorded on a Bruker HX90E instrument, and mass spectra were obtained on a VG ZAB 2HF spectrometer.

Magnetic susceptibilities were measured using a Johnson Matthey Magnetic Susceptibility Balance. Conductivity measurements were made using a locally made resistance bridge connected to a 1 cm cell having a cell constant of 0.77.

6.3. Electrochemical Procedures.

6.3.1. Electrochemical Cells. Electrochemical experiments were performed in a single compartment three electrode cell. The cell compartment consisted of a small glass vessel, fitted with a teflon cap. There were holes in the cap to accomodate the electrodes and the teflon tubing which carried the purging gas.

The reference electrode was a Saturated Calomel Electrode (Titron, Pty. Ltd.) and the counter electrode was a platinum wire. In non-aqueous solutions the working electrode was a commercially available platinum disc electrode (Bioanalytical Systems). For aqueous solutions, the working electrode was a glassy carbon disc. When a freshly polished electrode was used, this was a commercially available model (Bioanalytical Systems), and, when an activated electrode was used, the electrode was made locally by heat-shrinking a teflon shroud around a piece of glassy carbon rod.

6.3.2. Electrode Preparation. All electrodes were initially ground on a high speed polishing wheel with carborundum paper (600 grit). Platinum electrodes, and glassy carbon electrodes which were not to be activated were then polished with 1 μm alumina slurry, and then with 0.05 μm alumina slurry. Between each polishing step the electrodes were rinsed with a stream of high purity water and then washed in an ultrasonic bath for two minutes in high purity water. This rinsing and washing procedure was repeated twice. For polishing after normal use, the electrodes were polished with the 0.05 μm alumina slurry, and the same rinsing and washing procedure applied.

After the carborundum grinding step, glassy carbon electrodes which were to be activated were polished with 1 μm alumina slurry and then with 1 μm diamond paste. After the diamond paste polishing step, the electrodes were rinsed in a stream of high purity water and then cleaned in high purity water in an ultrasonic bath for two minutes. Following this, the ultrasonic washing was repeated, using ethanol, and then the ultrasonic washing with water was repeated.

Glassy carbon electrodes were activated using a modification of a method described in the literature. [4] In 0.1 mol dm^{-3} H_2SO_4, the potential of the glassy carbon electrode was held at +1.80 V for 30 seconds, and the potential was then changed to –0.20 V for 15 seconds. This cycle was performed six times, at which stage the state of activation was examined by determining a DPV of $[Ru(NH_3)_5(OH_2)]^{3+}$ at pH 4. Further activation cycles were applied, as required, until the peak height of the Ru^{4+}/Ru^{3+} couple remained constant relative to that of the Ru^{3+}/Ru^{2+} couple. The electrode was rinsed with water between the activating procedure and the recording of voltammograms, and was cleaned in an ultrasonic bath between the experiments in different electrochemical media. Freshly polished glassy carbon electrodes had a mirror-like surface and the surface of the activated electrodes was slightly dull, with a blue/bronze tinge.

6.3.3. Experimental Procedures. For studies in aqueous solution, the compound under investigation was dissolved in an electrochemical medium (approximately 5 mg of solid in 4 - 5 cm^3) containing 0.1 mol dm^{-3} sodium methanesulphonate as a supporting electrolyte and 0.02 mol dm^{-3} of the appropriate buffer. For experiments in acid solution, 0.1 mol dm^{-3} methanesulphonic acid fulfilled the requirements for buffer and supporting electrolyte. When monitoring preparative

reactions, 50 - 100µl of the reaction mixture was added by syringe to 4 - 5 cm^3 of the electrochemical medium. Points in the Pourbaix diagrams were fitted to straight lines by means of a regression analysis programme on a hand-held calculator. The data points for the line were chosen to give the largest value for the correlation coefficent, which was usually greater than 0.9.

For studies in non-aqueous solutions, about 5 mg of a solid sample was dissolved in 4 - 5 cm^3 of the solution containing 0.1 mol dm^{-3} sodium perchlorate as supporting electrolyte. The saturated calomel electrode was placed directly into the electrochemical medium, and no allowance was made for any possible liquid junction potential.

For all the voltammetric experiments, unless stated otherwise, there was a 2 second "quiet time" between the application of the initial potential and the commencement of the scan. Unless stated otherwise, cyclic voltammograms were recorded at 100 mV sec^{-1}. The standard conditions for recording sampled current polarography were: scan rate = 5 mV sec^{-1}, dropping time = 0.5 sec and sample width = 0.02 sec. The standard conditions for recording differential pulse voltammograms were: scan rate = 5 mV sec^{-1}, pulse amplitude = 5 mV, sample width = 0.02 sec, pulse width = 0.06 sec and pulse period = 0.5 sec. The standard conditions for recording Osteryoung square wave voltammograms were: square wave amplitude = 25 mV, square wave frequency = 15 Hz, potential step = 4 mV, with 256 sample points per line cycle.

6.4. Synthesis.

6.4.1. Starting Materials. $[Ru(NH_3)_5Cl]Cl_2$ [5], $[Ru(NH_3)_4C_2O_4]_2S_2O_6$ [6], and *cis* $[Ru(NH_3)_4(H_2O)_2](TFMS)_3$ [7] were prepared according to literature methods. $Ru(NH_3)_3Cl_3$ was prepared using the method of Banham. [8] $[Ru(NH_3)_4C_2O_4]_2S_2O_6$ (0.43 g, .60 mmol) was heated in refluxing hydrochloric acid (5 mol dm^{-3}, 35 cm^3) for 4 hours. The reaction mixture was then cooled in an ice bath for 1 hour. Red brown crystals were collected from a red mother liquor by vacuum filtration through a sintered glass funnel. The solid was washed with three 5 cm^3 portions of cold HCl (5 mol dm^{-3}), one 5 cm^3 portion of ethanol and then dried on a vacuum line for three hours. Yield = 0.2 g (0.77 mmol, 64%).

6.4.2. $[Ru(NH_3)_3(OH_2)_3](TFMS)_3$. Silver carbonate (0.957 g, 3.47 mmol) was dissolved in HTFMS (2 mol dm^{-3}, 20 cm^3) in a conical flask with heating on an oil bath at 45°C. $Ru(NH_3)_3Cl_3$ (0.6 g, 2.3 mmol) was then added, and washed in with an extra 5 cm^3 of the HTFMS solution. As the red ruthenium complex was dissolved by stirring a white, cloudy precipitate formed. The reaction was allowed to proceed for two hours, after which time, the reaction mixture was filered, hot, through a filter paper to give a clear, greenish-coloured filtrate. The precipitated silver chloride was washed with three 5 cm^3 portions of water, and the washings combined with the filtrate. Using a rotary

evaporator, the volume of the combined filtrate and washings was reduced to less than 10 cm^3. After cooling overnight in the refrigerator, the solution was filtered through a sintered glass funnel (porosity 3), yielding the product as pale pink, feathery crystals. The solid was washed with three portions of dry diethyl ether, and then dried on the vacuum line for four hours. Yield = 1.04 g (1.6 mmol, 69%) Analysis: Calc. for $RuC_3H_{15}N_3F_9S_3O_{12}$ (Mol. wt. 653.4) C - 5.51%, H - 2.31%, N - 6.43%. Found: C -5.53%, H - 2.34%, N - 6.66%.

6.4.2a. $[Ru(NH_3)_3(OH_2)_3](pTS)_3$. Silver carbonate (0.425 g, 1.54 mmol) was dissolved in pTSH (8 mol dm^{-3} 5 cm^3), and after effervescence had ceased, $Ru(NH_3)_3Cl_3$ (0.6 g, 1.03 mmol) was added, and washed in with an extra 5 cm^3 of the pTSH solution. The resulting mixture was heated at reflux for 1 hour. After cooling to room temperature, the mixture was then filtered to remove the silver chloride which had precipitated. The volume of the filtrate was reduced by half using the rotary evaporator, and the solution was then allowed to cool in an ice bath for one hour. Colourless needles were then collected by filtration, and washed with two 4 cm^3 portions of ethyl acetate and air dried. Yield = 0.06 g (0.08 mmol, 8%)

6.4.2b. $[Ru(NH_3)_3(OH_2)_3]^{2+}$. (1) $[Ru(NH_3)_3(OH_2)_3](TFMS)_3$ (0.02 g, .03 mmol) was dissolved in 0.1 mol dm^{-3} HTFMS (25 cm^3), and the uv/vis spectrum recorded. A 5 cm^3 aliquot was then degassed with argon, before amalgamated zinc was added and the mixture stirred under argon for 1 hour. The uv/vis spectrum of the golden yellow solution was recorded, and further reaction with the amalgamated zinc followed until there was no further change to the spectrum.
(2) $[Ru(NH_3)_3(OH_2)_3](TFMS)_3$ (0.02 g, .03 mmol) was dissolved in water (25 cm^3), and the uv/vis spectrum recorded. A 5 cm^3 aliquot was then degassed with argon, and hydrogen gas was then bubbled into the solution through a platinum black gauze for 1 hour. The uv/vis spectrum of the golden yellow solution was recorded, and further reaction with hydrogen followed until there was no further change to the spectrum.

6.4.2c. Mixed oxidation state species. (1) $[Ru(NH_3)_3(OH_2)_3](TFMS)_3$ (0.02 g, .03 mmol) was dissolved in pH 7.4 buffer containing 0.1 mol dm^{-3} sodium methanesulphonate (25 cm^3), and the solution was degassed with argon. Amalgamated zinc was then added, and the mixture stirred under argon. A blue colour developed after about 15 minutes, and became very intense over a period of 1 hour. Several samples were withdrawn to allow the uv/vis spectrum to be recorded, and voltammograms were recorded about 1 hour after the start of the reduction. After 4 hours, the blue colour of the solution faded to give a golden yellow solution, and the uv/vis spectrum of this solution was also recorded.
(2) $[Ru(NH_3)_3(OH_2)_3](TFMS)_3$ (0.02 g, .03 mmol) was dissolved in pH 7.4 buffer containing 0.1 mol dm^{-3} sodium methanesulphonate (25 cm^3), and the solution was degassed with argon. A similar

solution was made up in water, degassed with argon, and then hydrogen gas was bubbled into the solution through a platinum black gauze for 1 hour. SCP was used at this stage to determine that the ruthenium was in the +2 oxidation state. A 5 cm^3 aliquot of the Ru(II) solution was then added to an equal volume of the high pH Ru(III) solution, and the resulting solution stirred under argon. A blue colour became apparent after 15 minutes, and the uv/vis spectrum was determined after 1 hour.

6.4.2d. Oxidation of $[Ru(NH_3)_3(OH_2)_3]^{3+}$. $[Ru(NH_3)_3(OH_2)_3](TFMS)_3$ (0.008 g, .1.2 x 10^{-5} mol) was dissolved in pH 5 buffer (acetate, 3 cm^3) and an aliquot of hydrogen peroxide solution (0.1 mol dm^{-3}, 60 µl) was added. The reaction mixture was then heated on a steam bath at 50°C for 15 minutes. The solution turned red almost instantaneously, and then changed to a brown colour. The CV of the solution was then determined, and found to contain no peaks attributable to the $[Ru(NH_3)_3(OH_2)_3]^{3+}$ complex. The reaction was repeated at room temperature, but the same reactions were observed, occurring over about an hour.

6.4.3. Substituted Triammineruthenium(III) Complexes.

(a) $[Ru(NH_3)_3(acac)(OH_2]S_2O_6.2H_2O$. $[Ru(NH_3)_3(OH_2)_3](TFMS)_3$ (0.24 g, .37 mmol) was dissolved in ethanol (5 cm^3). The solution was stirred at 40°C for 2 hours in a round bottomed flask. 2,4-pentadione (38 µl, .38mmol) was then added to the solution, followed by lithium acetate (0.038 g, .37 mmol), which was washed in with ethanol (5 cm^3). The reaction was monitored by DPV until the peak at –0.09 V was no longer evident. The solvent was then removed using a rotary evaporator, and the residue dissolved in the minimum volume of dithionic acid (1.1 mol dm^{-3}). An equal volume of ethanol was then added, and the solution stored at –10°C for 80 hours. Purple crystals were collected from the mother liquor by vacuum filtration through a sintered glass funnel. The crystals were washed with two 3 cm^3 portions of ethanol, and one 5 cm^3 portion of dry diethyl ether then air dried by suction. Yield = 0.075 g (0.18 mmol, 49%). Analysis: Calc for $RuC_5H_{19}N_3S_2O_{11}$ (Mol. wt = 433.4) C - 12.90%, H - 4.76%, N - 9.03%. Found: C - 12.75%, H - 4.63%, N - 9.11%.

(b) $[Ru(NH_3)_3(dpm)(OH_2]S_2O_6$. $[Ru(NH_3)_3(OH_2)_3](TFMS)_3$ (0.25 g, .38 mmol) was dissolved in methanol (5 cm^3). The solution was stirred at 40°C for 2 hours in a round bottomed flask. 2,2,6,6-tetramethylhepta-3,5-dione in solution in methanol (34% solution, .205 g, .38 mmol) was added followed by lithium acetate (0.039 g, .38 mmol), which was washed into the flask with methanol (5 cm^3). The reaction was monitored by DPV until the peak at –0.09 V was no longer evident. The reaction mixture was then filtered to remove a solid impurity, and the solvent removed from the filtrate using a rotary evaporator. 5 cm^3 of dithionic acid (1.1 mol dm^{-3}) was added to the residue and a purple solid precipitated, which was collected from the mother liquor by vacuum filtration through a sintered glass funnel. The solid was washed with two 3 cm^3 portions of ethanol, and one

5 cm^3 portion of dry diethyl ether then air dried by suction. Yield = 0.08 g (0.16 mmol, 40%). Analysis: Calc for $RuC_{11}H_{30}N_3S_2O_9$ (Mol wt = 513.6) C - 25.73%, H - 5.89%, N - 8.18%. Found: C - 25.29%, H - 5.77%, N - 8.06%.

(c) $[Ru(NH_3)_3(hna)(OH_2]S_2O_6.H_2O$. $[Ru(NH_3)_3(OH_2)_3](TFMS)_3$ (0.12g, .18 mmol) was dissolved in ethanol (5 cm^3). The solution was stirred at 45°C for 1 hour in a round bottomed flask. 2-hydroxynaphthaldehyde (0.031 g µl, .18mmol) was then added to the solution, followed by lithium acetate (0.0184 g, .18 mmol), which was washed in with ethanol (5 cm^3). A green colour formed almost immediately after the addition of the solid materials. Stirring continued for 2 hours, after which time DPV analysis showed the reaction to be complete. The solvent was then removed using a rotary evaporator, and the residue dissolved in the minimum volume of dithionic acid (1.1 mol dm^{-3}). This solution was stored at –10°C for 60 hours. A dark green solid was collected from the mother liquor by vacuum filtration through a sintered glass funnel. The solid was washed with two 3 cm^3 portions of ethanol, and one 5 cm^3 portion of dry diethyl ether then air dried by suction. Yield = 0.052 g (0.10 mmol, 58%). Analysis: Calc for $RuC_{11}H_{18}N_3S_2O_9$ (Mol wt = 501.4) C - 26.33%, H - 3.62%, N - 8.38%. Found: C - 26.59%, H - 3.66%, N - 8.19%.

(d) $[Ru(NH_3)_3(oxine)(OH_2](TFMS)_2.H_2O$. $[Ru(NH_3)_3(OH_2)_3](TFMS)_3$ (0.17g, .27 mmol) was dissolved in ethanol (5 cm^3). The solution was stirred at 45°C for 1 hour in a round bottomed flask. 8-hydroxyquinoline (0.040 g µl, .28mmol) was then added to the solution, followed by lithium acetate (0.0265 g, .26 mmol), which was washed in with ethanol (5 cm^3). A green colour formed within half an hour of the addition of the solid materials. Stirring was continued for 4 hours, after which time DPV analysis showed the reaction to be complete. The solvent was then removed using a rotary evaporator, and the residue dissolved in 5 cm^3 HTFMS (3.5 mol dm^{-3}). The volume of the solution was reduced to half using a rotary evaporator, and the resulting solution was stored at –10°C for 85 hours. Dark green platelets were collected from the mother liquor by vacuum filtration through a sintered glass funnel. The solid was washed with three 3 cm^3 portions of dry diethyl ether then air dried by suction. Yield = 0.021 g (0.03 mmol, 12%). Attempts at isolating greater yields from the reaction, by further concentration of the mother liquor resulted in the formation of the starting material. Analysis: Calc for $RuC_{11}H_{19}N_4S_2F_6O_9$ (Mol wt = 628.5) C - 21.02%, H - 3.05%, N - 8.92%, . Found: C - 20.60%, H - 2.86%, N - 8.11%.

(e) $[Ru(NH_3)_3(C_2O_4)(H_2O)]_2S_2O_6.H_2O$. $[Ru(NH_3)_3(OH_2)_3](TFMS)_3$ (0.098g, .15 mmol) was dissolved in water (5 cm^3) in a round-bottomed flask fitted with an outflow bubbler. Oxalic acid dihydrate (0.011 g, .075 mmol) and sodium oxalate (0.0095 g, .075 mmol) were then added, and hydrogen gas was bubbled into the solution over a platinum black gauze for 1 hour without prior degassing. The red solution was then heated on an oil bath at 50°C for 1 hour, at which time the

colour of the solution had changed to yellow and DPV analysis showed the reaction to be complete. The solvent was then removed using a rotary evaporator, and the residue treated with dithionic acid (1 cm^3, 0.25 mol dm^{-3}). A pale yellow solid precipitated immediately. The mixture was stored a 4°C for 1 hour, and the product was collected by vacuum filtration through a sintered glass funnel. The solid was washed with two 3 cm^3 portions of ethanol, and one 5 cm^3 portion of dry diethyl ether then air dried by suction. Yield = 0.038 g (0.11 mmol, 75%). Analysis: Calc for $Ru_2C_4H_{24}N_6S_2O_7$ (Mol wt = 676.5) C - 6.92%, H - 3.48%, N - 12.10%. Found: C - 6.90%, H - 3.37%, N - 11.93%.

(f) $[Ru(NH_3)_3(sal)(H_2O)]^{2+}$. $[Ru(NH_3)_3(OH_2)_3](TFMS)_3$ (0.17g, .26 mmol) was dissolved in ethanol (5 cm^3). The solution was stirred at 45°C for 1 hour in a round bottomed flask. Salicylaldehyde (0.032 g, .26 mmol) was then added to the solution, followed by lithium acetate (0.027 g, .26 mmol), which was washed in with ethanol (5 cm^3). A green colour formed almost immediately after the addition of the solid materials. Stirring continued for 2 hours, after which time DPV analysis showed the reaction to be complete. 100 µl samples of the solution were added to 5 cm^3 aliquots of the aqueous electrochemical media, and the CV determined at several pH values.

(g) $[Ru(NH_3)_3(bzac)(H_2O)]^{2+}$. $[Ru(NH_3)_3(OH_2)_3](TFMS)_3$ (0.51g, .79 mmol) was dissolved in ethanol (5 cm^3). The solution was stirred at 45°C for 1 hour in a round bottomed flask. 1-phenylbuta-2,4-dione (0.127 g , .79 mmol) was then added to the solution, followed by lithium acetate (0.080 g, .79 mmol), which was washed in with ethanol (5 cm^3). A red colour formed almost immediately after the addition of the solid materials, and slowly changed to purple. Stirring continued for 2 hours, after which time DPV analysis showed the reaction to be complete. 100 µl samples of the solution were added to 5 cm^3 aliquots of the aqueous electrochemical media and, after filtering off a white precipitate, the CV of the purple aqueous solutions were determined at several pH values.

6.4.4. Substituted Triammineruthenium(II) Complexes.

(a) $[Ru(NH_3)_3(phen)(H_2O)](PF_6)_2$. Two procedures were used which gave the same products but with varying yield: (1) $[Ru(NH_3)_3(OH_2)_3](TFMS)_3$ (0.235g, .36 mmol) was dissolved in water (5 cm^3), the solution was degassed by bubbling argon through it and hydrogen gas was then bubbled into the solution through a platinum black gauze for 1 hour. The golden yellow solution of $[Ru(NH_3)_3(OH_2)_3]^{2+}$ was then filtered through a Schlenk filter into a round-bottomed Schlenk flask. 1,10-phenanthroline hydrate (0.065 g, .36 mmol) was then added and the reaction mixture stirred under argon for 4 hours, at which time DPV analysis showed the reaction to be complete. An excess of NH_4PF_6 was added to the solution and the mixture was then stirred under argon for 15 minutes, before being stored at –10°C for 5 hours. The brick red solid was collected by vacuum

filtration through a sintered glass funnel. The product was washed with two 5 cm^3 portions of ice-cold water, and one 3 cm^3 portion of dry diethyl ether then air dried by suction. Yield = 0.104 g (0.16 mmol, 45%). Analysis: Calc for $RuC_{12}H_{19}N_5P_2F_{12}O$ (Mol wt = 642.5) C - 22.51%, H - 2.99%, N - 10.94%. Found: C - 22.08%, H - 3.10%, N - 10.80%.

(2) $[Ru(NH_3)_3(OH_2)_3](TFMS)_3$ (0.25g, .38 mmol) was dissolved in water (10 cm^3), and the solution was degassed by bubbling argon through it. 1,10-phenanthroline hydrate (0.076 g, .38 mmol) was added and hydrogen gas was then bubbled into the solution through a platinum black gauze. After 2 hours, at which time DPV analysis showed the reaction to be complete, the deep red solution was filtered through a Schlenk filter, and excess NH_4PF_6 was added to the solution. The mixture was stirred under argon for 15 minutes, and then stored at –10°C for 5 hours. The brick red solid was collected by vacuum filtration through a sintered glass funnel. The product was washed with two 5 cm^3 portions of ice-cold water, and one 3 cm^3 portion of dry diethyl ether then air dried by suction. Yield = 0.195 g (0.11 mmol, 80%).

(b) $[Ru(NH_3)_2(bpy)_2](PF_6)_2$. $[Ru(NH_3)_3(OH_2)_3](TFMS)_3$ (0.191g, .29 mmol) was dissolved in water (10 cm^3), the solution was degassed by bubbling argon through it and hydrogen gas was then bubbled into the solution through a platinum black gauze for 1 hour. The golden yellow solution of $[Ru(NH_3)_3(OH_2)_3]^{2+}$ was then filtered through a Schlenk filter into a round-bottomed Schlenk flask containing a degassed solution 2,2'-bipyridine (0.063 g, .40 mmol) in ethanol (12 cm^3) and the reaction mixture was stirred under argon for 4 hours. An excess of NH_4PF_6 was then added to the solution and the mixture was stirred under argon for 15 minutes, before being stored at –10°C for 16 hours. The brick red solid was collected by vacuum filtration through a sintered glass funnel. The product was washed with two 3 cm^3 portions of ice-cold ethanol, and one 5 cm^3 portion of dry diethyl ether, then air dried by suction. Yield = 0.043 g (0.058 mmol, 20%). Analysis: Calc for $RuC_{20}H_{24}N_6P_2F_{12}$ (Mol wt = 741.6) C - 32.39%, H - 3.26%, N - 11.33%. Found: C - 32.41%, H - 2.85%, N - 11.09%.

(c) $[Ru(NH_3)_3(py)_3](ClO_4)_2$. Following the method of Ford & Sutton [9], a 1 mol dm^{-3} pyridine/pyridinium buffer was prepared by mixing pyridine (2 cm^3) and $MeSO_3H$ (2.4 mol dm^{-3}, 5 cm^3) and making up to 25 cm^3 with water. $[Ru(NH_3)_3(OH_2)_3](TFMS)_3$ (0.159g, .244 mmol) was dissolved in this buffer (10 cm^3), and the solution was degassed by bubbling argon through it. Amalgamated zinc was then added, and the reaction mixture stirred under argon for 6.5 hours, at which time DPV analysis showed the reaction to be complete. The bright gold-coloured solution was then filtered through a Schlenk filter into a round-bottomed Schlenk flask. An excess of $NaClO_4$ was then added and a cloudy precipitate formed almost immediately. The mixture was cooled on an ice bath for 1 hour, and the product was collected as a yellow powder by vacuum filtration through a sintered glass funnel. The product was washed with two 5 cm^3 portions of ice-

cold sodium perchlorate solution, and one 5 cm^3 portion of dry diethyl ether, then air dried by suction. The crude product was recrystallized from hot methanol, yielding bright yellow cubic crystals. Yield = 0.077 g (0.12 mmol, 48%). Analysis: Calc for $RuC_{15}H_{24}N_6O_8Cl_2$ (Mol wt = 588.37) C - 30.62%, H - 4.11%, N - 14.29%, Cl - 12.05%. Found: C - 30.05%, H - 4.5%, N - 14,5%, Cl - 12.3%.

(d) $[Ru(NH_3)_3(py)_3](Br)_2$. $[Ru(NH_3)_3(py)_3](ClO_4)_2$ (0.077 g, .12 mmol) was dissolved in butanone (10 cm^3), and then an excess of tetra(n-butyl)ammonium bromide was added to the solution. A pale precipitate formed almost immediately, and the mixture was stirred for 0.5 hour. After cooling in ice for 1 hour, the pale yellow solid was collected by vacuum filtration through a sintered glass funnel. The product was washed with two 5 cm^3 portions of butanone, and one 5 cm^3 portion of dry diethyl ether, then air dried by suction. Yield = 0.063 g (0.11 mmol, 96%).

(e) $[Ru(NH_3)_3(MeCN)_3]Cl_2.2H_2O$. $[Ru(NH_3)_3(OH_2)_3](TFMS)_3$ (0.236g, .36 mmol) was dissolved in 0.01 mol dm^{-3} HTFMS (10 cm^3), and then acetonitrile (1.5 cm^3) was added. The solution was degassed by bubbling argon through it, then amalgamated zinc was added and the mixture stirred for 4.5 hours, at which time DPV analysis showed the reaction to be complete. The golden yellow solution was then filtered through a Schlenk filter into a round-bottomed Schlenk flask and an excess of NH_4PF_6 was added to the solution. The mixture was then stirred under argon for 15 minutes, before being stored at –10°C for 2 hours. The pale yellow solid was collected by vacuum filtration through a sintered glass funnel. The product was washed with one 5 cm^3 portion of ice-cold water, and one 3 cm^3 portion of dry diethyl ether. This solid was dissolved in butanone (10 cm^3), and then a solution of tetra(n-butyl)ammonium chloride (0.5 g) in butanone (3 cm^3) was added. A pale precipitate formed almost immediately, and the mixture was stirred for 5 minutes. After cooling at –10°C for 2 hours, the pale yellow solid was collected by vacuum filtration through a sintered glass funnel and washed with two 5 cm^3 portions of butanone, and one 5 cm^3 portion of dry diethyl ether, then air dried by suction. The crude product was recrystallized from methanol/butanone, resulting in pale yellow, feathery crystals. Yield = 0.051 g (0.13 mmol, 37%). Analysis: Calc for $RuC_6H_{22}N_6Cl_2O_2$ (Mol wt = 382.3) C - 18.85%, H - 5.96%, N - 21.99%, Cl - 18.85%. Found: C - 18.80%, H - 5.77%, N - 21.72%, Cl - 18.27%.

(f) $[Ru(NH_3)_3(MeCN)_3]Br_2$. $[Ru(NH_3)_3(MeCN)_3](PF_6)_2$ was prepared as described in (e) above. This solid was then dissolved in butanone (10 cm^3), and an excess of tetra(n-butyl)ammonium bromide was added to the solution. A pale precipitate formed almost immediately, and the mixture was stirred for 5 minutes. After cooling at –10°C for 2 hours, the pale yellow solid was collected by vacuum filtration through a sintered glass funnel and washed with two 5 cm^3 portions of butanone,

and one 5 cm^3 portion of dry diethyl ether, then air dried by suction. Yield = 0.084 g (0.19 mmol, 42%).

(g) $[Ru(NH_3)_3(ampy)(H_2O)](PF_6)_2$. $[Ru(NH_3)_3(OH_2)_3](TFMS)_3$ (0.27g, .41 mmol) was dissolved in water (5 cm^3), and the solution was degassed by bubbling argon through it. Hydrogen gas was then bubbled into the solution through a platinum black gauze for 0.75 hour before 2(aminomethylpyridine) was added (20% solution in ethanol, 275 µl, .41 mmol). The treatment with hydrogen was continued for 0.5 hour, and then the solution was stirred at 40°C for 5 hours, at which time DPV analysis showed the reaction to be complete. The solution was then filtered through a Schlenk filter into a round-bottomed Schlenk flask and an excess of NH_4PF_6 was added to the filtrate. The mixture was stirred under argon for 15 minutes, and then cooled in an ice bath for 1 hour. The yellow solid which precipitated was collected by vacuum filtration through a sintered glass funnel. The product was washed with two 3 cm^3 portions of ice-cold ethanol, and one 5 cm^3 portion of dry diethyl ether, then air dried by suction. Yield = 0.106 g (0.18 mmol, 44%). The product underwent decomposition before the microanalysis could be performed. Freshly prepared samples were used to determine the pH-dependent electrochemistry.

6.4.5. Triammine(tripod)ruthenium(II) Complexes.

(a) $[Ru(NH_3)_3\{(py)_3COH\}]Br_2$. $[Ru(NH_3)_3(OH_2)_3](TFMS)_3$ (0.172g, .26 mmol) was dissolved in water (7 cm^3), and the solution was degassed by bubbling argon through it. Hydrogen gas was then bubbled into the solution through a platinum black gauze for 1.5 hours. Tris(pyridyl)methanol (0.068 g, .26 mmol) was then added and the treatment with hydrogen continued for 45 minutes. The reaction mixture was then stirred under argon until DPV analysis showed the reaction to be complete. The dark golden solution was filtered through a Schlenk filter, and excess NH_4PF_6 was added to the filtrate. The mixture was stirred under argon for 15 minutes and then stored at –10°C for 24 hours. The yellow solid was collected by vacuum filtration through a sintered glass funnel and washed with two 5 cm^3 portions of ice-cold ethanol, and one 3 cm^3 portion of dry diethyl ether then air dried by suction. The crude product (0.108 g, 55%) was dissolved in butanone (5 cm^3) and excess tetra(n-butyl)ammonium bromide was added to the solution. A flocculent precipitate formed almost immediately, and the mixture was stirred for 5 minutes. After cooling at –10°C for 16 hours, the pale yellow solid was collected by vacuum filtration through a sintered glass funnel and washed with two 3 cm^3 portions of butanone, and one 5 cm^3 portion of dry diethyl ether, then air dried by suction. Yield = 0.068 g (0.12 mmol, 46%). The crude bromide salt was recrystallized from methanol/butanone. Analysis: Calc for $RuC_{16}H_{22}N_6OBr_2$ (Mol wt = 575.3) C - 33.41%, H - 3.85%, N - 14.61%. Found: C - 32.57%, H - 3.71%, N - 13.71%.

(b) $[Ru(NH_3)_3\{(py)_3CH\}]Br_2$. $[Ru(NH_3)_3(OH_2)_3](TFMS)_3$ (0.18g, .27 mmol) was dissolved in water (5 cm^3), and the solution was degassed by bubbling argon through it. Hydrogen gas was then bubbled into the solution through a platinum black gauze for 45 minutes. Tris(pyridyl)methane (0.067 g, .27 mmol) was then added and the treatment with hydrogen continued for 1 hour. The reaction mixture was stirred under argon for 2.5 hours, at which time DPV analysis showed the reaction to be complete. The bright yellow solution was filtered through a Schlenk filter, and excess NH_4PF_6 was added to the filtrate. The mixture was stirred under argon in an ice bath for 2 hours. The yellow solid was collected by vacuum filtration through a sintered glass funnel and washed with two 5 cm^3 portions of ice-cold water, and one 3 cm^3 portion of dry diethyl ether then air dried by suction. The crude product was dissolved in butanone (5 cm^3) and excess tetra(n-butyl)ammonium bromide was added to the solution. A flocculent precipitate formed almost immediately, and the mixture was stirred for 5 minutes. After cooling at –10°C for 16 hours, the pale yellow solid was collected by vacuum filtration through a sintered glass funnel and washed with two 3 cm^3 portions of butanone, and one 5 cm^3 portion of dry diethyl ether, then air dried by suction. Yield = 0.052 g (0.09 mmol, 33%). The crude bromide salt was recrystallized from methanol/butanone. Analysis: Calc for $RuC_{16}H_{22}N_6Br_2$ (Mol wt = 559.3) C - 34.36%, H - 3.96%, N - 15.03%, Br - 28.57%. Found: C - 34.52%, H - 4.37%, N - 11.95%, Br - 28.04%.

(c) $[Ru(NH_3)_3\{(py)_3N\}](ClO_4)_2$. Tris(pyridyl)amine (0.026 g, .105 mmol) was added to a 2-neck reaction vessel. $[Ru(NH_3)_3(OH_2)_3](TFMS)_3$ (0.07g, .107 mmol) was added and washed into the flask with water (8 cm^3). The solution was degassed by bubbling argon through it and hydrogen gas was then bubbled into the solution through a platinum black gauze for 3.5 hours, at which time DPV analysis showed the reaction to be complete. The golden yellow solution was filtered through a Schlenk filter, and excess NH_4PF_6 was added to the filtrate. The mixture was stirred under argon for 8 hours. The yellow solid was collected by vacuum filtration through a sintered glass funnel and washed with two 5 cm^3 portions of ice-cold water, and one 3 cm^3 portion of dry diethyl ether then air dried by suction. Crude yield = 0.04g (0.063 mmol, 60%). A sample of the crude product (26 mg) was dissolved in the minimum volume of hot water. This solution was filtered through a plug of cotton wool and excess sodium perchlorate was added to the filtrate and dissolved with stirring. The mixture was stored at –10°C for 2 hours and a yellow powder was collected by vacuum filtration through a sintered glass funnel and washed with two 5 cm^3 portions of ice-cold water, and one 3 cm^3 portion of dry diethyl ether, then air dried by suction. Yield = 0.01 g (after accidental spillage). Analysis: Calc for $RuC_{15}H_{21}N_6Cl_2O_8$ (Mol wt = 599.4) C - 30.06%, H - 3.53%, N - 16.36%, Cl - 11.83%. Found: C - 30.47%, H - 3.58%, N - 15.96%, Cl - 11.65%.

6.4.6. Bis(tridentate)ruthenium Complexes.

(a) $Ru(bzacBH)_2.H_2O$. N'-(1-methyl-3-oxo-3-phenylpropylidene)benzohydrazide (H_2bzacBH,

0.385 g, 1.37 mmol) and lithium acetate (0.288 g, 2.82 mmol) were added to $RuCl_3.3H_2O$ (0.175 g, .669 mmol), the mixture was dissolved in ethanol (30 cm^3) and heated at reflux for 4 hours. The solvent volume was then reduced to 10 cm^3 on a rotary evaporator, and the concentrated solution stored at –10°C overnight. Black crystals were collected by vacuum filtration through a sintered glass funnel, washed with two 10 cm^3 portions of ice-cold ethanol, and three 5 cm^3 portion of dry diethyl ether, then air dried by suction. Yield = 0.162 g (0.24 mmol, 36%). Analysis: Calc for $RuC_{34}H_{30}N_4O_5$ (Mol wt = 677) C - 60.44%, H - 4.47%, N - 8.29%. Found: C - 60.88%, H - 4.39%, N - 8.46%

(b) Ru(bzac-pCl-BH)$_2$.H$_2$O. N'-(1-methyl-3-oxo-3-phenylpropylidene)-4-chlorobenzohydrazide (H_2bzac-pCl-BH, 0.340 g, 1.08 mmol) and lithium acetate (0.222 g, 2.18 mmol) were added to $RuCl_3.3H_2O$ (0.340 g, .547 mmol), the mixture was dissolved in ethanol (11 cm^3) and heated at reflux for 4 hours. The solvent volume was then reduced by half on a rotary evaporator, and the concentrated solution stored at –10°C overnight. Black crystals were collected by vacuum filtration through a sintered glass funnel, washed with two 10 cm^3 portions of ice-cold ethanol, and three 5 cm^3 portion of dry diethyl ether, then air dried by suction. Yield = 0.126 g (0.17 mmol, 31%). Analysis: Calc for $RuC_{34}H_{28}N_4O_5Cl_2$ (Mol wt = 745.9) C - 56.08%, H - 3.79%, N - 7.52%, Cl - 9.52%. Found: C - 55.16%, H - 3.70%, N - 7.51%, Cl - 10.31%.

(c1) Ru(hnaBH)$_2$.H$_2$O. N'-(2-hydroxynaphthylmethylidene)benzohydrazide (H_2hnaBH, 0.409 g, 1.41 mmol) and lithium acetate (0.294 g, 2.88 mmol) were added to $RuCl_3.3H_2O$ (0.185 g, .70 mmol), the mixture was dissolved in ethanol (11 cm^3) and heated at reflux for 4 hours. The solvent volume was then reduced by half on a rotary evaporator, and the concentrated solution stored at –10°C overnight. A brown powder precipitated which was collected by vacuum filtration through a sintered glass funnel, washed with two 10 cm^3 portions of ice-cold ethanol, and three 5 cm^3 portion of dry diethyl ether, then air dried by suction. Yield = 0.184 g (0.26 mmol, 37%). Analysis: Calc for $RuC_{36}H_{26}N_4O_5$ (Mol wt = 696) C - 62.15%, H - 3.77%, N - 8.05%. Found: C - 61.26%, H - 3.76%, N - 7.62%.

(c2) Ru(hnaBH)$_2$.H$_2$O. N'-(2-hydroxynaphthylmethylidene)benzohydrazide (H_2hnaBH, 0.80 g, 2.76 mmol) and triethylamine (0.77 cm^3, 5.52 mmol) were added to $RuCl_3.3H_2O$ (0.361 g, 1.38 mmol), the mixture was dissolved in ethanol (15 cm^3) and heated at reflux for 4 hours. The solvent volume was then reduced by half on a rotary evaporator, and the concentrated solution stored at –10°C overnight. A brown powder precipitated which was collected by vacuum filtration through a sintered glass funnel, washed with two 10 cm^3 portions of ice-cold ethanol, and three 5 cm^3 portion of dry diethyl ether, then air dried by suction. Yield = 0.2g (0.26 mmol, 37%). Analysis: Calc for

$RuC_{42}H_{40}N_5O_4$ (based on $Et_3NH[Ru(hnaBH)_2]$) (Mol wt = 779.9) C - 64.68%, H - 5.177%, N - 8.98%. Found: C - 62.12%, H - 3.98%, N - 9.82%.

(d) Ru(hna-pCl-BH)$_2$.H$_2$O. N'-(2-hydroxynaphthylmethylidene)-4-chlorobenzohydrazide (H_2hna-pCl-BH, 0.529 g, 1.63 mmol) and lithium acetate (0.333 g, 3.26 mmol) were added to $RuCl_3.3H_2O$ (0.204 g, .814 mmol), the mixture was dissolved in ethanol (24 cm^3) and heated at reflux for 4 hours. The solvent volume was then reduced to 10 cm^3 on a rotary evaporator, and the concentrated solution stored at –10°C overnight. A brown powder precipitated which was collected by vacuum filtration through a sintered glass funnel, washed with two 10 cm^3 portions of ice-cold ethanol, and three 5 cm^3 portion of dry diethyl ether, then air dried by suction. Yield = 0.153 g (0.2 mmol, 25%). Analysis: Calc for $RuC_{36}H_{24}N_4O_5Cl_2$ (Mol wt = 764.9) C - 56.55%, H - 3.16%, N - 7.33%, Cl - 9.27%. Found: C - 55.82%, H - 3.31%, N - 7.04%, Cl - 9.26%.

(e) Ru(hapBH)$_2$.H$_2$O. N'-(1-(2-hydroxy)phenylethylidene)benzohydrazide (H_2hapBH, 0.314 g, 1.23 mmol) and lithium acetate (0.255 g, 2.50 mmol) were added to $RuCl_3.3H_2O$ (0.159 g, .62 mmol), the mixture was dissolved in ethanol (13 cm^3) and heated at reflux for 4 hours. The solvent volume was then reduced by half on a rotary evaporator, and the concentrated solution stored at –10°C overnight. A brown powder precipitated which was collected by vacuum filtration through a sintered glass funnel, washed with two 10 cm^3 portions of ice-cold ethanol, and three 5 cm^3 portion of dry diethyl ether, then air dried by suction. Yield = 0.160 g (0.25 mmol, 41%). Analysis: Calc for $RuC_{30}H_{26}N_4O_5$ (Mol wt = 627.6) C - 57.75%, H - 4.20%, N - 8.98%. Found: C - 58.03%, H - 4.17%, N - 8.86%.

(f) Ru(bzacSalH)$_2$.H$_2$O. N'-(1-methyl-3-oxo-3-phenylpropylidene)-2-hydroxybenzohydrazide (H_2bzacSalH, 0.512 g, 1.73 mmol) and lithium acetate (0.364 g, 3.57 mmol) were added to $RuCl_3.3H_2O$ (0.232 g, .899 mmol), the mixture was dissolved in ethanol (13 cm^3) and heated at reflux for 4 hours. The solvent volume was then reduced by half on a rotary evaporator, and the concentrated solution stored at –10°C overnight. A brown powder precipitated which was collected by vacuum filtration through a sintered glass funnel, washed with two 10 cm^3 portions of ice-cold ethanol, and three 5 cm^3 portions of dry diethyl ether, then air dried by suction. Yield = 0.044 g (after accidental spillage). Analysis: Calc for $RuC_{34}H_{30}N_4O_7$ (Mol wt = 691.1) C - 57.70%, H - 4.27%, N - 7.62%. Found: C - 56.06%, H - 4.18%, N - 7.62%.

(g) Ru(salBH)$_2$.0.5EtOH. N'-(2-hydroxyphenylmethylidene)benzohydrazide (H_2salBH, 0.242 g, 0.92 mmol) and lithium acetate (0.186 g, 1.82 mmol) were added to $RuCl_3.3H_2O$ (0.117 g, .453 mmol), the mixture was dissolved in ethanol (13 cm^3) and heated at reflux for 4 hours. The reaction mixture was filtered through a sintered glass funnel after standing overnight. The black crystals so obtained were washed with two 10 cm^3 portions of ethanol, and three 5 cm^3 portion of dry diethyl

ether, then air dried by suction. Yield = 0.196 g (0.30 mmol, 66%). Analysis: Calc for $RuC_{29}H_{23}N_4O_{4.5}$ (Mol wt = 650.1) C - 57.78%, H - 4.20%, N - 8.98%. Found: C - 57.63%, H - 3.95%, N - 9.27%.

(h) Ru(bzacOAP)$_2$. N'-(1-methyl-3-oxo-3-phenylpropylidene)-2-hydroxyphenylimine (H_2bzacOAP, 0.269 g, 1.06 mmol) and lithium acetate (0.218 g, 2.12 mmol) were added to $RuCl_3.3H_2O$ (0.137 g, .531 mmol), the mixture was dissolved in ethanol (10 cm^3) and heated at reflux for 5 hours. Black crystals precipitated which were collected by vacuum filtration through a sintered glass funnel, washed with two 10 cm^3 portions of ethanol, and three 5 cm^3 portions of dry diethyl ether, then air dried by suction. Yield = 0.04 g (0.06 mmol, 11%). Analysis: Calc for $RuC_{32}H_{26}N_2O_4$ (Mol wt = 605) C - 63.67%, H - 4.34%, N - 4.64%. Found: C - 53.38%, H - 3.99%, N - 3.86%. Fits $Ru_2C_{32}H_{26}N_2O_4$. C - 53.18%, H - 3.90%, N - 3.88%.

(i) Attempted preparation of Ru(acacBH)$_2$. Following the procedure of Diamantis & Vanzo [11], tris(pentanedionato)ruthenium(III) (0.2 g, .5 mmol) was dissolved in methanol and benzoylhydrazine (0.138 g 1.01 mmol) was added. The reaction mixture was heated at reflux, in air, for 3 hours. At this stage the reaction mixture still had the red colour of Ru(acac)$_3$, and its uv/vis spectrum was consistent with the presence of this compound, implying that reaction had not occurred.

6.4.7. Nitrosyl Complexes.

(a) [Ru(NH$_3$)$_3$(Cl)$_2$NO]Cl. $Ru(NH_3)_3Cl_3$ (0.16 g, .61 mmol) was added to water (9 cm^3) in a round-bottomed flask fitted with an outflow bubbler. The mixture was degassed by bubbling nitrogen gas through it and nitric oxide was then bubbled through the mixture for 2 hours while it was stirred at 70°C. After this period, any nitric oxide remaining in the solution was removed by passing nitrogen through the solution for 30 minutes. The reaction mixture was filtered by gravity, yielding a bright red filtrate. The volume of the filtrate was reduced to 1 cm^3 by evaporation on a steam bath. As the concentrated solution cooled, red crystals precipitated, and the precipitation was enhanced by the addition of a few drops of ethanol. The product was collected by vacuum filtration through a sintered glass funnel and washed with two 2 cm^3 portions of ethanol, and one 2 cm^3 portion of dry diethyl ether, then air dried by suction. Yield = 0.123 g (0.43 mmol, 70%). Analysis: Calc for $RuH_9N_4Cl_3O$ (Mol wt = 288.5) H - 3.14%, N - 19.42%, Cl - 36.87%. Found: H - 2.91%, N - 18.55%, Cl - 35.5%.

(b) [Ru(NH$_3$)$_3$(Br)$_2$NO]Br. $[Ru(NH_3)_3(Cl)_2NO]Cl$ (0.05 g, .17 mmol) was heated on a steam bath in 5 mol dm^{-3} HBr (10 cm^3) for 2 hours. The solution was then cooled in ice and filtered to yield a pale orange filtrate. The volume of the filtrate was reduced using a rotary evaporator, and an excess of ethanol was added. An orange powder precipitated from the solution and was collected by vacuum filtration through a sintered glass funnel and washed with two 2 cm^3 portions of ethanol, and one 2

cm^3 portion of dry diethyl ether, then air dried by suction. Yield = 0.027 g (0.06 mmol, 35%). Analysis: Calc for $RuH_9N_4Br_3O$ (Mol wt = 421.5) H - 2.15%, N - 13.28%, Br - 56.82%. Found: H - 1.17%, N - 7.13%, Br - 37.0%. (Contaminated sample)

(c) $[Ru(NH_3)_3(C_2O_4)NO]_2C_2O_4$. Lithium acetate (0.077g, .7 mmol) and oxalic acid dihydrate (0.042 g, .3 mmol) were added to $[Ru(NH_3)_3(Cl)_2NO]Cl$ (0.06 g, .2 mmol) in water (20 cm^3), and the mixture was heated at reflux for 30 minutes. Most of the solvent was then evaporated from the resultant orange solution, and the concentrated solution was cooled on an ice bath. Ethanol was added, dropwise, until a faint cloudiness appeared, and orange crystals then precipitated from solution. The product was collected by vacuum filtration through a sintered glass funnel and washed with two 2 cm^3 portions of ethanol, and one 2 cm^3 portion of dry diethyl ether, then air dried by suction. Yield = 0.031 g (0.05 mmol, 50%). Analysis: Calc for $RuC_6H_9N_4O_{13}$ (Mol wt = 628.4) C - 11.47%, H - 2.89%, N - 17.83%. Found: C - 11.37%, H - 3.09%, N - 16.66%.

(d) Attempted synthesis of $[Ru(NH_3)_3(bpy)NO]Cl_3$. $[Ru(NH_3)_3(Cl)_2NO]Cl$ (0.19 g, .66 mmol) was dissolved in a 75/25 mixture of water and ethanol (20 cm^3), 2.2'-bipyridine (0.11 g, .7 mmol) was added and the mixture was heated at reflux for 30 minutes. Most of the solvent was then evaporated from the resultant orange solution, ethanol (1 cm^3)was added, and the concentrated solution was then cooled on an ice bath. Orange crystals precipitated from solution. The product was collected by vacuum filtration through a sintered glass funnel and washed with two 2 cm^3 portions of ethanol, and one 2 cm^3 portion of dry diethyl ether, then air dried by suction. Yield = 0.025 g. Analysis: Calc for $RuC_{10}H_{17}N_6OCl_3$ (Mol wt = 444.7) C - 27.01%, H - 3.85%, N - 18.90%, Cl - 23.92. Found: C - 0.57%, H - 4.08%, N - 22.45%, Cl - 34.14%. For $[Ru(NH_3)_4(Cl)NO]Cl_2$, calc for $RuH_{12}N_5OCl_3$: C - 0%, H - 4.00%, N - 22.92%, Cl - 34.80%.

6.4.8. Dinitrogen Complexes.

(a) $[Ru(NH_3)_3(OH_2)_2NO](PF_6)_2$. Following the method of Bottomley [10], $[Ru(NH_3)_3(Cl)_2NO]Cl$ (0.05 g, .18 mmol) was dissolved in water (20 cm^3) in a Schlenk tube, and the solution degassed by bubbling nitrogen through it for 10 minutes. Against a flow of nitrogen, a 50% solution of hydrazine hydrate (1 cm^3, 10 mmol) was then added, causing effervescence to occur. After 30 minutes, NH_4PF_6 (1 g) was added and stirred into the solution, and the mixture was then cooled on an ice bath for 30 minutes. A pale precipitate formed, which was collected by vacuum filtration through a sintered glass funnel and washed with two 2 cm^3 portions of ethanol, and one 2 cm^3 portion of dry diethyl ether, then air dried by suction. Yield = 0.045 g (0.09 mmol, 50%). Analysis: Calc for $RuH_{13}N_4O_2P_2F_{12}$ (Mol wt = 506.1) H - 2.59%, N - 13.84%, P - 12.24%. Found: H - 3.16%, N - 18.46%, P - 12.1%. For $[Ru(NH_3)_4(N_2H_4)(H_2O)(N_2)](PF_6)_2$, calc for $RuH_{15}N_7OP_2F_{12}$: H - 2.90%, N - 18.82%, P - 11.89%.

The same procedure was used to prepare samples containing the triammine dinitrogen complex containing the anions Br^-, I^- and BF_4^-, by using the appropriate sodium salt instead of NH_4PF_6.

(b) $[Ru(NH_3)_3(Cl)_2N_2]$. $[Ru(NH_3)_3(Cl)_2NO]Cl$ (0.081 g, .28 mmol) was suspended in methanol (20 cm^3) in a Schlenk tube, and the solvent degassed by bubbling nitrogen through it for 10 minutes. Against a flow of nitrogen, hydrazine hydrate (1 cm^3, 10 mmol) was then added, causing effervescence to occur. After 30 minutes, the red reaction mixture was filtered, and ethanol (10 cm^3) was added to the filtrate. A pale precipitate formed on cooling at –10°C for three hours, and this was collected by vacuum filtration through a sintered glass funnel and washed with two 2 cm^3 portions of ethanol, and one 2 cm^3 portion of dry diethyl ether, then dried on a vacuum line. Yield = 0.047 g (0.19 mmol, 68%). Because the uv/vis spectrum was indicative of substantial contamination with $[Ru(NH_3)_3(Cl)_2]N_2$, no analysis was attempted.

(c) Attempted preparations of terminal dinitrogen complexes from $[Ru(NH_3)_3(OH_2)_3]^{2+}$.
(1) $[Ru(NH_3)_3(OH_2)_3](TFMS)_3$ (0.172g, .26 mmol) was dissolved in saturated $NaBF_4$ solution (4 cm^3) at 0°C, and the solution was degassed by bubbling argon through it. Hydrogen gas was then bubbled into the solution through a platinum black gauze for 1.5 hours. The golden yellow solution was then filtered using a Schlenk filter and, while the filtrate was kept cool, nitrogen gas was bubbled through it. After 2 hours of reaction with nitrogen, there was no sign of any precipitate, though the solution was cloudy. After storing the mixture overnight at –10°C, $NaBF_4$ was filtered from the yellow solution. The uv/vis spectrum of the filtrate contained bands attributable to the terminal and bridged dinitrogen complexes.

(2) $[Ru(NH_3)_3(OH_2)_3](TFMS)_3$ (0.17g, .26 mmol) was dissolved in saturated $NaBF_4$ solution (7 cm^3), and the solution was degassed by bubbling argon through it. Hydrogen gas was then bubbled into the solution through a platinum black gauze for 1.5 hours. The golden yellow solution was then filtered using a Schlenk filter and transferred, under nitrogen, to a high pressure reaction vessel which had previously been flushed with nitrogen. The reaction vessel was pressurized to 20 atmospheres pressure with nitrogen, and maintained at this pressure for two hours. At the end of this period, the pressure was released and the vessel opened. Bubbles were observed in the solution, indicative of the slow release of nitrogen. The uv/vis spectrum of the solution contained bands attributable to the terminal and bridged dinitrogen complexes.

(3) $[Ru(NH_3)_3(OH_2)_3](TFMS)_3$ (0.15g, .23 mmol) was dissolved in saturated $NaBF_4$ solution (4 cm^3), and the solution was degassed by bubbling argon through it. Amalgamated zinc was added to the flask and the mixture was stirred while a stream of nitrous oxide was passed through it for 2

hours. There was no noticeable precipiate, and the uv/vis spectrum of the solution contained bands attributable to the terminal and bridged dinitrogen complexes.

References.

(1) L. Sacconi, *Z. Anorg. Allg. Chem.*, **275**, 249(1954)

(2) D. J. Szalda, F. R. Keene, *Inorg. Chem.*, **25**, 2795(1986)

(3) J. P. Wibaut, A. P. de Jonge, H. G. P. Van der Voort, H. L. Otto, *Rec. Trav. Chim. Pay-Bas.*, **70**, 1054(1951)

(4) G. E. Cabaniss, A. A. Diamantis, W. R. Murphy, L. W Linton, T. J. Meyer, *J. Amer. Chem. Soc.*, **107**,1845(985)

(5) F. M. Lever, A. R. Powell, *J. Chem., Soc., A.*, 1477(**1969**)

(6) S. Pell, J. N. Armor, *Inorg. Chem.*, **12**, 873(1973)

(7) D. M. D. Goswick, G. M. Brown, H. Taube, *Inorg. Chem.*, **22**, 1975(1983)

(8) P. W. Banham, Honours Thesis, The University of Adelaide, 1980.

(9) P. C. Ford, C. Sutton, *Inorg. Chem.*, **8**, 1544(1969)

(10) F. Bottomley, J. R. Crawford, *Chem. Commun.*, 200(**1971**)

(11) A.A. Diamantis, M. R. Snow, J. A. Vanzo, *J. Chem. Soc., Chem. Comm.*, 264(**1976**)